

**Biodiversity patterns of herbivore scarab chafers
of Sri Lanka with particular reference to
DNA based species delimitation, taxonomy,
morphospace, and assemblage composition
(Coleoptera: Scarabaeidae)**

Dissertation

zur

Erlangung des Doktorgrades (Dr. rer. nat.)

der

Mathematisch-Naturwissenschaftlichen Fakultät

der

Rheinischen Friedrich-Wilhelms-Universität Bonn

vorgelegt von

Sasanka Ranasinghe

aus

Kegalle, Sri Lanka

Bonn August, 2022



Angefertigt mit Genehmigung der Mathematisch-Naturwissenschaftlichen
Fakultät
der Rheinischen Friedrich-Wilhelms-Universität Bonn

Die Arbeit wurde am Zoologischen Forschungsmuseum Alexander Koenig in
Bonn durchgeführt.

Betreut von: Dr. Dirk Ahrens

Gutachter: Prof. Dr. Bernhard Misof

Gutachter: Prof. Dr. Christoph Scherber

Fachnahes Kommissionsmitglied: Prof. Dr. Gerhard von der Emde

Fachfremdes Kommissionsmitglied: Prof. Dr. Gabriele König

Tag der Promotion: 03. November 2022

Erscheinungsjahr: 2022

Summary

Biodiversity patterns of herbivore scarab chafers of Sri Lanka with particular reference to DNA based species delimitation, taxonomy, morphospace, and assemblage composition (Coleoptera: Scarabaeidae)

The thesis consists of six independent chapters covering DNA-based species delimitation, taxonomy, morphometrics, and synecology. The organism group on which the study focussed on was herbivore scarabs which represent a very diverse group of organisms. My work comprised four main field expeditions which were performed for quantitative sampling with multiple UV light traps during wet and dry seasons in Sri Lanka (chapter 2). Standardized sampling encompassed in total 15 localities (L1–L15), covering different forest types (evergreen wet lowland forests, evergreen dry lowland forest, sub-montane forests and montane forests) along an elevational gradient (0–2500m). Freshly sampled and well-preserved ethanol specimens was the critical point for the molecular work of this study.

Herbivore scarabs referred to as "pleurostict chafers" (Coleoptera: Scarabaeidae) are represented in Sri Lanka principally by the subfamilies Dynastinae, Melolonthinae, and Rutelinae. They are example study group because of their high diversity, presence of strongly differentiated male genitalia that allow precise species diagnostics based on morphology and high regional endemism. A total of 4901 pleurostict scarab chafer specimen representing 105 morphospecies have been examined. Multiple samples were DNA barcoded and delimited to species using several de-novo species delimitation methods. Based on resulting molecular operational taxonomic units (MOTUs), their species diversity, assemblage composition and pattern of morphospace across different spatial scales was inferred, also in comparison to morphospecies entities.

Chapter 3 DNA barcoding approaches have been widely used to explore the diversity in biodiversity hotspots. However, DNA barcoding (i.e., species delimitation and specimen identification based on a single gene fragment, e.g., *COI* sequences) also has been critically discussed due to many problems including the nature of the used single mtDNA marker gene. While results of *COI* barcoding have been so far mainly compared with morphospecies entities, the congruence of the outcome of different DNA-based species delimitations has only rarely been analyzed in detail. Outcomes have often been characterized as "different" without quantifying the difference, particularly in relation to delimitations based on morphology. This chapter focused to explore how well *COI* barcode data reflects morphological species entities and thus its utility for accelerated species

inventorization. This was studied by the example of the chafer lineage Sericini, which is particularly species rich in Sri Lanka. Morphological sorting of captured specimens (ca. 2300) resulted in a total of 45 morphospecies of which 280 individuals were selected for sequencing. These species included 41 Sri Lankan endemics and representatives from all five Sericini genera occurring in Sri Lanka. Eleven morphospecies were represented only by singletons. Different delimitation methods were performed to investigate the congruence of morphology-based species identifications with species entities (molecular operational taxonomic units (MOTUs)) that were inferred based on *COI* data. These analyses included the Poisson tree processes (PTP) model, statistical parsimony analysis (TCS), Automatic Barcode Gap Discovery (ABGD), Assemble Species by Automatic Partitioning (ASAP) and Barcode Index Number (BIN) assignments. Delimitation methods resulted in different numbers of MOTUs. All methods showed both over-splitting and lumping of species identified by morphology. Only 18 of the observed 45 morphospecies perfectly matched MOTUs in all delimitation methods. The congruence of delimitation between MOTUs and morphospecies expressed by the match ratio was low, ranging from 0.57 to 0.67. The study showed that empirical focused tests (this study) continue to be necessary to further develop our understanding of frequently employed taxonomic markers and methods, particularly in the light of potential drawbacks for accuracy of newly emerging approaches such as metabarcoding or “exclusively *COI* barcode-based species definitions”. The study confirmed that *COI* barcode data alone is unlikely to correctly delimit all species, in particular, when using only a single delimitation approach and suggested the integration of various approaches and data, particularly morphology, to validate species boundaries. A comparison of the outcome of all DNA-based species delimitation methods using Principal Coordinate Analysis (PCoA) based on pairwise match ratios, in which no method neither matched the other nor the morphospecies, confirmed this further.

Chapter 4 DNA-based species delimitation has become increasingly popular for biodiversity assessments and their robustness is often measured by integrative approaches by congruence of outcome from multiple delimitation methods. However, often incongruent outcomes of species delimitation methods provide may cause ambiguities for synecological studies. Here I investigated how contrasting results of different species delimitations translate into conclusions of synecological studies, exemplified by assemblages of phytophagous scarab beetles in Sri Lanka in different elevations and forest types. Particularly, species estimates based on complete assemblages and on cumulated species inventories inferred from individually analysed subclades were investigated. These patterns of assemblage similarity were analysed across different spatial scales with reference to morphospecies and haplotypes. Such outcome is important for providing a

robust and stable reference point with biodiversity assessments, particularly for those that have potential impact on decisions of conservation management. The study revealed method-related ambiguity of species estimates, which included particularly also subclade inferences, affected severely the certainty of biodiversity patterns at most spatial scales. To bypass some of these difficulties of incongruence with morphospecies or with the accurate species delimitation, particularly with mtDNA data and single marker data (e.g., COI), the use of haplotype data alone have been proposed as an unbiased and even more objective measure for biodiversity. However, in this case study of tropical beetles, haplotypes provided only very little explanatory information, since genetically highly diverse populations widely lacked shared haplotypes for almost all investigated entities.

Chapter 5 and 6 Fourteen new species of the Tribe Sericini Kirby, 1837 from Sri Lanka, belonging to the genera *Maladera* Mulsant & Rey, 1871, *Neoserica* Brenske, 1894 and *Selaserica* Brenske, 1897 were described. The descriptions are completed by illustrations of their genitalia and the habitus and included distribution maps and photos of the habitats. Chapter V presented the results of the first field expedition and described four new Sericini species: *Selaserica athukoralai* Ranasinghe et al., 2020, *Neoserica dharmapriyai* Ranasinghe et al., 2020, *Maladera cervicornis* Ranasinghe et al., 2020, *M. galdaththana* Ranasinghe et al., 2020. Chapter VI presented the results of the three subsequent expeditions, which were able to discover further ten new species; *Sel. fabriziae* Ranasinghe et al., 2022, *Sel. sororinitida* Ranasinghe et al., 2022, *N. pophami* Ranasinghe et al., 2022, *M. haniel* Ranasinghe et al., 2022, *M. kishi* Ranasinghe et al., 2022, *M. windy* Ranasinghe et al., 2022, *M. karunaratnae* Ranasinghe et al., 2022, *M. hiyarensis* Ranasinghe et al., 2022, *M. dambullana* Ranasinghe et al., 2022, and *M. deenstana* Ranasinghe et al., 2022. Further, new locality records for 33 previously known species were reported and the identification key to the *Maladera fistulosa* group was updated, due to the addition of nine new species. The study once more revealed a large amount of endemism, confirming that Sri Lanka remains unexplored, and that night active chafers are still rather poorly represented in material from occasional, non-specialized field surveys. The two chapters updated the results of a previous monograph of Sericini of the Sri Lanka (Fabrizi & Ahrens 2014), comprising now 91 species, 81 of them are endemic.

Chapter 7 Evolutionary success of lineages becomes visible by species diversity or morphological disparity, but the link between both phenomena is poorly investigated for invertebrates, particularly considering various ecochorological scales. This chapter focused to investigate the morphospace, morphological disparity, and species diversity for forest types, elevation zones, and each

collection site. Furthermore, the study attempted to quantify the effect of direct competition among species by investigating local scale vs. higher spatial scale patterns of the assemblages. Morphospace of phytophagous scarab lineages reflects well general niche occupation at global scale according to their different microhabitats and foraging behaviour. However, in previous studies single lineages showed only little divergence and sampling was not yet considering local assemblages. Therefore I explored at hand of these data, whether direct competition between species is likely to occur. Twenty linear distance measurements were taken from 384 adult specimens of 105 species. Morphospace and morphological disparity was analysed separately for three different monophyletic lineages (1) the entire assemblage, and two sister subclades, 2) Sericini, and 3) Pleurosticti excluding Sericini. These analyses were performed for three major chorological and landscape entities (1) forest type, 2) elevation zone, and 3) sampling locality. At locality-level, morphospace occupation referred to actually co-occurring species. The results corroborated a general correlation between morphological disparity and species richness among phytophagous chafers at different ecochorological scales showing contrasting patterns of lineages at different geographical scales. The relation disparity versus species diversity followed two distinctive patterns, one for the entire assemblage and Pleurosticti excluding Sericini, and one for Sericini. For the first I found a significant correlation between diversity and disparity between different forest types and elevation zone with size-corrected data. The opposite was the case for the different sampling locations in which Sericini showed significance, however, the other two lineages not. These patterns were corroborated by body size variation of the entire assemblage which was observed to shrink towards higher altitudes with the general decrease of species diversity and morphological disparity. The reason might be at larger geographical scales the relation of species diversity vs. disparity is determined by the historical integration of a multitude of species or lineages, while at local scale assembled species compete for space and resources. However, future studies need to explore more rigorously community composition at different landscape scales to disentangle the driving forces of diversity vs disparity in the context of assemblage evolution among pleurostict chafers.

Chapter 8 Very little is known about factors determining assemblage structure of megadiverse tropical polyphagous-herbivore scarab chafers. Knowledge about their actual assemblages, differences between habitats is even rarer. Most available studies on chafer assemblages include either mostly only a part of the assemblage, or assemblages from a single or a few distant localities. Factors determining the assemblage composition so far never have been explored. This chapter investigated the patterns of diversity and turnover of tropical pleurostict

chafers in Sri Lanka across different forest types, elevation zones, localities, and habitats to examine which spatial component determines the assemblage composition, and at which extent. Further the influence of lineage membership and body size in shaping the species composition was assessed. The study is based on 4847 specimens of 105 chafer morphospecies belonging to Rutelinae, Melolonthinae, and Dynastinae recorded from 11 localities across Sri Lanka. Species richness estimators suggested >89% of total species inventory had been captured. While 82% of the individual locality assemblages showed more than 84% of sampling completeness (in terms of species composition), in two case sampling completeness was quite a low with less than 50% (L9, L14). The species accumulation curves for individual localities showed that about 80% or slightly more of the expected species has been captured before the sixth trapping event (i.e., half of the total trapping events for each individual trap). Many species were geographically restricted, 67 species (from 105 total species) were found exclusively in just one site.

Ordination analysis on species presence/absence data of the full chafer assemblage generally showed different patterns between the different spatial components. The results revealed that assemblages were shaped mainly by locality stochastics, and to minor extent by the ecoclimatic conditions. Here, locality stochastics represent a not further investigated multi-factor ensemble that includes all environmental conditions at local scale such macrohabitat, biogeography, edaphic conditions, land use, local climate and exposition to rain and radiation. Macrohabitat had little effect on the assemblage composition. This was true for the entire chafer assemblage but also for all single lineages or different body size classes. However, in medium and large specimens contrasts between localities were less pronounced, which was not the case for the lineages. Contrasts of assemblage similarity between localities were much more evident than those of forest types and elevation zones. Significant correlation between species composition and geographic distance was found only for the assemblage of small-bodied specimens. In general, species richness and abundance varied significantly between collection seasons. But seasonal change (dry-wet) in species composition was minor and only measurable in a few localities.

Contents

Summary	v
Contents	vi
List of figures	viii
List of tables	x
Acknowledgments	xii
Chapter 1. General Introduction	1
Research question and aims	7
References	9
Chapter 2. Field expeditions and sampling	17
2.1. Study area	17
2.2. Sampling methods and sampling design	17
2.3. Collection and export permits	20
References	21
Chapter 3: Multiple species delimitation approaches with COI barcodes poorly fit each other and morphospecies – an integrative taxonomy case of Sri Lankan Sericini chafers (Coleoptera: Scarabaeidae)	22
Abstract	23
3.1 Introduction	24
3.2 Materials and Methods	26
3.3 Results	31
3.4 Discussion	36
3.5 References	43
3.6 Supplementary Figures to chapter 3	57
Chapter 4: Contrasting results of multiple species delimitation approaches cause uncertainty in synecological studies	60
Abstract	61
4.1 Introduction	61
4.2 Materials and Methods	64
4.3 Results	68
4.4 Discussion	72
Conclusion	76
4.5 References	77
4.6 Supplementary Figures to chapter 4	90
Chapter 5: New species of Sericini from Sri Lanka (Coleoptera, Scarabaeidae) Part I	98
Abstract	98
5.1 Introduction	99

5.2 Materials and Methods	99
5.3 Results	100
5.3.1 Taxonomy	102
5.3.2 New distribution records	113
5.4 Discussion	120
5.5 References	121
Chapter 6: New species of Sericini from Sri Lanka (Coleoptera, Scarabaeidae) Part II	122
Abstract	122
6.1 Introduction	123
6.2 Materials and Methods	123
6.3 Results	124
6.3.1 Taxonomy	124
6.3.2 Updated and corrected key to species of the <i>Maladera fistulosa</i> group	166
New distribution records	171
6.4 Discussion	186
6.5 References	187
Chapter 7: Chorological scale and lineage shape the correlation between morphospace disparity and species diversity in phytophagous scarab beetles	188
Abstract	189
7.1 Introduction	189
7.2 Materials and Methods	191
7.3 Results	194
7.4 Discussion	198
7.5 References	201
7.6 Supplementary Figures to chapter 7	206
Chapter 8: Local stochasticity and ecoclimatic situation shape phytophagous chafer assemblage composition	211
Abstract	212
8.1 Introduction	212
8.2 Materials and Methods	214
8.3 Results	217
<i>Spatial turnover</i>	218
<i>Seasonal turnover</i>	220
8.4 Discussion	222
8.5 References	226
8.6 Supplementary Figures to chapter 8	231
Chapter 9. General Discussion and Conclusions	234
References	237

Chapter 10. Appendix	
<i>Supplementary Tables to chapter 3</i>	238
<i>Supplementary Tables to chapter 4</i>	249
<i>Supplementary Tables to chapter 7</i>	274
<i>Supplementary Tables to chapter 8</i>	297
Declaration	310

List of Figures

Figure 1.1	Pleurostict chafers in the field	3
Figure 1.2	Sericini collected during field work	4
Figure 1.3	The geological history of India and Sri Lanka	5
Figure 2.1	Map of Sri Lanka showing sampling sites	18
Figure 2.2	Images of sampling habitats represent different forest types	19
Figure 2.3	Light trap in the field. Manual collecting from a white sheet illuminated with UV light in the field	20
Figure 3.1	Map of Sri Lanka showing collecting sites for this study	27
Figure 3.2	Maximum likelihood tree with morphospecies assignments and results of species delimitations	33
Figure 3.3	Principal Coordinate Analysis (PCoA) of different species delimitation methods and morphospecies	37
Figure S3.1	Maximum likelihood tree from PhyML analysis	57
Figure S3.2	Split network of all examined specimens.	59
Figure 4.1	Principal coordinate analyses (PCoA) of results of different species delimitation methods	69
Figure 4.2	Number of “species entities” reported for for forest types, elevation zones and sampling localities	71
Figure 4.3	Clustering analysis based on the Jaccard index	73
Figure S4.1	Maximum likelihood tree with morphospecies and results of species delimitations	90
Figure S4.2	NMDS analysis for total assemblage and cumulative subclades	93
Figure S4.3	Number of putative species entities reported in forest types, elevation zones and sampling localities	94
Figure S4.4	Clustering analysis (Jaccard Index) based on presence/absence for four subclade analysis	95
Figure S4.5	NMDS analysis for four subclade analysis	96
Figure S4.6	Frequency of intra-and interspecific distances of the phytophagous scarab chafer data from Sri Lanka	97

Figure 5.1	Map of Sri Lanka showing collecting sites for this study.	101
Figure 5.2	Light trap in the field and live Sericini	102
Figure 5.3	Plate of <i>Selaserica athukoralai</i> sp. n. (holotype), <i>Neoserica dharmapriyai</i> sp.n. (holotype),	107
Figure 5.4	Plate of <i>Maladera galdaththana</i> sp. n. (holotype), <i>M. cervicornis</i> sp. n. (holotype)	110
Figure 5.5	Distribution of the new species	114
Figure 5.6	Photos of the habitats of the new species	115
Figure 6.1	Map of Sri Lanka showing collecting sites for this study	125
Figure 6.2	Manual collecting from a white sheet illuminated with UV light	126
Figure 6.3	Plate of <i>Selaserica fabriziae</i> sp. nov., (holotype), <i>Selaserica sororinitida</i> sp.nov., (holotype), <i>Neoserica pophami</i> sp. nov.	130
Figure 6.4	Plate of <i>Maladera haniel</i> sp. nov., (holotype), <i>M. kishi</i> sp. nov., (holotype), <i>M. windy</i> sp. nov., (holotype)	148
Figure 6.5	Plate of <i>Maladera karunaratnae</i> sp. nov., (holotype), <i>M. hiyarensis</i> sp. nov., (holotype)	155
Figure 6.6	Plate of <i>M. dambullana</i> sp. nov., (holotype), <i>M. deenstana</i> sp. nov. (holotype)	165
Figure 6.7	Distribution of ten new species	166
Figure 6.8	Photographs of the habitats of the new species	167
Figure 7.1	Map illustrating the location of sampling sites	193
Figure 7.2	Illustration of the measured morphological traits.	194
Figure 7.3	Lineage-specific disparity and body size variation partitioned by forest type, elevation and location	196
Figure 7.4	Patterns of morphospace disparity of lineages partitioned by forest type, elevation and location	197
Figure S7.3	Biplots of PC1 and 2 from principal components analysis, illustrating trait contribution	206
Figure S7.4.	Patterns of morphospace disparity derived from log-normalized data	207
Figure S7.5a.	Patterns of morphospace disparity of all Pleurostictids in individual localities.	208
Figure S7.5b.	Patterns of morphospace disparity of Sericini in individual localities	209
Figure S7.6:	Patterns of morphospace disparity of Sericini chafers partitioned for forest types, elevation zones, localities	210
Figure 8.1	Total number of species (species richness) in different locations and in four field campaigns	218
Figure 8.2	Dendrogram from species presence data	219
Figure 8.3	NMDS analyses of assemblages separated by taxa and different spatial and eco-spatial partitions	220
Figure 8.4	NMDS analyses of assemblages separated by body size classes and different spatial and eco-spatial partitions	221

Figure 8.5	Correlation between species compositional similarity and pairwise geographic distance	222
Figure 8.6	NMDS analyses of assemblages from single trapping events separated by sampling locality	223
Figure S8.1	Map of Sri Lanka showing sampling sites	231
Figure S8.2	Species accumulation curves for each sampling locality for total species and subfamily level	232
Figure S8.3	No. of species and no. of individuals of Sericini chafers among twelve months	233

List of Tables

Table 3.1	Match ratio of DNA-based species delimitation methods	37
Table 7.1	Pearson correlation between the mean disparity and species diversity	198
Table S3.1	Details of species	238
Table S4.1	Sample details: voucher number, species identification, locality id, BIN, GenBank accession numbers	249
Table S4.2	Number of MOTUs, number of matches and match ratios of DNA-based species delimitation methods	271
Table S4.3	Species similarity among different forest types and elevation zones among morphospecies, haplotypes and MOTUs	272
Table S7.1	Details of sampling sites	274
Table S7.2	Morphometric measurements and metadata of all studied specimens	275
Table S7.3	Variance explained by principal component analysis for the complete sampling	287
Table S7.4	Euclidean distances of species disparity partitioned by forest types and lineages	288
Table S7.5	Euclidean distances of species disparity partitioned by elevational zones and lineages	289
Table S7.6	Euclidean distances of species disparity partitioned by localities (L1-14), and lineages	290
Table S7.7	Pairwise p-values from non-parametric MANOVA on PCA loadings and partitioned for forest types and lineages	292
Table S7.8	Pairwise p-values from non-parametric MANOVA on PCA loadings and partitioned for elevational zones and lineages	293
Table S7.9	Pairwise p-values from non-parametric MANOVA on PCA loadings and partitioned for localities and lineages from raw data	294
Table S7.10	Pairwise p-values from non-parametric MANOVA on PCA loadings and partitioned for localities and lineages from log normalized data	296

Table S8.1	Details of sampling sites, habitat types	297
Table S8.2	Details of species, recorded localities and their presence	299
Table S8.3	Individuals, observed species richness (Sobs) and percentages of inventory completeness and diversity indices of scarab beetles in all sampling locations	303
Table S8.4	Pearson correlation between the similarity of chafer assemblage (sorted body size and for separate lineages) with geographic distance	304
Table S8.5	Kruskal-Wallis test for species turnover in localities between four field campaigns	305
Table S8.6	Similarity in species composition among campaigns for total assemblage and assemblage sorted for body size and lineages	306
Table S8.7	Comparison of species occurrence in different months (only for Tribe Sericini)	307

Acknowledgements

First and foremost I would like to express my deep gratitude to my principal supervisor Dr. Dirk Ahrens for his guidance, immense knowledge, constant supervision, advices, care and encouragement provided throughout this study, while improving each chapter from basic to standard level. I consider myself very fortunate for being able to work with him. I learnt a lot, none of any words can describe my gratitude.

I would like to express my deep gratitude to Dr. Jonas Eberle for his immense support, and guidance whenever needed. He supported me from my starting point at the ZFMK, for field expeditions, during lab work and analysis then to manuscript corrections. I am fortunate to having such a collaborator for this study.

I would like to express my deep gratitude to Prof. Suresh Benjamin, for his excellent support, and advices whenever needed from my M.Phil. to Ph.D. journey. Also obtaining research and collection permits, which is the most important initial step for the whole study.

I would also like to thank to the doctoral committee members, Prof. Dr. Bernhard Misof, Prof. Dr. Christoph Scherber, Prof. Dr. Gerhard von der Emde and Prof. Gabriele König for their willingness to for accepting to review my thesis in a very restricted time schedule.

I greatly acknowledge the funding for my Ph.D. study received from German Academic Exchange Services (DAAD). I also acknowledge the funding received for field expeditions from the Alexander Koenig Stiftung, German Academic Exchange Services (DAAD) with additional supported through ZFMK institutional funding.

I am grateful to Mr. Namal Athukorala (NIFS) for his continuous support in the field in all four expeditions even in the Corona pandemic. I am thankful to my colleagues Dilini, Abira, Mathura, Chaturi (NIFS) & Supipi (UoP) for support for the fieldwork.

Further, I owe my special thanks to Frau. Claudia Eitzbauer and Frau. Jana Thormann (ZFMK) for the lab work in the molecular laboratory. Thank you for your nice coordination.

I am grateful to (late) Frau. Silvia Fabrizi, who cared me as a family member during my stay in Germany, without let me feel homesick at the beginning. You are always in my heart, Silvia! Also my heartiest thank goes to Claudia Bohacz, for being a wonderful friend for sharing happy and stressful moments. Also, my

heartiest thank goes to Benedict Wipfler for supporting at work in the museum and also being a helpful landlord. I am grateful to Frau. Karin Ulmen and Christina Blume for their kind support in the museum, also guiding translations of German-English documents, whenever I needed. Further my heartiest thanks go to Daniel Lukic, Neha Singh, Hans-Joachim Krammer, Adelfia Papu, Jana Flury, Alina Schüller and Sergio Avila-Calero for being friendly and supportive. Further I am thankful to all the people in the Arthropoda section (ZTE/ZFMK).

I would like to thank the Zoological Research Museum A. Koenig for providing me with the Research Infrastructure and for being an excellent place to work. Further, I would like to thank the National Institute of Fundamental Studies, Kandy, Sri Lanka for providing me with the working place during my fieldwork stay and remote working time during the pandemic.

I am grateful to Prof. Inoka Karunaratne, (UoP), for her kind support, especially for providing necessary items to continue Scarab genital preparation in my remote working time. I wish to express special thanks to Prof. Siril Wijesundara and Chanaka Lekamge for making available facilities in the NIFS Arboretum. Also thanks to Madhura de Silva, Sampath for facilities in the Hiyare Conservation Center. Further I am thankful to all wildlife rangers (Nuwara Eliya, Hiyare, Horton Plains), regional forest officers (Kandy, Knuckles, Nuwara Eliya, Kottawa, Kanneliya) and army officers (Piduruthalagala) who helped me to conduct fieldwork. Special thanks to N. Ramanayake and N. Gunathilake (Department of Wildlife Conservation, Sri Lanka) for processing export permits. Also, I would like to acknowledge Frau. Annete La Roch and Frau. Soulbieu Lara for doing administrative documentary work relevant for my field expeditions.

My deepest gratitude go to my loving parents, brother, my husband and husband's family who are the driving force behind my education and who always unconditionally stood by me every moment in my life. Especially my loving husband Dharmapriya, who dedicates whole four years, allowing me to do one of my most wanted wish in my academic career, without his permission and support I cannot do this! Thanks for giving me patience, strength, motivating, and being my inspiration.

Finally, I wish to thank all the others who helped me in numerous ways during my research work.

Chapter 1

Introduction

Biodiversity is threatened mainly by habitat loss and degradation, but also invasive alien species, over-exploitation of natural resources, pollution, diseases, and climate change (Isbell et al., 2017; Di Marco et al., 2019; Baguette et al., 2022). Describing and analysing biodiversity and its major patterns (e.g., Gaston, 2000; Holt et al., 2013) is key to investigate the underlying processes, causes of diversification and to generate a solid knowledge basis for any conservation effort. Many biogeographical and some macroecological patterns such as species turnover, alpha diversity at various geographical scales and species evolution can be assessed already at hand of material from natural history collections. However, the investigation of most macroecological patterns requires the knowledge of small-scale patterns of diversification including habitat specificity, species assemblage composition, or species turnover. All which have to be inferred by a dedicated sampling design.

Vertebrates including mammals, birds, reptiles, and amphibians are intensively studied components of tropical rainforests, but make up only a small fraction of the total number of species (Corlett & Primack, 2011; Pillay et al., 2022). In contrast, invertebrates, and especially insects, are the dominant fauna of the rainforest contributing the majority of species (Erwin, 1982; Corlett & Primack, 2011). Arthropods, which represent 80-90% of known species on earth (Stork et al., 2015), are known only fragmentarily in many aspects such as taxonomy, ecology, and distribution; and comprehensive data on them are rare (Kitching et al., 2001; Beck & Kitching, 2007; Beck et al., 2007; see also Hortal *et al.*, 2015; shortfalls of biodiversity). In most cases our knowledge relies only on museum's specimens and thus suffer largely from sampling bias (Santos & Quicke, 2011). Specifically, macroecological research until now has largely been driven by data already available (Grytnes & Romdal, 2008; Decaëns, 2010; Economo et al., 2015; Echevarría Ramos & Hulshof, 2019), revealing two major shortcomings: limited coverage of biomes, taxa and spatial scales, and insufficient or unknown data quality (Beck et al., 2012; Jetz et al., 2012). Observed large-scale biogeographical patterns are known to differ strongly between different lineages

and ecological guilds (e.g., Currie, 1991; Nielsen, 2019); thus, it may be expected that this is eventually also the case at smaller geographical scales. Nevertheless, restricted dispersal capacities and occurrence in micro-niches results in patterns of higher endemism and reveal often finer and still unknown patterns (Buckley & Jetz, 2007; Daru et al., 2020). At smaller scale diversity patterns the situation is complicated, since studies often do not rely on proper species identifications (Oliver & Beattie, 1996) and on representative species sampling (e.g., Kemp et al., 2017).

For the present study, dedicated field surveys were conducted in Sri Lanka to collect poorly studied pleurostict scarab chafers (Coleoptera: Scarabaeidae), particularly the species-rich and highly endemic Sericini chafers, and to study their biodiversity patterns. This study includes six independent chapters focus on taxonomic revisions, species delimitation analyses, the study of morphospace variation at different taxonomic scales and in different ecochorological scales, and of spatiotemporal turnover across localities and different habitats. In outcome of the study, several new species of the Sericini chafers were described.

Phytophagous scarab beetles - the study group

Beetles (Coleoptera) is the largest of all orders on the earth and comprise about 400,000 species. They constitute almost 40% of described insects and can be considered as one of the most successful animals distributed in almost every terrestrial natural habitat around the world (Crowson, 1981), with a huge variety of living habits and various locomotion modes (Carpenter, 1899; Chapman, 1998). Approximately 90% of the lineages in Coleoptera emerged in the Mesozoic, especially during the Jurassic–Cretaceous period. At the same time, the tremendous success of the angiosperms (flowering plants) replacing rapidly the dominating gymnosperms had dramatic environmental effects and led to an autocatalytic soil revolution which impacted not only the interaction between phytophagous insects and related plant groups but also for most soil living insects (e.g., litter revolution; see Ahrens et al., 2014).

Phytophagous insects, which feed on various parts of plants, including roots, stems, leaves, flowers, and fruits, either as larvae or as adults or in both stages, constitute more than one quarter of all known animal species (Mitter et al., 1988). Phytophagous scarabs are among the largest phytophagous beetle lineages, as a very diverse group of some 30,000 described species of beetles (Scholtz & Grebennikov, 2005) which includes more than two thirds of all species in the superfamily Scarabaeoidea. Phytophagous scarab chafers represent as a

monophyletic clade (Ahrens et al., 2014; McKenna et al., 2019) which is referred to as "pleurostict chafers" or pleurosticts (Erichson, 1847; Ritcher, 1958; Ahrens et al., 2014). Pleurosticts are usually subdivided into four major subfamilies including: Dynastinae, Rutelinae, Melolonthinae (cock chafers), and Cetoniinae (rose chafers), plus several other small groups (Smith, 2006). Most chafer species of Dynastinae, Rutelinae, Melolonthinae are highly polyphagous, feeding on a wide range of plant taxa with the adults generally feeding on leaves, while their larvae primarily feed on soil humus, living roots. In contrast to that, Cetoniinae, but also a few Rutelinae and Melolonthinae feed on flowers or pollen, their larvae on decaying wood and humus (Figure 1.1) (Ritcher, 1958; Ahrens et al., 2014).



Figure 1.1. Pleurostict chafers in the field. Most species are highly polyphagous, generally feeding on leaves, flowers or pollen of a wide range of plants (Photos: J. Eberle).

The present studies focused on the three, principally herbivorous subfamilies (Dynastinae, Rutelinae, Melolonthinae) which are all in majority active at night and can be collected by light traps (Ahrens et al., 2007; García-Lopez et al., 2013; Eberle et al., 2014, 2016, 2017; Šípek et al., 2016). Pleurostict chafers, particularly Sericini chafers (Figure 1.2) can be considered as suitable model organisms because of many aspects: 1) their extreme diversity, especially in tropical forests; 2) their strongly differentiated male genitalia, which allows clear species diagnoses based on morphology, and especially genital morphology (Dalstein et al., 2019; Lukic et al., 2021); 3) their high regional endemism (Ahrens, 2004). Numerous recent studies from the host lab (e.g., Fabrizi & Ahrens, 2014, 2018, 2019; Liu et al., 2014a-c, 2015, 2016, 2017a,b, 2019; Ahrens et al., 2014a-c; Ahrens & Fabrizi, 2016; Rana et al. 2017; Shrestha et al. 2012; Sreedevi et al. 2018, 2019) have discovered an enormous amount of new species from Asian biodiversity hotspots and exhibited high levels of endemism. These

have improved our knowledge of the distribution of many species and opened up the possibility to investigate more in detail their macroecology and factors that determine their diversity under the influence of the species relationships in their natural assemblages.



Figure 1.2. Sericini collected during field work: Left side: *Maladera* sp., female; right side: *Selaserica* sp. Sericini species are subject of all chapters of this thesis (Photos: J. Eberle).

The causes for the high diversity of pleurostict chafers are yet poorly understood (Ahrens et al., 2014; Eberle et al., 2014). Since they rapidly diversified with the rise of angiosperms during the Late Cretaceous – Early Paleogene, one hypothesis for their great species diversity is explained by insect-host plant co-diversification (Ehrlich & Raven, 1964; Mitter et al., 1991; Farrell, 1998). Specifically, increased differentiation among populations by more patchily distributed host resources (niches, new plants) might cause increased speciation (Janz et al., 2006). However, since many pleurosticts being polyphagous and not host specific (e.g., *Popilia japonica* (Rutelinae) is known to feed on 435 plant species out of 95 families; Fleming, 1972; Lessio et al., 2021), the “insect-host plant co-diversification” cannot be the right hypothesis to explain their diversity. Thus, alternative explanations are needed to explain their successful diversification (Eberle et al., 2014).

Sri Lanka - study area and world biodiversity hotspot

Since Darwin’s (1859) time islands have provided natural laboratories for the study of evolution, speciation and biodiversity (Veron et al., 2019). Sri Lanka is a tropical island country which is part of the same shallow continental shelf as India, and separated by an inlet of the Bay of Bengal known as the Palk Strait

(Pathirana, 1980). From biogeographic point of view, Sri Lanka has always been connected to the Indian subcontinent that was part of Gondwana (Figure 1.3). Since the Pliocene, Sri Lanka's geographic position has been similar to today. Periodic low sea levels in the Pleistocene generated from time to time land connections to India (Cooray, 1984) and facilitated a two-way dispersal of fauna across the Palk Strait in repeated waves.

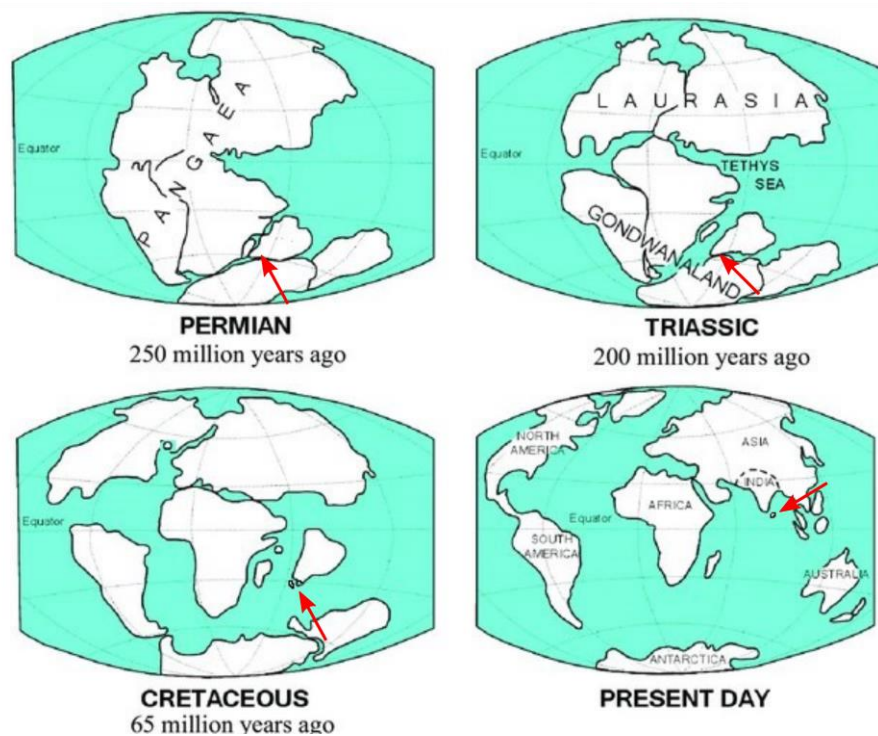


Figure 1.3. The geological history of India and Sri Lanka (red arrow) in relation to plate tectonics. Sri Lanka has always been part of the Indian subcontinent (modified from Dittus, 2017).

Wallace (1876) considered Sri Lanka, together with South India, as a distinct sub-region of the Oriental region, thereby recognizing the distinction of its biota from that of the rest of India. Later, Western Ghats together with Sri Lanka have been identified as a biodiversity hotspot, which represents a 0.7% (2180 species) of global endemic plants and 1.3% (355 species) of global endemic vertebrates (Myers et al., 2000). Especially the perhumid South-West Sri Lanka can be considered as a refugium (species survived when the climate was unsuitable in the surrounding matrix and eventually expanded their ranges in favourable climates) on account of its extraordinary endemism (Ashton, 2014; Gunatilleke, 2017; Ranasinghe & Benjamin, 2018; Ellepola et al., 2022). Central highlands in Sri Lanka were also recognized as endemic spots (Meegaskumbura & Manamendra-

Arachchi, 2005; Benjamin & Kanesharatnam, 2016; Bopearachchi & Benjamin, 2021). However, the area above 500m contour covers only ca 9% of the total area of the island (Wickramagamage, 2017). The combinations of the varied climate, and the diverse topography have created a variety of ecosystems that harbour a wide range of species and makes it a suitable study area to investigate the effect of various ecoclimatic parameters in insect assemblage composition.

Beetle fauna exploration in Sri Lanka

The insect fauna of Sri Lanka is exceptionally rich representing 53% of the total species diversity of the island (Wijesekara & Wijesinghe, 2003; Dangalle et al., 2014). According to Bambaradeniya et al., (2006) 3,033 species of Coleoptera belonging to 50 families were recorded from Sri Lanka so far, representing thus the largest animal group in the island. However, many invertebrates including beetles have not received much scientific attention. The exploration of the Sri Lankan chafer fauna and descriptions of species is relatively limited during the past few decades (Gunawardena & Gunatilake, 1993; Mayadunnage et al., 2007; Dangalle et al., 2011a,b, 2012a,b, 2014; 2017, 2018; Kudavidanage and Lekamge, 2012; Wijekoon et al., 2012; Thotagamuwa et al., 2016, 2019; Hewavithana et al., 2016; Abeywardhana et al., 2020; 2021a,b; Frolov & Akhmetova 2021). Fabrizi & Ahrens (2014) have done an extensive taxonomic and biogeographic study on Sericini chafers (Coleoptera: Scarabaeidae) from Sri Lanka based on collections preserved in numerous European and North American museums as well as in numerous private collections which resulted in 77 known species (76 endemics).

Overview on research question and aims

All studies related to biodiversity rely on an accurate delimitation of species which is also crucial for a stable taxonomy. Therefore, beside determining species based on morphological features, such as male genital structures, I used DNA sequences to infer independently species entities and to build a first DNA barcode reference library for the fauna. This way, I was able to explore ecological patterns not only in the traditional way, based on morphology, but also based on state-of-the-art DNA-based species delimitation methods.

My doctoral research work addressed the below shortly explained research questions. The thesis consisted with six independent chapters covering species delimitation and DNA barcoding, taxonomy, morphometrics, and synecology. The present study contributes to a better understanding of megadiverse phytophagous

scarab evolutionary biology on several levels, from the delimitation of species, as its results translate into conclusions of synecological studies, the description of new species, morphospace pattern and exploration of factors determining assemblage composition exemplified by phytophagous scarab beetles in Sri Lanka.

DNA-based species delimitation has become increasingly popular for such biodiversity assessments. While results of *COI* barcoding have been so far mainly compared with morphospecies entities, the congruence of the outcome of different DNA-based species delimitations has only rarely been analysed in detail. A detailed case study was performed using DNA barcode data along with a morphospecies approach and explored how well *COI* barcode data reflects morphological species entities and thus its utility for accelerated species inventorization. The chapter 3 focused on the investigation of the match of morphospecies with the entities (MOTUs) inferred by commonly used species delimitation algorithms (de novo species delimitation techniques including both tree-based (mPTP, bPTP, mlPTP) and distance-based methods (AGBD, TCS, ASAP)) based on a single gene fragment, i.e., *COI* sequences) and to investigate how well these resulting MOTUs reflected species entities in a megadiverse chafer group. So the study focused to investigate the performance of *COI* barcode data, under a multi-specimen sampling within different geographic context, since *COI* barcodes are widely used as a proxy for species taxonomy and for ecological monitoring. Such empirical focused tests continue to be necessary to further develop the understanding of frequently employed taxonomic markers and methods.

The chapter 4 focused to explore how contrasting results of different species delimitations translate into conclusions of synecological studies, exemplified by assemblages of phytophagous scarab beetles in Sri Lanka from different elevations and forest types. Further, to investigate species estimates based on complete assemblages and on cumulated species inventories inferred from individually analyzed subclades and to analyze patterns of assemblage similarity across different spatial scales with reference to morphospecies and haplotypes. To bypass some of these difficulties of incongruence with morphospecies or with the accurate species delimitation, particularly with mtDNA data and single marker data (e.g., *COI*), the use of haplotype data alone have been proposed as an unbiased and even more objective measure for biodiversity. Therefore, the study also focused to observe the use of haplotypes in compositional comparisons within genetically highly diverse populations in tropics. At the same time, the study aimed to build a phylogenetic tree based on *COI* barcode data for Sri

Lankan pleurostict scarab chafer assemblages using multiple specimens per species in different geographic sites.

Many invertebrates including beetles have not received much scientific attention in Sri Lanka, a part of the world's biodiversity hotspots. The exploration of the Sri Lankan chafer fauna and descriptions of species is relatively limited. The chapter 5 and 6 focused to describe new species of the Sericini chafers with their illustrations and distribution maps in Sri Lanka. Further, to report new locality records for previously known species and to update the identification key to the *Maladera fistulosa* group, due to addition of new species. These two chapters were updating the results of a previous monograph of Sericini of the Sri Lanka (Fabrizi & Ahrens, 2014).

Body size and shape variation (i.e., morphospace) are assumed to reflect differences in the species ecology and behaviour. However, there have been few studies on this to date, and these focused on large-scale spatial patterns of taxonomic richness vs morphological diversity, with only sparse reference to local phenomena. The chapter 7 focused to investigate the morphospace, morphological disparity, and species diversity for three major levels of chorological and landscape partition from regional to local scale, represented by forest types, elevation zones, and collection sites. Further, the study attempted to quantify the effect of direct competition among species by investigating local scale vs. higher spatial scale patterns of the assemblages.

The chapter 8 focused to investigate the patterns of diversity and turnover of tropical pleurostict chafers in Sri Lanka across different forest types, elevation zones, localities, and habitats and to examine which spatial component determines the assemblage composition, and at which extent. Further the study aimed to assess the influence of lineage membership and body size in shaping the species composition at different spatial scales, and to estimate association between qualitative species composition similarity and geographic distances. This way, the study expected to elucidate the dynamics of community assembly and differentiation and to get insight to explain the high species richness and local endemism in tropical chafers.

References

- Abeywardhana, D.L., Dangalle, C.D., Nugaliyadde, A., & Mallawarachchi, Y.W. (2020). Selecting the most suitable classification algorithm for tiger beetle identification using morphometric data and habitat data, *Proceedings of the Annual Research Symposium*, 2020, University of Colombo, 41
- Abeywardhana, L., Mallawarachchi, Y., & Dangalle, C.D. (2021a). The arboreal tiger beetles (Coleoptera: Cicindelidae) of Sri Lanka recorded from recent investigations. *Zootaxa*, 5068(3), 378–398.
- Abeywardhana, D.L., Dangalle, C.D., & Mallawarachchi, Y.W. (2021b). Arboreal Tiger Beetles Recorded from Lowland Crop Cultivations in Sri Lanka, *The Journal of Agricultural Sciences - Sri Lanka*, 16, 1, 135–142.
- Ahrens, D. (2004). Monographie der Sericini des Himalaya (Coleoptera, Scarabaeidae). Dissertation.de - Verlag im Internet GmbH, Berlin, 534pp.
- Ahrens, D., Monaghan, M.T. & Vogler, A.P. (2007). DNA-based taxonomy for associating adults and larvae in multi-species assemblages of chafers (Coleoptera: Scarabaeidae). *Molecular Phylogenetics and Evolution*, 44, 436–449.
- Ahrens, D., Schwarzer, J., & Vogler, A.P. (2014). The evolution of scarab beetles tracks the sequential rise of angiosperms and mammals. *Proceedings of the Royal Society B*, 281, 20141470.
- Ahrens, D., Liu, W.G., Fabrizi, S., Bai, M., & Yang, X.K., (2014a). A taxonomic review of the *Neoserica* (sensu lato) *abnormis* group (Coleoptera: Scarabaeidae: Sericini). *ZooKeys*, 439, 28–82.
- Ahrens, D. Liu, W.G., Fabrizi, S., Bai, M., & Yang, X.K. (2014b). A taxonomic review of the *Neoserica* (sensu lato) *septemlamellata* group (Coleoptera: Scarabaeidae: Sericini). *ZooKeys*, 402, 76-102.
- Ahrens, D., Liu, W.G., Fabrizi, S., Bai, M., & Yang, X.K. (2014c). A revision of the species of the *Neoserica* (sensu lato) *vulpes* group (Coleoptera: Scarabaeidae: Sericini). *Journal of Natural History*, 49 (17-18), 1073–1130.
- Ahrens, D. & Fabrizi, S. (2016). A monograph of the Sericini of India (Coleoptera: Scarabaeidae). *Bonn Zoological Bulletin*, 65, 1–355.
- Ashton, P.S. (2014). *On the forests of tropical Asia: lest the memory fade*. 670 pp. Royal Botanic Gardens, Kew and Arnold Arboretum of Harvard University, USA.
- Bambaradeniya, C.N.B. (2006). The Fauna of Sri Lanka: Status of Taxonomy, Research, and Conservation. Amazon.com. Google books. Retrieved 23 January 2022.
- Baguette, F., Harryba, S., Baboorun, T., Adam, P., Senterre, B. (2022).

- Characterization and evolution of the lowland tropical rain forest of the smallest oceanic Gondwana fragments, with implications for restoration and invasion ecology, *Forest Ecology and Management*, 504,
- Beck, J. & Kitching, I.J. (2007). Estimating regional species richness of tropical insects from museum data: a comparison of a geography-based and sample-based methods. *Journal of Applied Ecology*, 44, 672–681.
- Beck, J., Kitching, I.J., & Haxaire, J. (2007). The latitudinal distribution of Spingid species richness in continental Southeast Asia: what causes the biodiversity 'hotspot' in northern Thailand? *The Raffles Bulletin of Zoology* ; 55(1), 179–185.
- Beck, J., Ballesteros-Mejia, L., Buchmann, C.M., Dengler, J., Fritz, S.A., Gruber, B., Hof, C., Jansen, F., Knapp, S., Krefl, H., Schneider, A.K., Winter, M., & Dormann, C.F. (2012). What's on the horizon for macroecology? *Ecography*, 35, 673–683.
- Benjamin, S.P., & Kanesharatnam, N. (2016). Description of three new species of the tropical Asian jumping spider genus *Onomastus* Simon, 1900 from high altitude cloud forests of Sri Lanka (Araneae: Salticidae). *Zootaxa*, 9, 4205(5).
- Bopearachchi, D.P., & Benjamin, S.P. (2021). Phylogenetic placement of *Flacillula* Strand, 1932 with seven new species from Sri Lanka (Araneae: Salticidae). *Journal of Zoological Systematics and Evolutionary Research*, 59, 1255–1272.
- Buckley, L.B., & Jetz, W. (2007). Environmental and historical constraints on global patterns of amphibian richness. *Proceedings of the Royal Society B*, 274, 1167–1173.
- Carpenter, G.H. (1899). *Insects, their structure and life*. J.M. Dent & Co., London
- Chapman, R.F. (1998). *The insects: structure and function*, 4th edn. Cambridge University Press, Cambridge
- Corlett, R.T., & Primack, R.B. (2011). *Tropical Rain Forests: An Ecological and Biogeographical Comparison* (2nd ed.). Hoboken, NJ: Wiley-Blackwell. <https://doi.org/10.1002/9781444392296>
- Cooray, P.G. (1984). *The Geology of Sri Lanka (Ceylon)*. National Museums of Sri Lanka Publication, Colombo, pp. 340.
- Crowson, R.A. (1981). *The biology of the Coleoptera*, 1st ed, Elsevier. 1–802, Academic Press. <https://doi.org/10.1016/B978-0-12-196050-6.50024-5>
- Currie, D.J. (1991). Energy and Large-Scale Patterns of Animal- and Plant-Species Richness. *The American Naturalist* 137, 27–49.
- Dalstein, V., Eberle, J., Fabrizi, S., Eitzbauer, C., & Ahrens, D. (2019). COI-based species delimitation in Indochinese Tetraserica chafers reveal hybridisation despite strong divergence in male copulation organs. *Organisms Diversity and Evolution*, 19, 277–286.

- Dangalle, C., Pallewatta, N., & Vogler, A. (2011a). The current occurrence, habitat and historical change in the distributional range of an endemic tiger beetle species *Cicindela (Ifasina) willeyi* Horn (Coleoptera: Cicindelidae) of Sri Lanka. *Journal of Threatened Taxa*, 3(2), 1493–1505.
- Dangalle, C., Pallewatta, N., & Vogler, A. (2011b). The occurrence of the endemic tiger beetle *Cicindela (Ifasina) waterhousei* in Bopath Ella, Ratnapura, Sri Lanka. *Journal of the National Science Foundation of Sri Lanka*, 39(2), 163–168.
- Dangalle, C.D., Pallewatta, N., & Vogler, A.P. (2012a). Habitat specificity of tiger beetle species (Coleoptera, Cicindelidae) of Sri Lanka. *Cicindela*, 44(1), 1–32.
- Dangalle, C., Pallewatta, N., & Vogler, A. (2012b). Tiger beetles (Coleoptera: Cicindelidae) of ancient reservoir ecosystems of Sri Lanka. *Journal of Threatened Taxa*, 4(4), 2490–2498.
- Dangalle, C. D., Pallewatta, N., & Vogler, A. P. (2014). Inferring population history of tiger beetle species of Sri Lanka using mitochondrial DNA sequences. *Ceylon Journal of Science (Bio. Sci.)*, 43(2), 47–63.
- Dangalle, C.D., Dangalle, N.K., & Pallewatta, N. (2017). Historical and Current records on the Tiger Beetle, *Calomera angulata*, Fabricius of Sri Lanka. *Journal of Biology and Nature*, 7, 91–99.
- Dangalle, C.D. (2018). The forgotten tigers: The arboreal tiger beetles of Sri Lanka. *Journal of the National Science Foundation of Sri Lanka*, 46. doi: 10.4038/jnsfsr.v46i3.8477
- Daru, B.H., Farooq, H., Antonelli, A., & Faurby, S. (2020). Endemism patterns are scale dependent. *Nature Communications*, 11, 2115.
- Darwin, C. (1859). *On the Origin of Species by Means of Natural Selection*. London: John Murray, London, p. 502. doi: 10.1016/S0262-4079(09)60380-8.
- Decaëns, T. (2010). Macroecological patterns in soil communities. *Global Ecology and Biogeography*, 19, 287–302.
- Di Marco, M., Ferrier, S., Harwood, T.D., et al. (2019). Wilderness areas halve the extinction risk of terrestrial biodiversity. *Nature*, 573, 582–85.
- Dittus, W.P.J. (2017). The biogeography and ecology of Sri Lankan mammals point to conservation priorities, *Ceylon Journal of Science*, 46 (Special Issue), 33–64.
- Eberle, J., Myburgh, R., & Ahrens, D. (2014). The Evolution of morphospace in phytophagous scarab chafers: no competition - no divergence? *PLoS ONE* 9(5), e98536.
- Eberle, J., Fabrizi, S., Lago, P., & Ahrens, D. (2016). A historical biogeography of megadiverse Sericini – another story out of Africa? *Cladistics*, 33, 183–197.

- Eberle, J., Rödder, D., Beckett, M., & Ahrens, D. (2017). Landscape genetics indicate recently increased habitat fragmentation in African forest-associated chafers. *Global Change Biology*, 23, 1988–2004.
- Echevarría Ramos, M., & Hulshof, C.M. (2019). Using digitized museum collections to understand the effects of habitat on wing coloration in the Puerto Rican monarch. *Biotropica*, 51, 477–483.
- Economo, E.P., Klimov, P., Sarnat, E.M., Guénard, B., Weiser, M.D., Lecroq, B., & Knowles, L.L. (2015). Global phylogenetic structure of the hyperdiverse ant genus *Pheidole* reveals the repeated evolution of macroecological patterns, *Proceedings of the Royal Society B*, <http://doi.org/10.1098/rspb.2014.1416>
- Ehrlich, P. & Raven, P. (1964). Butterflies and plants: A study in coevolution. *Evolution*, 18, 586–608.
- Ellepola, G., Pie, M.R., Pethiyagoda, R. et al. (2022). The role of climate and islands in species diversification and reproductive-mode evolution of Old World tree frogs. *Communication Biology*, 5, 347. <https://doi.org/10.1038/s42003-022-03292-1>
- Erichson, W.F. (1847). *Naturgeschichte der Insecten Deutschlands. Erste Abtheilung. Coleoptera. vol. 3, Li.* Berlin: Nicolaische Buchhandlung.
- Erwin, T.L. (1982). Tropical forests: their richness in Coleoptera and other arthropod species. *Coleopta Bulletin*, 36, 74–75.
- Fabrizi, S. & Ahrens, D. (2014). A Monograph of the Sericini of Sri Lanka (Coleoptera: Scarabaeidae). *Bonn Zoological Bulletin Supplements*, 61, 1–124.
- Fabrizi, S. & Ahrens, D. (2018). Two new Gastroserica species from Vietnam (Coleoptera, Scarabaeidae: Sericini). *Entomologische Zeitschrift*, 128, 177–180.
- Fabrizi, S. Dalstein, V., & Ahrens, D. (2019). A monograph on the genus *Tetraserica* from the Indochinese region (Coleoptera, Scarabaeidae, Sericini). *Zookeys*, 837, 1–155.
- Farrell, B.D. (1998). “Inordinate Fondness” explained: Why are there so many beetles? *Science*, 281, 555–559.
- Fleming, W. E. (1972). Biology of the Japanese beetle. *Technical Bulletin*, 1449.
- Frolov, A.V., & Akhmetova, L.A. (2021). Review of the Orphninae (Coleoptera: Scarabaeidae) of Sri Lanka, with description of a new species of genus *Orphnus* Macleay, 1819. *European Journal of Taxonomy*, 767, 40–54.
- Gaston, K.J. (2000). Global patterns in biodiversity. *Nature*, 405, 220–227.
- García-Lopez, A., Mico, E., Murria, C., Galante, E., & Vogler, A.P. (2013). Beta diversity at multiple hierarchical levels: explaining the high diversity of scarab beetles in tropical montane forests. *Journal of Biogeography*, 40, 2134–2145.

- Grytnes, J.A., & Romdal, T.S. (2008). Using museum collections to estimate diversity patterns along geographical gradients. *Folia Geobotanica*, 43(3), 357–369.
- Gunatilleke, N. (2017). Biogeography of Sri Lanka, *Ceylon Journal of Science*, 46 (Special Issue), 1–3
- Gunawardena, N.E. & Gunatilake, R. (1993). Preliminary Studies on a host attractant of the coconut pest *Rhynchophorus Ferrugineus* (Coleoptera), *Journal of the National Science Council of Sri Lanka*, 21(1), 93–101.
- Hewavithana, D.K., Wijesinghe, M.R., Dangalle, C.D., & Dharmarathne, H. A. S. G. (2016). Habitat and dung preferences of scarab beetles of the subfamily Scarabaeinae: a case study in a tropical monsoon forest in Sri Lanka, *International Journal of Tropical Insect Science*, 36, 2, 97–105.
- Holt, B.G., Lessard, J.P., Borregaard, M.K., Fritz, S., Arajo, M.B., Dimitrov, D., Fabre, P.H., Graham, C.H., Graves, G.R., Jonsson, K., Nogués-Bravo, D., Wang, Z., Whittaker, R.J., Fjelds., J. & Rahbek, C. (2013). An update of Wallace’s zoogeographic regions of the world. *Science*, 339, 74–78.
- Hortal, Joaquin , de Bello, Francesco, Alexandre, Jos’e, Diniz-Filho, F., Lewinsohn, T. M., Lobo, J. M. and Ladle, R. J. (2015). Seven shortfalls that beset large-scale knowledge of biodiversity. *Annual Review of Ecology, Evolution, and Systematics*, 46, 523–549.
- Isbell, F., Gonzalez, A., Loreau, M., et al. (2017). Linking the influence and dependence of people on biodiversity across scales. *Nature*, 546, 65–72.
- Janz, N., Nylin, S., & Wahlberg, N. (2006). Diversity begets diversity: host expansions and the diversification of plant-feeding insects. *BMC Evolutionary Biology*, 6, 4. doi: 10.1186/1471-2148-6-4.
- Jetz, W., Thomas, G.H., Joy, J.B., Hartmann, K., & Mooers, A.O. (2012). The global diversity of birds in space and time. *Nature*, 491, 444–448.
- Kemp, J.E., Linder, H.P., & Ellis, A.G. (2017). Beta diversity of herbivorous insects is coupled to high species and phylogenetic turnover of plant communities across short spatial scales in the Cape Floristic Region. *Journal of Biogeography*, 44, 1813–1823.
- Kitching, R.L., Eastwood, R. & Hurley, K. (2001). Butterflies and Wallace’s Line: faunistic patterns and explanatory hypotheses within the south-east Asian butterflies. pp. 269–286. In: Metcalfe, I., Smith, J., Morwood, M., Davidson, I. (eds) *Faunal and Floral Migrations and Evolution in SE Asia-Australasia*. Lisse: A A Balkema Publishers.
- Kudavidanage, E.P., & Lekamge, D. (2012). A provisional checklist of dung beetles (Coleoptera; Scarabaeidae) in Sri Lanka, pp. 438–444. In *The National Red List 2012 of Sri Lanka; Conservation Status of the Fauna and Flora* (edited by D. K.Weerakoon and S.Wijesundara). Ministry of Environment, Colombo, Sri Lanka.

- Lessio, F., Pisa, C.G., Luca, P., Ciampitti, M., Cavagna, B., & Alma, A. (2021). An immunomarking method to investigate the flight distance of the Japanese beetle. *Entomologia Generalis*, 10.1127/entomologia/2021/1117.
- Liu, W.G., Fabrizi, S., Bai, M., Yang, X.K., & Ahrens, D. (2014a). A taxonomic revision of the *Neoserica* (s.l.) *pilosula* group (Coleoptera, Scarabaeidae, Sericini). *Zookeys*, 440, 89–113.
- Liu, W.G., Fabrizi, S., Bai, M., Yang, X.K., & Ahrens, D. (2014b). A taxonomic revision of the *Neoserica* (sensu lato) *calva* group (Coleoptera, Scarabaeidae, Sericini). *ZooKeys*, 448, 47–81.
- Liu, W.G., Fabrizi, S., Bai, M., Yang, X.K., & Ahrens, D. (2014c). A review of the *Tetraserica* species of China (Coleoptera, Scarabaeidae, Sericini). *ZooKeys*, 448, 83–121.
- Liu, W.G., Bai, M., Yang, X.K., & Ahrens, D. (2015). New species and records of the *Neoserica* (sensu stricto) group (Coleoptera, Scarabaeidae, Sericini). *Journal of Natural History*, 49 (39–40), 2379–2395.
- Liu, W.G., Fabrizi, S., Bai, M., Yang, X.K., & Ahrens, D. (2016). A taxonomic revision of *Neoserica* (sensu lato): the species groups *N. lubrica*, *N. obscura*, and *N. silvestris* (Coleoptera, Scarabaeidae, Sericini). *Zookeys*, 635, 123–160.
- Liu, W.G., Bai, M., Yang, X.K., & Ahrens, D. (2017a). New species and records of *Lasioserica* and *Gynaecoserica* from China (Coleoptera, Scarabaeidae, Sericini). *Bonn Zoological Bulletin*, 66(1), 29–36.
- Liu, W.G., Fabrizi, S., Bai, M., Yang, X.K., & Ahrens, D. (2017b). New species of *Nipponoserica* and *Paraserica* from China (Coleoptera: Scarabaeidae: Sericini). *ZooKeys*, 721, 65–91.
- Liu, W.G., Fabrizi, S., Bai, M., Yang, X.K., & Ahrens, D. (2019). A taxonomic revision of Chinese *Neoserica* (sensu lato): final part (Coleoptera: Scarabaeidae: Sericini). *Bonn Zoological Bulletin Supplement*, 64, 1–71.
- Lukic, D., Eberle, J., Thormann, J., Holzschuh, C., & Ahrens, D. (2021). Excluding spatial sampling bias does not eliminate over-splitting in DNA-based species delimitation analyses. *Ecology and Evolution*, 11, 10327–10337.
- Mayadunnage, S., Wijayagunasekara, H.N.P., Hemachandra, K.S., & Nugaliyadde, L. (2007). Predatory Coccinellids (Coleoptera: Coccinellidae) of Vegetable Insect Pests: A survey in Mid Country of Sri Lanka, *Tropical Agricultural Research*, 19, 69–77.
- McKenna, D.D. et al. (2019). The evolution and genomic basis of beetle diversity. *Proceedings of the National Academy of Sciences*, 116, 24729–24737.
- Meegaskumbura, M., & Manamendra-Arachchi, K. (2005). Description of eight new species of shrub frogs (Ranidae: Rhacophorinae: Philautus) from Sri Lanka. *The Raffles Bulletin of Zoology*, 12, 305–338.

- Mitter, C., Farrell, B., & Wiegmann, B., (1988). The phylogenetic study of adaptive zones: has phytophagy promoted insect diversification? *American Naturalist*, 132, 107–128.
- Mitter, C., Farrell, B., & Futuyma, D.J. (1991). Phylogenetic Studies of Insect-Plant Interactions: Insights into the Genesis of Diverstiy. *Trends in Ecology & Evolution*, 6, 290–293.
- Myers, N., Mittermeier, R., Mittermeier, C., da Fonseca, G. A. B., & Kent, J. (2000). Biodiversity hotspots for conservation priorities. *Nature*, 403, 853–858.
- Nielsen, U.N. (2019). Soil Fauna Assemblages. Global to local scales. Cambridge University Press, Cambridge, New York, Port Melbourne, 365pp.
- Oliver, I., & Beattie, A.J. (1996). Invertebrate morphospecies assurogates for species: a case study. *Conservation Biology*, 10, 99–109.
- Pathirana, H.D.N.C. (1980). Geology of Sri Lanka in relation to Plate Tectonics; *Journal of the National Science Council of Sri Lanka* 8(1), 75–85.
- Pillay, R., Venter, M., Aragon-Osejo, J., González-del-Pliego, P., Hansen, A.J., Watson, J.E.M., & Venter, O. (2022). *Frontiers in Ecology and the Environment*, 20 (1), 10– 15.
- Rana, P.S., Fabrizi, S., Ahrens, D. (2017). New records of Sericini and a new *Serica* (s. str.) species from Nepal (Coleoptera: Scarabaeidae: Sericini). *Entomologische Zeitschrift*, 127, 144–148.
- Ranasinghe U.G.S.L., & Benjamin, S.P. (2018). Taxonomic descriptions of nine new species of the goblin spider genera *Cavisternum*, *Grymeus*, *Ischnothyreus*, *Opopaea*, *Pelycinus* and *Silhouettella* (Araneae, Oonopidae) from Sri Lanka. *Evolutionary Systematics*, 2, 65–80.
- Ritcher, P.O. (1958). Biology of Scarabaeidae. *Annual Review of Entomology*, 3, 311–334.
- Santos, A.M.C. & Quicke, D. (2011). Large-scale diversity patterns of parasitoid insects. *Insect Science*, 14, 371–382.
- Scholtz, C.H., & Grebennikov, V.V. (2005). Scarabaeoidea Latreille, 1802. In: Rolf Beutel RABL, Coleoptera, beetles: Morphology and systematics (Archostemata, Adephaga, Myxophaga, Polyphaga partim), Band 1. Walter de Gruyter. p. 567.
- Shrestha, J., Eberle, J., & Ahrens, D. (2012). Further data on the distribution of Himalayan Sericini from the collection of Naturel History Museum Erfurt (Insecta: Coleoptera: Scarabaeidae) with description of a new *Xenoserica* from West-Nepal. *Vernate*, 31,379-386.
- Šípek, P., Fabrizi, S., Eberle, J., & Ahrens, D. (2016). A molecular phylogeny of rose chafers (Coleoptera: Scarabaeidae: Cetoniinae) reveals a complex and concerted morphological evolution related to their flight mode. *Molecular Phylogenetics and Evolution*, 101, 163–175.

- Smith, A.B.T. (2006). A Review of the Family-group Names for the Superfamily Scarabaeoidea (Coleoptera) with Corrections to Nomenclature and a Current Classification. *The Coleopterists Society Monographs*, 5, 144–204.
- Sreedevi, K., Speer J., Fabrizi S., & Ahrens D. (2018). New records and species of Sericini from Indian subcontinent (Coleoptera: Scarabaeidae). *ZooKeys*, 772, 97–128.
- Sreedevi, K., Ranasinghe S., Fabrizi S., & Ahrens D. (2019). New species and records of Sericini scarab beetles from the Indian subcontinent (Coleoptera, Scarabaeidae) II. *European Journal of Taxonomy*, 567, 1–26.
- Stork, N. E., McBroom, J, Gely, C., & Hamilton, A.J. (2015). New approaches narrow global species estimates for beetles, insects, and terrestrial arthropods. *Proceedings of the National Academy of Sciences*, 112, 201502408.
- Thotagamuwa, A., Dangalle, C.D., Pallewatta, N. & Lokupitiya, E. (2016). Tiger beetles (Coleoptera: Cicindelidae) of Sri Lanka's coastal zone: present distribution and diversity. *Sri Lanka Journal of Marine Environmental Sciences*, 1, 33–43.
- Thotagamuwa, A., Lokupitiya, E, Lokupitiya R.S., Dangalle, C.D., Pallewatta, N. & Dayananda, K.S. (2019). The effects of incident microclimatic and soil parameters on the population sizes of selected tiger beetle species in Sri Lanka, *International Journal of Tropical Insect Science*, <https://doi.org/10.1007/s42690-019-00058-x>
- Veron, S., Haevermans, T., Govaerts, R. *et al.* (2019). Distribution and relative age of endemism across islands worldwide. *Scientific Reports*, 9, 11693 <https://doi.org/10.1038/s41598-019-47951-6>
- Wallace, A. R. (1876). The geographical distribution of animals, with a study of the relations of living and extinct faunas as elucidating the past changes of the earth's surface. Harper and Brothers, New York.
- Wickramagamage, P. (2017). Role of human agency in the transformation of the biogeography of Sri Lanka, *Ceylon Journal of Science*, 46 (Special Issue) 19–31.
- Wijekoon, W. M.C.D., Wegiriya, H.C.E., & Bogahawatta, C.N.L. (2012). Regional diversity of fireflies of the subfamily Luciolinae (Coleoptera: Lampyridae) in Sri Lanka. *Lampyrid*, 2, 138–141.
- Wijesekara, A. & Wijesinghe, D.P. (2003). History of insect collection and a review of insect diversity in Sri Lanka. *Ceylon Journal of Science (Biological Science)*, 31, 43–59.

Chapter 2

Field expeditions and sampling

2.1. Study area

Sri Lanka has a total area of 65,610 km² with a length of 432 km (268 miles) and a maximum width of 224 km (139 miles). It is the twenty-fifth largest island in the world by area, with latitudes ranging from 5°55'N to 9°51'N and longitudes from 79°41'E to 81°53'E, which is near-equator position (Erdelen, 1988). Two principle monsoon rainfall seasons; southwest monsoon from May to September and northeast monsoon from December to February and two inter-monsoon rainfall seasons; first inter-monsoon from March to April and second inter-monsoon from October to November has identified (Domroes, 1974). The variation of rainfall is mainly affected by these monsoonal winds, the southwest monsoon brings moist air from the Indian Ocean and provides rainfall to the southwestern part and the Central Highland slopes; the northeast monsoon brings moist air from the Bay of Bengal and causes rainfall across the whole country; distinct inter-monsoonal periods receive conventional rains and cyclones. Based on annual precipitation, three distinct tropical climatic zones are distinguished as; the 'wet', 'dry' and 'intermediate zones' (Puvaneswaran, Smithson, 1993). These regions receive more than 2,500 mm; between 1,750 to 2,500 m and less than 1,750 mm of rain respectively. In addition, two small areas at the extreme northwest and southeast of the country have a very dry climate and are arid zones (Wijesinghe et al., 1993). Average annual temperature is ranging from 28 °C to 31 °C in the lowlands and decreases (16°C) rapidly in the highlands. The island's elevation ranges from the sea level to over 2,500m, and can also be divided as lowland (<1000 m), midland (1000-1500 m) and highland (1500-2500 m) on the basis of elevation.

2.2. Sampling methods and sampling design

Four field expeditions were conducted during 2019 and 2020 (in February-March/ October-November and June-July/ November-December, respectively) in Sri Lanka (Figure 2.1). Sampling encompassed 15 localities covering different forest types (lowland wet evergreen, lowland dry evergreen, sub-montane and montane

forest) and altitudinal zones (0-2500m) of Sri Lanka (Figure 2.2). These sampling periods met both rainy and dry seasons in the respective localities.

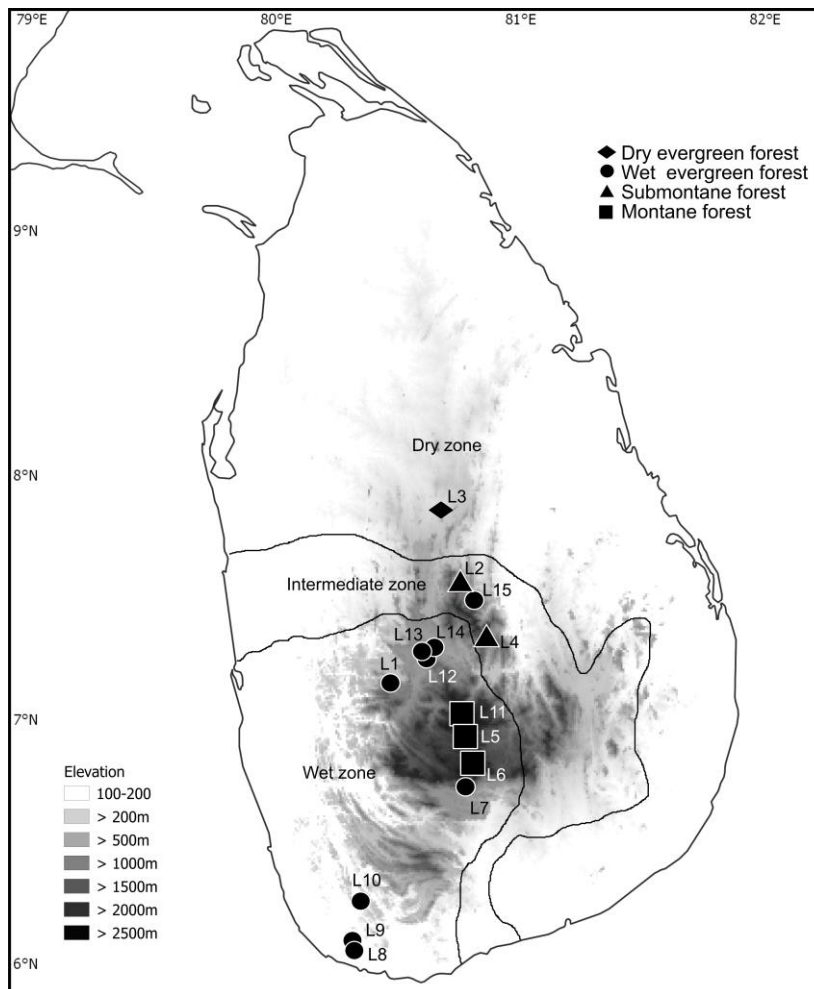


Figure 2.1. Map of Sri Lanka showing sampling sites. L1: Aranayake; L2: Riverston; L3: NIFS Arboretum; L4: Deenston; L5: Nuwara Eliya; L6: Horton Plains; L7: Belihuloya; L8: Hiyare; L9: Kottawa; L10: Kanneliya; L11: Piduruthalagala; L12: Uda Peradeniya; L13: Gannoruwa; L14: Udawattakele; L15: Sera Ella. Symbols represent different forest types.

Mainly three different methods were used to capture beetles; i) UV-light traps, ii) manual collecting from a white sheet being illuminated with UV, blue and green LEDs (LepiLED, © WIF, Dr Gunnar Brehm, Jena, Germany) (Figure 2.3) and iii) some additional specimens were hand-collected during the day (partly by netting).

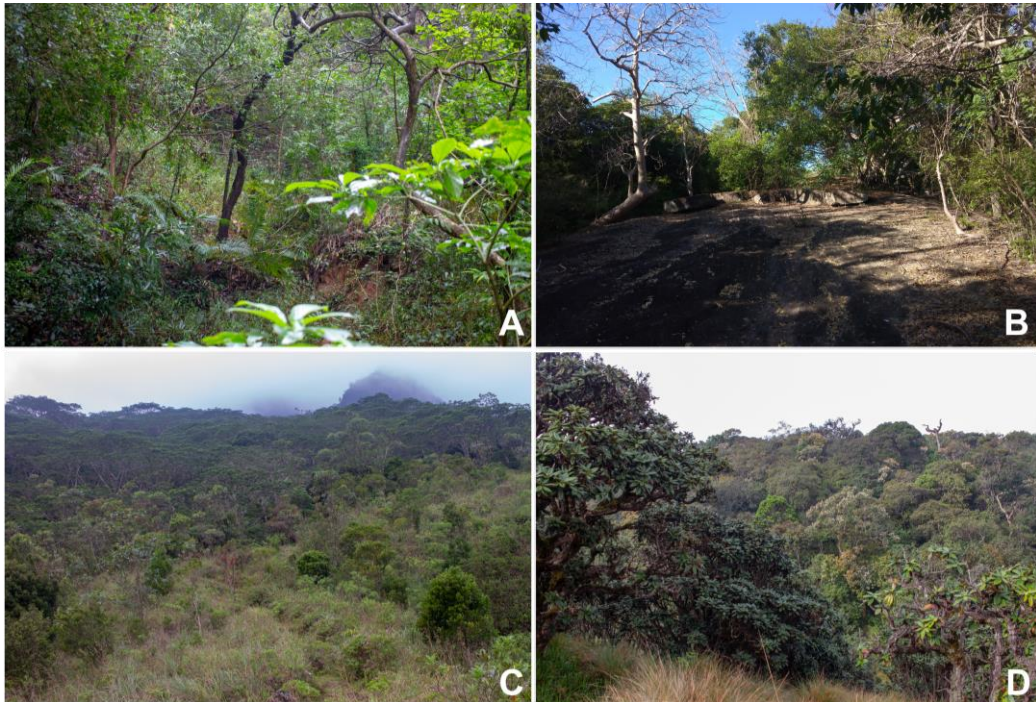


Figure 2.2. Images of sampling habitats represent different forest types; **A.** lowland wet evergreen forest, **B.** lowland dry evergreen forest, **C.** sub-montane, **D.** montane forest.

i) Light traps (Night sampling)

Six UV-light traps were placed in different sites (i.e., habitats) at each locality to collect quantitatively comparable samples that are sufficiently complete to represent the local assemblages. All traps were separated by at least 100 - 500m distance depending on the landscape of the locality in order to not influence each other. The traps were placed at a height of approximately 2 m above the ground and positioned at the same spot for 2–3 consecutive days. Traps were unattended during activity and a timer activated the light from dusk to almost midnight (6 pm to 11 pm). Beetles that were attracted to the light traps were stopped by transparent polystyrene plates (32 cm in width) and fell into a sampling container with preservation liquid (96% ethanol). Specimens were stored and in 96% ethanol for later identification and/or DNA sequencing.

ii) Light sheet (Night sampling)

A white sheet was hanged under the bulb of UV, blue and green LEDs (LepiLED, © WIF, Dr Gunnar Brehm, Jena, Germany). The Scarab beetles were selectively collected from the sheet. This method followed every day from 6.30pm to 11.00pm. The sheet was set towards the forest as much as possible. Target beetles

selectively collected from the sheet and preserve. When light was off other insects fly away for their destinations.



Figure 2.3. Light trap in the field (left). Manual collecting from a white sheet illuminated with UV light in the field (right).

iii) Sweep netting/hand collection (Day sampling)

The net was held with the hoop end and swing the net from side to side (back and forth) in a full 180-degree arc through the ground vegetation. Targeted Scarab beetles collected and preserved. This method performed only during the daytime.

The non-targeted insects preserved and stored (-20C) in the projects' collaborative institute "National Institute of Fundamental Studies, Kandy, Sri Lanka" for future research purposes or to extend the proposed project further.

2.3. Collection and export permits

Permits for sample collection in Sri Lanka obtained through the projects' collaborative institute "National Institute of Fundamental Studies, Kandy, Sri Lanka" (Prof. Suresh Benjamin). Collection permits were issued by the Department of Wildlife Conservation, Sri Lanka (permit no: WL/3/2/61/18), and the Department of Forest Conservation, Sri Lanka (permit no: R&E/RES/NFSRCM/2019-01 & R&E/RES/NFSRCM/ EXTENSION/2020). Further by the Divisional Forest Office, Kandy, Sri Lanka (permit no:

K/G/01/06/03); Galle (M/0/03/2019). However, the current legal framework for biodiversity conservation allowing the export of specimens outside Sri Lanka is very restrictive (Dias et al., 2020). Therefore permit process was taken more time than expected.

References

- Dias, R.K.S., Guénard, B., Akbar, S.A., Economo, E.P., Udayakantha, W.S., & Wachkoo, A.A. (2020). The Ants (Hymenoptera, Formicidae) of Sri Lanka: a taxonomic research summary and updated checklist. *ZooKeys* 967, 1–142.
- Domrös, M. (1974). The agro-climate of Ceylon, Vol. 2. Franz Steiner Verlag. Gmbh Wiesbaden, 5–65.
- Erdelen, W. (1988). Forest ecosystems and nature conservation in Sri Lanka. *Biological Conservation*, 43, 2, 115–135.
- Puvaneswaran, K.M., & Smithson, P.A. (1993). An objective classification of homogeneous rainfall regimes in Sri Lanka. *Theoretical and Applied Climatology*, 48, 133–145.
- Wijesinghe, L.C.A.de S., Gunatilleke, I.A.U.N., Jayawardana, S.D.G., Kotagama, S.W., & Gunatilleke, C.V. (1993). *Biological Conservation in Sri Lanka: A National Status Report*. Colombo: IUCN, Sri Lanka.

Chapter 3

Multiple species delimitation approaches with *COI* barcodes poorly fit each other and morphospecies – an integrative taxonomy case of Sri Lankan Sericini chafers (Coleoptera: Scarabaeidae)

This chapter is published in:

Ranasinghe, U.G.S.L., Eberle, J., Thormann, J., Bohacz, C., Benjamin, S., Ahrens, D., (2022). Multiple species delimitation approaches with COI barcodes poorly fit each other and with morphospecies – an integrative taxonomy case of Sri Lankan Sericini chafers (Coleoptera: Scarabaeidae), *Ecology and Evolution*, 12, e8942. <https://doi.org/10.1002/ece3.8942>

Authors' contributions to the original article:

SR, JE, CB: fieldwork collections; JT, SR: molecular lab work; SR: sequence assembly and alignments, phylogenetic inference, DNA-based species delimitation; SR, DA: writing-original draft; DA, JE, SB, SR: manuscript review and editing.

Abstract

DNA taxonomy including barcoding and metabarcoding is widely used to explore the diversity in biodiversity hotspots. In most of these hotspot areas, chafers are represented by a multitude of species, which are well defined by the complex shape of male genitalia. Here, we explore how well *COI* barcode data reflect morphological species entities and thus their usability for accelerated species inventorization. We conducted dedicated field surveys in Sri Lanka to collect the species-rich and highly endemic Sericini chafers (Coleoptera: Scarabaeidae). Congruence among results of a series of protocols for *de novo* species delimitation and with morphology-based species identifications was investigated. Different delimitation methods, such as the Poisson tree processes (PTP) model, statistical parsimony analysis (TCS), Automatic Barcode Gap Discovery (ABGD), Assemble Species by Automatic Partitioning (ASAP) and Barcode Index Number (BIN) assignments, resulted in different numbers of molecular operational taxonomic units (MOTUs). All methods showed both over-splitting and lumping of morphologically identified species. Only 18 of the observed 45 morphospecies perfectly matched MOTUs from all methods. The congruence of delimitation between MOTUs and morphospecies expressed by the match ratio was low, ranging from 0.57 to 0.67. TCS and multi-rate PTP (mPTP) showed the highest match ratio, while (BIN) assignment resulted in the lowest match ratio and most splitting events. mPTP lumped more species than any other method. Principal Coordinate Analysis (PCoA) on a match ratio-based distance matrix revealed incongruent outcomes of multiple DNA delimitation methods, although applied to the same data. Our results confirm that *COI* barcode data alone is unlikely to correctly delimit all species, in particular, when using only a single delimitation approach. We encourage the integration of various approaches and data, particularly morphology, to validate species boundaries.

Keywords. taxonomic match ratio, barcoding, integrative taxonomy.

3.1 Introduction

Many regions on Earth that are exceptionally rich in endemic species are facing massive habitat loss (Costello et al., 2013). Most of those areas have been identified as ‘biodiversity hotspots’ (Myers et al., 2000). In order to be able to conserve the vast diversity of currently largely unknown species, one necessity is to recognize them (Smith et al., 2005; Costello et al., 2013; Modica et al., 2014). For this purpose, DNA barcoding approaches have been widely used to explore diversity of both flora and fauna, especially in biodiversity hotspots where efficient conservation priorities are imperative (e.g., Hebert et al., 2003a,b; Hebert et al., 2004; Smith et al., 2005; Barber & Boyce, 2006; Lahaye et al., 2008, Kadarusman et al., 2012; Nagy et al., 2012; Geiger et al., 2014; Grosjean et al., 2015; Bezeng et al., 2017; Boissin et al., 2017; Barman et al., 2018; Oberprieler et al., 2018; Jamaluddin et al., 2019). These techniques attempt species delimitation and specimen identification based on a single gene fragment, e.g., from the *COI* gene. The state of the art, advantages and drawbacks, as well as their current usage have been extensively discussed in a number of works (e.g., Vogler & Monaghan, 2007; Leliaert et al., 2014; Luo et al., 2018; Dellicour & Flot, 2018; DeSalle & Goldstein, 2019; Rannala & Yang, 2020). Subsequently, approaches have been employed (metabarcoding), which allow large-scale assessments of biodiversity through environmental DNA (Taberlet et al., 2012; Heyde et al., 2020; Hobern, 2021) in both terrestrial (Holdaway et al., 2017; Fernandes et al., 2018) and aquatic habitats (Leduc et al., 2019). With such metabarcoding approaches it is not only possible to rapidly assess biodiversity, but also to investigate external impacts on poorly studied invertebrate communities in highly diverse ecosystems (Dopheide et al., 2020; Vogler et al., 2021).

However, DNA barcoding also has been critically discussed since its first emergence due to many problems coming particularly from the nature of the used single mtDNA marker gene (Ballard & Whitlock, 2004; Krishnamurthy & Francis, 2012; Eberle et al., 2020). Many empirical studies investigated the robustness of DNA barcoding and the used species delimitation methods, particularly in the context of inherent natural bias of species such as fluctuating effective population size or unbalanced representation of specimen samples (e.g., Esselstyn et al., 2012; Fujisawa & Barraclough, 2013; Ahrens et al., 2016).

While results of *COI* barcoding have been so far mainly compared with morphospecies entities, the congruence of the outcome of different DNA-based species delimitations has only rarely been analyzed in detail. Outcomes have often

been characterized as "different" without quantifying the difference (e.g., Ahrens et al., 2016; Dalstein et al., 2019; Lukic et al., 2021). These differences are explored here in detail, exemplified by a case study of Sri Lankan Sericini chafers.

Sri Lanka, together with Southern Indian Western Ghats, is one of the world's outstanding biodiversity hotspots, harbouring unique and threatened biota (Myers, 2000). So far, only a handful of larger barcoding studies have been conducted on the Indian subcontinent. These include the identification of disease vectors (Tabanid flies: Banerjee et al., 2015; sand flies: Gajapathy et al., 2016; biting midges Culicoides: Harrup et al., 2016; mosquitos: Weeraratne et al., 2018), and also of highly invasive agricultural pests (Fruit fly: Khamis et al., 2012; tea mosquito bugs: Rebijith et al., 2012; Pentatomomorpha bugs: Tembe et al., 2014; Kaur & Sharma, 2016; thrips: Tyagi et al., 2017; fall armyworm: Nanayakkara et al., 2020). Further, barcoding approaches have been used to resolve taxonomic questions in butterflies (Rajpoot et al., 2018; Goonesekera et al., 2019), fishes (Senevirathna & Munasinghe, 2013; Dhaneesh et al., 2015; Lakra et al., 2016; Raja & Perumal, 2017; Ekanayake et al., 2021), frogs (Biju et al., 2014; Meegaskumbura et al., 2015), freshwater crabs (Beenaerts et al., 2010), spiders (Ileperuma Arachchi & Benjamin, 2019; Kanesharatnam & Benjamin, 2019), snakes (Pyron et al., 2013) and snails (Raheem et al., 2017). Concerted and comprehensive initiatives, which coordinate the sampling and data basing efforts, as known from Europe and northern America for example, are yet missing.

For the highly diverse beetles, apart from a few isolated studies that were very limited in taxon sampling (Dangalle et al., 2014; Asha & Sinu, 2020), DNA taxonomy approaches including barcoding have not yet been applied in the Western Ghats hotspot. This is even true for herbivore scarab chafers, of which some species appear to be serious crop pests despite being highly endemic (Ahrens, 2004; Ahrens & Fabrizi, 2016). In the last decade dozens of new herbivore scarab species have been discovered from the subcontinent, and Asia in general (e.g., Fabrizi & Ahrens, 2014; Liu et al., 2014a-c, 2015, 2016; Ahrens et al., 2014a-c; Ahrens & Fabrizi, 2016).

Given the great use of *COI* barcode data for biodiversity assessments (e.g., Arribas et al., 2020, 2021), we were interested in expanding the existing punctual assessments of DNA barcoding (Ahrens et al., 2016; Dalstein et al., 2019; Lukic et al., 2021) and in exploring, how well *COI* barcode data reflect species entities in a understudied tropical hotspot. We chose Sericini chafer beetles (Coleoptera: Scarabaeidae: Melolonthinae) as example study group, because species can be well defined by strongly differentiated male genitalia (e.g., Eberle et al., 2016;

Dalstein et al., 2019). We performed dedicated field surveys in Sri Lanka and investigated the match of morphospecies with the entities inferred by commonly used species delimitation algorithms based on the sequenced *COI* barcode data. Such focused tests continue to be necessary to further develop our understanding of frequently employed taxonomic markers in different organism groups, particularly in the light of potential drawbacks for accuracy of newly emerging approaches such as metabarcoding or “exclusively *COI* barcode-based species definitions” (Sharkey et al., 2021a,b).

3.2 Materials and Methods

Specimen sampling

Sampling of adult Sericini chafers (Coleoptera: Scarabaeidae) was carried out at twelve localities in Sri Lanka (Figure 3.1) during 2019-2020. These sites included different forest types in different ecozones. Beetles were captured using UV-light traps and manual collecting from a white sheet being illuminated with UV, blue and green LEDs (LepiLED, © WIF, Dr Gunnar Brehm, Jena, Germany). Some additional specimens were hand-collected during the day. All specimens were preserved in 96% ethanol after collecting.

The collected specimens were presorted to morphospecies. For this purpose, all male genitalia were dissected and labelled. Identification to species level was done using recent literature (Fabrizi & Ahrens, 2014; Ahrens & Fabrizi, 2016; Ranasinghe et al., 2020) and, in some cases, by comparison with type specimens. Three to seven male individuals of each morphospecies per location were selected for DNA extraction and subsequent sequencing (in total 280 individuals). The species' habitus and male genitalia were photographed of one selected specimen per species, using a Zeiss AxioCam HRc camera (SteREO Discovery. V20). Images at several focal points were taken using the Zeiss Axio Vision (ZEN pro) software package and stacked with Zerene Stacker (Version 1.04) (<http://www.zerene.com>).

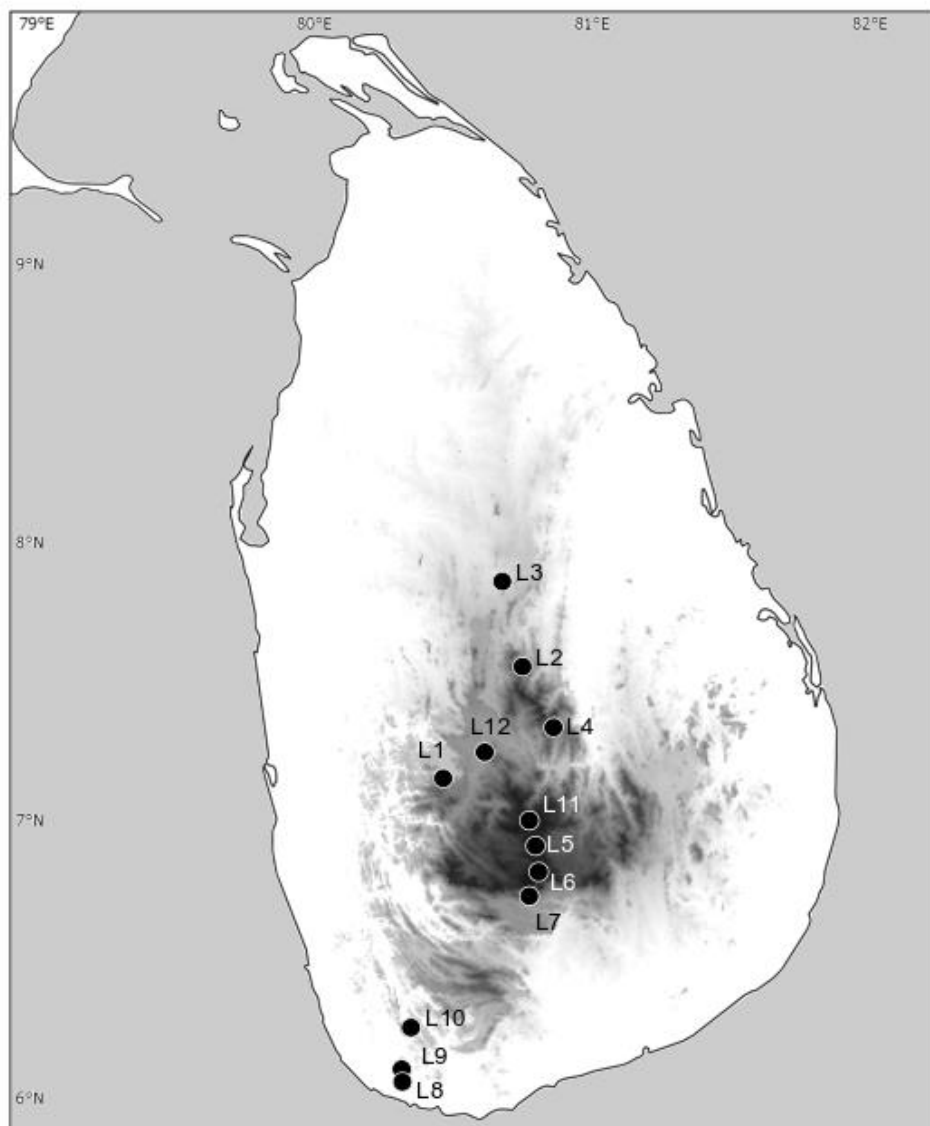


Figure 3.1. Map of Sri Lanka showing collecting sites for this study. IDs refer to major sampling localities: L1: Aranayake; L2: Riverston; L3: NIFS Arboretum; L4: Deenston; L5: Nuwara Eliya; L6: Horton Plains; L7: Belihuloya; L8: Hiyare; L9: Kottawa; L10: Kanneliya; L11: Piduruthalagala; L12: Uda Peradeniya.

DNA sequencing

DNA was extracted from mesothoracic leg and attached muscles using the Qiagen® DNeasy Blood and Tissue Kit (Hilden, Germany) or the Qiagen® BioSprint 96 magnetic bead extractor (Hilden, Germany). Lab work followed the standard protocols of the German Barcode of Life project (Geiger et al., 2016). The primers LCO1490-JJ [5'-CHACWAAYCATAAAGATATYGG-3'] and

HCO2198-JJ [5'-AWACTTCVGGRTGVCC AAARAATCA-3'] (Astrin & Stüben, 2008) were used to amplify a 658 bp fragment at the 5'-end of the mitochondrial gene cytochrome c oxidase subunit 1. PCRs of 90 samples were performed using the QIAGEN® Multiplex PCR Kit. The amplification products were subsequently checked by electrophoresis on a 1.5% agarose gel containing GelRed®. Successfully amplified DNA fragments were purified using Illustra™ ExoProStar™ Enzymatic PCR and Sequencing Clean-Up Kit. Forward and reverse strands were sequenced by Macrogen Europe (Macrogen, Amsterdam, the Netherlands; www.macrogen.com). PCRs for 190 samples were done in 96-well-plates. Unpurified PCR products were subsequently sent for purification and bidirectional Sanger sequencing to BGI Tech Solutions (Hongkong, China). Sequences were assembled, edited and aligned using Geneious R7 (version 7.1.9, Biomatters Ltd.). All data are deposited in BOLD (project: SCOIB) and GenBank (accession numbers MW698204 - MW698469) (see Supplement Table S3.1).

Phylogenetic analysis

Maximum likelihood (ML; Felsenstein, 1973) searches were performed in IQ-TREE version 1.6.12 (Nguyen et al., 2015) under the (GTR+F+I+G4) model of nucleotide substitution that was inferred as the best fit model by ModelFinder (Kalyaanamoorthy et al., 2017). A total of 1000 ultrafast bootstrap (Hoang et al., 2018) replicates were done to assess branch supports. The tree search was repeated ten times with the above parameters and the tree with highest likelihood was selected for further analysis. The resulting tree was rooted with *Apogonia* sp (X-SR0095) in FigTree v.1.4.4 (available from <http://tree.bio.ed.ac.uk/software/figtree>). Split networks as implemented in SplitsTree4 v.4.16.2 (available from <http://www.splitstree.org>) (Huson & Bryant, 2006) were used to represent incompatible and ambiguous signals in the *COI* dataset. Additionally, maximum likelihood searches were performed in PhyML using automatic model selection by Smart Model Selection (SMS) (Lefort et al., 2017) on the web server version (<http://www.atgc-montpellier.fr/phyml/>) (Guindon et al., 2010).

Species delimitation

DNA-based species delimitation was performed using the Poisson tree processes (PTP) model (Zhang et al., 2013), Statistical parsimony analysis (TCS) (Templeton et al., 1992; 2001), Automatic Barcode Gap Discovery (ABGD) (Puillandre et al., 2012), Assemble Species by Automatic Partitioning (ASAP)

(Puillandre et al., 2021) and Barcode Index Number (BIN) assignments (Ratnasingham & Hebert, 2013).

Poisson tree process modeling was performed with PTP web server (<https://species.h-its.org/>; accessed on 09 February 2021) using the maximum likelihood implementation (hereafter mlPTP; Zhang et al., 2013) with a single Poisson distribution, as well as the Bayesian implementation (bPTP), which adds Bayesian support (pp) values for putative species to branches in the input tree. The PTP method infers speciation events based on a shift in the number of substitutions between internal nodes (Zhang et al., 2013).

Further, multi-rate PTP (<https://mptp.h-its.org/#/tree>; accessed on 23 July 2021) was performed. Multi-rate PTP (hereafter mPTP; Kapli et al., 2017) is an improved method of PTP which does not require user-defined parameter as input and using MCMC it computes the support values for each clade, which can be used to assess the confidence of the ML delimitation. The IQ-TREE result from previous phylogenetic analysis was used as input for all PTP analysis.

Statistical parsimony analysis was performed as implemented in TCS v.1.21 (Clement et al., 2000). The procedure partitions the sequence data into clusters, i.e. subgroups (or networks) of closely related haplotypes connected by changes with a <95% probability to be non-homoplastic. Resulting networks have been found to be largely congruent with morphospecies at the 95% threshold (Meier et al., 2006; Ahrens et al., 2007) and are considered here as molecular operational taxonomic units (MOTUs).

Automatic Barcode Gap Discovery (ABGD) was conducted using the ABGD webserver (<https://bioinfo.mnhn.fr/abi/public/abgd/abgdweb.html>; accessed on 09 February 2021) with default parameters (i.e., using Jukes-Cantor model (JC69) distances, a relative gap width of 1 and 50 steps, Pmin=0.001, Pmax=0.1, Nb bins for distance distribution= 20) (Puillandre et al., 2012). ABGD applies a set of prior intraspecific divergences to detect the position of the barcode gap, which are iteratively refined. Alternatively, we reran the ABGD analysis with a distance matrix generated through IQ-TREE analysis as the input file. This maximum likelihood distance values (mldist file) reflected pairwise distances corrected by the GTR-model.

Assemble Species by Automatic Partitioning (ASAP) was conducted using the ASAP webserver (<https://bioinfo.mnhn.fr/abi/public/asap/> accessed on 23 July 2021) using the distance matrix generated through IQ-TREE analysis (Puillandre et al., 2020). ASAP divides species partitions based on pairwise genetic distances. ASAP also computes a probability of panmixia (p-val), a relative gap width

metric (W), and ranked results by the ASAP-score: the lower the score, the better the partitioning (Puillandre et al., 2021). Number of MOTUs predicted by ASAP 1st and ASAP 2nd scores were selected and compared with other methods. Finally, MOTUs from Barcode Index Number (BIN) assignments (Ratnasingham & Hebert, 2013) obtained from the BOLD data base (Project - SCOIB: Sericini *COI* Barcoding) were included and compared with other delimitation results.

The accuracy of DNA-based methods with prior morphospecies assignment was assessed by the match ratio (Ahrens et al., 2016): $2 \times N_{\text{match}} / (N_{\text{mol}} + N_{\text{morph}})$, where N_{match} is the number of exact matches of morphospecies (all individuals) with MOTUs of different delimitation methods, N_{mol} is the number of MOTUs that resulted from different delimitation methods, and N_{morph} is the number of morphospecies (Table 3.1). All morphospecies were mapped onto the terminals of the maximum likelihood tree along with the images of their male genitalia (lateral view) and MOTUs obtained from different species delimitation methods (Figure 3.2). Further, the match ratios for all pairs of delimitation methods were calculated and compared in a similarity matrix. The matrix was transformed into a distance matrix and a Principal Coordinate Analysis (PCoA) was performed in PAST v. 3.25 (Hammer et al., 2001) in order to compare similarity between different methods.

Data handling

All raw data produced in the project are freely accessible and deposited in dedicated databases for secure and curated long-term storage. Extracted DNA is stored at -80 °C in the DNA bank collection of the ZFMK (<https://www.zfmk.de/en/biobank>). Obtained nucleotide sequences were submitted to NCBI (accession numbers MW698204 - MW698469) and BOLD databases (project: SCOIB) (see Supplement Table S3.1). Voucher specimens are deposited in the insect collections of the ZFMK, each with a unique voucher ID that is linked to the corresponding DNA extract from that sample, to the DNA sequences, and to the morphological data and images. Voucher-related data and IDs were stored in the ZFMK's digital collection database.

3.3 Results

Morphological sorting of captured scarab specimens (total ca. 2300) resulted in a total of 45 Sericini morphospecies of which 280 individuals were selected for sequencing. These species included 41 Sri Lankan endemics and representatives from all five Sericini genera occurring in Sri Lanka. Thirty-four morphospecies were represented by more than one individual and 11 were singletons. For 266 specimens, we successfully obtained *COI* sequences (658 bp). From 266 individuals, 257 were assigned to putative morphospecies using male genital preparations. Nine specimens were females which did not have suitable diagnostic characters for morphospecies assignment; they were subsequently assigned to species using the DNA sequences as they were clearly nested in the relevant species clades (seven specimens: SR0088, SR0100, SR0118, SR0186, SR0190, SR0350; SR0881) or unambiguously assigned to a species in all delimitation methods (two specimens: SR0089, SR0095). Despite our repeated extensive sampling (Figure 3.1), 75.5% of the taxa (34 morphospecies) were collected from only single localities. For example, nine species (20% of all recorded species) were only found at Deanston (L4), 10 species (22.2%) only at Dambulla (L3), six species (13.3%) only at Aranayake (L1). However, 11 morphospecies (24.5% of all recorded species) were represented in more than one locality, but no one was found in more than half of all localities: *Maladera badullana* (3 sites), *M. coxalis* (2 sites), *M. dubia* (3 sites), *M. hortonensis* (2 sites), *M. karunaratnae* (2 sites), *M. rufocuprea* (5 sites), *Serica fusa* (3 sites), *S. lurida* (2 sites), *Selaserica impexa* (2 sites), *Se. nitida* (2 sites), and *Se. pusilla* (2 sites).

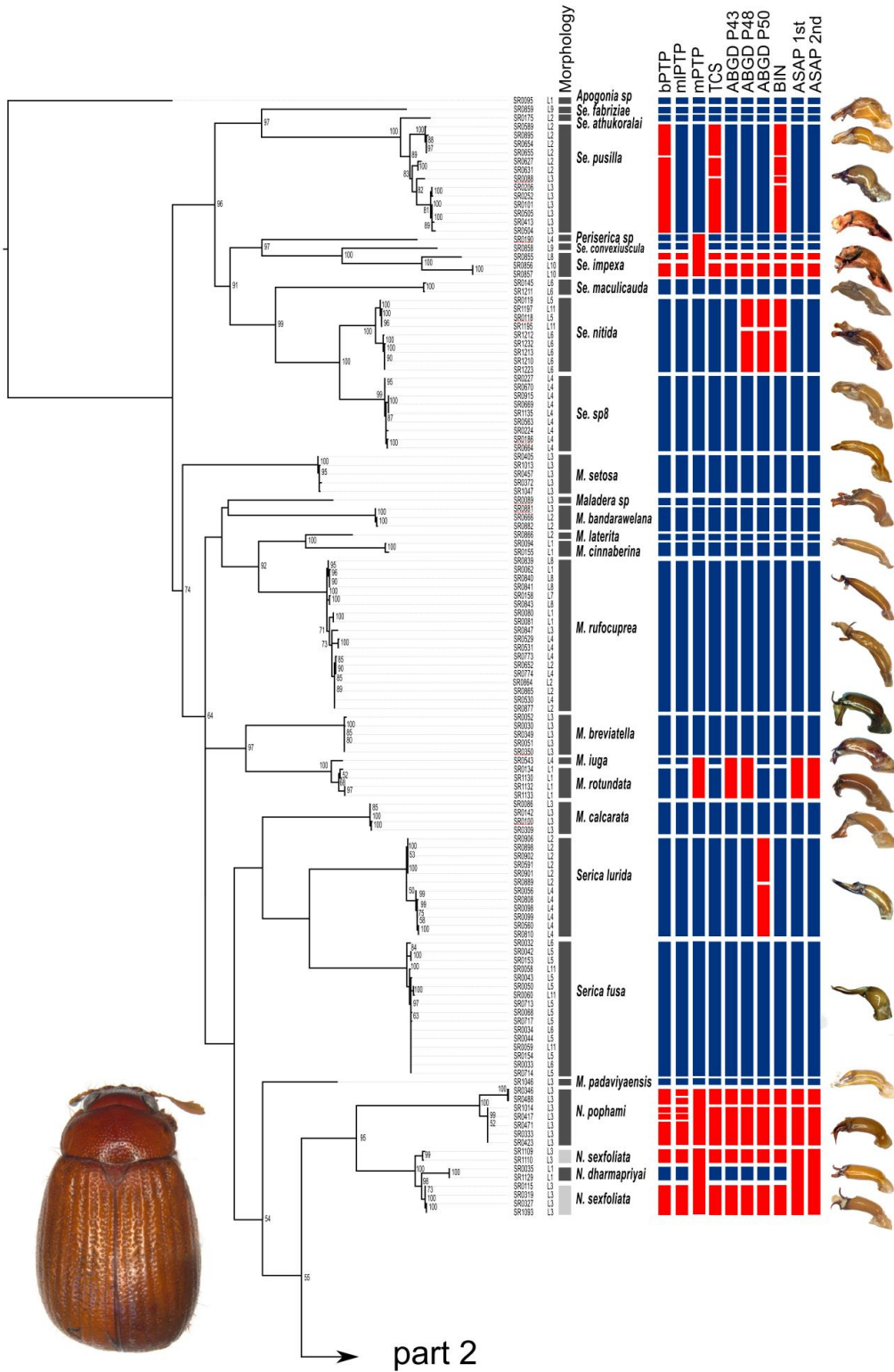
ML tree searches with IQ-TREE and PhyML obtained a similar tree topology (Figure 3.2, Supplement Figure S3.1), with the exception of three cases. With IQ-TREE, *M. hortonensis* was sister to *M. dubia* + *M. lindulana*, whereas in the PhyML tree *M. lindulana* was sister to *M. dubia* + *M. hortonensis*. In the second case, *Maladera* sp. (female specimen, SR0089) was sister to *M. bandarawelana* in the IQ-TREE tree and to *M. rotundata* + *M. igua* + *M. breviatella* in the PhyML tree. Finally, *M. igua* was nested within *M. rotundata* in the latter, whereas the IQ-TREE resolved them as two sister species. However, several distinct clades were equally recovered in both trees, such as the clade *Selaserica* + *Periserica*, the *Serica* clade, the *Neoserica* clade, and the *Maladera fistulosa* clade. The latter is a diverse, endemic radiation on the island that is characterized by entirely reduced parameres. It included eight so far new, unnamed species, which will be described in a separate publication.

Species delimitation

The different species delimitation methods (bPTP, mlPTP, mPTP, TCS, ABGD, ASAP, and BIN) resulted in different numbers of MOTUs (Table 3.1). We found relatively limited congruence between molecular operational taxonomic units (MOTUs) and morphospecies. None of the employed species delimitation methods correctly inferred the same species partition that was obtained from prior morphospecies assignments. The number of MOTUs varied from 35 to 61.

Parsimony network analysis subdivided the unique haplotypes into 53 different MOTUs (i.e., networks). Thirty-three of them perfectly matched with the morphospecies assignments and showed the highest, although moderate, match ratio of all delimitation methods (0.67). Most over-splitting events could be attributed to larger geographical sequence variation. Three different types of tree-based PTP analyses (bPTP, mlPTP, mPTP) resulted in varying numbers of MOTUs and matches with morphospecies. bPTP modelling showed low congruence, mainly due to oversplitting, and resulted in 57 MOTUs with 30 matches with the morphospecies, displaying the second lowest match ratio (0.59). mlPTP modeling resulted in 52 MOTUs with 32 matches with the morphospecies and the second highest match ratio of 0.66. mPTP produced 35 MOTUs with 27 matches and the highest match ratio (0.67) similar to TCS analysis.

ABGD failed to identify a clear barcoding gap and thus resulted in unreliable results that strongly depended on parameter choice. No consistent estimate of the number of species was recovered across a range of initial parameter values. We arbitrarily chose three partitions with a prior maximal distance (P) of 0.018, 0.015 and 0.010 that resulted in 43, 48, and 50 MOTUs, respectively (hereafter as P43, P48, and P50), and matched with 29, 29, and 30 morphospecies. All three choices showed both lumping and splitting, and obtained match ratios between 0.63-0.66. The performance of ABGD thus lied between bPTP and TCS. The two best scores of ASAP partitioned species into groups containing 40 and 41 entities, and matched with 27 and 28 morphospecies, respectively. The resulting match ratio was 0.63 for the best scored partition, and 0.65 for the second partitioning. BIN assignments revealed 61 MOTUs and matched with 30 morphospecies. It obtained the lowest match ratio (0.57). BIN assignments showed more splitting events than any other method, for example six MOTUs for 11 *M. coxalis* individuals collected from two different geographic locations, whereas all other methods resulted in a single MOTU for *M. coxalis*.



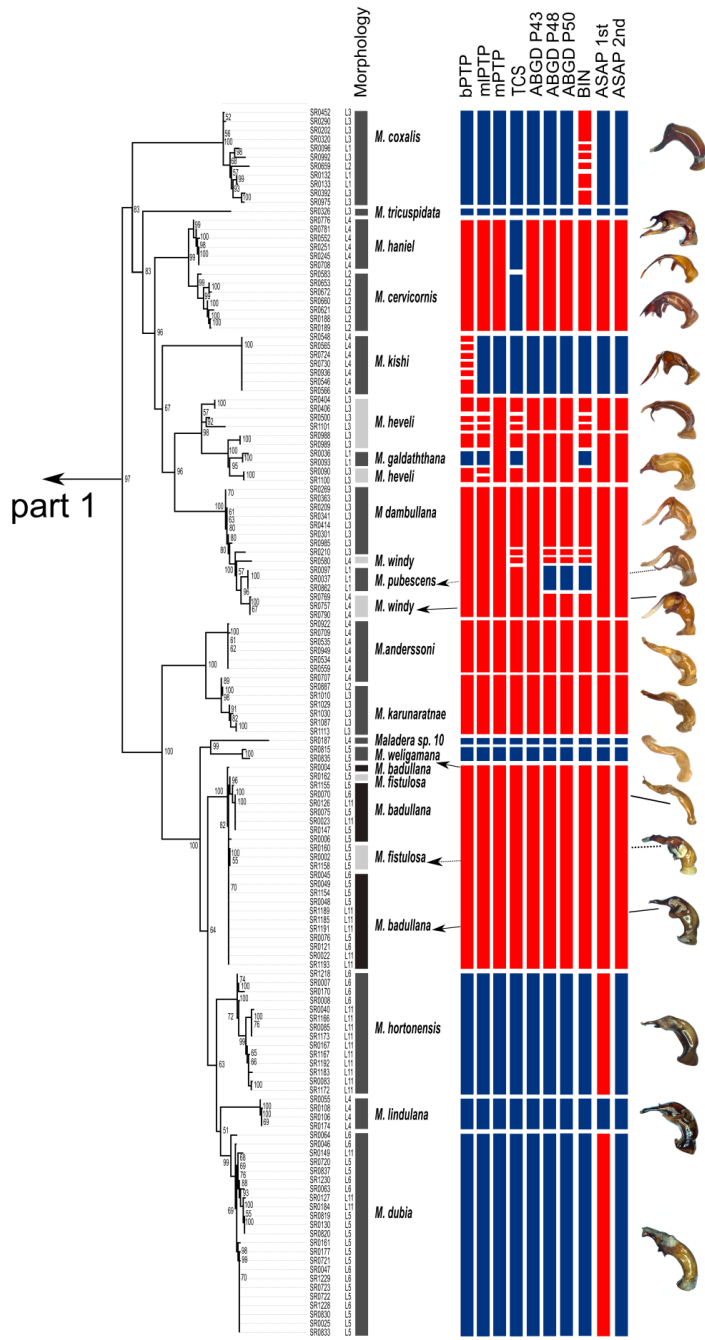


Figure. 3.2. Maximum likelihood tree with information about morphospecies assignments, sampling locations, results of species delimitations (bPTP, mlPTP, mPTP, TCS, ABGD, BINs and ASAP) and illustrations of the respective morphospecies' aedeagi in lateral view. Blue boxes indicate agreement between molecular species delimitation method and morphospecies assignment, while red boxes indicate disagreement. Ultrafast bootstrap supports (%) >50 are shown next to the branches.

Only 18 MOTUs were obtained from all methods and also perfectly matched morphospecies. This included haplotypes from different geographic locations (e.g., in *Maladera rufocuprea* and *Serica fusa*). Thirty-four morphospecies assignments entirely matched with MOTUs of at least one delimitation method. All methods showed both splitting (i.e., individuals of one morphospecies were separated into two or more different MOTUs) and lumping of morphospecies (i.e., individuals of two or more different morphospecies were joined in one MOTU) and produced different numbers of MOTUs and hence lower matching ratios (Table 3.1). Individuals of *Selaserica impexa* were split into different MOTUs according to their different geographic sampling locations with all delimitation methods except mPTP, while other species were only split by ABGD and BINs (*Se. nitida*), bPTP, BINs and TCS (*Se. pusilla*) or ABGD (*S. lurida*).

A few non-monophyletic species were observed: 1) *Neoserica dharmapriyai* was nested within *N. sexfoliata*; 2) *Maladera galdaththana* nested within *M. heveli*; 3) *M. pubescens* nested within *M. windy*; 4) one individual of *M. anderssoni* was placed in the *M. karunaratnae* clade; 5) *M. badullana* and *M. fistulosa* were mixed within one clade. Consequently, individuals of *N. sexfoliata*, *M. heveli* and *M. windy* split into two or more MOTUs, while nested species were resolved as one MOTU or lumped with its sister species, resulting in low matches with morphospecies. In the first case, *N. sexfoliata* split into two MOTUs and *N. dharmapriyai* recovered as one separate MOTU that was nested within *N. sexfoliata* in all methods except mPTP and ASAP where both species were lumped into one MOTU. In the second case, *M. galdaththana* was lumped with the four individuals of *M. heveli* in ABGD and ASAP, however, mlPTP, bPTP, TCS, and BINs correctly assigned the species as a single MOTU. In mPTP several but not all individuals of *M. galdaththana* and *M. heveli*, respectively, resulted as separate MOTUs. In the third case all individuals of *M. pubescens*, *M. dambullana*, and *M. windy* were lumped together (bPTP, mlPTP, mPTP, ASAP), whereas in TCS, ABGD and BIN additionally one individual from *M. dambullana* and *M. windy*, respectively, was split off resulting in two additional MOTUs. *M. pubescens* matched with prior morphospecies assignment in ABGD P48, ABGD P50, and BIN assignments. Both, fourth and fifth case showed mixing of two different morphospecies: one individual of *M. anderssoni* (SR0707) was placed in the *M. karunaratnae* clade in all methods; moreover, *M. badullana* and *M. fistulosa* were mixed in all methods thus both events resulted in lumping of species.

M. cervicornis and *M. haniel*, which differ very distinctly in shape of their male copulation organ, were lumped with all methods except in TCS. Whereas *M. iuga*

and *M. rotundata* lumped in mPTP, ABGD, and ASAP. *M. dubia* showed lumping with *M. hortonensis* only in ASAP 1st partition. Over-splitting was observed in *N. pophami* (SR0346, SR0488 in mlPTP), *M. heveli* (SR0090 and SR1100 in mlPTP), and *M. kishi* (all individuals in bPTP) despite having identical sequences and being sampled from the same locality. All those cases affect matches with prior morphospecies assignments, hence decrease the match ratio in different delimitation methods.

The PCoA ordination based on pairwise match ratios examined the similarity of the ten different delimitation methods, which were all based on the same *COI* fragment, and also in relation to their congruence with morphology-defined species (Figure. 3.3). For *COI*-based species delimitation, four distinct clusters were evident: one method resulted rather isolated (mPTP) and produced the lowest number of MOTUs ($n=35$). TCS, BIN, and bPTP formed a second cluster; a third cluster consisted of ABGD P48, ABGD P50 and mlPTP, while ASAP 1st, ASAP 2nd and ABGD P43 formed the last one. These clusters correspond basically to the number of MOTUs of these methods ($N_{\text{MOTU}} = 53-61, 48-52, \text{ and } 40-43$ for cluster 2-4, respectively) and they appear rather independent from prior morphospecies matches. This proposed ordination method can be used to show at one glance how different delimitation methods performed on a particular problem and to observe the similarity of *COI*-based delimitation compared to that of morphology.

3.4 Discussion

This study focused on the investigation of the performance of *COI* barcode data with various species delimitation approaches, since *COI* barcodes are widely used as a proxy for species taxonomy and for ecological monitoring. Specifically, we investigated how well the resulting MOTUs reflected species entities in a megadiverse chafer group. While being rather uniform in external appearance, Sericini chafers show extremely well differentiated genitalia even between closely related species (e.g., Ahrens et al., 2016; Dalstein et al., 2019). The correlation between divergent genital morphology and evolutionary entities was widely confirmed by integrative taxonomy studies (e.g., Ahrens & Ribera, 2009; Eberle et al., 2016), including even genomic data (Dietz et al., 2021). The resulting maximum likelihood trees represent the first molecular phylogenetic hypotheses for Sri Lankan Sericini. Two distinct clades of *Selaserica* that were previously

also characterized by morphological data (Fabrizi & Ahrens, 2014) could be confirmed in the present study. The two groups are characterized by the presence or absence of a carinate hypomeron for the *Selaserica splendifica* group and the *Se. nitida* group, respectively.

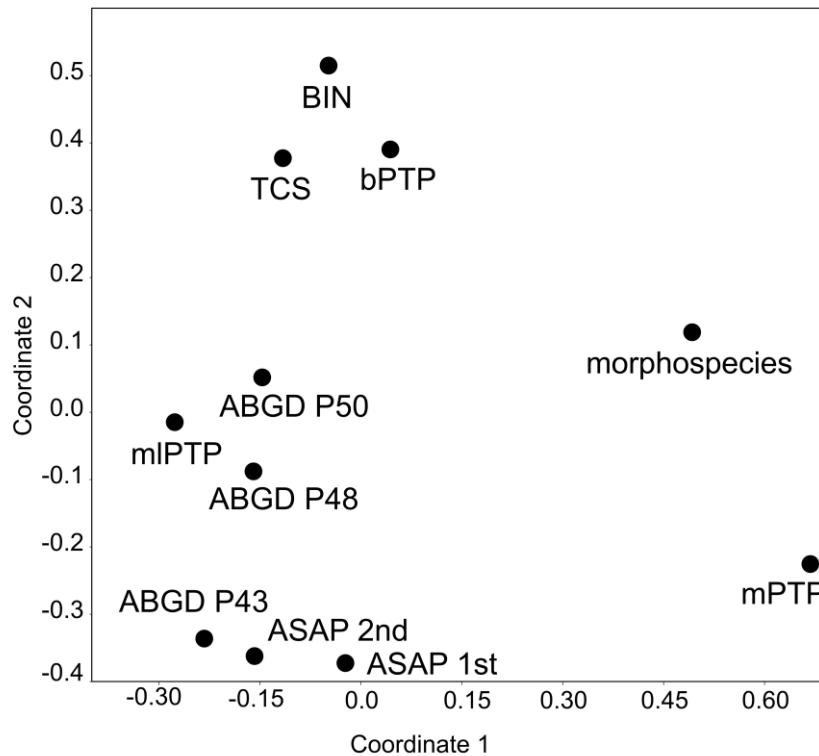


Figure 3.3. Principal Coordinate Analysis (PCoA) of different species delimitation methods and morphospecies based on pairwise match ratios.

Table 3.1. Match ratio (Ahrens et al., 2016) of DNA-based species delimitation methods on Sericini chafer data based on number of MOTUs and number of matches between MOTUs and morphospecies ($N_{\text{morph}}=45$). Match ratio = $2 \times N_{\text{match}} / (N_{\text{mol}} + N_{\text{morph}})$.

	bPTP	mIPTP	mPTP	TCS	ABGD P43	ABGD P48	ABGD P50	BIN	ASAP 1st	ASAP 2nd
N match	30	32	27	33	29	29	30	30	27	28
N MOTU	57	52	35	53	43	48	50	61	40	41
Match ratio	0.59	0.66	0.67	0.67	0.66	0.62	0.63	0.57	0.63	0.65

The here observed low congruence of MOTUs with morphospecies (match ratio: 0.57-0.67) was not unexpected since previous studies on tropical Sericini have showed similarly low match ratios (Ahrens et al., 2016, Dalstein et al., 2019, Lukic et al., 2021). Some of them were subject to strong variation (between 0.14 and 1) depending on the different selected subclades being analyzed (Ahrens et al., 2016). Even in absence of geographic sampling bias these have shown low match ratios (0.59-0.77) (Lukic et al., 2021). Also the congruence between the different delimitation methods, although using the same data, was moderate. This is in line with graphical summaries of many DNA-taxonomy studies that have shown rather inconsistent results among different species delimitation approaches using the same marker (see above; e.g., Bergsten et al., 2012; Magoga et al., 2021). However, some studies, particularly those with limited geographical (i.e., regional) scope in the northern hemisphere, showed almost perfect matches of MOTUs with morphospecies among nearly 90% of the studied species (e.g., Hendrich et al., 2015; Pentinsaari et al., 2014; Rulik et al., 2017). So far uninvestigated was their mutual multidimensional relations in terms of match ratios (Figure 3.3) (Ahrens et al., 2016). The observed divergent clusters in the plot of mutual match-similarity, also in context with morphospecies, provided insight to the robustness and confidence of the results in a range of the used species delimitation approaches. Even using the same genetic marker, results differed conspicuously and call for caution regarding premature conclusions (Ahrens et al., 2021).

Inconsistency between *COI* delimited species and morphospecies can have different causes. In several cases, non-monophyly of morphospecies was linked to splitting or lumping. Such cases were observed in the clades *M. fistulosa* group and in *Neoserica*. Non-monophyly of species could be a result of introgression by hybridization or incomplete lineage sorting (ILS). Both phenomena can result in similar *COI* haplotypes across species boundaries and may consequently lead to splitting and/or lumping. If this occurs in morphologically highly dissimilar species (under the assumption that morphologically highly dissimilar species in terms of male genital shape are not closely related), it would rather indicate hybridization (Dalstein et al., 2019). In this study, hybridization may have occurred in case of *M. galdaththana* and *M. heveli*. Both taxa have highly dissimilar genitalia. In morphologically very similar species, non-monophyly could be explained by either incomplete lineage sorting or introgressed DNA (Eberle et al., 2016; Dalstein et al., 2019). These cases were: 1) *Neoserica dharmapriyai* and *N. sexfoliata*; 2) *M. pubescens*, *M. dambullana* and *M. windy*; 3) *Maladera anderssoni* and *M. karunaratnae* and 4) *M. badullana* and *M. fistulosa*. There are several tests to distinguish hybridization from incomplete lineage sorting (Sang & Zhong, 2000; Joly et al., 2009), which is, however, often

difficult in reality (Eberle et al., 2016). Based on the available data (i.e., part of the *COI* gene), their application is impossible (Dalstein et al., 2019). Cross contamination of specimens during DNA-extraction or PCR preparation could be excluded based on the position of the single samples in the microtiter-plates, particularly for the case of *M. anderssoni* / *M. karunaratnae* (in which one individual of *M. anderssoni* was lumped with *M. karunaratnae* in all methods).

Inconsistency between MOTUs and morphospecies could have been caused by highly rapid speciation: *Maladera cervicornis* and *M. haniel*, which here both resulted as monophyletic sister taxa, have highly distinct male genitalia. They lumped in all methods except TCS. This could be indicative that divergence of their male genitalia is much faster and more distinct than mitochondrial molecular divergence and lineage sorting, which, although being complete, was not sufficient in terms of degree of divergence to delimit species unambiguously. Similar evidence for multiple species have been shown by Eberle et al. (2016) and confirmed with genomic data by Dietz et al. (2021).

Over-splitting of morphospecies encountered here was apparently also caused by relatively deep coalescence, for example by considerable geographically determined genetic variation of haplotypes (*Sel. impexa*). Specimens of this species originated from two isolated lowland forest reserves without any heterogeneous landscapes in between (L8 and L10; see Figure 3.1), so that individuals might not be able to migrate between these populations. Splitting of *Se. pusilla* (bPTP, TCS, BIN), *S. lurida* (ABGD), *M. coxalis* (BIN), and *Sel. nitida* (ABGD, BIN) also were determined by distant geographic sample locations of the specimens. *Maladera coxalis*, *Sel. nitida*, *Sel. pusilla*, and *S. lurida* were recorded from different forests in the central highlands with complex elevation patterns. A greater biodiversity is observed in these forests compared to lowland forests (Meegaskumbura et al., 2015), since they are separated by steep escarpments, gorges, parallel ridges, or peaks (Cooray, 1967), which may act as geographical barriers for dispersal and may result in partial reproductive isolation. However, spatial separation of individuals did not always cause over-splitting. Morphospecies of *M. dubia*, *M. hortonensis*, *M. rufocuprea*, and *Serica fusa* were collected from different geographical locations and still appeared as a single entity in all analyses.

In general, as a result of limited dispersal, a negative relationship is expected for the geographic distance and the mating probability of individuals, as predicted by isolation by distance (Perez et al., 2018). Heterogeneous landscapes additionally might affect levels of gene flow due to reduced dispersal in consequence of the patchiness of preferred habitats (van Strien et al., 2015; Perez et al., 2018). Thus,

it is obvious that low dispersal propensity contributes to an elevated but unknown extent of intraspecific, geographically structured divergence (Li et al., 2015). Alternatively, genetic divergence may also result from ecological adaptation or sexual selection (e.g., Boughman, 2001; Matsubayashi et al., 2013). What is actually more likely for each case under study is often unknown, as is the case of the Sri Lankan Sericini chafers studied here. Biased accumulation of mutations in mtDNA after population separation of widespread species can obscure the limits between putative species (e.g., Eberle et al., 2019). Restricted gene flow caused by large distances between populations can result in increased divergence (Perez et al., 2018; Bergsten et al., 2012) which can be exaggerated by (sex) biased or limited dispersal. In result numbers of delimited entities can exceed the true species numbers by orders of magnitude (Eberle et al., 2019). Moreover, the effect of geography-induced genetic divergence depends on the latitude as well as the involvement of diversity hotspots (Gaytán et al., 2020), which generally are also refugial areas (Ahrens et al., 2013), characterized by long-term climatic stability (Fjeldså et al., 1997, 1999; Harrison & Noss, 2017). All this would affect the output of different species delimitation methods and in fact, none of the used methods report accurate species numbers compared to prior morphospecies assignments.

Besides the above discussed issues like incomplete lineage sorting and introgression (e.g., Funk & Omland, 2003; Ballard & Whitlock, 2004), molecular species delimitation approaches based on information from a single gene such as the mitochondrial gene *COI*, are frequently hampered by pseudogene co-amplification or *Wolbachia* infections (e.g., Song et al., 2008; Smith et al., 2012), which may bias haplotype distributions. Furthermore, sampling size influences the results of delimitation methods (e.g., Ahrens et al., 2016; Luo et al., 2018). Low number of samples may affect species delimitation. Our sample size ranged from 5 to 10 individuals per species and sampling was the same for all delimitation methods, and therefore did not affect their comparison. The estimation of a tree topology also affects delimitation methods; relying on a single mitochondrial DNA marker system is prone to errors that can mislead species delimitation and identification (see Eberle et al., 2020).

The present study indicated that not the study organisms, i.e., the data itself is the sole cause for incongruent species entities that were proposed by different methods. If signals were inherent to the data that caused mismatches with morphospecies, the same pattern of over-splitting and lumping would be expected across all methods. This was not always the case (Figure 3.2). For example, lumping of *M. dubia* and *M. hortonensis* only in ASAP 1st partition, split of *M. coxilis* in BIN, split of *S. lurida* in ABGD P50 (Figure 3.2). However, several

species and species complexes were incongruent between morphospecies and several or all delimitation methods (e.g., *M. heveli* and *M. galdaththana* or *M. pubescens*, *M. dambullana*, and *M. windy*). We conclude that in these cases the used single marker system provided insufficient or misleading signal for accurate delimitation of species.

In order to bypass some of these difficulties of incongruence of morphospecies and species identification or delimitation with *COI* data, there have been proposals for a haplotype-based macroecology, as patterns of intraspecific genetic diversity were found to be correlated with species richness (Papadopoulou et al., 2011) even at different spatial scales (Baselga et al., 2015). This way, highly valuable and easily produced data from, e.g., metabarcoding can be used (Taberlet et al., 2012). This becomes especially relevant in absence of complete reference barcode libraries in order to avoid high amounts of data deletion due to impossible species assignments.

Our results confirm that *COI* DNA barcode data alone are inadequate to delimit species, in particular in this case of Sericini chafers. Using various levels of haplotype diversity for ecological or evolutionary assessments bear high levels of uncertainty, as they might reflect different patterns at variable scales in time and space. However, these patterns appear to be not entirely and stringently evolutionary significant, as are those ones reflected by species. Thus, although haplotype diversity and species diversity are correlated, any ecological approach that does not take (true) species entities and species diversity in account, might look at different ecological interrelationships and processes than those considering true species (Papadopoulou et al., 2011; Thormann et al., 2016). Also, our results strongly discourage approaches of a minimalist taxonomic procedure, defining (new) species based on *COI* barcode data alone, using a single species delimitation approach only without morphological reference diagnoses (Meierotto et al., 2019; Sharkey et al., 2021a,b) (see also Zamani et al., 2021; Ahrens et al., 2021; Meier, et al., 2021; Fernandez-Triana, 2022).

Due to the severe impact of human activities including climate change, numerous species risk going extinct before being discovered (Costello et al., 2013). An estimated 10 million species remain to be discovered (Dayrat, 2004). A stable and robust nomenclature is the basis of clear communication and scientific discussion about biodiversity. Including true species entities within biodiversity research incorporates evolutionary scales and processes at all time levels. In this manner, species entities and names provide the ‘anchor’ to which all taxonomic, ecological, molecular and conservation data are attached (International Trust for Zoological Nomenclature 2008). Legal protection and policy are also linked to

names (i.e., species), not to actual (mortal) individuals (or haplotypes), on the assumption that the groups indicated by the names are consistent through time and among places.

Conversely, recent integrative taxonomy studies revealed how difficult it actually is to infer species boundaries objectively and robustly and that, so far, no infallible method for species delimitation exists, even when using genomic data (e.g., Carstens et al., 2013; Rannala & Yang, 2020). New methods and data sources continue to be developed and examined empirically (e.g., Fujisawa & Barraclough, 2013; Ahrens et al., 2016; Eberle et al., 2019; Sukumaran & Knowles, 2017), gradually converging to detecting species boundaries (Eberle et al., 2020; Rannala & Yang, 2020; Dietz et al., 2021). However, issues of sampling and the inherent nature of species (e.g., the fluctuation of effective population size; Ahrens et al. 2016) are variables that will always impact large-scale approaches and require continued integration with other sources of evidence (Padial et al., 2010; Schlick-Steiner et al., 2010), thereby specifically accounting for characteristics of every single species (e.g., Dufresnes et al., 2020; Campillo et al., 2020; Hausdorf & Hennig, 2020).

Acknowledgments

We are thankful to the Alexander Koenig Stiftung for supporting field work in Sri Lanka. S.R. was funded by the German Academic Exchange Services (DAAD) with additional support through ZFMK institutional funding. We are extremely thankful to N. Athukorala (NIFS), S.R. family members; P.L. Dharmapriya, B. Ranasinghe & T.N. Dharmapriya for assistance in the fieldwork. We are furthermore thankful to D. Bopearachchi, A. Sathkunanathan, M. Tharmarajan, C. Jayatissa (all of the NIFS) & Supipi Wijesundara (UoP) assistance in the fieldwork. Prof. S. Wijesundara & Mr. C. Lekamge made available facility in the NIFS Arboretum. Also thanks to M. de Silva, Mr. Sampath for facilities in the Hiyare Conservation Center. We are thankful to all wildlife rangers (Nuwara Eliya, Hiyare, Horton Plains), regional forest officers (Kandy, Knuckles, Nuwara Eliya, Kottawa, Kanneliya) who helped us to conduct fieldwork. For providing research and collection permits to S.P.B, we thank the Department of Wildlife Conservation, Sri Lanka (permit no: WL/3/2/61/18), the Department of Forest Conservation, Sri Lanka (permit no: R&E/RES/NFSRCM/2019-01 & R&E/RES/NFSRCM/EXTENSION/2020), the Divisional Forest Office, Kandy, Sri Lanka (permit no: K/G/01/06/03); Galle (M/0/03/2019). Special thanks to N. Ramanayake (DWC) and N. Gunathilake (DWC) for processing permits on time.

3.5 References

- Ahrens, D. (2004). Phylogeny and zoogeography of the Sericini in the Himalayan region (Insecta: Coleoptera: Scarabaeidae) (PhD dissertation). Freie Universität Berlin.
- Ahrens, D., Monaghan, M.T., & Vogler, A.P. (2007). DNA-based taxonomy for associating adults and larvae in multi-species assemblages of chafers (Coleoptera: Scarabaeidae). *Molecular Phylogenetics and Evolution*, 44 (1), 436–449. DOI: 10.1016/j.ympev.2007.02.024.
- Ahrens, D. & Ribera, I. (2009). Inferring speciation modes in a clade of Iberian chafers from rates of morphological evolution in different character systems. *BMC Evolutionary Biology*, 9, 234.
- Ahrens, D., Fabrizi, S., Sipek, P., & Lago, P. (2013). Integrative analysis of DNA phylogeography and morphology of the European rose chafer (*Cetonia aurata*) to infer species taxonomy and patterns of postglacial colonisation in Europe. *Molecular Phylogenetics and Evolution*, 69, 83–94.
- Ahrens, D., Liu, W.G., Fabrizi, S., Bai, M., & Yang, X.K., (2014a). A taxonomic review of the *Neoserica* (sensu lato) *abnormis* group (Coleoptera: Scarabaeidae: Sericini). *ZooKeys*, 439, 28–82.
- Ahrens, D. Liu, W.G., Fabrizi, S., Bai, M., & Yang, X.K. (2014b). A taxonomic review of the *Neoserica* (sensu lato) *septemlamellata* group (Coleoptera: Scarabaeidae: Sericini). *ZooKeys*, 402, 76–102.
- Ahrens, D., Liu, W.G., Fabrizi, S., Bai, M., & Yang, X.K. (2014c). A revision of the species of the *Neoserica* (sensu lato) *vulpes* group (Coleoptera: Scarabaeidae: Sericini). *Journal of Natural History*, 49 (17–18), 1073–1130. DOI: 10.1080/00222933.2014.974707
- Ahrens, D., Fujisawa, T., Krammer H.J., Eberle, J., Fabrizi, S., & Vogler, A.P. (2016). Rarity and incomplete sampling in DNA based species delimitation. *Systematic Biology*, 65, 478–494.
- Ahrens, D. & Fabrizi, S. (2016). A monograph of the Sericini of India (Coleoptera: Scarabaeidae). *Bonn Zoological Bulletin*, 65, 1–355.
- Ahrens, D., Ahyong, S.T., Ballerio, A., Barclay, M.V.L., Eberle, J., Espeland, M., Huber, B.A., Mengual, X., Pacheco, T., Peters, R.S., Rulik, B., Vaz-de-Mello, F., Wesener, T., & Krell, F. (2021). Is it time to describe new species without diagnoses? - A comment on Sharkey et al. (2021). *Zootaxa*, 5027 (2), 151–159.
- Arribas, P., Andújar, C., Salces-Castellano, A., Emerson, B.C., & Vogler, A.P. (2020). The limited spatial scale of dispersal in soil arthropods revealed with whole-community haplotype-level metabarcoding. *Molecular Ecology*, 30, 48–61. <https://doi.org/10.1111/mec.15591>

- Arribas, P., Andújar, C., Bidartondo, M.I. *et al.* (2021). Connecting high-throughput biodiversity inventories: Opportunities for a site-based genomic framework for global integration and synthesis. *Molecular Ecology*, 30, 1120–1135.
- Asha, G. & Sinu, P.A. (2020). DNA barcode and phylogenetic analysis of dung beetles (Coleoptera: Scarabaeidae) from the Western Ghats biodiversity hotspot, India. *International Journal of Tropical Insect Science*, 41, 1419–1425 <https://doi.org/10.1007/s42690-020-00336-z>
- Astrin, J.J. & Stüben, P.E. (2008). Phylogeny in cryptic weevils: molecules, morphology and new genera of western Palaearctic Cryptorhynchinae (Coleoptera: Curculionidae). *Invertebrate Systematics*, 22 (5), 503–522. DOI: 10.1071/IS07057.
- Ballard, J.W. & Whitlock, M.C. (2004). The incomplete natural history of mitochondria. *Molecular Ecology*, 13, 729–744. doi: 10.1046/j.1365-294X.2003.02063.x
- Banerjee, D., Kumar, V., Maity, A., Ghosh, B., Tyagi, K., Singha, D., Kundu, S., Laskar, B.S., Naskar, A., & Rath, S. (2015). Identification through DNA barcoding of Tabanidae (Diptera) vectors of surra disease in India. *Acta Tropica*, 150, 52–58, <https://doi.org/10.1016/j.actatropica.2015.06.023>.
- Barber, P. & Boyce, S.L. (2006). Estimating diversity of Indo-Pacific coral reef stomatopods through DNA barcoding of stomatopod larvae. *Proceedings of the Royal Society B: Biological Sciences*, 273, 2053–2061.
- Barman, A.S., Singh, M., Singh, S.K., Saha, H., Singh, Y.J., Laishram, M., & Pandey, P.K. (2018). DNA Barcoding of Freshwater Fishes of Indo-Myanmar Biodiversity Hotspot. *Scientific Reports*, 8 (1). doi:10.1038/s41598-018-26976-3.
- Baselga, A., Gómez-Rodríguez, C., & Vogler, A.P. (2015). Multi-hierarchical macroecology at species and genetic levels to discern neutral and non-neutral processes. *Global Ecology and Biogeography*, 24, 873–882. <https://doi.org/10.1111/geb.12322>
- Beenaerts, N., Pethiyagoda, R., Ng, P.K.L., Yeo, D.C.J., Bex, G.J., Bahir, M.M., & Artois, T. (2010). Phylogenetic diversity of Sri Lankan freshwater crabs and its implications for conservation. *Molecular Ecology*, 19, 183–196. doi: 10.1111/j.1365-294X.2009.04439.x
- Bergsten, J., Bilton, D. T., Fujisawa, T., Elliott, M., Monaghan, M.T., Balke, M., & Vogler, A.P. (2012). The effect of geographical scale of sampling on DNA barcoding. *Systematic Biology*, 61, 851–869. <https://doi.org/10.1093/sysbio/sys037>
- Bezeng, B.S., Davies, T.J., Daru, B.H., Kabongo, R.M., Maurin, O., Yessoufou, K., van der Bank, H., & van der Bank, M. (2017). Ten years of barcoding

- at the African Centre for DNA Barcoding. *Genome*, 60(7), 629–638. doi:10.1139/gen-2016-0198.
- Biju, S.D., Garg, S., Mahony, S., Wijayathilaka, N., Senevirathne, G., & Meegaskumbura, M. (2014). DNA barcoding, phylogeny and systematics of Golden-backed frogs (*Hylarana*, Ranidae) of the Western Ghats-Sri Lanka biodiversity hotspot, with the description of seven new species. *Contributions to Zoology*, 83 (4), 269–335 (2014).
- Boissin, E., Hoareau, T.B., Paulay, G., & Bruggemann, J.H. (2017). DNA barcoding of reef brittle stars (Ophiuroidea, Echinodermata) from the southwestern Indian Ocean evolutionary hot spot of biodiversity. *Ecology and Evolution*, 7, 11197–11203. <https://doi.org/10.1002/ece3.3554>
- Boughman, J.W. (2001). Divergent sexual selection enhances reproductive isolation in sticklebacks. *Nature*, 411 (6840), 944–948. doi: 10.1038/35082064. PMID: 11418857.
- Campillo, L.C., Barley, A.J., & Thomson, R.C. (2020). Model-based species delimitation: Are coalescent species reproductively isolated? *Systematic Biology*, 69, 708–721.
- Carstens, B.C., Pelletier, T.A., Reid, N.M., & Satler, J.D. (2013). How to fail at species delimitation. *Molecular Ecology*, 22, 4369–4383.
- Clement, M., Posada, D., & Crandall, K.A. (2000). TCS: a computer program to estimate gene genealogies. *Molecular Ecology*, 9, 1657–1660.
- Cooray, P.G. (1967). An introduction to the geology of Ceylon. *Spolia Zeylanica*, 31, 1–314.
- Costello, M.J., Wilson, S., & Houlding, B. (2013). More Taxonomists Describing Significantly Fewer Species per Unit Effort May Indicate That Most Species Have Been Discovered. *Systematic Biology*, 62, 616–624, <https://doi.org/10.1093/sysbio/syt024>.
- Dalstein, V., Eberle, J., Fabrizi, S., Eitzbauer, C., & Ahrens, D. (2019). COI-based species delimitation in Indochinese Tetraserica chafers reveal hybridisation despite strong divergence in male copulation organs. *Organisms Diversity and Evolution*, 19, 277–286. DOI: 10.1007/s13127-019-00398-z.
- Dangalle, C.D., Pallewatta, N., & Vogler, A.P. (2014). Inferring Population History of Tiger Beetle Species of Sri Lanka using Mitochondrial DNA Sequences. *Ceylon Journal of Science (Biological Science)*, 43, 47–63. DOI: <http://dx.doi.org/10.4038/cjsbs.v43i2.7324>
- Dayrat, B. (2004). Towards integrative taxonomy. *Biological Journal of the Linnean Society*, 85, 407–415.
- Dellicour, S., & Flot, J. (2018). The hitchhiker’s guide to single-locus species delimitation. *Molecular Ecology Resources*, 18(6), 1234–1246. <https://doi.org/10.1111/1755-0998.12908>

- DeSalle, R. & Goldstein, P. (2019). Review and Interpretation of Trends in DNA Barcoding. *Frontiers in Ecology and Evolution*, 7, 302. doi: 10.3389/fevo.2019.00302
- Dhaneesh, K.V., Kumar, T.T.A., & Kumar, A.B. (2015). Barcoding, phylogeography and species boundaries in clownfishes of the Indian Ocean. *DNA Barcodes*, 3, 5–16.
- Dietz, L., Eberle, J., Mayer, C., Kukowka, S., Bohacz, C., Baur, H., Espeland, M., Huber, B.A., Hutter, C., Mengual, X., Peters, R.S., Vences, M., Wesener, T., Willmott, K., Misof, B., Niehuis, O., & Ahrens, D. (2021). Standardized nuclear markers advance metazoan taxonomy. *bioRxiv* 2021.05.07.443120; doi: <https://doi.org/10.1101/2021.05.07.443120>
- Dopheide, A., Makiola, A., Orwin, K.H., Holdaway, R.J., Wood, J.R., & Dickie, I.A. (2020). Rarity is a more reliable indicator of land-use impacts on soil invertebrate communities than other diversity metrics. *eLife*, 9, e52787 doi: 10.7554/eLife.52787
- Dufresnes, C., Pribille, M., Alard, B., Gonçalves, H., Amat, F., Crochet, P.A., Dubey, S., Perrin, N., Fumagalli, L., Vences, M., & Martínez-Solano, I. (2020). Integrating hybrid zone analyses in species delimitation: lessons from two anuran radiations of the Western Mediterranean. *Heredity*, 124, 423–438.
- Eberle, J., Warnock, R.C.M., & Ahrens, D. (2016). Bayesian species delimitation in *Pleophylla* chafers (Coleoptera) - the importance of prior choice and morphology. *BMC Evolutionary Biology*, 16, 94. DOI: 10.1186/s12862-016-0659-3.
- Eberle, J., Fabrizi, S., Bazzato, E., Rossi, Stella Columba, M., Cillo, D., Uliana M., Sparacio, I., Sabatinelli, G., Warnock, R.C.M., Carpaneto, G.M., Ahrens, D. (2019). Sex-Biased dispersal obscures species boundaries in integrative species delimitation approaches. *Systematic Biology*, 68, 441–459, doi: 10.1093/sysbio/syy072.
- Eberle, J., Ahrens, D., Mayer, C., Niehuis, O., & Misof, B. (2020). A plea for standardized nuclear markers in metazoan DNA taxonomy. *Trends in Ecology & Evolution*, 35(4), 336–345.
- Ekanayake, H., Perera, N., Ukuwela, K.D., Walpita, C.N., Kodithuwakku, S.P., & Perera, S.J. (2021). Cryptic species diversity and molecular diagnosis of *Channa orientalis*; an endemic freshwater fish of Sri Lanka. *Mitochondrial DNA Part A*, 32, 3, 77–84, DOI: 10.1080/24701394.2021.1876040.
- Esselstyn, J., Evans, B., Sedlock, J., Anwarali Khan, F., & Heaney, L. (2012). Single-locus species delimitation: a test of the mixed Yule-coalescent model, with an empirical application to Philippine round-leaf bats. *Proceedings of the Royal Society B: Biological Sciences*, 279, 3678–86. 10.1098/rspb.2012.0705.

- Fabrizi, S. & Ahrens, D. (2014). A Monograph of the Sericini of Sri Lanka (Coleoptera: Scarabaeidae). *Bonn Zoological Bulletin Supplements*, 61, 1–124.
- Fernandes, K., van der Heyde, M., Bunce, M., Dixon, K., Harris, R.J., Wardell-Johnson, G., & Nevill, P.G. (2018). DNA metabarcoding—a new approach to fauna monitoring in mine site restoration. *Restoration Ecology*, 26, 1098–1107. <https://doi.org/10.1111/rec.12868>
- Fernandez-Triana, J.L. (2022). Turbo taxonomy approaches: lessons from the past and recommendations for the future based on the experience with Braconidae (Hymenoptera) parasitoid wasps. *ZooKeys*, 1087, 199–220. <https://doi.org/10.3897/zookeys.1087.76720>
- Felsenstein, J. (1973). Maximum likelihood and minimum-step methods for estimating evolutionary trees from data on discrete characters. *Systematic Zoology*, 22, 240–249.
- Fjeldså, J., Ehrlich, D., Lambin, E. et al. (1997). Are biodiversity ‘hotspots’ correlated with current ecoclimatic stability? A pilot study using the NOAA-AVHRR remote sensing data. *Biodiversity and Conservation*, 6, 401–422 <https://doi.org/10.1023/A:1018364708207>
- Fjeldså, J., Lambin, E., & Mertens, B. (1999). Correlation between Endemism and Local Ecoclimatic Stability Documented by Comparing Andean Bird Distributions and Remotely Sensed Land Surface Data. *Ecography*, 22(1), 63–78.
- Fujisawa, T. & Barraclough, T.G. (2013). Delimiting species using single-locus data and the generalized mixed Yule coalescent approach: a revised method and evaluation on simulated data sets. *Systematic Biology*, 62, 707–724.
- Funk, D.J., & Omland, K.E. (2003). Species-level paraphyly and polyphyly: frequency, causes, and consequences, with insights from animal mitochondrial DNA. *Annual Review of Ecology, Evolution, and Systematics*, 34, 397–423.
- Gajapathy, K., Tharmasegaram, T., Eswaramohan, T., Peries, L.B.S.L., Jayanetti, R., & Surendran, S.N. (2016). DNA barcoding of Sri Lankan phlebotomine sand flies using cytochrome C oxidase subunit I reveals the presence of cryptic species. *Acta Tropica*, 161, 1–7. <http://dx.doi.org/10.1016/j.actatropica.2016.05.001>
- Gaytán, Á., Bergsten, J., Canelo, T., Pérez-Izquierdo, C., Santoro, M., & Bonal, R. (2020). DNA Barcoding and geographical scale effect: The problems of undersampling genetic diversity hotspots. *Ecology and Evolution*, 10, 10754–10772. <https://doi.org/10.1002/ece3.6733>
- Geiger, M.F., Herder, F., Monaghan, M.T., Almada, V., Barbieri, R., Bariche, M., Berrebi, P., Bohlen, J., Casal-Lopez, M., Delmastro, G.B., Denys, G.P.,

- Detta, A., Doadrio, I., Kalogianni, E., Kärst, H., Kottelat, M., Kovačić, M., Laporte, M., Lorenzoni, M., Marčić, Z., Özuluğ, M., Perdices, A., Perea, S., Persat, H., Porcelotti, S., Puzzi, C., Robalo, J., Šanda, R., Schneider, M., Šlechtová, V., Stoumboudi, M., Walter, S., & Freyhof, J. (2014). Spatial heterogeneity in the Mediterranean Biodiversity Hotspot affects barcoding accuracy of its freshwater fishes. *Molecular Ecology Resources*, 14(6), 1210–1221. doi: 10.1111/1755-0998.12257.
- Geiger, M. F., Moriniere, J., Hausmann, A., Haszprunar, G., Wägele, W., Hebert, P.D.N., & Rulik, B. (2016). Testing the global Malaise trap program - How well does the current barcode reference library identify flying insects in Germany? *Biodiversity Data Journal*, 4, e10671. DOI: 10.3897/BDJ.4.e10671.
- Goonesequera, K., Lee, P.L.M., van der Poorten, G., & Ranawaka, G.R. (2019). The phylogenetic history of the old world butterfly subtribe Mycalesina extended: the Mycalesis (Lepidoptera: Nymphalidae) of Sri Lanka. *Journal of Asia-Pacific Entomology*, 22, 121–133.
- Grosjean, S., Ohler, A., Chuaynkern, Y., Cruaud, C., & Hassanin, A. (2015). Improving biodiversity assessment of anuran amphibians using DNA barcoding of tadpoles. Case studies from Southeast Asia. *Comptes Rendus Biologies*, 338, 351–361. doi:10.1016/j.crvi.2015.03.015.
- Guindon, S., Dufayard, J.F., Lefort, V., Anisimova, M., Hordijk, W., & Gascuel, O. (2010). New algorithms and methods to estimate Maximum-Likelihood phylogenies: assessing the performance of PhyML 3.0. *Systematic Biology*, 59(3), 307–21.
- Hammer, O., Harper, D.A.T., & Ryan, P.D. (2001). Paleontological statistics software package for education and data analysis. *Palaeontologia Electronica*, 4, 1–9.
- Harrison, S. & Noss, R. (2017). Endemism hotspots are linked to stable climatic refugia. *Annals of Botany*, 119, 207–214. <https://doi.org/10.1093/aob/mcw248>
- Harrup, L.E., Laban, S., Purse, B.V. et al. (2016). DNA barcoding and surveillance sampling strategies for Culicoides biting midges (Diptera: Ceratopogonidae) in southern India. *Parasites Vectors*, 9, 461. <https://doi.org/10.1186/s13071-016-1722-z>.
- Hausdorf, B. & Hennig, C. (2020). Species delimitation and geography. *Molecular Ecology Resources*, 20, 950–960.
- Hebert, P.D.N., Cywinska, A., Ball, S.L., & DeWaard, J.R. (2003a). Biological identifications through DNA barcodes. *Proceedings of the Royal Society B: Biological Sciences*, 270, 313–321.
- Hebert, P.D.N., Ratnasingham, S., & deWaard, J.R. (2003b). Barcoding animal life: Cytochrome c oxidase subunit 1 divergences among closely related

- species. *Proceedings of the Royal Society B: Biological Sciences*, 270, S96–S99.
- Hebert, P.D.N., Penton, E.H., Burns, J.M., Janzen, D.H. & Hallwachs, W. (2004). Ten species in one: DNA barcoding reveals cryptic species in the neotropical skipper butterfly *Astrartes fulgerator*. *Proceedings of the National Academy of Sciences of the United States of America*, 101, 14812–14817.
- Hendrich, L., Morinière, J., Haszprunar, G., Hebert, P. D. N., Hausmann, A., Köhler, F., & Balke, M. (2015). A comprehensive DNA barcode database for Central European beetles with a focus on Germany: Adding more than 3,500 identified species to BOLD. *Molecular Ecology Resources*, 15, 795–818.
- Heyde, M. van der, Bunce, M., Wardell-Johnson, G., Fernandes, K., White, N.E., & Nevill, P. (2020). Testing multiple substrates for terrestrial biodiversity monitoring using environmental DNA metabarcoding. *Molecular Ecology Resources*, 20, 3, 732–745. <https://doi.org/10.1111/1755-0998.13148>
- Hoang, D.T., Chernomor, O., Haeseler, A. von, Minh, B.Q., & Vinh, L.S. (2018). UFBoot2: Improving the ultrafast bootstrap approximation. *Molecular Biology and Evolution*, 35, 518–522. <https://doi.org/10.1093/molbev/msx281>
- Hobern, D.G. (2021). BIOSCAN: DNA Barcoding to accelerate taxonomy and biogeography for conservation and sustainability. *Genome*, 64(3), 161–164. doi:10.1139/gen-2020-0009.
- Holdaway, R., Wood, J., Dickie, I., Orwin, K., Bellingham, P., Richardson, S., & Buckley, T. (2017). Using DNA metabarcoding to assess New Zealand’s terrestrial biodiversity. *New Zealand Journal of Ecology*, 41(2), 251–262. <http://www.jstor.org/stable/26198807>
- Huson, D. H. & Bryant, D. (2006). Application of phylogenetic networks in evolutionary studies. *Molecular Biology and Evolution*, 23 (2), 254–267. DOI:10.1093/molbev/msj030.
- Ileperuma Arachchi, I.S. & Benjamin, S.P. (2019). The crab spider genus *Tarrocanus* Simon, 1895 with notes on the genera *Alcimochthes* Simon, 1895 and *Domatha* Simon, 1895 (Araneae: Thomisidae). *Zootaxa*, 4613, 587–593. doi:10.11646/zootaxa.4613.3.10.
- International Trust for Zoological Nomenclature. (2008). Memorandum. House of Lords - Science and Technology - Written Evidence <https://publications.parliament.uk/pa/ld200708/ldselect/ldsctech/162/162we25.htm> (accessed, June 30th, 2021).
- Jamaluddin, J.A.F., Akib, N.A.M., Ahmad, S.Z., Halim, S.A.A.A., Hamid, N.K.A., & Nor, S.A.M. (2019). DNA barcoding of shrimps from a

- mangrove biodiversity hotspot. *Mitochondrial DNA. Part A*, 30(4), 618–625. DOI: 10.1080/24701394.2019.1597073.
- Joly, S., McLenachan, P. A., & Lockhart, P. J. (2009). A statistical approach for distinguishing hybridization and incomplete lineage sorting. *American Naturalist*, 174, E54–E70.
- Kadarusman, Hubert, N., Hadiaty, R.K., Sudarto, Paradis, E., & Pouyaud, L. (2012). Cryptic diversity in Indo-Australian rainbowfishes revealed by DNA barcoding: implications for conservation in a biodiversity hotspot candidate. *PLoS ONE*, 7(7), e40627. doi:10.1371/journal.pone.0040627.
- Kalyaanamoorthy, S., Minh, B.Q., Wong, T.K.F., Haeseler, A. von, & Jermin, L.S. (2017). ModelFinder: Fast model selection for accurate phylogenetic estimates. *Nature Methods*, 14, 587–589. <https://doi.org/10.1038/nmeth.4285>.
- Kanesharatnam, N. & Benjamin, S.P. (2019). Multilocus genetic and morphological phylogenetic analysis reveals a radiation of shiny South Asian jumping spiders (Araneae, Salticidae). *ZooKeys*, 839, 1–81. doi:10.3897/zookeys.839.28312
- Kapli, T., Lutteropp, S., Zhang, J., Kobert, K., Pavlidis, P., Stamatakis, A., & Flouri, T. (2017). Multi-rate Poisson tree processes for single-locus species delimitation under maximum likelihood and Markov chain Monte Carlo. *Bioinformatics*, 33(11), 1630–1638. doi:10.1093/bioinformatics/btx025
- Kaur, H. & Sharma, K. (2016). COI-based DNA barcoding of some species of Pentatomidae from North India (Hemiptera: Heteroptera), *Mitochondrial DNA Part A*, 28(5), 756–761. DOI: 10.1080/24701394.2016.1180513.
- Khamis, F.M., Masiga, D.K., Mohamed, S.A., Salifu, D., de Meyer, M., & Ekesi, S. (2012). Taxonomic Identity of the Invasive Fruit Fly Pest, *Bactrocera invadens*: Concordance in Morphometry and DNA Barcoding. *PLoS ONE*, 7(9), e44862. doi:10.1371/journal.pone.0044862
- Krishnamurthy, K.P. & Francis, R.A. (2012). A critical review on the utility of DNA barcoding in biodiversity conservation. *Biodiversity Conservation*, 21, 1901–1919.
- Lahaye, R., van der Bank, M., Bogarin, D. et al. (2008). DNA barcoding the floras of biodiversity hotspots. *Proceedings of the National Academy of Sciences of the United States of America*, 105, 2923–2928.
- Lakra, W.S., Singh, M., Goswami, M., Gopalakrishnan, A., Lal, K.K., Mohindra, V., Sarkar, U.K., Punia, P.P., Singh, K.V., Bhatt, J.P., & Ayyappan, S. (2016). DNA barcoding Indian freshwater fishes. *Mitochondrial DNA Part A*, 27:6, 4510–4517, DOI: 10.3109/19401736.2015.1101540.
- Lefort, V., Longueville, J.E. & Gascuel, O. (2017). SMS: Smart Model Selection in PhyML. *Molecular Biology and Evolution*, 34(9), 2422–2424.

- Leduc, N., Lacoursière-Roussel, A., Howland, K.L., et al. (2019). Comparing eDNA metabarcoding and species collection for documenting Arctic metazoan biodiversity. *Environmental DNA*, 1, 342–358. <https://doi.org/10.1002/edn3.35>
- Leliaert, F., Verbruggen, H., Vanormelingen, P., Steen, F., López-Bautista, J.M., Zuccarello, G.C. & De Clerck, O. (2014). DNA-based species delimitation in algae. *European Journal of Phycology*, 49,2, 179–196, DOI: 10.1080/09670262.2014.904524
- Li, Y., Gunter, N., Pang, H., & Bocak, L. (2015). DNA-based species delimitation separates highly divergent populations within morphologically coherent clades of poorly dispersing beetles. *Zoological Journal of the Linnean Society*, 175, 59–72.
- Liu, W.G., Fabrizi, S., Bai, M., Yang, X.K., & Ahrens, D. (2014a). A taxonomic revision of the *Neoserica* (s.l.) *pilosula* group (Coleoptera, Scarabaeidae, Sericini). *Zookeys*, 440, 89–113.
- Liu, W.G., Fabrizi, S., Bai, M., Yang, X.K., & Ahrens, D. (2014b). A taxonomic revision of the *Neoserica* (sensu lato) *calva* group (Coleoptera, Scarabaeidae, Sericini). *ZooKeys*, 448, 47–81.
- Liu, W.G., Fabrizi, S., Bai, M., Yang, X.K., & Ahrens, D. (2014c). A review of the *Tetraserica* species of China (Coleoptera, Scarabaeidae, Sericini). *ZooKeys* 448, 83–121.
- Liu, W.G., Bai, M., Yang, X.K., & Ahrens, D. (2015). New species and records of the *Neoserica* (sensu stricto) group (Coleoptera, Scarabaeidae, Sericini). *Journal of Natural History*, 49 (39–40), 2379–2395.
- Liu, W.G., Fabrizi, S., Bai, M., Yang, X.K., & Ahrens, D. (2016). A taxonomic revision of *Neoserica* (sensu lato): the species groups *N. lubrica*, *N. obscura*, and *N. silvestris* (Coleoptera, Scarabaeidae, Sericini). *Zookeys*, 635, 123–160.
- Lukic, D., Eberle, J., Thormann, J., Holzschuh, C., & Ahrens, D. (2021). Excluding spatial sampling bias does not eliminate over-splitting in DNA-based species delimitation analyses. *Ecology and Evolution*, 11, 10327–10337. <https://doi.org/10.1002/ece3.7836>
- Luo, A., Ling, C., Ho, S.Y.W., Zhu, C.D. (2018). Comparison of methods for molecular species delimitation across a range of speciation scenarios. *Systematic Biology*, 67, 830–846. <https://doi.org/10.1093/sysbio/syy011>
- Magoga, G., Fontaneto, D., & Montagna, M. (2021). Factors affecting the efficiency of molecular species delimitation in a species-rich insect family. *Molecular Ecology Resources*, 21, 1475–1489. <https://doi.org/10.1111/1755-0998.13352>
- Matsubayashi, K.W., Kahono, S., & Katakura, H. (2013). Divergent host plant preference causes assortative mating between sympatric host races of the

- ladybird beetle, *Henosepilachna diekei*. *Biological Journal of the Linnean Society*, 110, 606–614.
- Meegaskumbura, M., Wijayathilaka, N., Abayalath, N., & Senevirathne, G. (2015). Realities of rarity: climatically and ecologically restricted, critically endangered Kandian Torrent Toads (*Adenomus kandianus*) breed *en masse*. *PeerJ*, PrePrints. <https://doi.org/10.7287/peerj.preprints.1575v2> | CC
- Meier, R., Shiyang, K., Vaidya, G., & Ng, P. K. L. (2006). DNA barcoding and taxonomy in Diptera: a tale of high intraspecific variability and low identification success. *Systematic Biology*, 55 (5), 715–728. DOI: 10.1080/10635150600969864.
- Meier, R., Blaimer, B., Buenaventura, E., Hartop, E., von Rintelen, T., Srivathsan, A., & Yeo, D. (2021). A re-analysis of the data in Sharkey et al.'s (2021) minimalist revision reveals that BINs do not deserve names, but BOLD Systems needs a stronger commitment to open science. *Cladistics*. <https://doi.org/10.1111/cla.12489>
- Meierotto, S., Sharkey, M.J., Janzen, D.H., Hallwachs, W., Hebert, P.D.N., Chapman, E.G., & Smith, M.A. (2019). A revolutionary protocol to describe understudied hyperdiverse taxa and overcome the taxonomic impediment. *Deutsche Entomologische Zeitschrift*, 66 (2), 119–145.
- Modica, M.V., Puillandre, N., Castelin, M., Zhang, Y., & Holford, M. (2014). A good compromise: rapid and robust species proxies for inventorying biodiversity hotspots using the Terebridae (Gastropoda: Conoidea). *PLoS ONE*, 9(7), e102160. doi:10.1371/journal.pone.0102160.
- Myers, N., Mittermeier, R., Mittermeier, C., da Fonseca, G. A. B., & Kent, J. (2000). Biodiversity hotspots for conservation priorities. *Nature*, 403, 853–858. <https://doi.org/10.1038/35002501>
- Nagy, Z.T., Sonet, G., Glaw, F., & Vences, M. (2012). First large-scale DNA barcoding assessment of reptiles in the biodiversity hotspot of Madagascar, based on newly designed COI primers. *PLoS ONE*, 7(3), e34506. doi:10.1371/journal.pone.0034506.
- Nanayakkara, D., Jayatilake, D., & Kodithuwakku, S. (2020). Development of a single nucleotide polymorphism-based DNA marker for fall armyworm (Lepidoptera: Noctuidae) biotyping: a case study from the fall armyworm outbreak in Sri Lanka. *The Canadian Entomologist*, 152(6), 762–771. doi:10.4039/tce.2020.52.
- Nguyen, L.T., Schmidt, H.A., von Haeseler, A., & Minh, B.Q. (2015). IQ-TREE: A fast and effective stochastic algorithm for estimating maximum likelihood phylogenies. *Molecular Biology and Evolution*, 32, 268–274. <https://doi.org/10.1093/molbev/msu300>

- Oberprieler, S.K., Andersen, A.N., & Moritz, C.C. (2018). Ants in Australia's monsoonal tropics: CO1 barcoding reveals extensive unrecognised diversity. *Diversity*, 10, 36; doi:10.3390/d10020036
- Padial, J.M., Miralles, A., De la Riva, I., & Vences, M. (2010). The integrative future of taxonomy. *Frontiers in Zoology*, 7, 16. <https://doi.org/10.1186/1742-9994-7-16>.
- Papadopoulou, A., Anastasiou, I., Spagopoulou, F., Stalimerou, M., Terzopoulou, S., Legakis, A., & Vogler, A.P. (2011). Testing the species–genetic diversity correlation in the Aegean Archipelago: toward a haplotype-based macroecology? *The American Naturalist*, 178(2), 241–255.
- Pentinsaari, M., Hebert, P.D.N., Mutanen, M. (2014). Barcoding beetles: a regional survey of 1872 species reveals high identification success and unusually deep interspecific divergences. *PLoS ONE*, 9(9), e108651. <https://doi.org/10.1371/journal.pone.0108651>
- Perez, M.F., Franco, F.F., Bombonato, J.R., et al. (2018). Assessing population structure in the face of isolation by distance: Are we neglecting the problem? *Diversity and Distributions*, 24, 1883–1889. <https://doi.org/10.1111/ddi.12816>
- Puillandre, N., Lambert, A., Brouillet, S., & Achaz, G. (2012). ABGD, Automatic Barcode Gap Discovery for primary species delimitation. *Molecular Ecology*, 21, 1864–1877.
- Puillandre, N., Brouillet, S., & Achaz, G. (2021). ASAP: assemble species by automatic partitioning. *Molecular Ecology Resources*, 21, 609–620. <https://doi.org/10.1111/1755-0998.13281>.
- Pyron, R. A., Kandambi, H. K. D., Hendry, C. R., Pushpamal, V., Burbrink, F. T., & Somaweera, R. (2013). Genus-level phylogeny of snakes reveals the origins of species richness in Sri Lanka. *Molecular Phylogenetics and Evolution*, 66(3), 969–978. doi:10.1016/j.ympev.2012.12.004.
- Raheem, D.C., Breugelmans, K., Wade, C.M., Naggs, F.C., & Backeljau, T. (2017). Exploring the shell-based taxonomy of the Sri Lankan land snail *Corilla* H. and A. Adams, 1855 (Pulmonata: Corillidae) using mitochondrial DNA. *Molecular Phylogenetics and Evolution*, 107, 609–618. ISSN 1055-7903, <https://doi.org/10.1016/j.ympev.2016.12.020>.
- Raja, M. & Perumal, P. (2017). DNA Barcoding and Phylogenetic Relationships of Selected South Indian Freshwater Fishes Based on mtDNA COI Sequences. *Journal of Phylogenetics and Evolutionary Biology*, 5, 184. doi:10.4172/2329-9002.1000184.
- Rajpoot, A., Kumar, V.P., & Bahuguna, A. (2018). DNA barcodes and insights into the phylogenetic relationships of butterflies of the genus *Eurema* (Pieridae) from Uttarakhand, India. doi: <http://dx.doi.org/10.1101/242263>.

- Ranasinghe, S., Eberle J., Benjamin, S., & Ahrens, D. (2020). New species of Sericini from Sri Lanka (Coleoptera, Scarabaeidae). *European Journal of Taxonomy*, 621, 1–20.
- Rannala, B. & Yang, Z. (2020). Species Delimitation. p. 5.5:1–5.5:18. In: Scornavacca, C., Delsuc, F., Galtier, N. (eds) Phylogenetics in the genomic era. Authors open access book, <https://hal.inria.fr/PGE/>.
- Ratnasingham, S. & Hebert, P.D.N. (2013). A DNA-based registry for all animal species: the Barcode Index Number (BIN) system. *PLoS One*, 8, e66213.
- Rebijith, K.B., Asokan, R., Kumar, N.K.K., Srikumar, K.K., Ramamurthy, V.V., & Bhat, P.S. (2012). DNA Barcoding and Development of Species-Specific Markers for the Identification of Tea Mosquito Bugs (Miridae: Heteroptera) in India. *Molecular Ecology and Evolution*, 41(5), 1239–1245.
- Rulik, B., Eberle, J., Jung, M., Köhler, F., Apfel, W., Weigel, A., Kopetz, A., Köhler, J., Hadulla, K., Hartmann, M., Fritzlar, F., Schmidt, J., Astrin, J., Wägele, W., Geiger, M., Ahrens, D. (2017). Using taxonomic consistency with semi-automatized data preprocessing for high quality Barcode data. *Methods in Ecology and Evolution*, 8, 1878–1887.
- Sang, T. & Zhong, Y. (2000). Testing hybridization hypotheses based on incongruent gene trees. *Systematic Biology*, 49, 422–434.
- Schlick-Steiner, B.C., Steiner, F.M., Seifert, B., Stauffer, C., Christian, E., & Crozier, R.H. (2010). Integrative taxonomy: a multisource approach to exploring biodiversity. *Annual Review of Entomology*, 55, 421–438. <https://doi.org/10.1146/annurev-ento-112408-085432>
- Senevirathna, J.D.M. & Munasinghe, D.H.N. (2013). Identification of taxonomic status of spiny lobster species in Sri Lanka using DNA barcoding and its implications on fisheries and Conservation programs. *Tropical Agricultural Research*, 25, 96–108.
- Sharkey, M.J., Janzen, D.H., Hallwachs, W., Chapman, E.G., Smith, M.A., Dapkey, T., Brown, A., Ratnasingham, S., Naik, S., Manjunath, R., Perez, K., Milton, M., Hebert, P., Shaw, S.R., Kittel, R.N., Solis, M.A., Metz, M.A., Goldstein, P.Z., Brown, J.W., Quicke, D.L.J., van Achterberg, C., Brown, B.V., & Burns, J.M. (2021a). Minimalist revision and description of 403 new species in 11 subfamilies of Costa Rican braconid parasitoid wasps, including host records for 219 species. *ZooKeys*, 1013, 1–665.
- Sharkey, M., Brown, B., Baker, A. & Mutanen, M. (2021b). Response to Zamani *et al.* (2020). The omission of critical data in the pursuit of “revolutionary” methods to accelerate the description of species. *ZooKeys*, 1033, 191–201.
- Smith, M. A., Fisher, B. L., & Hebert, P. D. N. (2005). DNA barcoding for effective biodiversity assessment of a hyperdiverse arthropod group: the

- ants of Madagascar. *Philosophical Transactions of the Royal Society B: Biological Sciences*, 360(1462), 1825–1834. doi:10.1098/rstb.2005.1714.
- Smith, M.A., Bertrand, C., Crosby, K., Eveleigh, E.S., Fernandez-Triana, J., Fisher, B.L. et al. (2012). *Wolbachia* and DNA barcoding insects: patterns, potential, and problems. *PLoS ONE*, 7(5), e36514. <https://doi.org/10.1371/journal.pone.0036514>
- Song, H., Buhay, J.E., Whiting, M.F., & Crandall, K.A. (2008). Many species in one: DNA barcoding overestimates the number of species when nuclear mitochondrial pseudogenes are coamplified. *Proceedings of the National Academy of Sciences*, 105(36), 13486–13491; DOI: 10.1073/pnas.0803076105
- Sukumaran, J. & Knowles, L.L. (2017). Multispecies coalescent delimits structure, not species. *Proceedings of the National Academy of Sciences of the United States of America*, 114, 1607–1612.
- Taberlet, P., Coissac, E., Pompanon, F., Brochmann, C., & Willerslev, E. (2012). Towards next-generation biodiversity assessment using DNA metabarcoding. *Molecular Ecology*, 8, 2045–50. doi: 10.1111/j.1365-294X.2012.05470.x.
- Tembe, S., Shouche, Y., & Ghate, H.V. (2014). DNA barcoding of Pentatomomorpha bugs (Hemiptera: Heteroptera) from Western Ghats of India. *Meta Gene*, 2, 737–745.
- Templeton, A. R., Crandall, K. A., & Sing, C. F. (1992). A cladistic analysis of phenotypic associations with haplotypes inferred from restriction endonuclease mapping and DNA sequence data. III. Cladogram estimation. *Genetics*, 132 (2), 619–633.
- Templeton, A.R. (2001). Using phylogeographic analyses of gene trees to test species status and processes. *Molecular Ecology*, 10, 779–791.
- Thormann, B., Ahrens, D., Marín Armijos, D., Peters, M.K., Wagner, T., & Wägele, J.W. (2016) Exploring the leaf beetle fauna (Coleoptera: Chrysomelidae) of an Ecuadorian mountain forest using DNA barcoding. *PLoS ONE*, 11(2), e0148268. <https://doi.org/10.1371/journal.pone.0148268>
- Tyagi, K., Kumar, V., Singha, D., Chandra, K., Laskar, B.A., Kundu, S., Chakraborty, R., & Chatterjee, S. (2017). DNA Barcoding studies on Thrips in India: Cryptic species, Species complexes. *Scientific Reports*, 4898(7),1-14. Doi: 10.1038/s41598-017-05112-7
- van Strien, M. J., Holderegger, R., & Van Heck, H. J. (2015). Isolation-by-distance in landscapes: Considerations for landscape genetics. *Heredity*, 114(1), 27–37. <https://doi.org/10.1038/hdy.2014.62>

- Vogler, A.P. and Monaghan, M.T. (2007) Recent advances in DNA taxonomy. *Journal of Zoological Systematics and Evolutionary Research*, 45, 1–10. <https://doi.org/10.1111/j.1439-0469.2006.00384.x>
- Vogler, A.P., Rahman, Md. M., Burian, A., & Creedy, T.J. (2021). Metabarcoding to establish freshwater indicators of environmental degradation in the Indo-Burmese biodiversity hotspot. *ARPHA Conference Abstracts*, 4, e65364. <https://doi.org/10.3897/aca.4.e65364>
- Weeraratne, T.C., Surendran, S.N., Reimer, L.J., Wondji, C.S., Perera, M.D.B., Walton, C., & Karunaratne, S.H.P.P. (2018). Molecular characterization of Anopheline (Diptera: Culicidae) mosquitoes from eight geographical locations of Sri Lanka. *Malaria Journal*, 16, 234. DOI 10.1186/s12936-017-1876-y.
- Zamani, A., Vahtera, V., Sääksjärvi, I.E., & Scherz, M.D. (2021). The omission of critical data in the pursuit of ‘revolutionary’ methods to accelerate the description of species. *Systematic Entomology*, 46, 1–4.
- Zhang, J., Kapli, P., Pavlidis, P., & Stamatakis, A. (2013). A general species delimitation method with applications to phylogenetic placements. *Bioinformatics*, 29, 2869–2876.

3.6 Supplementary Figures



Figure S3.1 cont



Figure S3.1. Maximum likelihood tree from PhyML analysis. Approximate likelihood ratio test (aLRT) values >0.5 are shown next to the respective branches.



Figure S3.2. Split network of all examined specimens. Singletons are highlighted in blue squares, others in orange colours. Morphospecies nested within others are highlighted with red circles around them.

Chapter 4

Contrasting results of multiple species delimitation approaches cause uncertainty in synecological studies

This chapter is intended for publication in *Ecology Letters*:

Ranasinghe U.G.S.L., Thormann, J, Benjamin S.P., Bezděk, A., EberleJ, Ahrens D. (in-prep). Contrasting results of multiple species delimitation approaches cause uncertainty in synecological studies.

Authors' contributions to the original article:

SR, JE: fieldwork collections; JT, SR: molecular lab work; SR: sequence assembly and alignments, phylogenetic inference, DNA-based species delimitation, synecological analysis; JE: R scripts; AB: Diplotaxini identification; SR, DA: writing-original draft; DA, JE, SB, SR: manuscript review and editing.

Abstract

Biodiversity patterns are the sum of multiple overlapping species distributions. Their analysis therefore requires proper species inference. DNA-based species delimitation has become increasingly popular for such assessments and their robustness is often measured by congruence of multiple delimitation approaches. We explore how contrasting results of different species delimitations translate into conclusions of synecological studies, exemplified by assemblages of phytophagous scarab beetles in Sri Lanka from different elevations and forest types. Particularly, we compared estimates based on complete assemblages and on cumulated species inventories inferred from individually analysed subclades. These patterns of assemblage similarity were analysed across different spatial scales with reference to morphospecies and haplotypes. Method-related ambiguity of species estimates, which included particularly also subclade inferences, affected severely the certainty of biodiversity patterns at most spatial scales. In this case study of tropical beetles, haplotypes provided only very little explanatory information, since genetically highly diverse populations widely lacked shared haplotypes.

4.1 Introduction

Because of compelling advantage over traditional approaches in terms of speed and automation, DNA-based species identification has become a standardized and broadly used molecular approach for rapid biodiversity assessments (Sun et al., 2016; Gostel & Kress, 2022). Their use for biodiversity surveys compared to conventional taxonomy appears immense, including metabarcoding of whole organism communities (Creedy et al., 2022), environmental or extra-organismal DNA (eDNA; Taberlet et al., 2012), ingested DNA (iDNA; Schnell et al., 2012). All of them use high-throughput sequencing approaches (Leray & Knowlton, 2015), and are also comprised as next-generation biodiversity assessments (Elbrecht & Leese, 2015; Creedy et al., 2022; Huang et al., 2022; Steinke et al., 2022). This systematic large-scale DNA sequencing of entire communities allows the assessment of molecular diversity as well as the variation in community composition at species level and below (Baselga et al., 2015; Bush et al., 2019).

However, the success of DNA-based species inference heavily depends on a distinction between intraspecific and interspecific genetic variation across taxa (Phillips et al., 2019, 2022), which is often referred to as barcode gap (Meyer & Paulay, 2005; Ratnasingham & Hebert, 2013; Puillandre et al., 2012; 2021). For the recognition of this gap, each study requires sufficient sampling effort to capture adequate levels of within-species genetic variation (Meyer & Paulay, 2005; Eberle et al., 2020; Phillips et al., 2022). Independently of the type and number of marker used for the species delimitation, researchers from early on have recognized a certain incongruence between the outcome of DNA-based identification and morphology-based species assignments (e.g., Esselstyn et al., 2012; Fujisawa & Barraclough, 2013; Ratnasingham & Hebert, 2013; Ahrens et al., 2016). This was reasons why 1) the term molecular operational taxonomic units (MOTU) was introduced, which pragmatically defines groups of individuals by similarity that can but must not represent true species (Floyd et al., 2002; Blaxter et al., 2005), and 2) an integrative taxonomy and species delimitation was propagated (e.g., Padial et al., 2010; Schlick-Steiner et al., 2010; Carstens et al., 2013). Latter integrative framework would incorporate multiple lines of evidence but also alternative delimitation approaches and methods (e.g., threshold-based, character-based, tree- and coalescence-based methods) (Templeton et al., 1992; 2001; Will et al., 2005; Fujita et al., 2012; Puillandre et al., 2012; 2021; Zhang et al., 2013; Kapli et al., 2017). Beyond that, it was found that inherent characteristics of the species and assemblages itself such as fluctuating effective population size (Esselstyn et al., 2012; Fujisawa & Barraclough, 2013; Ahrens et al., 2016) and rareness of species (Lim et al., 2012; Ahrens et al., 2016) may have an important impact on the outcome of the species inference in which sampling design (i.e., the extent of taxa studied in a simultaneous species inferences step) becomes a crucial issue (Ahrens et al., 2016; Luo et al., 2018; Zhou et al., 2019).

To bypass some of these difficulties of incongruence with morphospecies or with the accurate species delimitation, particularly with mtDNA data and single marker data (e.g., COI), the use of haplotype data alone have been proposed as an unbiased and even more objective measure for biodiversity (Papadopoulou et al., 2011; García-Lopez et al., 2013; Baselga et al., 2015; Uscanga et al., 2021). A haplotype-based biodiversity research appeared to be completely independent from species concepts or delimitation methods including their assumptions (Thormann et al., 2016) and is currently extensively used in ecological metabarcoding studies (Gálvez-Reyes et al., 2020; Nogueras et al., 2021; Andujar et al., 2022). A haplotype-based macroecology (Baselga et al., 2013, Papadopoulou et al., 2011) was shown to work well for exploring macroecological patterns in poorly known biota and to predicting large-scale

biodiversity patterns by using haplotype diversity as a proxy for genetic and species diversity (Papadopoulou et al., 2011).

Among the different species delimitation methods proposed so far, the choice of a particular method has a considerable effect on estimated species entities and thus also on species richness estimates (Ahrens et al., 2016; Eberle et al., 2019; Zhou et al., 2019). With the ongoing employment of integrative approaches using multiple species delimitation methods, it became clear that neither of these always perfectly matches the morphospecies entities (e.g., Ahrens et al., 2013, 2016; Dalstein et al., 2019; Eberle et al., 2019; Lukic et al., 2021) nor do they rarely ever match among each other (Ranasinghe et al., 2022a). Although metabarcoding approaches use mainly distance based clustering algorithms with predefined thresholds for species circumscription (Callahan et al., 2017; Piper et al., 2019), several different pipelines or “cluster parameter values” are in use that may reveal alternative outcome (e.g., Potter et al., 2017; Alberdi et al., 2018; Creedy et al. 2019; Baitl et al., 2020) The threshold values used for sequence filtering and the number of reads for the identified MOTUs have an effect on the assessment accuracy of data (Edgar & Flyvbjerg, 2015; Potter et al., 2017; Piper et al., 2019, 2022; Meyer et al., 2021). The choice of the clustering threshold at 3% pairwise distance, as applied by the majority of studies (Elbrecht et al., 2017; Yu et al., 2012; Alberdi et al., 2018), or at 2% for similar taxa (Beentjes et al., 2019; Rossini et al., 2016; Smith et al., 2005) can have a significant impact on taxonomic inferences. Each step can potentially introduce its own sources of artefacts and biases which may inflate or deflate sample diversity estimates (Zinger et al., 2019; Liu et al., 2020).

In this study, we investigate the impact of alternative species estimates (MOTUs) on synecological analyses being applied to different entities of spatial scale (regional to local). Synecological studies bring together diversity measures at different collection points and integrate them into spatial entities with similar characteristics, such as species number and composition, which is why the methods that examine faunal similarity are applied in ecology as well as in biogeography. Outcome from both is important for providing a robust and stable reference point with biodiversity assessments, particularly for those that have potential impact on decisions of conservation management (e.g., van Jaarsveld et al., 1998; Ji et al., 2013; Floren et al., 2020; Uscanga et al., 2021; Yang et al., 2021).

4.2 Materials and Methods

Specimen sampling

The impact of alternative MOTU estimates for synecological analyses is investigated at hand of Sri Lankan species assemblages of phytophagous scarab chafers (Coleoptera: Scarabaeidae) (Ahrens et al., 2014). These beetles are polyphagous herbivorous and generally nocturnal; and represented in Sri Lanka by three subfamilies: Rutelinae, Melolonthinae and Dynastinae. Sampling of adult beetles was carried out at fifteen localities during 2019-2020 (Ranasinghe et al., 2020, 2022b) which included different forest types (evergreen wet lowland forest, evergreen dry lowland forest, sub-montane forest, and montane forest) and elevational zones. Beetles were captured using six UV-light traps per locality. All specimens (for collection details, see Table S4.1) were preserved in 96% ethanol after collecting. The collected specimens were presorted to morphospecies based on genital morphology using available taxonomic revisions and keys (Arrow, 1910; Endrödi, 1985; Ahrens et al., 2007; Fabrizi & Ahrens, 2014; Ahrens & Fabrizi, 2016; Ranasinghe et al., 2020, 2022b).

DNA sequencing

Three to seven individuals of each morphospecies per location were selected for DNA extraction and subsequent sequencing (in total 565 individuals). DNA was extracted from mesothoracic leg and attached muscles using the Qiagen® DNeasy Blood and Tissue Kit (Hilden, Germany) or the Qiagen® BioSprint 96 magnetic bead extractor (Hilden, Germany). Lab work followed the standard protocols of the German Barcode of Life project (Geiger et al., 2016). The primers LCO1490-JJ [5'-CHACWAAYCATAAAGATATYGG-3'] and HCO2198-JJ [5'-AWACTTCVGGRTGVCC AAARAATCA-3'] (Astrin & Stüben, 2008) were used to amplify a 658 bp fragment at the 5'-end of the mitochondrial gene cytochrome c oxidase subunit 1. PCRs of 90 samples were performed using the QIAGEN® Multiplex PCR Kit. The amplification products were subsequently checked by electrophoresis on a 1.5% agarose gel containing GelRed®. Successfully amplified DNA fragments were purified using Illustra™ ExoProStar™ Enzymatic PCR and Sequencing Clean-Up Kit. Forward and reverse strands were sequenced by Macrogen Europe (Macrogen, Amsterdam, the Netherlands; www.macrogen.com). PCRs for 475 samples were done in 96-well-plates. Unpurified PCR products were subsequently sent for purification and

bidirectional Sanger sequencing to BGI Tech Solutions (Hongkong, China). Sequences were assembled, edited and aligned using Geneious R7 (version 7.1.9, Biomatters Ltd.). All data are deposited in BOLD (project: SCOIB) and GenBank (accession numbers MW698204 - MW698469 (Sericini; Ranasinghe et al., 2022a) and XX-XX, (other taxa; see Table S4.1)).

Phylogenetic analysis

Maximum likelihood (ML; Felsenstein, 1973) searches were performed in IQ-TREE version 1.6.12 (Nguyen et al., 2015) under the (GTR+F+I+G4) model of nucleotide substitution that was inferred as the best fit model by ModelFinder (Kalyaanamoorthy et al., 2017). A total of 1000 ultrafast bootstrap (Hoang et al., 2018) replicates were done to assess branch supports. Then, the tree search was repeated ten times with the above parameters and the tree with highest likelihood was selected for further analysis.

Species delimitation

DNA-based species delimitation was performed using the multi-rate Poisson tree processes (mPTP) model (Zhang et al., 2013), statistical parsimony analysis using TCS (Templeton et al., 1992; 2001), Assemble Species by Automatic Partitioning (ASAP) (Puillandre et al., 2021). Poisson tree process modeling was performed on the mPTP web server (<https://mptp.h-its.org/#/tree>; accessed on 21 December 2021). mPTP (Kapli et al., 2017) is an improved method of PTP which does not require user-defined parameters. Using MCMC, it computes support values for each clade, which can be used to assess the confidence of the ML delimitation. The IQ-TREE result from previous phylogenetic analysis was used as input for all PTP analysis.

Statistical parsimony analysis was performed as implemented in TCS v. 1.21 (Clement et al., 2000). The procedure partitions the sequence data into clusters, i.e. subgroups (or networks) of closely related haplotypes connected by changes with a <95% probability to be non-homoplastic. Resulting networks have been found to be largely congruent with morphospecies at the 95 % threshold (Meier et al., 2006; Ahrens et al., 2007) and are considered here as MOTUs.

Assemble Species by Automatic Partitioning (ASAP) was conducted using the ASAP webserver (<https://bioinfo.mnhn.fr/abi/public/asap/> accessed on 21 December 2021) (Puillandre et al., 2020), using the distance matrix generated by

IQ-TREE. ASAP divides species partitions based on pairwise genetic distances. ASAP also computes a probability of panmixia (p-val), a relative gap width metric (W), and ranked results by the ASAP-score: the lower the score, the better the partition (Puillandre et al., 2021). The number of MOTUs predicted by ASAP's best score was selected and compared with other methods.

Furthermore, we employed clustering algorithms similar to those used in metabarcoding approaches, to explore the reliability of this critical step in current metabarcoding analysis pipelines (Macher et al., 2018). Distance-based clustering was done with the R-package (v. 4.1.2) spider (v. 1.5.0; Brown et al., 2012). A threshold of 3% was applied to the pairwise distance matrix of all specimens obtained from MEGA X (p-distance) (Kumar et al., 2018).

Since it is known that also the tree depth, i.e., the phylogenetic extent of sampling, may impact species delimitation analysis (Ahrens et al., 2016), we reanalyzed the current data set for its four principal monophyletic lineages as evident from the Maximum Likelihood tree obtained with IQ-TREE: clade 1: Rhizotrogini (+ Leucopholini); clade 2: Apogonia spp. (Diplotaxini); clade 3: Sericini; clade 4: Rutelinae + Dynastinae + Cetoniinae. Clade 1-3 formally comprise the subfamily Melolonthinae, which, however, in most current molecular phylogenies does not result monophyletic (Ahrens et al., 2014; McKenna et al., 2019). On these four subclades, the same delimitation methods as described above were applied (i.e., mPTP, TCS, ASAP, and 3% clustering).

The accuracy of DNA-based methods with prior morphospecies assignment was assessed by the match ratio (Ahrens et al., 2016): $2 \times N_{\text{match}} / (N_{\text{mol}} + N_{\text{morph}})$, where N_{match} is the number of exact matches of morphospecies (all individuals) with MOTUs of different delimitation methods, N_{mol} is the number of MOTUs that resulted from different delimitation methods, and N_{morph} is the number of morphospecies (Table S4.2). All morphospecies were mapped onto the terminals of the maximum likelihood tree and MOTUs obtained from different species delimitation methods, including subclade analysis (Fig. S1). Furthermore, the match ratios for all pairs of delimitation methods were calculated analogously as explained above and compared in a similarity matrix. Subsequently, the matrix was transformed into a distance matrix and a principal coordinate analysis (PCoA) was performed in PAST v.3.25 (Hammer et al., 2001) to visualize the similarity of outcome between the different methods (Ranasinghe et al., 2022a). The same was done for species inventories resulting from individual subclade analyses and cumulated inventories from individually performed species delimitation analyses on subclades, in which entities of each subclade delimitation were taken again

together for the entire assemblage, to explore whether species delimitation on subclades alone affected the overall outcome of delimitation analyses.

In addition, a few more alternative species delimitation approaches were conducted for the full assemblage data, for which, however, we did not perform synecological analyses, but we compared only the outcome of species delimitation. Poisson tree process modeling was performed with PTP web server (<https://species.h-its.org/>; accessed on 21 December 2021) using the maximum likelihood implementation (hereafter mlPTP; Zhang et al., 2013) with a single Poisson distribution, as well as the Bayesian implementation (bPTP), which adds Bayesian support (pp) values for putative species to branches in the input tree. Automatic Barcode Gap Discovery (ABGD) was conducted using the ABGD webserver (<https://bioinfo.mnhn.fr/abi/public/abgd/abgdweb.html>; accessed on 21 December 2021) using the distance matrix generated through IQ-TREE analysis with default parameters (i.e., a relative gap width of 1 and 50 steps, Pmin=0.001, Pmax=0.1, Nb bins for distance distribution= 20) (Puillandre et al., 2012). Distance-based clustering with 2% threshold was done with the R-package (v. 4.1.1). Then match ratio was calculated as above.

Synecological analysis

The analysis of species diversity and assemblage composition was performed for different spatial levels (forest type, elevation, locality) using morphospecies and the different MOTUs, namely haplotypes, mPTP clusters, TCS networks, ASAP clusters and 3% and 2% clusters. Species and MOTUs composition of each of these spatial entities was assessed for the entire assemblage, for individual subclades, and for cumulative MOTUs of subclades. Forest types included four entities: a) evergreen wet lowland forests, b) evergreen dry lowland forests, c) sub-montane forests, and d) montane forests. Elevational zones (EZ) included five entities: EZ1: 0–500 m, EZ2: 501–1000 m, EZ3: 1001–1500 m, EZ4: 1501–2000 m, and EZ5: 2001–2500 m. Localities included all 15 individual sampling localities. The dissimilarity in species/ MOTU composition of entities at each spatial level was measured using the Jaccard index (i.e., presence-absence data) using PAST v. 3.25 (Hammer et al., 2001). Results were visualized using non-metric multidimensional scaling (NMDS) and single linkage clustering (based on Jaccard index) at each spatial level.

Endemicity (unique vs shared occurrences) for entities at each spatial level was calculated for the morphospecies and MOTUs for the entire assemblage, single subclades, and cumulated species inventories from individually performed analyses of species delimitation for subclades.

4.3 Results

Of 4901 sampled specimens, 565 individuals were sequenced, of which 458 (81%) specimens representing 101 morphospecies were sequenced successfully and included 332 distinct haplotypes. Of the 101 morphospecies 27 were singletons (26.7% of all species), i.e., species represented by one specimen. Sixteen morphospecies (i.e., 15.8% of all species) had infraspecific distances larger than 3% (Fig. S6). Thirty-three morphospecies (or 12 haplotypes out of 332) were represented from more than one locality, but no one was found in more than half of all localities. The resulting maximum likelihood tree (Fig. S1) showed general agreement with subfamily and genus level classification (Ahrens et al., 2014; McKenna et al., 2019). Monophyletic clades resulted for all tribes (Diplotaxini, Sericini, Rhizotrogini and Leucopholini) and most subfamilies (Rutelinae and Dynastinae), the latter two formed a monophyletic sister clade. Melolonthinae was not monophyletic.

Species delimitation: full dataset vs subclade datasets

The different species delimitation methods (PTP, TCS, ASAP, 3% and 2% clustering) resulted in different numbers of MOTUs (Table S4.2). We found relatively limited congruence between molecular operational taxonomic units (MOTUs) and morphospecies as well as among the different DNA-based delimitation approaches (Figure S4.1). None of the employed species delimitation methods identically inferred species partitions, neither the prior morphospecies assignments. The total number of MOTUs varied from 82 to 129, compared to the morphospecies count of 101. These contradictions arise from splitting (the individuals of one morphospecies are assigned to two or more different MOTUs) or lumping phenomena (individuals of two or more different morphospecies are fused into one MOTU) (Figure S4.1). Only 37 MOTUs were obtained from all methods and also perfectly matched morphospecies. Eighty-three morphospecies assignments entirely matched with MOTUs of at least one delimitation method. Out of the 27 singleton morphospecies, 14 were also 'molecular singletons' for all delimitation methods, i.e. they were the unique representatives of a MOTU, while remaining 13 singletons, were lumped with other specimens into one MOTU.

Compared to the analyses of the full dataset, separate delimitation analyses on individual subclades showed minor differences (ASAP more splitting; PTP and TCS more lumping; 3%, 2% clustering with no differences). The match ratio was

higher in few cases (clade 4: ASAP; clade 3: TCS; clades 2 and 4: 3%, 2% clustering) for delimitation analyses on individual subclades (Table S4.2). The match ratio compared to the morphospecies assignments was lower for cumulative subclade analyses for ASAP, PTP, TCS, while for 3%, 2% it remained the same (Table S4.2). The number of summed MOTUs varied from 80 to 126 compared to 82 to 129 for the analysis of the full data set.

The PCoA ordination based on the similarity of pairwise match ratios of the different delimitation methods, also in relation to their match with morphospecies revealed contrasting patterns between the differently partitioned analyses (Figure 4.1); i.e. the full assemblage dataset, the four individual subclades, and for cumulative subclade analyses. None of the DNA-based methods conformed with prior morphospecies matches. Most importantly, the ordination patterns for the full assemblage dataset and cumulative subclade dataset are highly contrasting.

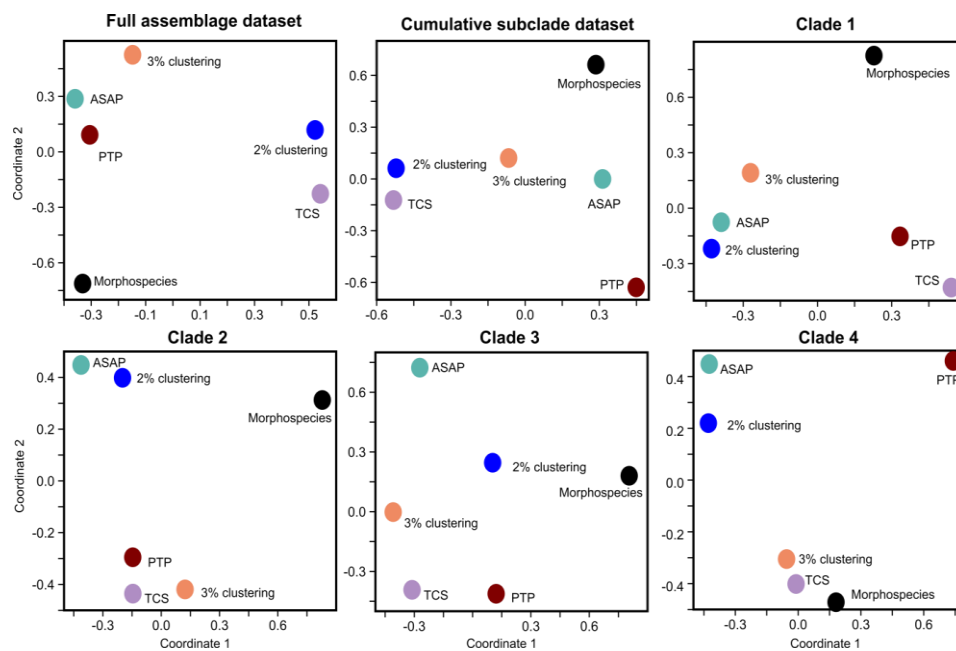
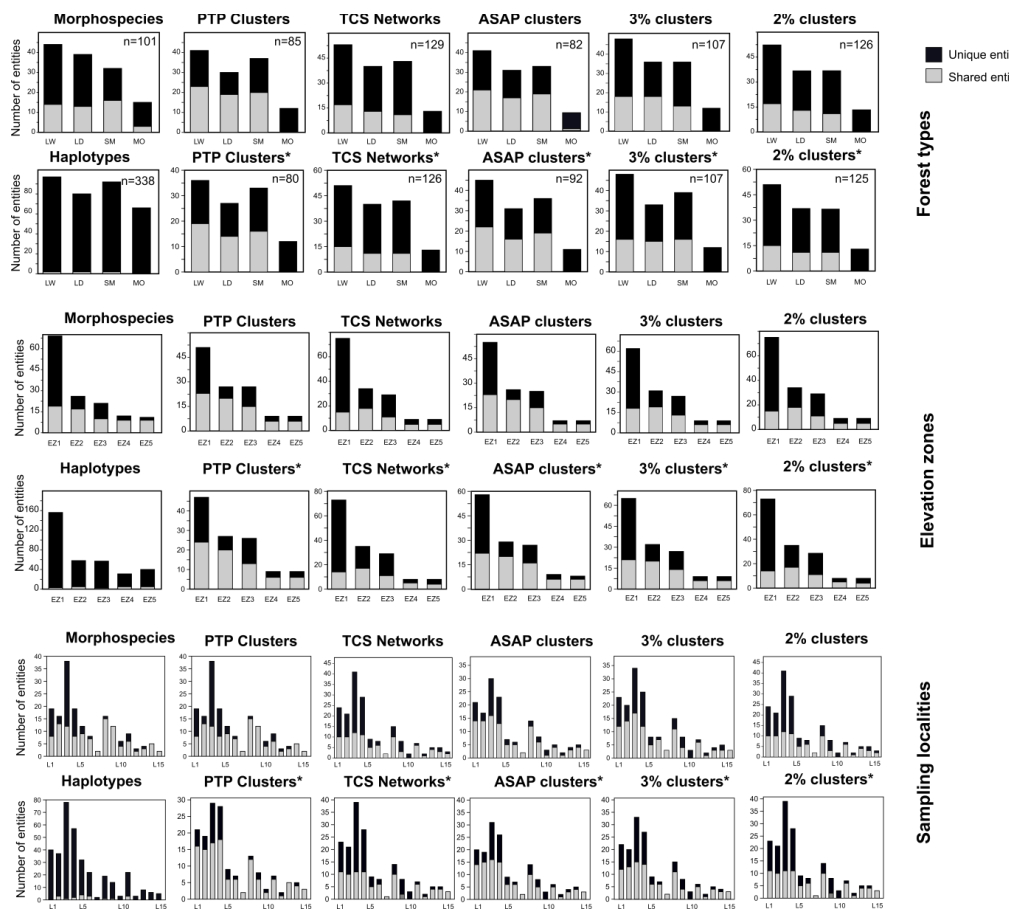


Figure 4.1. Principal coordinate analyses (PCoA) of results of different species delimitation methods based on pairwise match ratios for the total assemblage, individual subclades and cumulative subclade analyses. Clade 1: Rhizotrogini (+ Leucopholini); clade 2: *Apogonia* spp. (Diplotaxini); clade 3: Sericini; clade 4: Rutelinae + Dynastinae + Cetoniinae.

Species richness and assemblage similarity

The operational taxonomic entities (haplotypes, morphospecies, MOTUs) that were gained for the spatial partitions were similar between the full assemblage and the cumulative subclade analyses within each species delimitation approach, but differed strongly between the different delimitation approaches, also in comparison to the morphospecies (Figure 4.2, see Figure S4.3 for subclades). The numbers of unique and shared operational taxonomic entities for the spatial partitions were inconsistent between delimitations. All MOTUs (except one MOTU in ASAP) that occurred in montane forest were not found in other spatial partitions. The most striking result here was that almost all haplotypes were unique to each spatial entity and were restricted to either one forest type, elevation zone, or locality, except only few cases. Twelve haplotypes were shared among localities. This concerned in total only 10 morphospecies, in each case with single species that shared haplotypes at a maximum of three locations or a single species that shared haplotypes within two forest types (three individual cases) or adjacent elevation zones (ten individual cases). In contrast to exclusive haplotypes, morphospecies generally occurred at more than one locality and also higher level spatial zones. Some, however, also occurred exclusively at a single entity. Shared morphospecies were observed in 37 cases with a maximum of six localities; 21 cases for forest types and 30 cases for elevation zones and no species was found at all elevation zones.

The assemblage's compositional similarity (Jaccard index) was assessed for morphospecies, haplotypes and for MOTUs from the total dataset and cumulative subclade analysis. Outcome of the species delimitation approaches resulted in considerably different species compositions, leading to considerable variation in hierarchical clustering of spatial partitions (Figure 4.3; see Figure S4.4 for subclades). For the clustering of haplotype composition there were of course no alterations between full assemblage dataset or subclades (Figure 4.3; see Figure S4.4 for subclades). However, levels of haplotype sharing was by two magnitudes lower than that of MOTUs or of morphospecies (Table S4.3), which is why relations between spatial entities remain often unresolved, or very weakly connected.



4.2. Number of “species entities” reported for morphospecies, haplotypes, PTP-clusters, TCS networks, and distance clusters from the total assemblage and from cumulative subclade analyses (indicated by asterisk) for forest types, elevation zones and sampling localities. LW: wet lowland; LD: dry lowland; SM: sub-montane; MO: montane. EZ1: 0–500 m, EZ2: 501–1000 m, EZ3: 1001–1500 m, EZ4: 1501–2000 m, EZ5: 2001–2500 m. L1–L15 sampling localities.

Contrasting patterns of assembly composition were obtained between the full assemblage dataset vs the cumulative subclade analyses with PTP (forest types) and ASAP (elevation zone). Otherwise, very similar patterns were observed for the respective pairs of taxon sampling and delimitation strategies, despite generally differing total numbers of MOTUs. Match of compositional similarity with morphospecies pattern was rarely found, however. NMDS based on species compositional similarity (Jaccard index) showed similar results, although relations among haplotypes did not reveal with the plot that their NMDS “ecospace” was based simply on divergences rather than also on shared entities (Figure S4.2; see Figure S4.5 for subclades).

4.4 Discussion

Conflicts among different DNA-based species delimitation approaches are common (Zhou et al., 2019), but comparative studies to detect such conflicts and to show, how this translates into synecological signal in biodiversity assessments are rare, if not lacking at all, particularly when beyond species diversity also the similarity of the assessed probes or sites is investigated. Our study showed how contrasting results of species delimitation translate into conclusions of synecological studies, exemplified by assemblages of phytophagous scarab beetles in Sri Lanka. Method-related ambiguity of DNA-based species estimates, affected severely the certainty of biodiversity patterns at different spatial scales such as different elevations, forest types or sampling localities. We also demonstrated that differences in assemblage similarity patterns across different spatial scales emerged when DNA-based species estimates were based on the entire assemblage vs cumulatively composed assemblage with MOTUs delimited from subclade datasets.

Our results demonstrated that the congruence between the different delimitation methods was rather moderate as number of MOTUs varied from 82–129 (also 80–126 for cumulative analysis). TCS, 2%, 3% clustering produced higher species numbers (overestimation), while ASAP and mPTP lower numbers (underestimation) than prior morphospecies sorting. Consequently, patterns obtained by morphospecies, DNA-based delimitation methods and haplotypes were strongly contrasting each other in both total diversity and similarity patterns across different spatial scales and species turnover among assemblages (Fig. 2). Resulting MOTUs were often incongruent with the morphospecies due to lumping or splitting in different delimitation methods. In consequence, this resulted in different similarity patterns across which was more evident when various spatial scales were compared with reference to the morphospecies pattern. Shared MOTUs among allopatric, slightly divergent genetic clusters represent recently separated lineages that may have recently speciated or are still undergoing genetic differentiation. Since most diagnostic morphological characters such as genital organs in most insect are under strong selection they can evolve rapidly and often result in clearly definable morphospecies while species are not yet sorted by slowly recombining and possibly more slowly diverging mitochondrial haplotypes (Thompson, 1998; Gibbs, 2017; Eberle et al., 2016; Dietz et al. in review). On this may add patterns of introgression which is presumably more common in closely related species and may further confound specimen identification using mtDNA barcodes (Pentinsaari et al., 2014; Gibbs, 2017), which in the end will lead to contrasting synecological patterns.

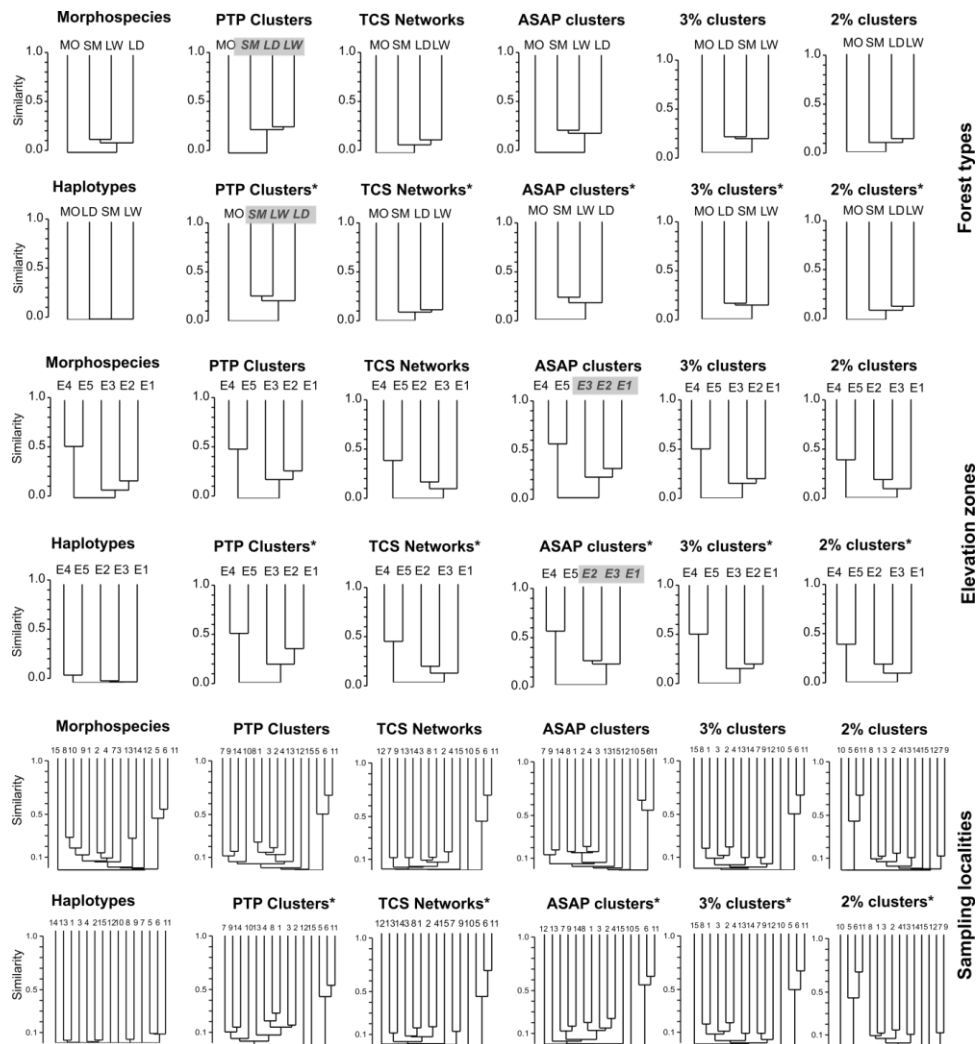


Figure 4.3. Clustering analysis based on the Jaccard index among morphospecies, haplotypes and MOTUs that result from delimitation of the total assemblage and from cumulative subclade analyses (indicated by asterisk) for forest types, elevation zones and sampling localities. Observed differences between total vs cumulative analyses are shown in bold italics. LW: wet lowland; LD: dry lowland; SM: sub-montane; MO: montane. EZ1: 0–500 m, EZ2: 501–1000 m, EZ3: 1001–1500 m, EZ4: 1501–2000 m, EZ5: 2001–2500 m. L1–L15 sampling localities.

Metabarcoding protocols for rapid biodiversity assessments, which also use COI as the frequent marker of choice as in DNA barcoding approaches (Deagle et al., 2014), include large-scale trapping, homogenised (‘souped’) mass-collected specimens, (optionally) mass-PCR-amplified for the barcode gene of interest and high-throughput sequencing and bioinformatic pipelines to process the resulting huge number of sequences down to a data set of manageable size (Yu et al.,

2012). As all other DNA-based species inference approaches, they suffer the same above-mentioned problems. Each one of their highly automatized steps (see above) can potentially introduce its own sources of artifacts and biases which inflate or deflate sample diversity estimates (Zinger et al., 2019; Liu et al., 2020). A majority of metabarcoding studies uses a 3% threshold clustering (Elbrecht et al., 2017; Yu et al., 2012; Alberdi et al., 2018), while alternative clustering thresholds with 2% may exaggerate the effect of species overestimation. Lineage-specific differences in the amount of interspecific divergence between species will lead to either overestimation or underestimation, depending on the cluster settings (Beentjes et al., 2019).

The choice of the ‘clustering threshold’ during species inference leads to different number of MOTUs (Smith et al., 2005), as confirmed also here (Fig. 1), which naturally alters the assemblage similarity. Barcoding studies suggest that there is no universal genetic distance threshold value (or ‘barcode gap’) to group species (Wiemers & Fiedler, 2007; Meier et al., 2008; Phillips et al., 2022). Using a fixed genetic threshold to distinguish taxa with different evolutionary histories may overestimate or underestimate species diversity (Meyer & Paulay, 2005; Ma et al., 2022). However, growing evidence suggests that the overlap between mean intra- and interspecific genetic distances is considerably greater with larger proportions of closely related taxa particularly also due to quite commonly occurring introgression (Ballard & Whitlock, 2004; Meyer & Paulay, 2005; Sun et al., 2016; Edelman & Mallet, 2021). Although, new software arises constantly and hardware improves rapidly in order to recover taxonomic information from a wider range of taxa by de novo OTU-picking pipelines (Yu et al., 2012; Elbrecht & Leese, 2015; Krehenwinkel et al., 2017), yet general problems given through the nature of species in diverse lineages will remain.

In our study case, we noted highest levels of intraspecific divergence at 10.46% (Figure S4.6), while in most species intraspecific divergences were rather low. But we found deep coalescence (i.e., distinct intraspecific phylogenetic structure), (e.g., *Sophrops* sp2, *Apogonia glabrilinea*, *A. coriacea*, *M. galdaththana*, *M. heveli*), so more than one of the DNA-based species delimitation methods split these morphospecies into different MOTUs. Such species with genetically well-differentiated populations occur in time and space, possibly due to lack of gene flow or by low dispersal between populations, for example, due to climatic fluctuation during the Pleistocene in geographically highly structured areas (Voris, 2000; Arora et al., 2010; Beck et al., 2017; Murria et al., 2017; Lukic et al., 2021; Dincă et al., 2021; French et al., 2022). Nevertheless, nature of maternal inheritance of mtDNA and its very low recombination rate also affects and partly causes the patterns of deep coalescence in mtDNA (Ballard & Whitlock, 2004).

This is one of a major reason encountered for inconsistencies in species delimitation output compared to morphospecies or nuclear genetic data.

Because of these problems, some previous studies on the genetic variation of mtDNA have used haplotypes as proxies for genetic diversity in the framework of a haplotype-based macroecology (Papadopoulou et al., 2011; Baselga et al., 2013). They demonstrated the utility of haplotype data for exploring macroecological patterns in poorly known biota and predicting largescale biodiversity patterns based on genetic inventories of local samples (Papadopoulou et al., 2011; Arribas et al., 2020). Metabarcoding-based haplotyping used this approach as it allows access to the intraspecific diversity and facilitated enhanced biodiversity monitoring (Sigsgaard et al., 2020; Shum & Palumbi, 2021).

Our results have shown, however, that the dissimilarity of assemblage composition between haplotypes at diverse spatial levels (Table S4.3) was extremely high. Almost all haplotypes were unique at any spatial entity, except a few rare cases. Therefore, clustering of haplotype composition (based on shared characteristics, i.e., haplotypes) resulted almost meaningless due to missing of shared haplotypes. Therefore, the basis for an ordination was the amount of divergence alone. This resulted in hierarchical clustering often in unresolved polytomy of entities (see Figures 4.3, S4.4) which makes haplotypes a poor proxy for compositional comparison of species diversity, at least in hyperdiverse and ancient tropical habitats (Barros et al., 2020; Cruz-Salazar et al., 2021; see also Rodríguez et al., 2015).

Haplotypes are simply products of divergence, species often carry more than a single haplotype (or can be even heteroplasmic: i.e., the presence of multiple haplotypes within an individual) (Gibbs, 2017). In contrast to that, species integrate different patterns by dispersal, inheritance, introgression, and recombination, all may occur at different intensity in time and space (Vellend & Geber, 2005; Epp et al., 2018), having thus a more complex, integrative, and significative meaning than simple diversity, i.e., the number of entities (e.g., MOTUs). Moreover, haplotype-derived patterns might be confounded if mtDNA groupings or genealogy does not reflect true species limits or the species' geographic extent (Murria et al., 2017; Paradis, 2018; Salinas-Ivanenko & Múrria, 2021).

Conclusion

DNA-based species identification is broadly used and popular for biodiversity assessments compared to conventional taxonomy. However due to incongruent outcomes from various species delimitation methods, particularly when researchers follow an integrative taxonomic approach (Carstens et al., 2013) provide certain ambiguities for synecological studies. Our study showed that such method-related ambiguity of DNA-based species estimates affected severely the patterns of faunal similarity and thus, the certainty of biodiversity patterns at different spatial scales such as elevations, forest types, or sampling localities. Nevertheless, even more contrasting patterns results from individual clade-wise analyses of faunal similarity or even from cumulated species inventories from individual clade-wise species delimitation analysis. In this context, our study underlines the need of awareness when synecological observations from different studies are integrated which use different species delimitation methods for their biodiversity assessment. At the same time, this shows why searching proper species boundaries should be the ultimate goal of biodiversity assessment to place the trust in species delimitations to give an enduring meaning to biodiversity research and its sustainable application (Carstens et al., 2013). In this even morphospecies, especially due to its globally complete and enormous reference system (Ahrens et al., 2021), remain a valid variable for biodiversity research.

Acknowledgments

Fieldwork for this study was fully funded by institutional funds of the ZFMK, Alexander Koenig Stiftung and by the German Academic Exchange Service (DAAD). S.R. was funded by the DAAD; S.P.B. were funded by the NIFS. We are extremely thankful to N. Athukorala (NIFS), S.R. family members; P.L. Dharmapriya, B. Ranasinghe & T.N. Dharmapriya for assistance in the fieldwork. We are furthermore thankful to C. Bohacz (ZFMK), D. Bopearachchi, A. Sathkunanathan, M. Tharmarajan, C. Jayatissa (all of the NIFS) & Supipi Wijesundara (UoP) assistance in the fieldwork. Prof. S. Wijesundara & Mr. C. Lekamge made available facility in the NIFS Arboretum. Also thanks to M. de Silva, Mr. Sampath for facilities in the Hiyare Conservation Center. We are thankful to all wildlife rangers (Nuwara Eliya, Hiyare, Horton Plains), regional forest officers (Kandy, Knuckles, Nuwara Eliya, Kottawa, Kanneliya) who helped us to conduct fieldwork. For providing research and collection permits to S.P.B, we thank the Department of Wildlife Conservation, Sri Lanka (permit no: WL/3/2/61/18), the Department of Forest Conservation, Sri Lanka (permit no:

R&E/RES/NFSRCM/2019-01 & R&E/RES/NFSRCM/EXTENSION/2020), the Divisional Forest Office, Kandy, Sri Lanka (permit no: K/G/01/06/03); Galle (M/0/03/2019).

4.5 References

- Ahrens, D. (2007). Beetle evolution in the Asian highlands: insight from a phylogeny of the scarabaeid subgenus *Serica* (Coleoptera, Scarabaeidae). *Systematic Entomology*, 32, 450–476.
- Ahrens, D., Monaghan, M.T. & Vogler, A.P. (2007). DNA-based taxonomy for associating adults and larvae in multi-species assemblages of chafers (Coleoptera. Scarabaeidae). *Molecular Phylogenetics and Evolution*, 44 (1), 436–449. doi: 10.1016/j.ympev.
- Ahrens, D., Zorn, C., Dhoj, G.C., Keller, S., & Nagel, P. (2007). Illustrated key of phytophagous scarabs of Nepal. – A Guide to white grubs and chafers of the lower central regions (Coleoptera, Scarabaeidae). *Opuscula Biogeographica basileensis*, 5, 1–44.
- Ahrens, D., Fabrizi, S., Sipek, P., & Lago, P. (2013). Integrative analysis of DNA phylogeography and morphology of the European rose chafer (*Cetonia aurata*) to infer species taxonomy and patterns of postglacial colonisation in Europe. *Molecular Phylogenetics and Evolution*, 69, 83–94.
- Ahrens, D., Schwarzer, J., & Vogler, A.P. (2014). The evolution of scarab beetles tracks the sequential rise of angiosperms and mammals. *Proceedings of the Royal Society B*, 281, 20141470.
- Ahrens, D. & Fabrizi, S. (2016). A monograph of the Sericini of India (Coleoptera: Scarabaeidae). *Bonn Zoological Bulletin*, 65, 1–355.
- Ahrens, D., Fujisawa, T., Krammer H.J., Eberle, J., Fabrizi, S., & Vogler, A.P. (2016). Rarity and incomplete sampling in DNA based species delimitation. *Systematic Biology*, 65, 478–494.
- Ahrens, D., Ahyong, S.T., Ballerio, A., Barclay, M.V.L., Eberle, J., Espeland, M., Huber, B.A., Mengual, X., Pacheco, T.L., Peters, R.S., Rulik, B., Vaz-de-Mello, F., Wesener, T., & Krell, F.T. (2021). Is it time to describe new species without diagnoses? - A comment on Sharkey et al. (2021). *Zootaxa*, 5027 (2), 151–159.
- Alberdi, A., Aizpurua, O., Gilbert, M.T.P., & Bohmann, K. (2018). Scrutinizing key steps for reliable metabarcoding of environmental samples. Mahon A, editor. *Methods in Ecology & Evolution*, 9, 134–147. <https://doi.org/10.1111/2041-210X.12849>

- Andujar, C., Arribas, P., López, H., Arjona, Y., P´erez-Delgado, A., Oromi, P., Vogler, A., & Emerson, B. (2022). Community assembly and metaphylogeography of soil biodiversity: insights from haplotype-level community DNA metabarcoding within an oceanic island. *Authorea*. doi: 10.22541/au.164212487.73179731/v1
- Astrin, J.J. & Stüben, P.E. (2008). Phylogeny in cryptic weevils: molecules, morphology and new genera of western Palaearctic Cryptorhynchinae (Coleoptera: Curculionidae). *Invertebrate Systematics*, 22 (5), 503–522. doi: 10.1071/IS07057.
- Arribas, P., Andujar, C., Salces-Castellano, A., Emerson, B.C., & Vogler, A.P. (2020). The limited spatial scale of dispersal in soil arthropods revealed with whole-community haplotype-level metabarcoding. *Molecular Ecology*, 30, 48–61 <https://doi.org/10.1111/mec.15591>
- Arora, N., Nater, A., van Schaik, C.P., Willems, E.P., van Noordwijk, M.A., Goossens, B., Morf, N., Bastian, M., Knott, C., Morrogh-Bernard, H., Kuze, N., Kanamori, T., Pamungkas, J., Perwitasari-Farajallah, D., Verschoor, E., Warren, K., Krützen, M., & Goodman, M. (2010). Effects of Pleistocene glaciations and rivers on the population structure of Bornean orangutans (*Pongo pygmaeus*). *Proceedings of the National Academy of Sciences of the United States of America*, 107(50), 21376–21381. <http://www.jstor.org/stable/25756892>
- Bailet, B., Apothéloz-Perret-Gentil, L., Baričević, A., Chonova, T., Franc, A., Frigerio, J., Kelly, M., Mora, D., Pfannkuchen, M., Proft, S., Ramon, M., Vasselon, V., Zimmermann, J. & Kahlert, M. (2020). Diatom DNA metabarcoding for ecological assessment: Comparison among bioinformatics pipelines used in six European countries reveals the need for standardization. *Science of the Total Environment*, 745, 140948. <https://doi.org/10.1016/j.scitotenv.2020.140948>.
- Ballard, J.W., & Whitlock, M.C. (2004). The incomplete natural history of mitochondria. *Molecular Ecology*, 13, 729–744. <https://doi.org/10.1046/j.1365-294X.2003.02063.x>
- Barros, M.J.F., Silva-Arias, G.A., Segatto, A.L.A., Reck-Kortmann, M., Fregonezi, J.N., Diniz-Filho, J.A.F., & Freitas, L.B. (2020). Phylogenetic niche conservatism and plant diversification in South American subtropical grasslands along multiple climatic dimensions. *Genetics and Molecular Biology*, 43, 2, e20180291
- Baselga, A., Gómez-Rodríguez, C., Novoa, F., & Vogler, A.P. (2013a). Rare failures of DNA barcodes to separate morphologically distinct species in a biodiversity survey of Iberian leaf beetles. *PloS ONE* 8(9), e74854. doi:10.1371/journal.pone.0074854

- Baselga, A., Fujisawa, T., Crampton-Platt, A., Bergsten, J., Foster, P.G., Monaghan, M.T., & Vogler, A.P. (2013). Whole-community DNA barcoding reveals a spatio-temporal continuum of biodiversity at species and genetic levels. *Nature Communications*, 4, 1892.
- Baselga, A., Gómez-Rodríguez, C., & Vogler, A.P. (2015). Multi-hierarchical macroecology at species and genetic levels to discern neutral and non-neutral processes. *Global Ecology and Biogeography*, 24, 873–882. <https://doi.org/10.1111/geb.12322>
- Bawa, K.S., Das, A., Krishnaswamy, J., Karanth, K.U., Kumar, S., & Rao, M. (2007). Ecosystem Profile: Western Ghats and Sri Lanka Biodiversity Hotspot Western Ghats Region. A report by Critical Ecosystem Partnership Fund, 95 pp.
- Beck, S.V., Carvalho, G.R., Barlow, A., Ruber, L., Tan, H.H, Nugroho, E., Wowor, D., Nor, S.A.M., Herder, F., Muchlisin, Z.A., & de Bruyn, M. (2017). Plio- Pleistocene phylogeography of the Southeast Asian Blue Panchax killifish, *Aplocheilus panchax*. *PloS One*, 12(7), e0179557. <https://doi.org/10.1371/journal.pone.0179557>
- Blaxter, M., Mann, J., Chapman, T., Thomas, F., Whitton, C., Floyd, R., & Abebe, E. (2005). Defining operational taxonomic units using DNA barcode data. *Philosophical Transactions of the Royal Society B: Biological Sciences*, 360(1462), 1935–1943.
- Beentjes, K.K., Speksnijder, A.G.C.L., Schilthuizen, M., Hoogeveen, M., Pastoor, R., & van der Hoorn, B.B. (2019). Increased performance of DNA metabarcoding of macroinvertebrates by taxonomic sorting. *PloS One*, 14(12), e0226527. <https://doi.org/10.1371/journal.pone.0226527>
- Brown, S.D.J., Collins, R.A., Boyer, S., Lefort, M.C., Malumbres-Olarte, J., Vink, C. J., & Cruickshank, R.H. (2012). SPIDER: An R package for the analysis of species identity and evolution, with particular reference to DNA barcoding. *Molecular Ecology Resources*, 12, 562–565.
- Bush, A., Compson, Z.G., Monk, W.A., Porter, T.M., Steeves, R., Emilson, E., Gagne, N., Hajibabaei, M., Roy, M, & Baird, D.J. (2019). Studying ecosystems with DNA Metabarcoding: Lessons from biomonitoring of aquatic macroinvertebrates. *Frontiers in Ecology and Evolution*, 7, 434. doi: 10.3389/fevo.2019.00434
- Callahan, B., McMurdie, P. & Holmes, S. (2017). Exact sequence variants should replace operational taxonomic units in marker-gene data analysis. *International Society for Microbial Ecology Journal*, 11, 2639–2643. <https://doi.org/10.1038/ismej.2017.119>
- Carstens, B.C., Pelletier, T.A., Reid, N.M. & Satler, J.D. (2013). How to fail at species delimitation. *Molecular Ecology*, 22, 4369–4383. <https://doi.org/10.1111/mec.12413>

- Clement, M., Posada, D., & Crandall, K. A. (2000). TCS: a computer program to estimate gene genealogies. *Molecular Ecology*, 9, 1657–1660.
- Coddington, J.A., Agnarsson, I., Miller, J.A., Kuntner, M., & Hormiga, G. (2009). Undersampling bias: the null hypothesis for singleton species in tropical arthropod surveys. *Journal of Animal Ecology*, 78, 573–584. doi: 10.1111/j.1365-2656.2009.01525.x PMID: 19245379.
- Coyne, J.A., & Orr, H.A. (2004). Speciation. Sinauer Associates, Inc., Sunderland, Mass.
- Creedy, T.J., Ng, W.S., & Vogler, A.P. (2019). Toward accurate species-level metabarcoding of arthropod communities from the tropical forest canopy. *Ecology and Evolution*, 9 (6), 3105–3116. <https://doi.org/10.1002/ece3.4839>
- Creedy, T.J., Andújar, C., Meramveliotakis, E., Noguerales, V., Overcast, I., Papadopoulou, A., Morlon, H., Vogler, A.P., Emerson, B.C., & Arribas, P. (2022). Coming of age for COI metabarcoding of whole organism community DNA: Towards bioinformatic harmonisation. *Molecular Ecology Resources*, 22, 847–861. <https://doi.org/10.1111/1755-0998.13502>
- Cruz-Salazar, B., Ruiz-Montoya, L., Ramírez-Marcial, N., García-Bautista, M. (2021). Relationship between genetic variation and diversity of tree species in tropical forests in the El Ocote Biosphere Reserve, Chiapas, Mexico. *Tropical Conservation Science*, 14, 1–14. <https://doi.org/10.1177/1940082920978143>
- Dalstein, V., Eberle, J., Fabrizi, S., Eitzbauer, C., & Ahrens, D. (2019). COI-based species delimitation in Indochinese *Tetraserica* chafers reveal hybridisation despite strong divergence in male copulation organs. *Organisms Diversity and Evolution*, 19, 277–286. doi: 10.1007/s13127-019-00398-z.
- Deagle, B.E., Jarman, S.N., Coissac, E., Pompanon, F., & Taberlet, P. (2014). DNA metabarcoding and the cytochrome c oxidase subunit I marker: not a perfect match. *Biology Letters*, 10, 20140562. <http://dx.doi.org/10.1098/rsbl.2014.0562>
- Dellicour, S., & Flot, J. (2018). The hitchhiker’s guide to single-locus species delimitation. *Molecular Ecology Resources*, 18(6), 1234–1246. <https://doi.org/10.1111/1755-0998.12908>
- Dincă, V., Dapporto, L., Somervuo, P., Vodă, R., Cuvelier, S., Gascoigne-Pees, M., Huemer, P., Mutanen, M., Hebert, P.D.N., & Vila, R. (2021). High resolution DNA barcode library for European butterflies reveals continental patterns of mitochondrial genetic diversity. *Communications Biology*, 4(1), 315.

- Eberle, J., Warnock, R.C.M., & Ahrens, D. (2016). Bayesian species delimitation in Pleophylla chafers (Coleoptera) –The importance of prior choice and morphology. *BMC Evolutionary Biology*, 16, 94. <https://doi.org/10.1186/s12862-016-0659-3>
- Eberle, J., Ahrens, D., Mayer, C., Niehuis, O., & Misof, B. (2020). A plea for standardized nuclear markers in metazoan DNA taxonomy. *Trends in Ecology & Evolution*, 35(4), 336–345.
- Edelman, N.B. & Mallet, J. (2021). Prevalence and adaptive impact of introgression. *Annual Review of Genetics*, 55, 265–83.
- Edgar, R.C. & Flyvbjerg, H. (2015). Error filtering, pair assembly and error correction for next-generation sequencing reads. *Bioinformatics*, 31, 3476–3482.
- Elbrecht, V. & Leese, F. (2015). Can DNA-based ecosystem assessments quantify species abundance? Testing primer bias and biomass—sequence relationships with an innovative metabarcoding protocol. *Plos One*, 10, e0130324
- Elbrecht, V., Vamos, E.E., Meissner, K., Aroviita, J., & Leese, F. (2017). Assessing strengths and weaknesses of DNA metabarcoding-based macroinvertebrate identification for routine stream monitoring. *Methods in Ecology and Evolution*, 8, 1265–1275. <https://doi.org/10.1111/2041-210x.12789>
- Endrödi, S. (1985). The Dynastinae of the world. Dordrecht, Boston, Lancaster: Dr. W. Junk Publishers, 800pp. Pls I-XXXI.
- Epp, L.S., Kruse, S., Kath, N.J. Stoof-Leichsenring, K.R., Tiedemann, R., Pestryakova, L.A., & Herzsuh, U. (2018). Temporal and spatial patterns of mitochondrial haplotype and species distributions in Siberian larches inferred from ancient environmental DNA and modeling. *Scientific Reports*, 8, 17436. <https://doi.org/10.1038/s41598-018-35550-w>
- Erichson, W.F. (1847). Naturgeschichte der Insecten Deutschlands. Erste Abtheilung. Coleoptera. vol. 3, Li. Berlin: Nicolaische Buchhandlung.
- Esselstyn, J., Evans, B., Sedlock, J., Anwarali Khan, F., & Heaney, L. (2012). Single-locus species delimitation: a test of the mixed Yule-coalescent model, with an empirical application to Philippine round-leaf bats. *Proceedings of the Royal Society B: Biological Sciences*, 279, 3678–86. [10.1098/rspb.2012.0705](https://doi.org/10.1098/rspb.2012.0705).
- Fabrizi, S. & Ahrens, D. (2014). A Monograph of the Sericini of Sri Lanka (Coleoptera: Scarabaeidae). *Bonn Zoological Bulletin Supplements*, 61, 1–124.
- Fan, X., Njeri, H.K., Pu, Y., La, Q., Li, W., Li, X., & Chen, Y. (2021). Contrasting relationships between genetic diversity and species diversity in conserved and disturbed submerged macrophyte communities of Honghu

- Lake, a typical freshwater lake of Yangtze River Basin. *Global ecology and conservation*, 31, e01873. doi: 10.1016/j.gecco.2021.e01873.
- Felsenstein, J. (1973). Maximum likelihood and minimum-step methods for estimating evolutionary trees from data on discrete characters. *Systematic Zoology*, 22, 240–249.
- Floren, A., von Rintelen, T., Hebert, P.D.N. et al. (2020). Integrative ecological and molecular analysis indicate high diversity and strict elevational separation of canopy beetles in tropical mountain forests. *Scientific Reports*, 10, 16677. <https://doi.org/10.1038/s41598-020-73519-w>
- Floyd, R., Abebe, E., Papert, A., & Blaxter, M. (2002). Molecular barcodes for soil nematode identification. *Molecular Ecology*, 11(4), 839–850. doi: 10.1046/j.1365-294X.2002.01485.x.
- French, C.M., Bertola, L.D., Carnaval, A.C., Economo, E.P., Kass, J.M., Lohman, D.J., Marske, K.A., Meier, R., Overcast, I., Rominger, A.J., Staniczenko, P., & Hickerson, M.J. (2022). Global determinants of the distribution of insect genetic diversity, *bioRxiv*, doi: <https://doi.org/10.1101/2022.02.09.479762>
- Fujisawa, T. & Barraclough, T.G. (2013). Delimiting species using single-locus data and the generalized mixed Yule coalescent approach: a revised method and evaluation on simulated data sets. *Systematic Biology*, 62, 707–724.
- Fujita, M.K., Leaché, A.D., Burbrink, F.T., McGuire, J.A., & Moritz, C. (2012). Coalescent-based species delimitation in an integrative taxonomy. *Trends in Ecology and Evolution*, 27(9), 480-8. doi: 10.1016/j.tree.2012.04.012. Epub 2012 May 25. PMID: 22633974.
- Gálvez-Reyes, N., Arribas, P., Andujar, C., Emerson, B., Píñero, D., & Mastretta-Yanes, A. (2020). Local-scale dispersal constraints promote spatial structure and arthropod diversity within a tropical sky-island. *Authorea*. DOI: 10.22541/au.160193334.45224582/v1
- García-Lopez, A., Mico, E., Murria, C., Galante, E., & Vogler, A.P. (2013). Beta diversity at multiple hierarchical levels: explaining the high diversity of scarab beetles in tropical montane forests. *Journal of Biogeography*, 40, 2134–2145.
- Geiger, M.F., Moriniere, J., Hausmann, A., Haszprunar, G., Wägele, W., Hebert, P.D.N., & Rulik, B. (2016). Testing the global Malaise trap program - How well does the current barcode reference library identify flying insects in Germany? *Biodiversity Data Journal*, 4, e10671.
- Gibbs, J., (2017). DNA barcoding a nightmare taxon: assessing barcode index numbers and barcode gaps for sweat bees. *Genome*, 61(1), 21–31. <https://doi.org/10.1139/gen-2017-0096>

- Gostel, M.R., & Kress, W.J., (2022). The Expanding Role of DNA Barcodes: Indispensable Tools for Ecology, Evolution, and Conservation. *Diversity*, 14, 213. <https://doi.org/10.3390/d14030213>
- Hammer, O, Harper, D.A.T., & Ryan, P.D. (2001). Paleontological statistics software package for education and data analysis. *Palaeontologia Electronica*, 4, 1–9.
- Hoang, D.T., Chernomor, O., Haeseler, A. von, Minh, B.Q., & Vinh, L.S. (2018). UFBoot2: Improving the ultrafast bootstrap approximation. *Molecular Biology and Evolution*, 35, 518–522. <https://doi.org/10.1093/molbev/msx281>
- Huang, J., Miao, X., Wang, Q., Menzel, F., Tang, P., Yang, D., Wu, H., & Vogler, A. P. (2022). Metabarcoding reveals massive species diversity of Diptera in a subtropical ecosystem. *Ecology and Evolution*, 12, e8535. <https://doi.org/10.1002/ece3.8535>
- Ji, Y. et al. (2013). Reliable, verifiable and efficient monitoring of biodiversity via metabarcoding. *Ecology Letters*, 16, 1245–1257. (doi:10.1111/ele.12162)
- Kapli, T., Lutteropp, S., Zhang, J., Kobert, K., Pavlidis, P., Stamatakis, A., & Flouri, T. (2017). Multi-rate Poisson tree processes for single-locus species delimitation under maximum likelihood and Markov chain Monte Carlo. *Bioinformatics*, 33(11), 1630–1638. doi:10.1093/bioinformatics/btx025
- Kalyaanamoorthy, S., Minh, B.Q., Wong, T.K.F., Haeseler, A. von, & Jermini, L.S. (2017). ModelFinder: Fast model selection for accurate phylogenetic estimates. *Nature Methods*, 14, 587–589. <https://doi.org/10.1038/nmeth.4285>
- Kamenova, S. (2020). A flexible pipeline combining clustering and correction tools for prokaryotic and eukaryotic metabarcoding. *Peer Community in Ecology*, 100043. [10.24072/pci.ecology.100043](https://doi.org/10.24072/pci.ecology.100043)
- Krehenwinkel, H., Wolf, M., Lim, J. Y., Rominger, A. J., Simison, W. B., & Gillespie, R. G. (2017). Estimating and mitigating amplification bias in qualitative and quantitative arthropod metabarcoding. *Scientific Reports*, 7(1), 1–12. <https://doi.org/10.1038/s41598-017-17333-x>
- Kumar, S., Stecher, G., Li, M., Knyaz, C., & Tamura, K. (2018). MEGA X: Molecular Evolutionary Genetics Analysis across computing platforms. *Molecular Biology and Evolution*, 35, 1547–1549.
- Leray, M., & Knowlton, N. (2015). DNA barcoding and metabarcoding of standardized samples reveal patterns of marine benthic diversity. *Proceedings of the National Academy of Sciences*, 112 (7), 2076–2081 <https://doi.org/10.1073/pnas.1424997112>
- Lim, G., Balke, M., & Meier, R. (2012). Determining species boundaries in a world full of rarity: Singletons, species delimitation methods. *Systematic Biology*, 61, 165–169.

- Liu, M., Clarke, L.J., Baker, S.C., Jordan, G.J., & Burridge, C.P. (2020). A practical guide to DNA metabarcoding for entomological ecologists. *Ecological Entomology*, 45, 373–385. <https://doi.org/10.1111/een.12831>
- Lukic, D., Eberle, J., Thormann, J., Holzschuh, C., & Ahrens, D. (2021). Excluding spatial sampling bias does not eliminate over-splitting in DNA-based species delimitation analyses. *Ecology and Evolution*, 11, 10327–10337. <https://doi.org/10.1002/ece3.7836>
- Luo, A., Ling, C., Ho, S.Y.W., & Zhu, C.D. (2018). Comparison of methods for molecular species delimitation across a range of speciation scenarios. Mueller R, editor. *Systematic Biology*, 67, 830–846. <https://doi.org/10.1093/sysbio/syy011> PMID: 29462495
- Ma, Z. Ren, J. & Zhang, R. (2022). Identifying the Genetic Distance Threshold for Entiminae (Coleoptera: Curculionidae) Species Delimitation via COI Barcodes. *Insects*, 13, 261. <https://doi.org/10.3390/insects13030261>
- Macher, J.N., Vivancos, A., Piggott, J.J., Centeno, F.C., Matthaei, C.D., & Leese, F. (2018). Comparison of environmental DNA and bulk-sample metabarcoding using highly degenerate cytochrome c oxidase I primers. *Molecular Ecology Resources*, 18(6), 1456–1468. <https://doi.org/10.1111/1755-0998.12940>
- Mattsson, E., Persson, U.M., Ostwald, M., & Nissanka, S.P. (2012). REDD+ readiness implications for Sri Lanka in terms of reducing deforestation. *Journal of Environmental Management*, 100, 29–40. <https://doi.org/10.1016/j.jenvman.2012.01.018>
- McKenna, D.D. et al. (2019). The evolution and genomic basis of beetle diversity. *Proceedings of the National Academy of Sciences*, 116, 24729–24737. (<https://doi.org/10.1073/pnas.1909655116>)
- Meegaskumbura, M., Wijayathilaka, N., Abayalath, N., & Senevirathne, G. (2015). Realities of rarity: climatically and ecologically restricted, critically endangered Kandian Torrent Toads (*Adenomus kandianus*) breed en masse. *PeerJ, PrePrints*. <https://doi.org/10.7287/peerj.preprints.1575v2> | CC
- Meier, R., Shiyang, K., Vaidya, G., & Ng, P. K. L. (2006). DNA barcoding and taxonomy in Diptera: a tale of high intraspecific variability and low identification success. *Systematic Biology*, 55 (5), 715–728. DOI: 10.1080/10635150600969864.
- Meier, R., Zhang, G., & Ali, F. (2008). The use of mean instead of smallest interspecific distances exaggerates the size of the “Barcoding Gap” and leads to misidentification. *Systematic Biology*, 57, 5809–813, <https://doi.org/10.1080/10635150802406343>
- Meier, R., Blaimer, B.B., Buenaventura, E., Hartop, E., von Rintelen, T., Srivathsan, A. & Yeo, D. (2022). A re-analysis of the data in Sharkey

- et al.'s (2021) minimalist revision reveals that BINs do not deserve names, but BOLD Systems needs a stronger commitment to open science. *Cladistics*, 38: 264–275. <https://doi.org/10.1111/cla.12489>
- Meierotto, S., Sharkey, M.J., Janzen, D.H., Hallwachs, W., Hebert, P.D.N., Chapman, E.G., & Smith, M.A. (2019). A revolutionary protocol to describe understudied hyperdiverse taxa and overcome the taxonomic impediment. *Deutsche Entomologische Zeitschrift*, 66 (2), 119–145.
- Meyer, C.P., & Paulay, G. (2005). DNA barcoding: error rates based on comprehensive sampling. *PLoS Biol*, 3, 2229–2238.
- Meyer, A., Boyer, F., Valentini, A., Bonin, A., Ficetola, G.F., Beisel, J., Bouquerel, J., Wagner, P., Gaboriaud, C., Leese, F., Dejean, T., Taberlet, P., & Usseglio-Polater, P. (2021). Morphological vs. DNA metabarcoding approaches for the evaluation of stream ecological status with benthic invertebrates: Testing different combinations of markers and strategies of data filtering. *Molecular Ecology*, 30, 3203–3220. <https://doi.org/10.1111/mec.15723>
- Murria, C., Bonada, N., Vellend, M., Zamora-Munoz, C., Alba-Tercedor, J., Elisa Sainz-Cantero, C., Garrido, J., Acosta, R., El Alami, M., Barquin, J., Derka, T., Alvarez-Cabria, M., Sainz-Bariain, M., Filipe, A.F., & Vogler, A.P. (2017). Local Environment Rather than Past Climate Determines Community Composition of Mountain Stream Macroinvertebrates across Europe. *Molecular Ecology* 26(21), 6085–6099.
- Noguerales, V., Meramveliotakis, E., Castro-Insua, A., Andújar, C., Arribas, P., Creed, T. J., Overcast, I., Morlon, H., Emerson, B. C., Vogler, A. P., & Papadopoulou, A. (2021). Community metabarcoding reveals the relative role of environmental filtering and spatial processes in metacommunity dynamics of soil microarthropods across a mosaic of montane forests. *Molecular Ecology*, 00, 1– 19. <https://doi.org/10.1111/mec.16275>
- Papadopoulou, A., Anastasiou, I., Spagopoulou, F., Stalimerou, M., Terzopoulou, S., Legakis, A., & Vogler, A.P. (2011). Testing the species–genetic diversity correlation in the Aegean Archipelago: toward a haplotype-based macroecology? *The American Naturalist*, 178(2), 241– 255.
- Papadopoulou, A., Cardoso, A., & Gomez-Zurita, J. (2013). Diversity and diversification of Eumolpinae (Coleoptera: Chrysomelidae) in New Caledonia. *Zoological Journal of the Linnean Society*, 168, 473–495. doi: 10.1111/ zoj.12039
- Paradis, E. (2018). Analysis of haplotype networks: The randomized minimum spanning tree method. *Methods in Ecology and Evolution*, 9, 1308–1317. <https://doi.org/10.1111/2041-210X.12969>
- Pentinsaari, M., Mutanen, M., & Kaila, L. (2014). Cryptic diversity and signs of mitochondrial introgression in the *Agrilus viridis* species complex

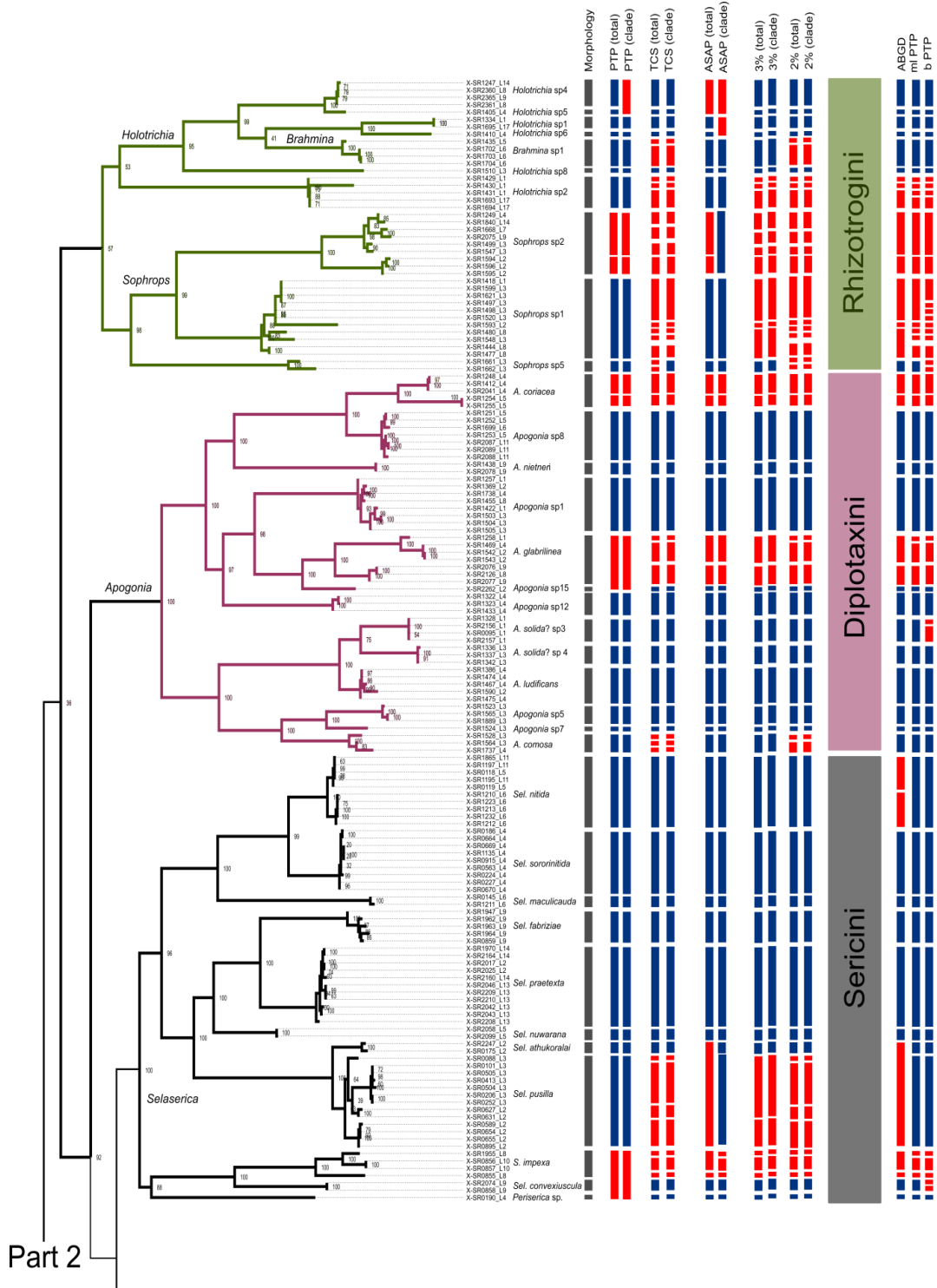
- (Coleoptera: Buprestidae). *European journal of entomology*, 111(4), 475–486. doi:10.14411/eje.2014.072)
- Phillips, J.D., Gillis, D.J., & Hanner, R.H. (2022). Lack of statistical rigor in DNA barcoding likely invalidates the presence of a true species' barcode gap. *Frontiers in Ecology and Evolution*, 10, 859099. doi: 10.3389/fevo.2022.859099
- Piper, A.M., Cunningham, J.P., Cogan, N.O.I. & Blacket, M.J. (2022). DNA metabarcoding enables high-throughput detection of spotted wing *Drosophila* (*Drosophila suzukii*) within unsorted trap catches. *Frontiers in Ecology and Evolution*, 10, 822648. doi: 10.3389/fevo.2022.822648
- Piper, A.M., Batovska, J., Cogan, N.O.I., Weiss, J., Cunningham, J.P., Rodoni, B.C., et al. (2019). Prospects and challenges of implementing DNA metabarcoding for high-throughput insect surveillance. *Gigascience*, 8, giz092. doi: 10.1093/gigascience/giz092
- Potter, C., Tang, C.Q., Fonseca, V., Lallias, D., Gaspar, J.M., Thomas, K., & Creer, S. (2017). De novo species delimitation in metabarcoding datasets using ecology and phylogeny. *PeerJ Preprints*, 5, e3121v1 <https://doi.org/10.7287/peerj.preprints.3121v1>
- Phillips, J.D., Gillis, D.J., & Hanner, R.H. (2019). Incomplete estimates of genetic diversity within species: implications for DNA barcoding. *Ecology and Evolution*, 9, 2996–3010. doi: 10.1002/ece3.4757
- Phillips, J.D., Gillis, D.J. & Hanner, R.H. (2022). Lack of Statistical Rigor in DNA Barcoding Likely Invalidates the Presence of a True Species' Barcode Gap. *Frontiers in Ecology and Evolution*, 10, 859099. doi: 10.3389/fevo.2022.859099
- Puillandre, N., Lambert, A., Brouillet, S., & Achaz, G. (2012). ABGD, Automatic Barcode Gap Discovery for primary species delimitation. *Molecular Ecology*, 21, 1864–1877.
- Puillandre, N., Brouillet, S., & Achaz, G. (2021). ASAP: assemble species by automatic partitioning. *Molecular Ecology Resources*, 21, 609–620. <https://doi.org/10.1111/1755-0998.13281>.
- Rannala, B. & Yang, Z. (2020). Species Delimitation. p. 5.5:1–5.5:18. In: Scornavacca, C., Delsuc, F., Galtier, N. (eds) *Phylogenetics in the genomic era*. Authors open access book, <https://hal.inria.fr/PGE/>.
- Ranasinghe, S., Eberle, J., Bohacz, C., Benjamin, S., & Ahrens, D. (2020). New species of Sericini from Sri Lanka (Coleoptera, Scarabaeidae). *European Journal of Taxonomy*, 621, 1–20.
- Ranasinghe, U.G.S.L., Eberle, J., Thormann, J., Bohacz, C., Benjamin, S., & Ahrens D. (2022a). Multiple species delimitation approaches with COI barcodes poorly fit each other and with morphospecies – an integrative

- taxonomy case of Sri Lankan Sericini chafers (Coleoptera: Scarabaeidae), *Ecology and Evolution*, 12, e8942. <https://doi.org/10.1002/ece3.8942>
- Ranasinghe, S., Eberle, J., Athukorala, N., Benjamin, S., & Ahrens, D. (2022b). New species of Sericini from Sri Lanka (Coleoptera, Scarabaeidae) II. *European Journal of Taxonomy*, 821, 57–101.
- Ratnasingham, S. & Hebert, P.D.N. (2013). A DNA-based registry for all animal species: the Barcode Index Number (BIN) system. *PLoS One*, 8, e66213
- Rathnayake, C., Jones, S. & Soto-Berelov, M. (2020). Mapping Land Cover Change Over a 25-Year Period (1993–2018) in Sri Lanka Using Landsat Time-Series. *Land*, 9, 27; doi:10.3390/land9010027
- Richer, P.O. (1958). Biology of Scarabaeidae. *Annual Review of Entomology*, 3, 311–334. <https://doi.org/10.1146/annurev.en.03.010158.001523>
- Rodríguez, A., Börner, M., Pabijan, M., Gehara, M., Haddad, C.F.B., & Vences, M. (2015). Genetic divergence in tropical anurans: deeper phylogeographic structure in forest specialists and in topographically complex regions. *Evolutionary Ecology*, 29, 765–785 <https://doi.org/10.1007/s10682-015-9774-7>
- Rossini, B.C., Oliveira, C.A.M., de Melo, F.A.G., Bertaco, V.D., de Astarloa, J.M.D., Rosso, J.J., et al. (2016). Highlighting Astyanax species diversity through DNA barcoding. *PLoS One*, 11, e0167203.
- Salinas-Ivanenko, S., & Múrria, C. (2021). Macroecological trend of increasing values of intraspecific genetic diversity and population structure from temperate to tropical streams. *Global Ecology and Biogeography*, 30, 1685–1697. <https://doi.org/10.1111/geb.13344>
- Schnell, I.B., Thomsen, P.F., Wilkinson, N., Rasmussen, M., Jensen, L.R.D., Willerslev, E., Bertelsen, M.F., & Gilbert, M.T.P. (2012). Screening mammal biodiversity using DNA from leeches. *Current Biology*, 22(8), R262–R263. <https://doi.org/10.1016/j.cub.2012.02.058>
- Sigsgaard, E.E., Jensen, M.R., Winkelmann, I.E., Møller, P.R., Hansen, M.M., & Thomsen, P.F. (2020). Population-level inferences from environmental DNA—Current status and future perspectives. *Evolutionary Applications*, 13, 245–262. <https://doi.org/10.1111/eva.12882>
- Shum, P., & Palumbi, S.R. (2021). Testing small-scale ecological gradients and intraspecific differentiation for hundreds of kelp forest species using haplotypes from metabarcoding. *Molecular Ecology*, 30, 3355–3373. <https://doi.org/10.1111/mec.15851>
- Smith, M.A., Fisher, B.L., & Hebert, P.D.N. (2005). DNA barcoding for effective biodiversity assessment of a hyperdiverse arthropod group: the ants of Madagascar. *Philosophical Transactions of the Royal Society B: Biological Sciences*, 360, 1825–34.

- Steinke, D., deWaard, S.L., Sones, J.E., Ivanova, N.V., Prosser, S.W. J., Perez, K., Braukmann, T.W.A., Milton, M., Zakharov, E.V., deWaard, J.R., Ratnasingham, S., & Hebert, P.D.N. (2022). Message in a Bottle—Metabarcoding enables biodiversity comparisons across ecoregions, *GigaScience*, 11, giac040, <https://doi.org/10.1093/gigascience/giac040>
- Sun, S. et al. (2016). DNA barcoding reveal patterns of species diversity among northwestern Pacific molluscs. *Scientific Reports*, 6, 33367; doi: 10.1038/srep33367.
- Taberlet, P., Coissac, E., Pompanon, F., Brochmann, C., & Willerslev, E. (2012). Towards next-generation biodiversity assessment using DNA metabarcoding. *Molecular Ecology*, 8, 2045–2050. <https://doi.org/10.1111/j.1365-294X.2012.05470.x>
- Templeton, A.R., Crandall, K.A., & Sing, C.F. (1992). A cladistic analysis of phenotypic associations with haplotypes inferred from restriction endonuclease mapping and DNA sequence data. III. Cladogram estimation. *Genetics*, 132 (2), 619–633.
- Templeton, A.R. (2001). Using phylogeographic analyses of gene trees to test species status and processes. *Molecular Ecology*, 10, 779–791.
- Thompson, J.N. (1998). Rapid evolution as an ecological process. *Trends Ecology and Evolution*, 13(8), 329–332. doi:10.1016/S0169-5347(98)01378-0. PMID:21238328.)
- Uscanga, A., López, H., Piñero, D., Emerson, B.C., Mastretta-Yanes, A. (2021). Evaluating species origins within tropical sky-islands arthropod communities. *Journal of Biogeography*, 48, 2199–2210. <https://doi.org/10.1111/jbi.14144>
- van Jaarsveld A.S., Freitag, S., Chown, S.L., Muller, C., Koch, S., Hull, H., Bellamy, C., Krüger, M., Endrödy-Younga, S., Mansell, M.W., & Scholtz, C.H. (1998). Biodiversity assessment and conservation strategies. *Science*, 279, 2106–2108.
- Vellend, M., & Geber, M.A. (2005). Connections between species diversity and Genetic diversity: species diversity and genetic diversity. *Ecology Letters*, 8(7), 767–781.
- Voris, H.K. (2000). Maps of Pleistocene sea levels in Southeast Asia: shorelines, river systems and time durations. *Journal of Biogeography*, 27, 1153–1167. <https://doi.org/10.1046/j.1365-2699.2000.00489.x>
- Wiemers, M., & Fiedler, K. (2007). Does the DNA barcoding gap exist? – a case study in blue butterflies (Lepidoptera: Lycaenidae). *Frontiers in Zoology*, 4, 8 <https://doi.org/10.1186/1742-9994-4-8>

- Will, K.W., Mishler, B.D., & Wheeler, Q.D. (2005). The Perils of DNA Barcoding and the Need for Integrative Taxonomy, *Systematic Biology*, 54, 5, 844–851, <https://doi.org/10.1080/10635150500354878>
- Yang, J., Zhang, X., Jin, X., Seymour, M., Richter, C., Logares, R., Khim, J.S. & Klymus, K. (2021). Recent advances in environmental DNA-based biodiversity assessment and conservation. *Diversity and Distribution*, 27, 1876-1879. <https://doi.org/10.1111/ddi.13415>
- Yu, D.W., Ji, Y., Emerson, B.C., Wang, X., Ye, C., Yang, C., & Ding, Z. (2012). Biodiversity soup: metabarcoding of arthropods for rapid biodiversity assessment and biomonitoring. *Methods in Ecology and Evolution*, 3, 613–623. (doi:10.1111/j.2041-210X.2012.00198.x)
- Zinger, L., Bonin, A., Alsos, I.G., Bálint, M., Bik, H., Boyer, F., Chariton, A.A., Creer, S., Coissac, E., Deagle, B.E., De Barba, M., Dickie, I.A., Dumbrell, A.J., Ficetola, G.F., Fierer, N., Fumagalli, L., Gilbert, M.T.P., Jarman, S., Jumpponen, A., Kausarud, H., Orlando, L., Pansu, J., Pawlowski, J., Tedersoo, L., Thomsen, P.F., Willerslev, E. & Taberlet, P. (2019). DNA metabarcoding—Need for robust experimental designs to draw sound ecological conclusions. *Molecular Ecology*, 28, 1857–1862. <https://doi.org/10.1111/mec.15060>
- Zhang, J., Kapli, P., Pavlidis, P., & Stamatakis, A. (2013). A general species delimitation method with applications to phylogenetic placements. *Bioinformatics*, 29, 2869–2876.
- Zhou, Z., Guo, H., Han, L. Chai, J., Che, X., & Shi, F. (2019). Singleton molecular species delimitation based on COI-5P barcode sequences revealed high cryptic/undescribed diversity for Chinese katydids (Orthoptera: Tettigoniidae). *BMC Ecology and Evolution*, 19, 79. <https://doi.org/10.1186/s12862-019-1404-5>

4.6 Supplementary Figures



Part 2

Figure S4.1a. part 1 cont.

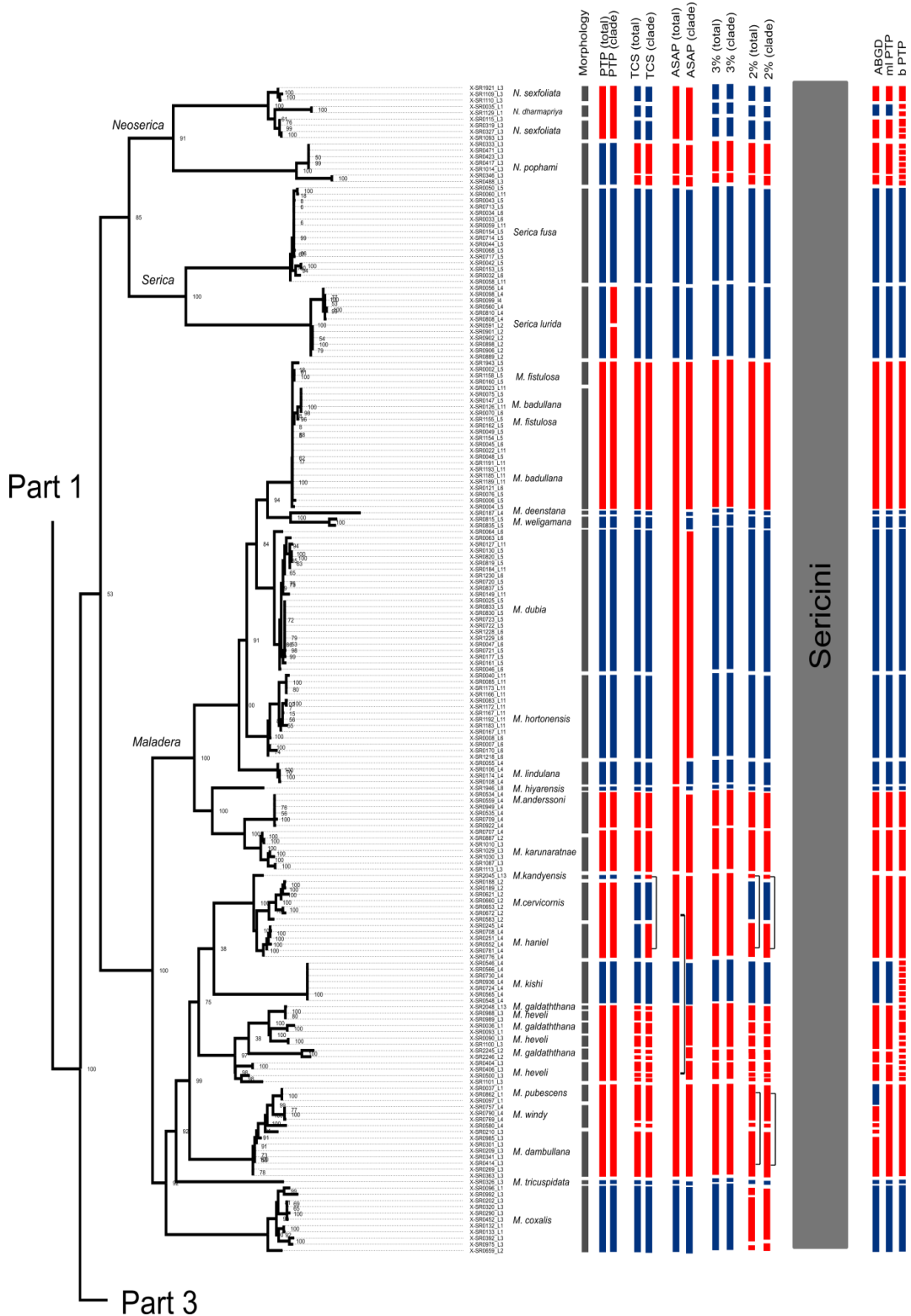


Figure S4.1b.cont.

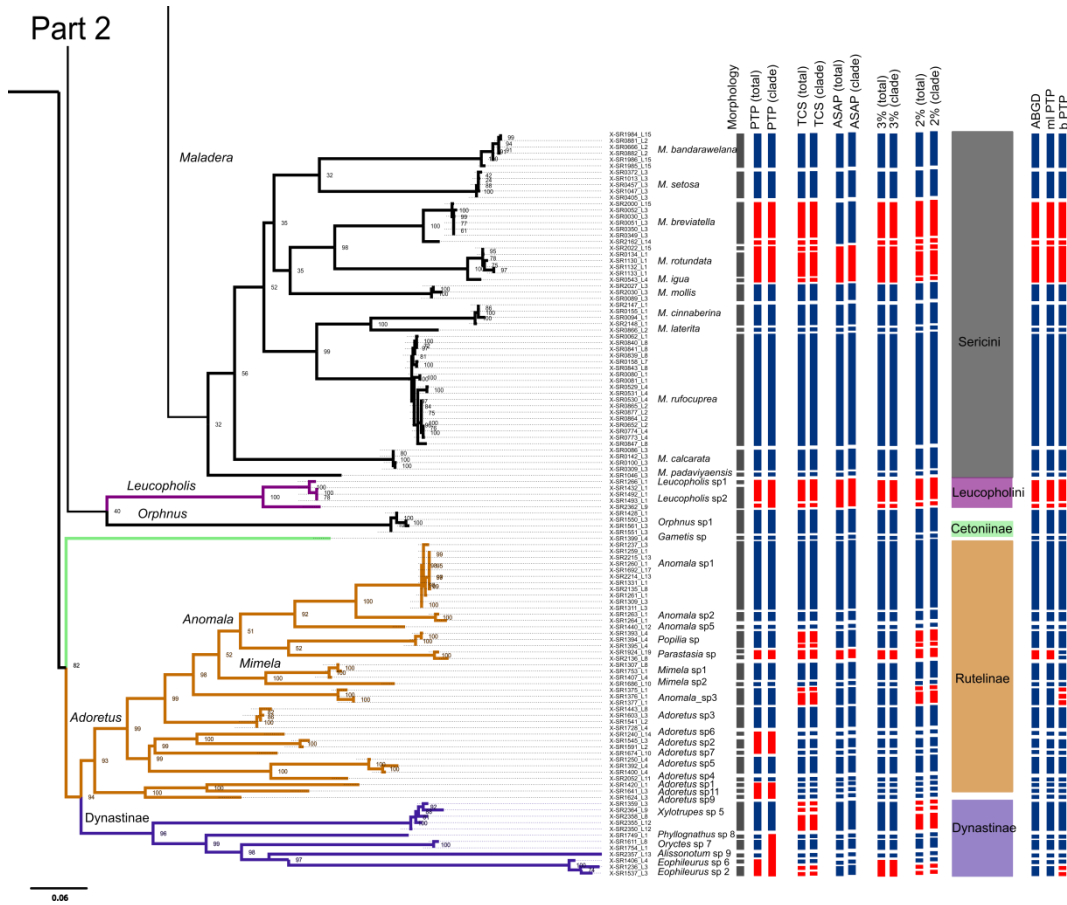


Figure S4.1c.

Figure S4.1. Maximum likelihood tree with information about morphospecies assignments, sampling locations, results of species delimitations (mPTP, TCS, ASAP, 3%, 2% clustering). Blue boxes indicate agreement between molecular species delimitation method and morphospecies assignment, while red boxes indicate disagreement. Results from subclade analyses are shown in a separate column indicated by “clade”. Ultrafast bootstrap supports (%) >50 are shown next to the branches.

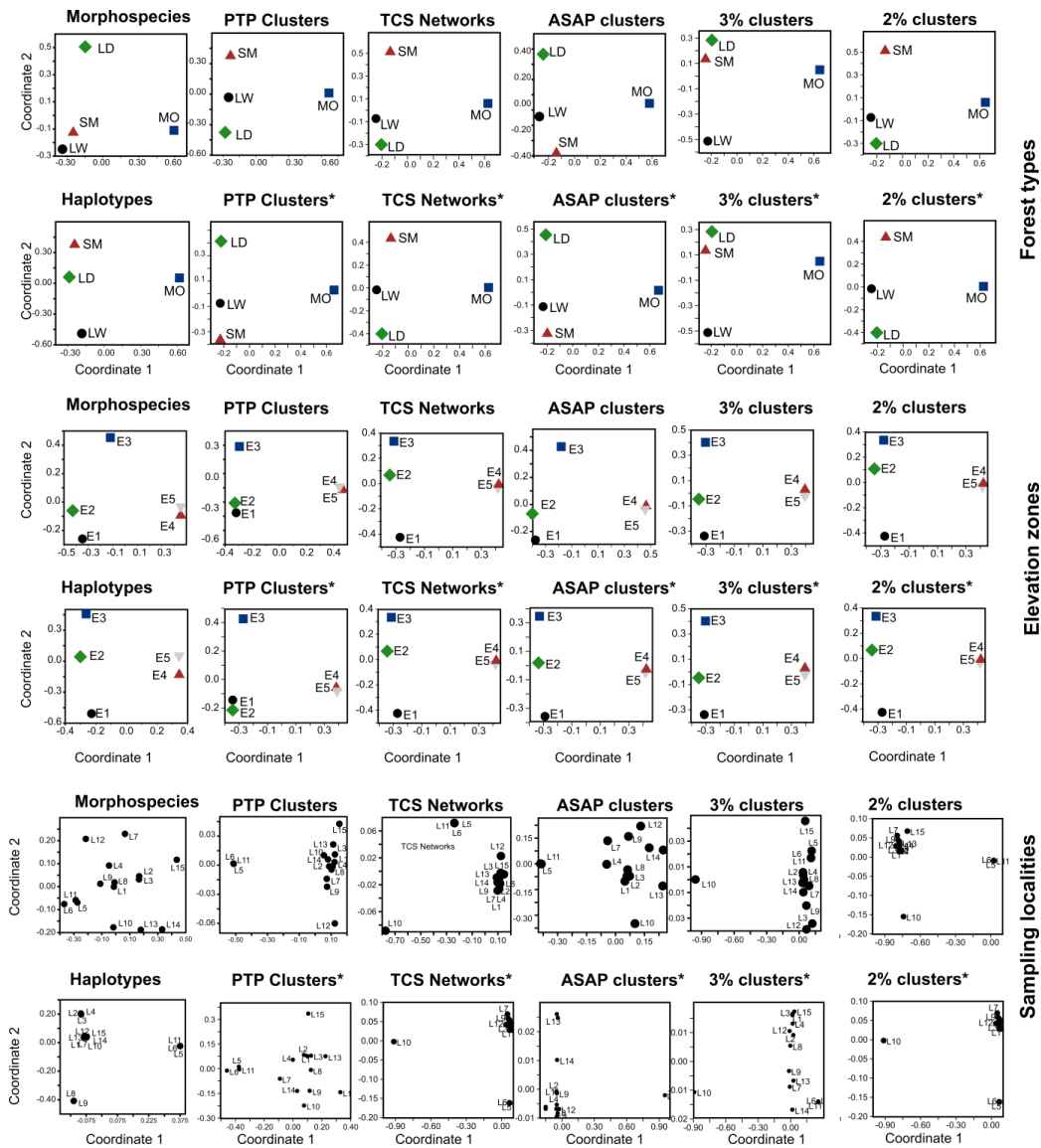


Figure S4.2. NMDS analysis (Non-metric Multidimensional Scaling; Jaccard index) for morphospecies, haplotypes and MOTUs that resulted from delimitation of the total assemblage and from cumulative subclade analyses (indicated by asterisk) for forest types, elevation zones and sampling localities.

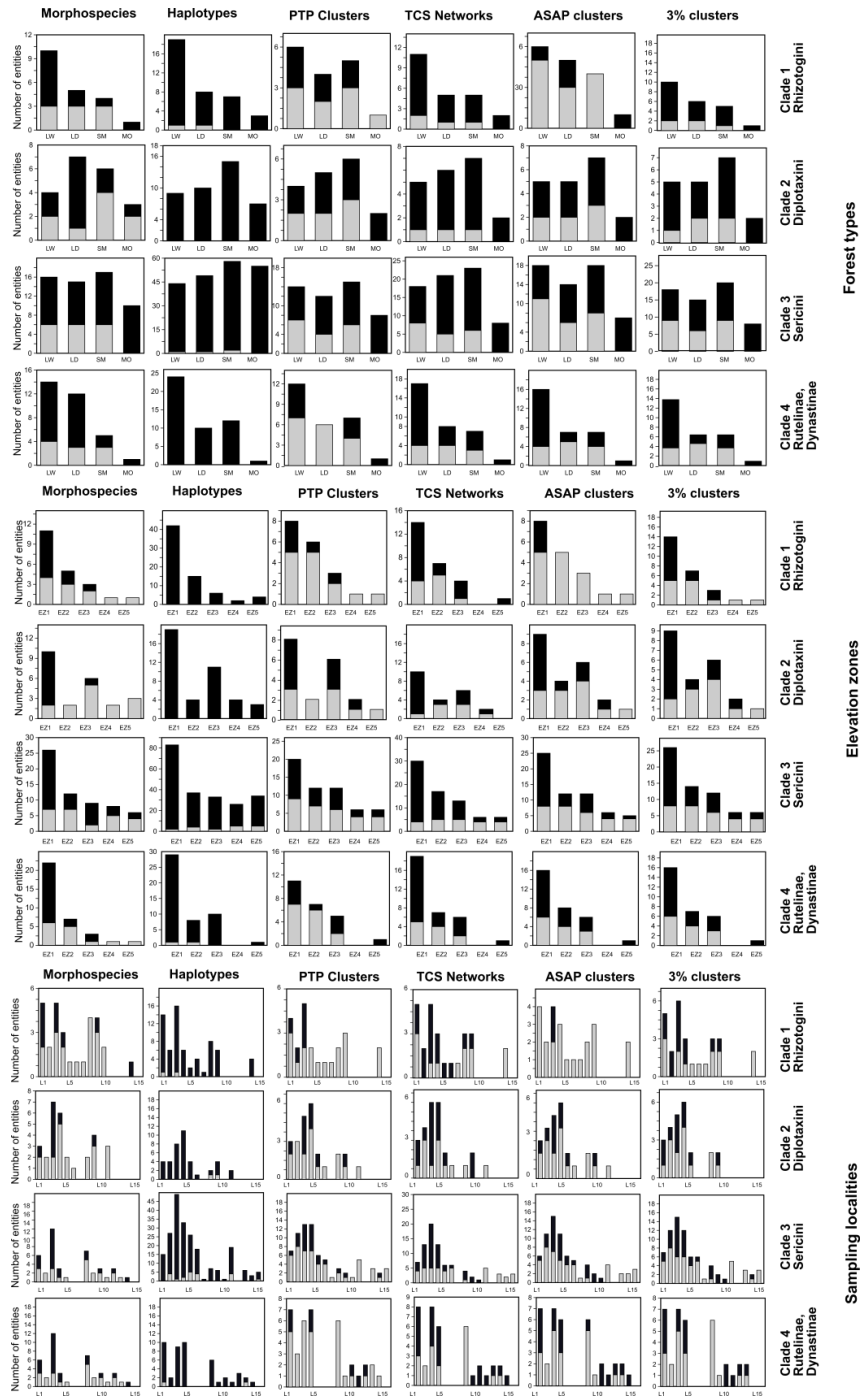


Figure S4.3. Number of putative species entities reported in forest types, elevation zones and sampling localities as morphospecies, haplotypes, PTP-clusters, TCS networks, distance clusters for subclades.

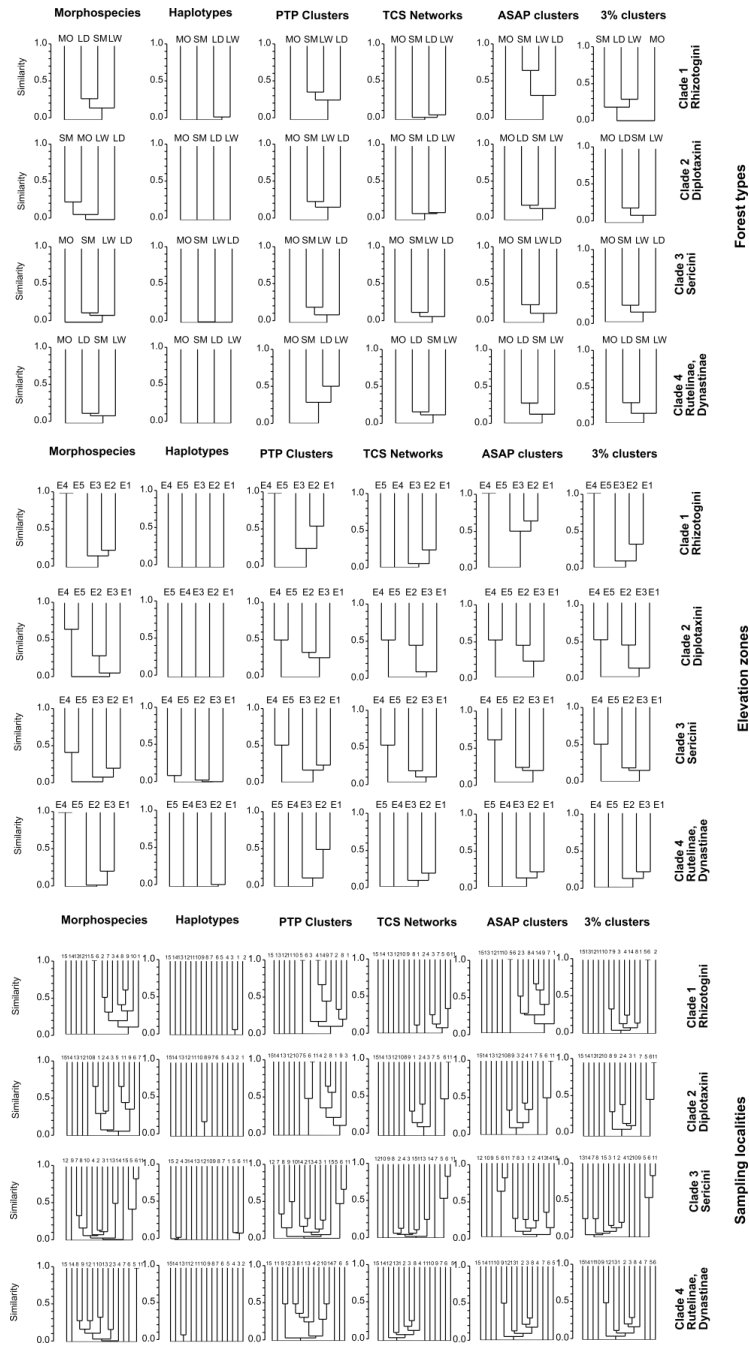


Figure S4.4. Clustering analysis (Jaccard Index) based on presence/absence for forest types, elevation zones and sampling localities for morphospecies, haplotypes and MOTUs for four subclade analysis. LW: wet lowland; LD: dry lowland; SM: sub-montane; MO: montane. EZ1: 0–500 m, EZ2: 501–1000 m, EZ3: 1001–1500 m, EZ4: 1501–2000 m, EZ5; 2001–2500 m. L1–L15 sampling localities.

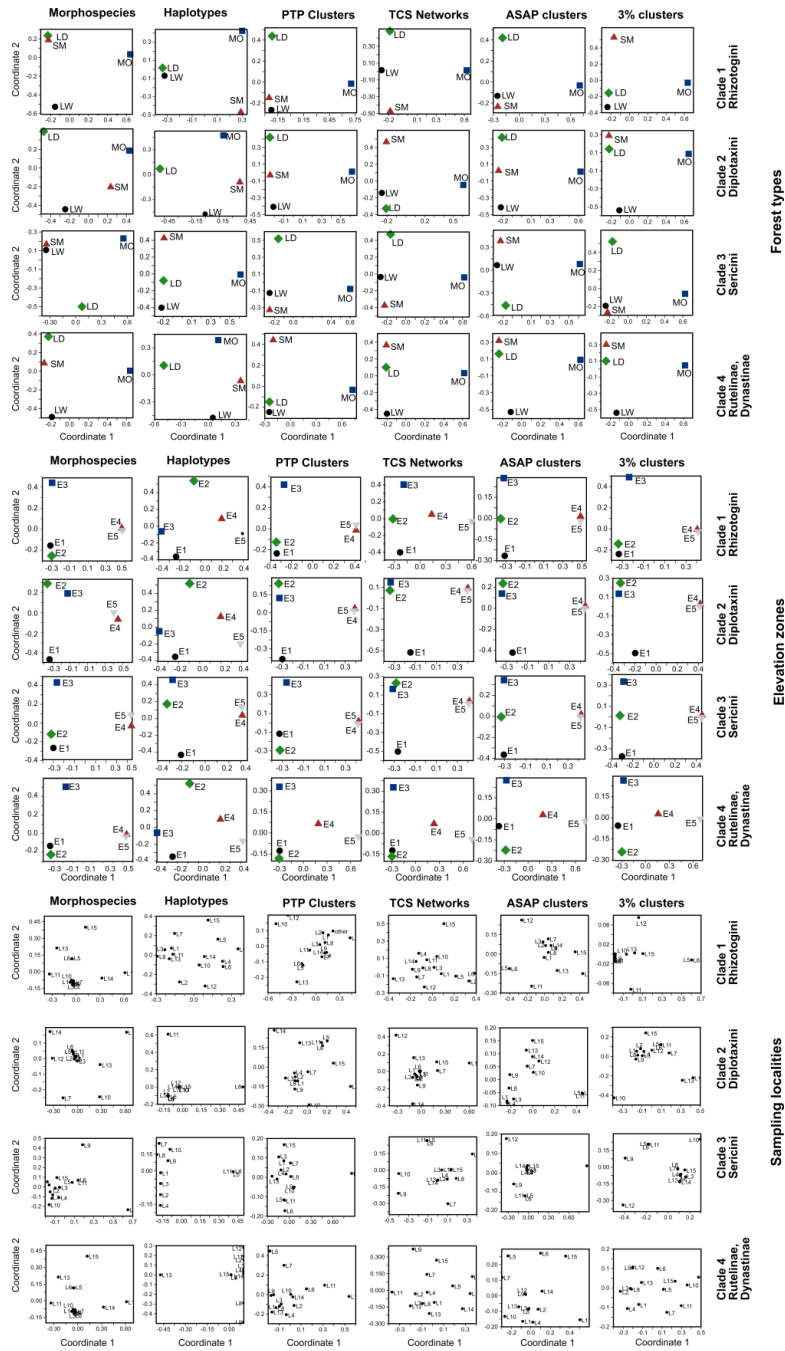


Figure S4.5. NMDS (non-metric multidimensional scaling: Jaccard index) based on presence/absence of specis. Analyses were done for forest types, elevation zones and sampling localities and for morphospecies, haplotypes and MOTUs and four subclade analysis. LW: wet lowland; LD: dry lowland; SM: sub-montane; MO: montane. E1: 0–500 m, E2: 501–1000 m, E3: 1001–1500 m, E4: 1501–2000 m, E5: 2001–2500 m. L1–L15 sampling localities.

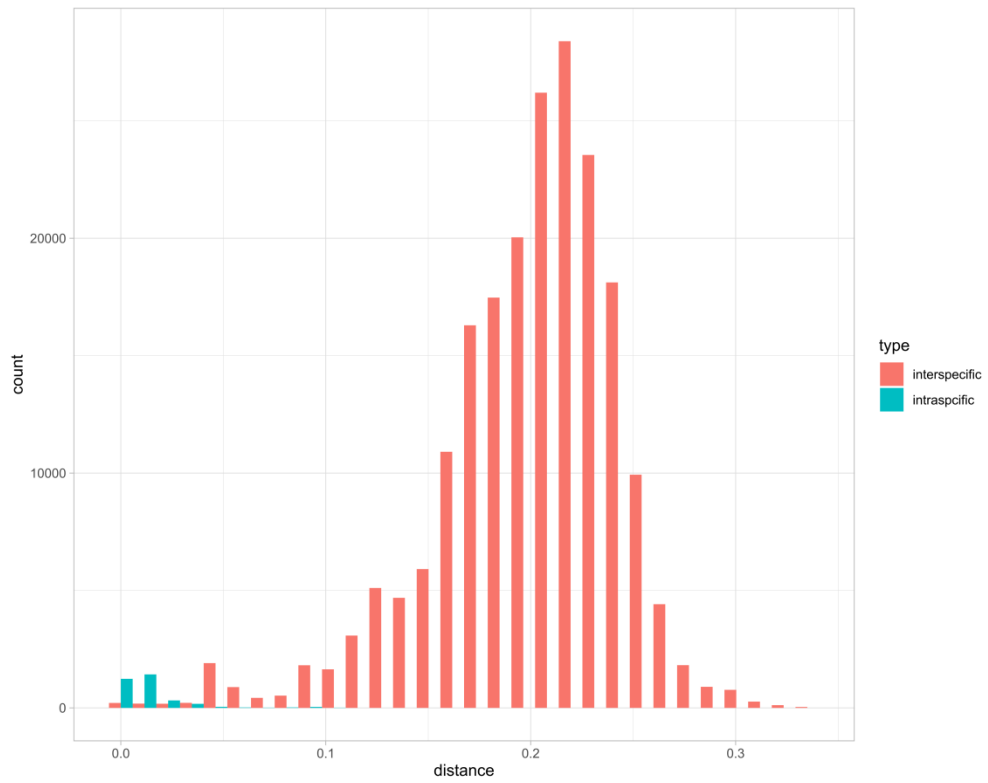


Figure S4.6. Frequency of intra- and interspecific distances of the phytophagous scarab chafer data from Sri Lanka

Chapter 5

New species of Sericini from Sri Lanka (Coleoptera, Scarabaeidae) Part I

This chapter is published in:

Ranasinghe S., Eberle J., Benjamin S.P. & Ahrens D. (2020). New species of Sericini from Sri Lanka (Coleoptera, Scarabaeidae). *European Journal of Taxonomy*, 621, 1–20. <https://doi.org/10.5852/ejt.2020.621>

Authors' contributions to the original article:

SR, JE: fieldwork collections; SR, DA: species identification, writing-original draft; DA, JE, SB, SR: manuscript review and editing.

Abstract

In a recent project, extensive fieldwork was carried out in several parts of Sri Lanka to investigate scarab biodiversity. Here we present the first results of this survey and describe four new Sericini species: *Selaserica athukoralai* sp. nov., *Neoserica dharmapriyai* sp. nov., *Maladera cervicornis* sp. nov., *M. galdathhana* sp. nov. Further, new locality records for 20 already known species are given. The genitalia and the habitus of all new species are illustrated and photos of the habitats of the new species are given.

5.1 Introduction

After a detailed taxonomic treatment of specimens from numerous museums and private collections, Fabrizi & Ahrens (2014) documented 77 valid species of Sericini for Sri Lanka. Among them only one species (*Maladera rufocuprea*) is widely distributed in the Oriental region, while some species are reported as endemic to Southern India and Sri Lanka (e.g., *Neoserica sexfoliata*, *Selaserica meridionalis*). However, the majority (67 species) are restricted to Sri Lanka, which suggests that their distribution is likely relative to the ecoclimatic particularities but also due to the long periods of isolation of the island.

The study of Fabrizi & Ahrens (2014) raised questions on the phylogenetic position of several lineages within Sericini which need to be further explored. In particular the endemic and very likely monophyletic *Maladera fistulosa* group, characterized by entirely reduced parameres, the *Serica fusa* group, as well as the genera *Periserica* and *Selaserica*. The way of choice to resolve this is a thorough phylogenetic analysis of a data matrix that includes the islands scarab biodiversity to the existing molecular data of Eberle *et al.* (2016) in which endemic taxa of the Indian subcontinent and in particular those from Sri Lanka were underrepresented or missing. Thus, a series of field expeditions to Sri Lanka was initiated in early 2019, with the aim of collecting fresh material for both morphological as well as molecular phylogenetic studies.

Here we present the first results from this fieldwork, describing four new species from Sri Lanka, belonging to the genera *Maladera*, *Neoserica* and *Selaserica*, and report new locality records of twenty previously known species.

5.2 Material and methods

Sampling of adult Sericini (Coleoptera: Scarabaeidae) was carried out in seven different localities (Figure 5.1) in the Kandy, Matale, Nuwara Eliya and Rathnapura Districts from February to March 2019. Beetles were captured using UV-light traps (Figure 5.2A). The traps were placed at a height of approximately 1–2 m above the ground and positioned at the same spot for 2-3 consecutive days. A timer activated the light from dusk to midnight (6.00pm to 11.00pm). Beetles

that were attracted to the light traps were stopped by transparent polystyrene plates (32 cm in width) and fell into a container where they were preserved. Whenever the circumstances at the sampling site allowed, we additionally used a LepiLED® lamp (spectrum: mixed radiation) which was placed near a white sheet and manually collected selected Sericini specimens (Figures. 5.2B–C). Some specimens were hand-collected during the day. All specimens were preserved in vials containing 96% ethanol.

The specimens were examined under a Wild M3Z stereomicroscope. Male genitalia were dissected and glued to a pointed card. Identification to species level was done using recent literature (Ahrens & Fabrizi 2016, Fabrizi & Ahrens, 2014) and comparison with type specimens (deposited in ZFMK).

Newly discovered species and their genitalia were photographed using a Zeiss AxioCam HRc camera. Multifocal images were taken using the Zeiss Axio Vision software package, and stacked with Zerene Stacker (www.zerene.com) to obtain a single image with the entire area in focus. Maps of sample sites and species distribution were prepared using Quantum GIS 3.6.2 (available on <https://www.qgis.org>).

Abbreviations

ZFMK – Zoological Research Museum A. Koenig, Bonn, Germany;
NIFS – National Institute of Fundamental Studies, Kandy, Sri Lanka;
SNR – Strict Nature Reserve;
FR – Forest Reserve.

5.3 Results

Class Insecta Linnaeus, 1758
Subclass Pterygota Lang, 1888
Superfamily Scarabaeoidea Latreille, 1802
Family Scarabaeidae Latreille, 1802
Subfamily Melolonthinae Leach, 1819
Tribe Sericini Kirby, 1837

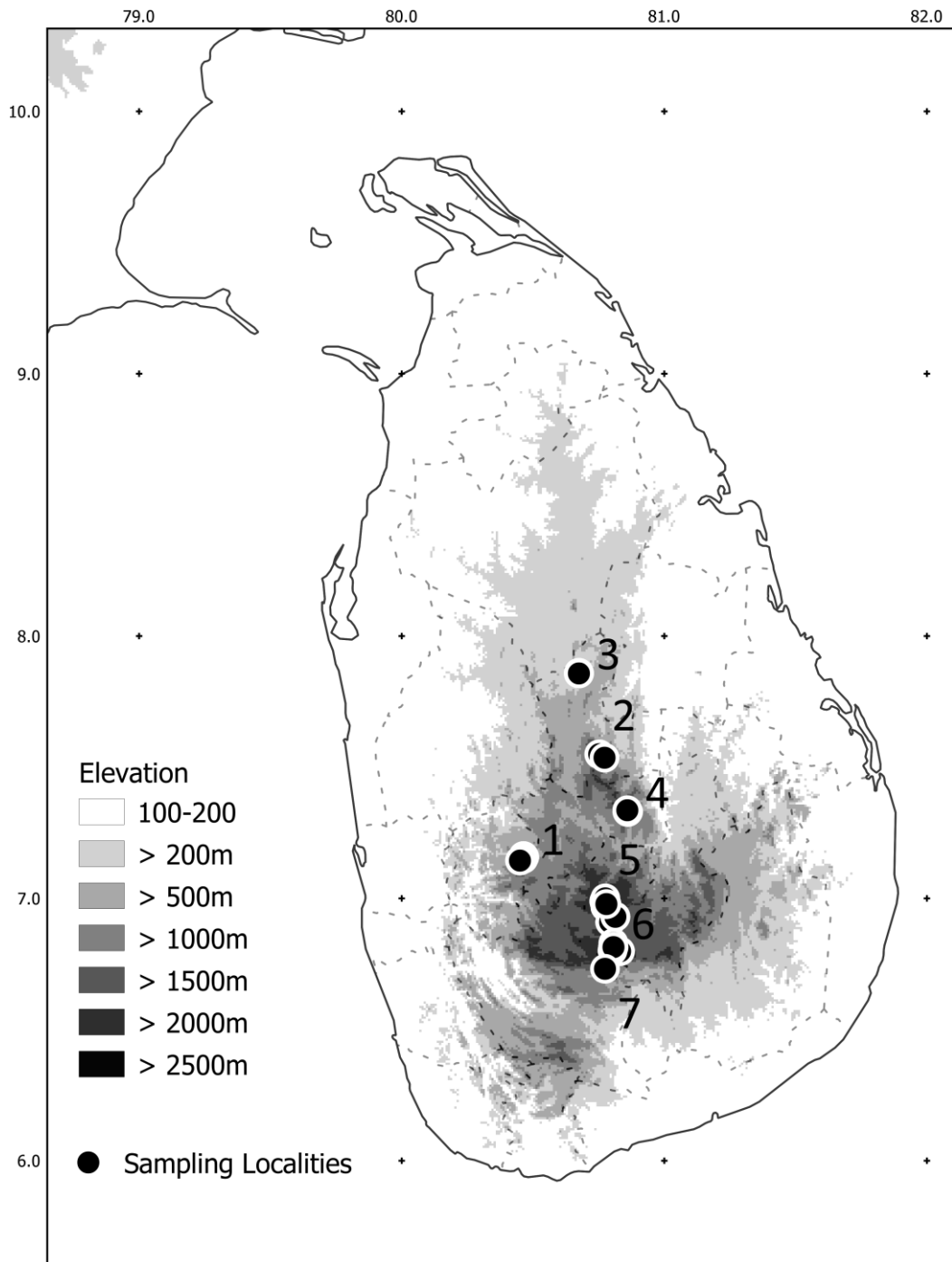


Figure 5.1. Map of Sri Lanka showing collecting sites for this study. Numbers refers to major sampling localities. 1, Aranayake; 2, Riverston; 3, NIFS Arboretum; 4, Deenston; 5, Nuwara Eliya; 6, Horton Plains; 7, Belihuloya.

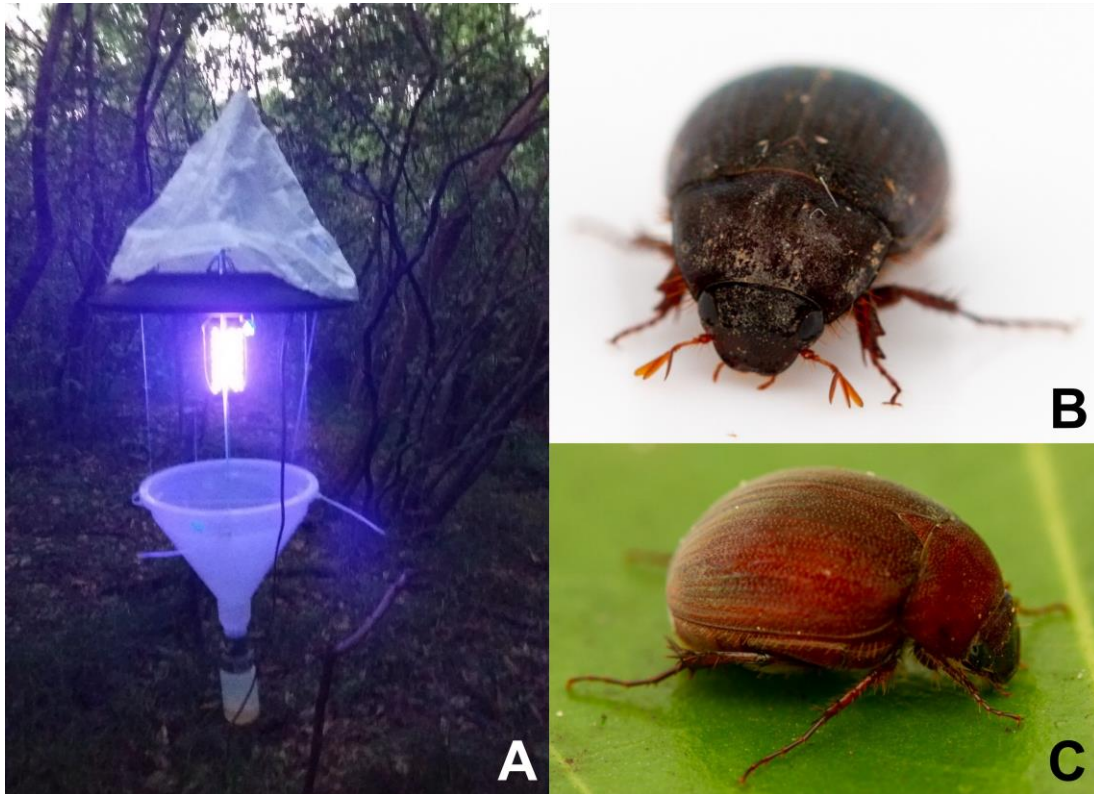


Figure 5.2. A Light trap in the field. B–C Live Sericini collected from the field A *Maladera breviatella* male, C. *Maladera* sp. female. (Photos by JE).

5.3.1 Taxonomy

Selaserica athukoralai sp. n.

Figures. 5.3A–D

Type material examined.

Holotype

SRI LANKA • ♂; Matale District, Riverston, Thelgamu oya bangalow;
7.53635607°N, 80.77234267°E; 509m; 15 Feb. 2019; Eberle & Ranasinghe leg.;
Black light; X-SR0175, 1036 Sericini Asia spec; ZFMK.

Description. Length: 7.0 mm, length of elytra: 5.2 mm, width: 4.5 mm. Body oval, reddish brown, antenna yellow, dorsal surface shiny and glabrous.

Labroclypeus subtrapezoidal, distinctly wider than long, widest at base, lateral margins convex and strongly convergent to blunt anterior angles, lateral border and ocular canthus producing an indistinct blunt angle, margins weakly reflexed, anteriorly distinctly sinuate medially; surface nearly flat, shiny, finely and densely punctate, distance between punctures subequal to their diameter, with a few fine setae anteriorly; frontoclypeal suture feebly impressed and weakly angled medially; smooth area in front of eye approximately twice as wide as long; ocular canthus moderately long and narrow, sparsely punctate, with a single short terminal seta. Frons shiny, with fine, moderately dense punctures, in posterior half impunctate, surface glabrous except for a few setae beside eyes. Eyes moderately large, ratio of diameter/ interocular width: 0.73. Antenna yellowish, with ten antennomeres; club with four antennomeres, 1.2 times as long as remaining antennomeres combined. Mentum elevated and anteriorly flattened.

Pronotum moderately wide, widest at posterior third, lateral margins convex and evenly narrowed to the anterior and posterior angles, anterior angles moderately produced and sharp, posterior angle strongly rounded; anterior marginal line narrowly incomplete medially, anterior margin moderately produced medially; surface densely and coarsely punctate, with microscopic setae in the punctures and two long erect setae on each side; anterior and lateral borders sparsely setose, basal margin without marginal line; hypomeron ventrobasally carinate, weakly produced ventrally, on the carina with fine setae. Scutellum small, triangular, dull, with fine and sparse punctures, each bearing a single very minute seta.

Elytra oblong, widest in posterior third, striae indistinctly impressed, finely and densely punctate, intervals almost flat, with fine, sparse punctures concentrated along the striae, punctures with minute setae, odd intervals with some erect long setae; epipleural edge fine, ending at the convex external apical angle of elytra, epipleura densely setose, apical border broadly membranous.

Ventral surface dull, thorax and metacoxa with large and dense punctures, sparsely finely setose, metacoxa glabrous except for numerous short setae laterally; each abdominal sternite with generally distributed fine and dense punctures, each with a moderately long setae, with a transverse row of coarse punctures each bearing a long seta, penultimate sternite apically with a shiny smooth but very short chitinous border. Mesosternum between mesocoxae as wide as mesofemur. Ratio of length of metepisternum/ metacoxa: 1/ 1.1. Pygidium

weakly convex, shiny, finely and densely punctate, with a narrow, smooth midline, beside apical border with some long setae.

Legs moderately broad; femur shiny, with two longitudinal rows of setae, finely and sparsely punctate; metafemur almost impunctate, its anterior edge acute, with a very fine, closely adjacent serrated line, anterior longitudinal row of setae not reduced; posterior ventral margin almost straight, weakly widened in apical half, nor ventrally nor dorsally serrated, glabrous. Metatibia moderately broad and long, widest behind middle, dorsal and ventral margins in posterior two thirds subparallel, ratio width/ length: 1/ 3.1, dorsally longitudinally convex, with two groups of spines, basal one at middle, apical one at four fifths of metatibial length, basally beside dorsal margin with a long serrated line, which ends shortly before the middle of metatibia, adjacent to it some single punctures each bearing a single spine; lateral face longitudinally convex, impunctate and glabrous; ventral margin with three fine spines equidistant from each other, medial face smooth, apex anteriorly near tarsal articulation shallowly concave, nearly truncate. Tarsomeres impunctate dorsally, ventrally with dense, fine setae; metatarsomeres ventrally with a strongly serrated ridge, beside which is no strong longitudinal carina; first metatarsomere little shorter than the two following tarsomeres combined and twice as long as the dorsal tibial spur. Protibia moderately long, tridentate. All claws symmetrical, feebly curved and long, with normally developed basal tooth.

Aedeagus: Fig. 5.3A–C. Habitus: Fig. 5.3D. Female unknown.

Diagnosis. *Selaserica athukoralai* sp. n. is in shape of aedeagus very similar to *Selaserica pusilla* Arrow, 1916 and *S. splendifica* (Brenske, 1898). From both latter taxa the new species differs by the different shape of parameres as well as by the long lateral process on the right apex of the phallobase.

Etymology. The new species is named after Mr. N.P. Athukorala (NIFS) who supported our expedition in many ways (species name, noun in the genitive case).

Distribution. See Fig. 5.5A.

***Neoserica dharmapriyai* sp. n.**

Figs. 5.3E–I

Type material examined.**Holotype**

SRI LANKA • ♂; Kegalle District, Pannala, Galdaththa, Aranayake;
7.16154167°N, 80.46388889°E; 294m; 03 Mar. 2019; Eberle & Ranasinghe leg.;
Black light; X-SR0035, 1035 Sericini Asia spec; ZFMK.

Description. Length: 7.5 mm, length of elytra: 5.2 mm, width: 4.5 mm. Body oval, reddish brown, antenna pale, labroclypeus shiny, dorsal surface dull, except the dense pilosity on head dorsal surface almost glabrous.

Labroclypeus broad and subtrapezoidal, widest at base, lateral margins convex and strongly convergent anteriorly, anterior angles including anterior margin strongly rounded, not sinuate medially, all margins strongly reflexed, lateral margins producing a very indistinct angle with the ocular canthus; surface flat, finely and densely punctate, densely erectly setose in coarser punctures mixed with the fine ones; frontoclypeal suture finely incised, not elevated and weakly angled medially; smooth area anterior to eye wide, almost flat, three times as wide as long; ocular canthus long and broad (one third of ocular diameter), coarsely and densely punctate, with a single terminal seta. Frons dull, with fine, moderately dense punctures, with a few erect setae behind the frontoclypeal suture. Eyes moderately large, ratio diameter/ interocular width: 0.66. Antenna with ten antennomeres; club in male with five antennomeres and straight, 0.8 times as long as remaining antennomeres combined. Mentum elevated and slightly flattened anteriorly.

Pronotum widely transverse, widest at base, lateral margins in basal half almost straight and slightly convergent anteriorly, in anterior half weakly convex and evenly convergent anteriorly, anterior angles distinctly produced and acute, posterior angles blunt; anterior margin indistinctly produced medially, with a fine and complete marginal line, base of pronotum without marginal line; surface densely and finely punctate, punctures with very minute setae only, otherwise glabrous; lateral and anterior margin densely setose; hypomerion carinate, ventrally slightly produced. Scutellum wide, triangular, at apex moderately pointed, with fine, evenly dense punctures, with only very minute setae.

Elytra widest at middle, striae finely impressed, finely and moderately densely punctate, intervals weakly convex, with fine and evenly dense punctures, except

very minute setae in punctures only a few short setae on lateral odd intervals; epipleural edge robust, ending at strongly curved external apical angle of elytra, epipleura densely setose; apical border of elytra with a fine rim of microtrichomes (100x).

Ventral surface dull, coarsely and densely punctate, metepisternum distally impunctate, metasternum sparsely covered with fine, short or very minute setae, metacoxa glabrous, with a few single setae laterally; abdominal sternites finely and densely punctate, with a transverse row of coarse punctures, each bearing a robust seta, the two basal sternites additionally with dense setae beside the row. Mesosternum between mesocoxae 1.5 times as wide as the width of mesofemur. Ratio of length of metepisternum/ metacoxa: 1/ 1.62. Pygidium strongly convex at apex and dull, coarsely and densely punctate, without smooth midline, glabrous except some longer setae along the apical margin.

Legs broad and moderately long; femur with two longitudinal row of setae, finely and sparsely punctate; metafemur dull, behind the posterior longitudinal row of setae punctures finer and slightly denser, anterior margin acute, without serrated line behind anterior edge, posterior margin smooth ventrally, strongly widened, posterior margin finely serrated over its entire length dorsally, with just a few short setae basally. Metatibia wide and flattened, short, widest at middle of metatibial length, ratio of width/ length: 1/ 2.46, sharply carinate dorsally, with two groups of spines, basal group at first third, apical group at three quarters of metatibial length, basally with a few short robust single spines; lateral face weakly longitudinally convex, finely and sparsely punctate, glabrous, smooth along the middle; ventral margin finely serrated, with four robust equidistant setae; medial face smooth and glabrous; apex finely serrated, interiorly near tarsal articulation weakly concavely sinuate. Tarsomeres dorsally smooth and glabrous, neither laterally nor dorsally carinate, ventrally robustly densely setose; metatarsomeres with a strongly serrated ridge and a smooth subventral longitudinal carina; first metatarsomere slightly shorter than following two tarsomeres combined and slightly longer than dorsal tibial spur. Protibia short, bidentate; anterior claws symmetrical, basal tooth of both claws bluntly truncate at apex.

Aedeagus: Fig. 5.3E–H. Habitus: Fig. 5.3I. Female unknown.

Diagnosis. The new species resembles to *Neoserica sexfoliata* Moser, 1915 in external appearance of the body and in the shape of parameres. *Neoserica dharmapriyai* sp. n. may be distinguished from the former by the shorter antennal club being composed of only five antennomeres, and by the shape of parameres: the right paramere is only half as long as the left one, in *N. sexfoliata* both are subequal in length.

Etymology. The new species is named after Sasanka's husband Prasanna Dharmapriya for his dedication to this project (species name, noun in the genitive case).

Distribution. See Fig. 5.5B.

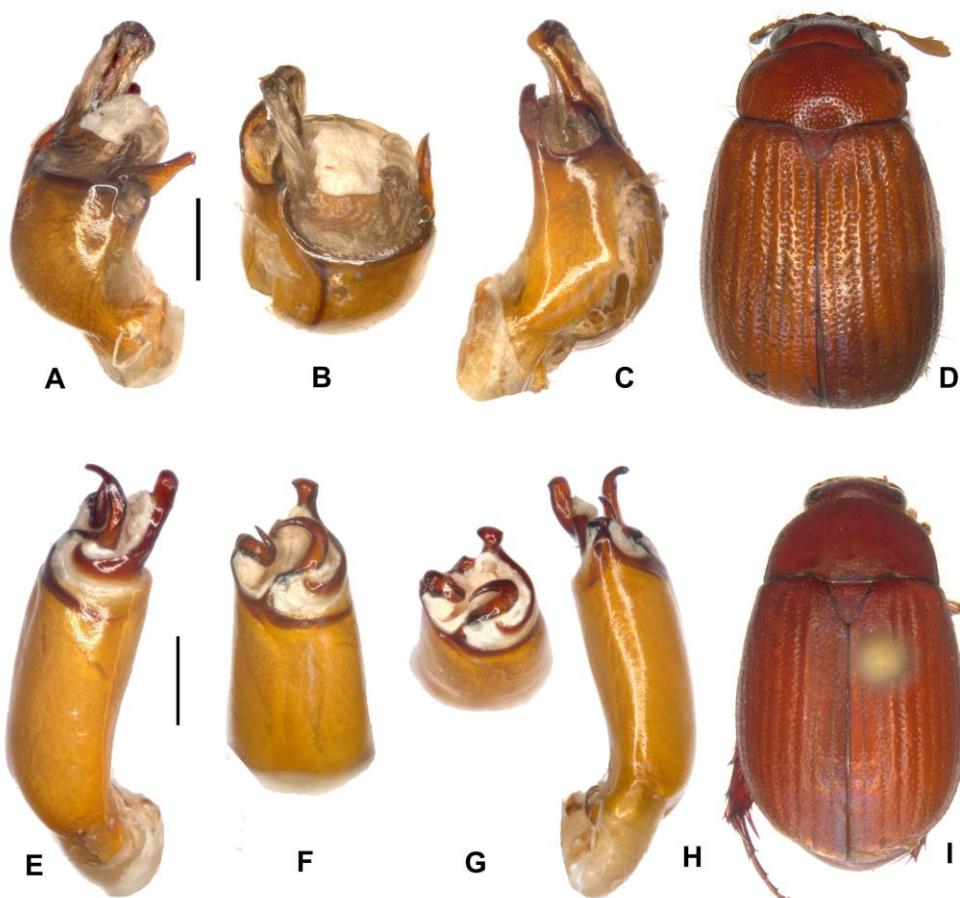


Figure 5.3. A–D *Selaserica athukoralai* sp. n. (holotype) E–I *Neoserica dharmapriyai* sp. n. (holotype). A, E aedeagus, left side lateral view C, H aedeagus, right side lateral view B, F, G parameres, dorsal view D, I habitus (not to scale). Scale: 0.5 mm.

***Maladera galdaththana* sp. n.**

Figs. 5.4A–D

Type material examined.**Holotype**

SRI LANKA • ♂; Kegalle District; Pannala, Galdaththa, Aranayake;
7.16154167°N, 80.46388889°E; 294m; 03 Mar. 2019; Eberle & Ranasinghe leg.;
Black light; X-SR0036, 1033 Sericini Asia spec; ZFMK.

Paratype

SRI LANKA • 1 ♂; Kegalle District; Alic Land Estate; 7.14420175°N,
80.4502789°E; 405m; 04 Mar. 2019; Eberle & Ranasinghe leg.; Black light; X-
SR0093; ZFMK.

Description. Length: 7.4 mm, length of elytra: 5.4 mm, width: 4.5 mm. Body oval, dark brown, antenna dark yellowish, labroclypeus moderately shiny, dorsal surface dull, with fine, sparse erect setae on the head, pronotum, and elytra.

Labroclypeus trapezoidal, distinctly wider than long, widest at base, lateral margins convex and strongly convergent to broadly rounded anterior angles, lateral border and ocular canthus produce an indistinct blunt angle, margins weakly reflexed, anteriorly weakly medially; surface weakly convex, moderately shiny, basis narrowly dull, coarsely and densely punctate, distance between punctures less than their diameter, with erect setae in larger punctures; frontoclypeal suture feebly impressed and weakly angled medially; smooth area in front of eye approximately twice as wide as long; ocular canthus moderately long and narrow, finely punctate, with a single short terminal seta. Frons with fine, dense punctures, with dense erect setae being partly bent backwards. Eyes moderately large, ratio of diameter/ interocular width: 0.66. Antenna yellow, with ten antennomeres; club with three antennomeres, slightly longer than remaining antennomeres combined. Mentum elevated and anteriorly flattened.

Pronotum widest at base, lateral margins nearly straight and convergent anteriorly, in anterior third evenly convex and convergent to the anterior angles, anterior angles moderately produced and moderately acute, anterior margin straight, anterior marginal line very fine but complete medially; surface with fine dense punctures mixed with large dense punctures, with fine adpressed white setae in smaller punctures and long erect setae in larger ones; anterior and lateral borders setose, basal margin without marginal line; hypomeron ventrobasally carinate and

slightly produced ventrally. Scutellum broad, triangular, with fine and dense punctures each bearing a single fine seta.

Elytra oblong, widest at middle, striae distinctly impressed, finely and densely punctate, intervals weakly convex, with fine, dense punctures concentrated along striae, with dense short white setae in punctures, odd intervals anteriorly with a few long erect setae; epipleural edge robust, ending at the weakly convex external apical angle of elytra, epipleura densely setose; apical border membranous, apex covered with short microtrichomes.

Ventral surface partly dull partly moderately shiny, thorax and metacoxa with large and dense punctures, densely shortly setose, including metacoxa, the latter with numerous long setae laterally; each abdominal sternite, in addition to generally distributed fine and dense punctures with a distinct transverse row of coarse punctures each bearing a short seta, remainder punctures with short white setae, penultimate sternite apically with a shiny smooth chitinous border which is one third as long as sternite. Mesosternum between mesocoxae as wide as mesofemur. Ratio of length of metepisternum/ metacoxa: 1/ 2.11. Median apophysis of metacoxa with normal fine setae. Pygidium moderately convex, coarsely and densely punctate, with a narrow, smooth midline, punctures with short white setae and with numerous erect setae of different length.

Legs wide; femur with two longitudinal rows of setae, finely and densely punctate; metafemur shiny, anterior edge acute, lacking an adjacent serrated line, posterior ventral margin medially feebly concave, strongly widened in apical half and indistinctly serrate apically, dorsally not serrated, glabrous. Metatibia wide and short, widest at middle, ratio width/ length: 1/ 2.1, dorsally sharply carinate, with two groups of spines, basal one shortly behind middle, apical one at four fifths of metatibial length, basally beside dorsal margin with two robust spines; lateral face longitudinally convex, with dense, fine punctures, along the middle before apex impunctate, with minute setae in punctures; ventral margin with five strong spines equidistant from each other; medial face impunctate, apex interiorly near tarsal articulation shallowly concave. Meso- and metatarsomeres sparsely punctate dorsally and minutely setose, ventrally with sparse, short setae; metatarsomeres ventrally with a strongly serrated ridge, beside which is a strong longitudinal carina; first metatarsomere distinctly longer than following two tarsomeres and slightly shorter than extremely long (as long as metatarsomeres 1 and 2) and apically ventrally curved ventral tibial spur. Protibia short, bidentate. All claws symmetrical, feebly curved and long, with normally developed basal tooth.

Aedeagus: Fig. 5.4A–C. Habitus: Fig. 5.4D.

Diagnosis. *Maladera galdaththana* sp. n. is in shape of aedeagus rather similar to *M. woodii* Fabrizi & Ahrens, 2014. The new species differs by the shorter parameres being at base also wider, by the denser long pilosity, and by the extremely long ventral metatibial spur which is apically curved ventrally.

Variation. Length: 7.4–8.2 mm, length of elytra: 5.4–5.6 mm, width: 4.5–4.8 mm.

Etymology. The new species is named after its type locality ‘Galdaththa’, a small undisturbed forest patch on a rock (adjective in the nominative singular).

Distribution. See Fig. 5.5C.

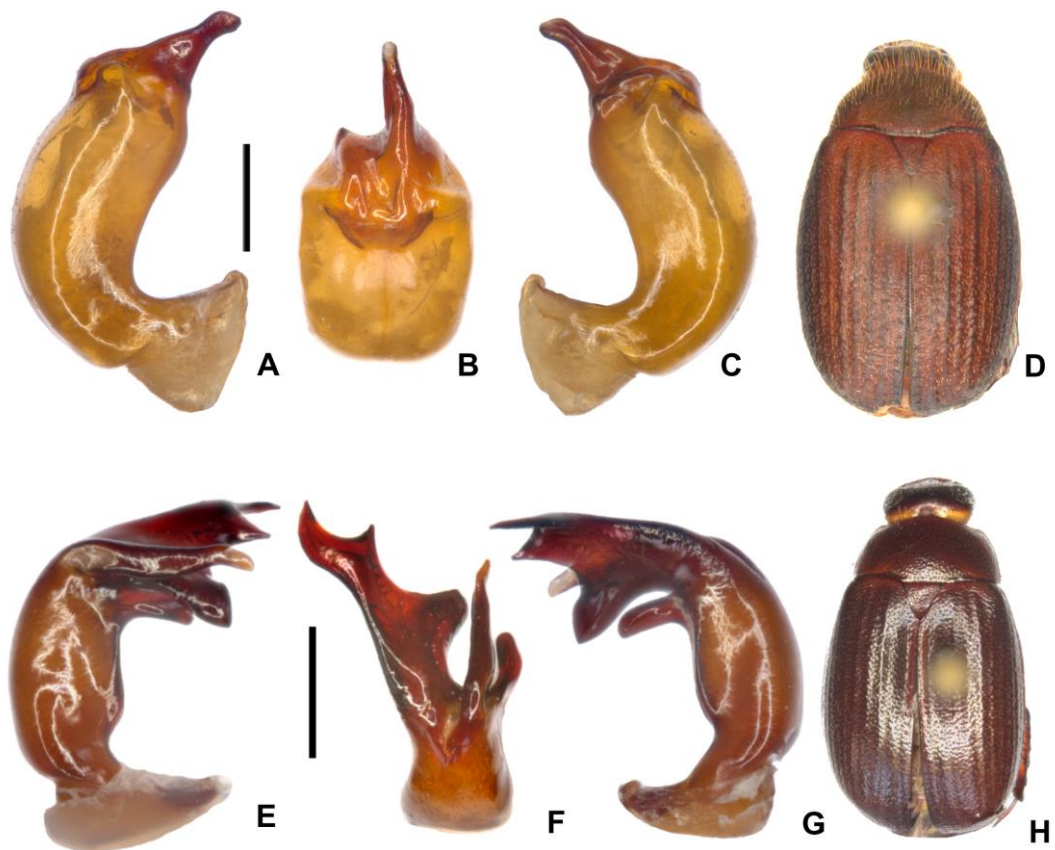


Figure 5.4. A–D *Maladera galdaththana* sp. n. (holotype) E–H *M. cervicornis* sp. n. (holotype) A, E aedeagus, left side lateral view C, G aedeagus, right side lateral view B, F parameres, dorsal view D, H habitus (not to scale). Scale: 0.5 mm.

***Maladera cervicornis* sp. n.**

Figs. 5.4E–H

Type material examined.**Holotype**

SRI LANKA • 1 ♂; Matale District; holotype of *M. cervicornis* sp. n.; Riverston, Pitawala Pathana; 7.54976718°N, 80.75212294°E; 902m; 15 Feb. 2019; Eberle & Ranasinghe leg.; Black light; X-SR0188, 1034 Sericini Asia spec; ZFMK.

Paratype

SRI LANKA • 1 ♂; Matale District; Riverston, Pitawala Pathana; 7.54976718°N, 80.75212294°E; 902m; 15 Feb. 2019; Eberle & Ranasinghe leg.; Black light; X-SR0189; ZFMK.

Description. Length: 7.2 mm, length of elytra: 5.4 mm, width: 4.4 mm. Body short oval, dark brown, antenna yellow, dorsal surface shiny, nearly completely glabrous.

Labroclypeus short and rectangular, wider than long, widest at base, lateral margins moderately convex and convergent to broadly rounded anterior angles, lateral border and ocular canthus producing an indistinct blunt angle, margins weakly reflexed, anterior margin almost feebly sinuate medially; surface slightly convex, finely and densely punctate, distance between punctures smaller than their diameter, with numerous erect setae in larger punctures; frontoclypeal suture indistinctly incised and bluntly bent medially; smooth area in front of eye approximately three times as wide as long; ocular canthus long and narrow, minutely and superficially punctate, without a single short terminal seta. Frons with fine, dense punctures, with a few long erect setae in larger punctures. Eyes very large, ratio of diameter/ interocular width: 0.97. Antenna yellow, with ten antennomeres; club with three antennomeres, as long as remaining antennomeres combined. Mentum elevated and anteriorly flattened.

Pronotum wide, widest at base, lateral margins weakly convex and evenly narrowed to the anterior angles, anterior angles moderately produced and sharp, anterior marginal line very fine but complete medially, anterior margin straight; surface finely densely punctate, except a few short and fine setae laterally glabrous; anterior and lateral borders setose, basal margin without marginal line; hypomeron ventrobasally carinate and slightly produced ventrally. Scutellum short and broad, triangular, with fine and dense punctures, glabrous.

Elytra short oval, widest shortly behind middle, striae distinctly impressed, finely and densely punctate, intervals weakly convex, with moderately fine, dense punctures and with dense, fine, short setae; epipleural edge fine, ending at the weakly convex external apical angle of elytra, epipleura densely setose; apical border narrowly membranous, apex covered with short microtrichomes.

Ventral surface shiny, thorax and metacoxa with large and dense punctures, sparsely setose, metacoxa with minute adjacent setae in the punctures except for numerous long setae laterally, apical margin weakly convex, without a broad rim of long white microtrichomes; each abdominal sternite, in addition to evenly distributed fine and dense punctures bearing each a fine seta, with a distinct transverse row of coarse punctures each bearing a long and more robust seta, 3rd sternite with a sharp median tubercle being half as high as sternite length, penultimate sternite apically with a shiny smooth chitinous border, which is a quarter as long as the sternite. Mesosternum between mesocoxae as wide as mesofemur, with a semi-circular ridge bearing robust setae. Ratio of length of metepisternum/ metacoxa: 1/ 1.89. Pygidium moderately convex, moderately finely and densely punctate, without smooth midline, punctures with short and moderately dense, adjacent setae or with moderately dense, long, erect setae.

Legs short and wide; femur with two longitudinal rows of setae, finely and densely punctate; metafemur shiny, anterior edge acute, lacking an adjacent serrated line, ventral surface densely punctate and setose, posterior ventral margin straight, only little widened in apical half, finely serrate apically, dorsally not serrated, glabrous. Metatibia short, widest at middle, posteriorly only very little narrowed, ratio width/ length: 1/ 2.87, dorsally sharply carinate, with two groups of spines, basal one at middle, apical one at three quarters of metatibial length, basally beside dorsal margin with two single punctures with serrated margins, each bearing a single robust spine and beside them a longitudinal serrated line; lateral face almost flat, with dense, large but superficial punctures and with minute setae in the punctures; ventral margin with four strong spines equidistant from each other, medial face smooth, apex interiorly near tarsal articulation shallowly concave. Meso- and metatarsomeres finely and sparsely punctate but glabrous dorsally, ventrally with sparse, short setae; metatarsomeres ventrally with a strongly serrated ridge, beside which is a strong longitudinal carina; first metatarsomere as long as following two tarsomeres combined and as long as dorsal tibial spur. Protibia short, bidentate. All claws symmetrical, feebly curved and long, with normally developed basal tooth.

Aedeagus: Fig. 5.4E–G. Habitus: Fig. 5.4H. Female unknown.

Diagnosis. *Maladera cervicornis* sp. n. is in external morphology very similar to *M. kandyensis* Fabrizi & Ahrens, 2014. The new species differs by the tubercle on 3rd abdominal sternite as well as by the shape of parameres.

Etymology. The name of the new species is derived from the combined Latin nouns *cornu* (horn) and *cervus* (deer), with reference to the shape of the parameres, resembling the horns of a deer (noun in nominative case).

Variation. Length: 7.2-7.8 mm, length of elytra: 5.4-5.8 mm, width: 4.4-4.5 mm.

Distribution. See Fig. 5.5D.

5.3.2 New distribution records:

Maladera badullana Fabrizi & Ahrens, 2014

Material examined.

SRI LANKA • 1 ♂; Nuwara Eliya District, Horton Plains; 6.80133047°N, 80.80275893°E; 2116m; 28 Feb. 2019; Eberle & Ranasinghe leg.; Hand collecting; X-SR0070; ZFMK • 3 ♂♂; Horton Plains; 6.81278056°N, 80.80444444°E; 2147m; 26 Feb. 2019; Eberle & Ranasinghe leg.; Black light; X-SR0179, X-SR0180, X-SR0181; ZFMK • 1 ♂; Horton Plains; 6.81437222°N, 80.80638889°E; 2146m; 28 Feb. 2019; Eberle & Ranasinghe leg.; Light sheet; X-SR0121; ZFMK • 1 ♂; Horton Plains; 6.82978333°N, 80.80611111°E; 2154m; 26 Feb. 2019; Eberle & Ranasinghe leg.; Black light; X-SR0045; ZFMK • 3 ♂♂; Hakgala SNR, Near Kande Ela reservoir; 6.90995856°N, 80.79366605°E; 1917m; 24 Feb. 2019; Eberle & Ranasinghe leg.; Black light; X-SR0075, X-SR0076, X-SR0077; NIFS • 9 ♂♂; Hakgala SNR, Near Kande Ela reservoir; 6.91085232°N, 80.79427602°E; 1914m; 23-24 Feb. 2019; Eberle & Ranasinghe leg.; Black light; X-SR0011- X-SR0014, X-SR0027, X-SR0028, X-SR0136- X-SR0138; ZFMK • 3 ♂♂; Hakgala SNR, Near Kande Ela reservoir; 6.91133456°N, 80.79475087°E; 1907m; 23 Feb. 2019; Eberle & Ranasinghe leg.; Black light; X-SR0020, X-SR0139, X-SR0140; ZFMK • 7 ♂♂; Hakgala SNR, Near Kande Ela reservoir; 6.91179564°N, 80.79491161°E; 1882m; 23-24 Feb. 2019; Eberle & Ranasinghe leg.; Black light; X-SR0004- X-SR0006, X-SR0103, X-SR0104, X-SR0176, X-SR0178; ZFMK • 1 ♂; Hakgala SNR, Seetha Eliya; 6.9304544°N, 80.81356983°E; 1789m; 24 Feb. 2019; Eberle & Ranasinghe leg.; Black light; X-SR0001; (ZFMK) • 4 ♂♂; Hakgala SNR, Seetha Eliya; 6.93074021°N, 80.8134195°E; 1773m; 24 Feb. 2019; Eberle & Ranasinghe leg.;

Black light; X-SR0067, X-SR0129, X-SR0159, X-SR0163; ZFMK• 2 ♂♂; Galways Land NP; 6.96616216°N, 80.77744079°E; 1931m; 23 Feb. 2019; Eberle & Ranasinghe leg.; Black light; X-SR0048, X-SR0049; ZFMK• 1 ♂; Galways Land NP; 6.96747401°N, 80.77677784°E; 1982m; 23 Feb. 2019; Eberle &

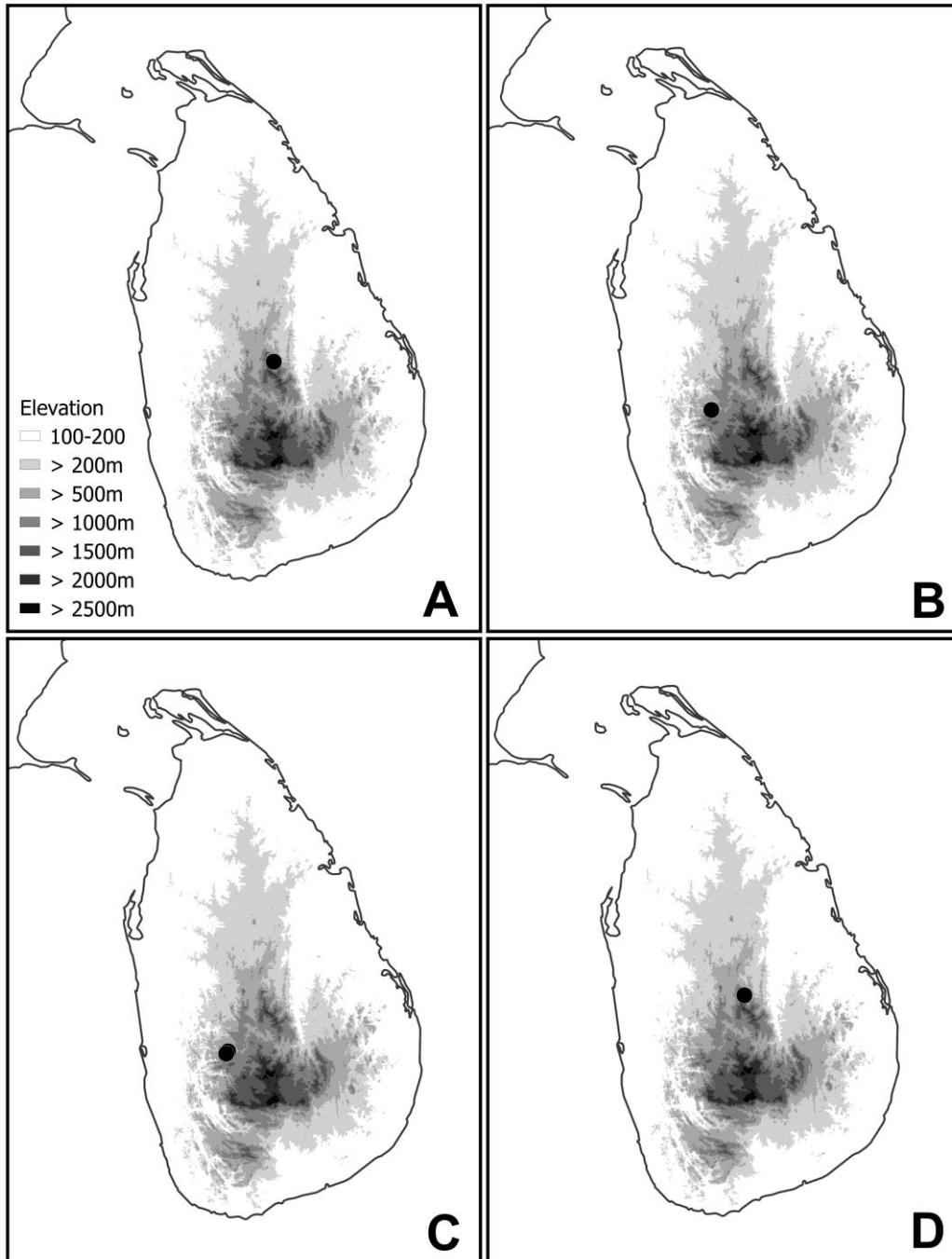


Figure 5.5. Distribution of the new species **A**, *Selaserica athukoralai* sp. n. **B**, *Neoserica dharmapriyai* sp. n. **C**, *Maladera galdaththana* sp. n. **D**, *M. cervicornis* sp. n.



Figure 5.6. Photos of the habitats of the new species **A**, *Selaserica athukoralai* sp. n. **B**, *Neoserica dharmapriyai* sp. n. **B–C**, *Maladera galdaththana* sp. n. **D**, *M. cervicornis* sp. n.

Ranasinghe leg.; Black light; X-SR0147; ZFMK• 1 ♂; Piduruthalagala FR_outside; 6.97845°N, 80.77944444°E; 2013m; 25 Feb. 2019; Eberle & Ranasinghe leg.; Black light; X-SR0151; ZFMK• 4 ♂♂; Piduruthalagala FR; 6.98299444°N, 80.77305556°E; 2073m; 25 Feb. 2019; Eberle & Ranasinghe leg.; Black light; X-SR0126, X-SR0128, X-SR0148, X-SR0150; ZFMK• 2 ♂♂; Piduruthalagala FR; 6.98955278°N, 80.77138889°E; 2192m; 25 Feb. 2019; Eberle & Ranasinghe leg.; Black light; X-SR0022, X-SR0023; ZFMK

***Maladera breviatella* Fabrizi & Ahrens, 2014**

Material examined.

SRI LANKA • 1 ♂; Matale District, Dambulla, NIFS Arboretum; 7.85783259°N, 80.67391938°E; 167m; 17 Feb. 2019; Eberle & Ranasinghe leg.; Black light; X-SR0030; ZFMK• 1 ♂; Dambulla, NIFS Arboretum; 7.86011766°N, 80.67441844°E; 187m; 16 Feb. 2019; Eberle & Ranasinghe leg.; Light sheet; X-SR0156; NIFS • 4 ♂♂; Dambulla, NIFS Arboretum; 7.86011766°N, 80.67441844°E; 187m; 17 Feb. 2019; Eberle & Ranasinghe leg.; Light sheet; X-SR0051 to X-SR0054; ZFMK.

***Maladera calcarata* (Brenske, 1898)**

Material examined.

SRI LANKA • 1 ♂; Matale District, Dambulla, NIFS Arboretum; 7.85766783°N, 80.67474244°E; 174m; 16 Feb. 2019; Eberle & Ranasinghe leg.; Black light; X-SR0086; ZFMK• 1 ♂; Dambulla, NIFS Arboretum; 7.85783259°N, 80.67391938°E; 167m; 18 Feb. 2019; Eberle & Ranasinghe leg.; Black light; X-SR0142; NIFS • 1 ♂; Dambulla, NIFS Arboretum; 7.85897387°N, 80.67533196°E; 203m; 16 Feb. 2019; Eberle & Ranasinghe leg.; Black light; X-SR0100; ZFMK.

***Maladera cinnaberina* (Brenske, 1898)**

Material examined.

SRI LANKA • 1 ♂; Kegalle District, Aranayake, near tea estate; 7.15068199°N, 80.46286137°E; 252m; 03 Mar. 2019; Eberle & Ranasinghe leg.; Black light net; X-SR0094; ZFMK• 1 ♂; Pannala, Polwaththa, Aranayake; 7.15828056°N, 80.46666667°E; 238m; 03 Mar. 2019; Eberle & Ranasinghe leg.; Black light; X-SR0155; ZFMK.

***Maladera coxalis* (Moser, 1915)**

Material examined.

SRI LANKA • 3 ♂♂; Kegalle District, Pannala, Galdaththa, Aranayake; 7.16154167°N, 80.46388889°E; 294m; 03 Mar. 2019; Eberle & Ranasinghe leg.; Black light; X-SR0096, X-SR0132, X-SR0133; ZFMK.

Maladera dubia* (Arrow, 1916)*Material examined.**

SRI LANKA • 2 ♂♂; Nuwara Eliya District, Horton Plains; 6.80133047°N, 80.80275893°E; 2116m; 28 Feb. 2019; Eberle & Ranasinghe leg.; Hand collecting; X-SR0069, X-SR0071; NIFS • 1 ♂; Horton Plains; 6.81437222°N, 80.80638889°E; 2146m; 28 Feb. 2019; Eberle & Ranasinghe leg.; Light sheet; X-SR0120; ZFMK • 6 ♂♂; Horton Plains; 6.82978333°N, 80.80611111°E; 2154m; 26 Feb. 2019; Eberle & Ranasinghe leg.; Black light; X-SR0046, X-SR0047, X-SR0063 to X-SR0065, X-SR0168; ZFMK • 1 ♂; Hakgala SNR, Near Kande Ela resorviour; 6.91179564°N, 80.79491161°E; 1882m; 23 Feb. 2019; Eberle & Ranasinghe leg.; Black light; X-SR0177; ZFMK • 1 ♂; Hakgala SNR, Seetha Eliya; 6.9304544°N, 80.81356983°E; 1789m; 24 Feb. 2019; Eberle & Ranasinghe leg.; Black light; X-SR0025; ZFMK • 2 ♂♂; Hakgala SNR, Seetha Eliya; 6.93074021°N, 80.8134195°E; 1773m; 24 Feb. 2019; Eberle & Ranasinghe leg.; Black light; X-SR0130, X-SR0161; ZFMK • 2 ♂♂; Piduruthalagala FR; 6.98299444°N, 80.77305556°E; 2073m; 25 Feb. 2019; Eberle & Ranasinghe leg.; Black light; X-SR0127, X-SR0149; ZFMK • 2 ♂♂; Piduruthalagala FR; 6.98955278°N, 80.77138889°E; 2192m; 25 Feb. 2019; Eberle & Ranasinghe leg.; Black light; X-SR0184, X-SR0185; ZFMK.

Maladera fistulosa* (Brenske, 1898)*Material examined.**

SRI LANKA • 1 ♂; Nuwara Eliya District, Hakgala SNR, Seetha Eliya; 6.9304544°N, 80.81356983°E; 1789m; 24 Feb. 2019; Eberle & Ranasinghe leg.; Black light; X-SR0002; ZFMK • 2 ♂♂; Hakgala SNR, Seetha Eliya; 6.93074021°N, 80.8134195°E; 1773m; 24 Feb. 2019; Eberle & Ranasinghe leg.; Black light; X-SR0160, X-SR0162; ZFMK.

Maladera heveli* Fabrizi & Ahrens, 2014*Material examined.**

SRI LANKA • 1 ♂; Matale District, Dambulla, NIFS Arboretum; 7.85766783°N, 80.67474244°E; 174m; 18 Feb. 2019; Eberle & Ranasinghe leg.; Black light; X-SR0090; ZFMK.

Maladera hortonensis* Fabrizi & Ahrens, 2014*Material examined.**

SRI LANKA • 2 ♂♂; Nuwara Eliya District, Horton Plains; 6.80735°N, 80.80472222°E; 2138m; 26 Feb. 2019; Eberle & Ranasinghe leg.; Black light; X-SR0007, X-SR0008; ZFMK • 1 ♂; Horton Plains; 6.82978333°N, 80.80611111°E; 2154m; 26 Feb. 2019; Eberle & Ranasinghe leg.; Black light; X-SR0170; ZFMK •

1 ♂; Piduruthalagala FR; 6.98955278°N, 80.77138889°E; 2192m; 25 Feb. 2019; Eberle & Ranasinghe leg.; Black light; X-SR0182; NIFS • 4 ♂♂; Piduruthalagala FR; 7.00029167°N, 80.77527778°E; 2483m; 25 Feb. 2019; Eberle & Ranasinghe leg.; Black light; X-SR0083, X-SR0085, X-SR0167, X-SR0040; ZFMK.

***Maladera lindulana* Fabrizi & Ahrens, 2014**

Material examined.

SRI LANKA • 1 ♂; Kandy District, Deenston, Knuckles South; 7.32972685°N, 80.86098159°E; 1169m; 21 Feb. 2019; Eberle & Ranasinghe leg.; Black light; X-SR0108; ZFMK • 1 ♂; Deenston, Knuckles South; 7.32991027°N, 80.86093445°E; 1142m; 20 Feb. 2019; Eberle & Ranasinghe leg.; Light sheet; X-SR0106; ZFMK • 1 ♂; Deenston, Knuckles South; 7.33077851°N, 80.86049097°E; 1156m; 19 Feb. 2019; Eberle & Ranasinghe leg.; Black light; X-SR0174; ZFMK • 1 ♂; Deenston, Knuckles South; 7.33097004°N, 80.85934859°E; 1190m; 20 Feb. 2019; Eberle & Ranasinghe leg.; Black light; X-SR0055; ZFMK • 1 ♂; Deenston, Knuckles South; 7.33616555°N, 80.85907541°E; 1197m; 21 Feb. 2019; Eberle & Ranasinghe leg.; Black light; X-SR0123; NIFS.

***Maladera pubescens* (Arrow, 1916)**

Material examined.

SRI LANKA • 2 ♂♂; Kegalle District, Pannala, Galdaththa, Aranayake; 7.16154167°N, 80.46388889°E; 294m; 03 Mar. 2019; Eberle & Ranasinghe leg.; Black light; X-SR0037, X-SR0097; ZFMK.

***Maladera rotundata* (Walker, 1859)**

Material examined.

SRI LANKA • 1 ♂; Kegalle District, Pannala, Galdaththa, Aranayake; 7.16154167°N, 80.46388889°E; 294m; 03 Mar. 2019; Eberle & Ranasinghe leg.; Black light; X-SR0134; ZFMK.

***Maladera rufocuprea* (Blanchard, 1850)**

Material examined.

SRI LANKA • 1 ♂; Ratnapura District, Belihuloya; 6.731762°N, 80.773989°E; 750m; 01 Mar. 2019; Eberle & Ranasinghe leg.; Black light; X-SR0158; ZFMK • 1 ♂; Kegalle District, Aranayake, near tea estate; 7.15050176°N, 80.46239683°E; 245m; 12 Feb. 2019; Eberle & Ranasinghe leg.; Black light; X-SR0062; NIFS • 3 ♂♂; Kegalle District, Aranayake, near tea estate; 7.15068199°N, 80.46286137°E; 252m; 10 Feb. 2019; Eberle & Ranasinghe leg.; Black light; X-SR0080 to X-SR0082; ZFMK.

Maladera weligamana* (Brenske, 1900)*Material examined.**

SRI LANKA • 1 ♂; Kandy District, Deenston, Knuckles South; 7.33082417°N, 80.86203243°E; 1108m; 20 Feb. 2019; Eberle & Ranasinghe leg.; Black light; X-SR0187; ZFMK.

Selaserica maculicauda* (Arrow, 1916)*Material examined.**

SRI LANKA • 1 ♂; Nuwara Eliya District, Horton Plains; 6.7987251°N, 80.83160249°E; 2146m; 27 Feb. 2019; Eberle & Ranasinghe leg.; Black light; X-SR0145; ZFMK.

Selaserica nitida* (Candèze, 1861)*Material examined.**

SRI LANKA • 1 ♂; Nuwara Eliya District, Hakgala SNR, Seetha Eliya; 6.92999891°N, 80.81359713°E; 1794m; 24 Feb. 2019; Eberle & Ranasinghe leg.; Black light; X-SR0119; ZFMK.

Selaserica pusilla* Arrow, 1916*Material examined.**

SRI LANKA • 1 ♂; Matale District, Dambulla, NIFS Arboretum; 7.85897387°N, 80.67533196°E; 203m; 16 Feb. 2019; Eberle & Ranasinghe leg.; Black light; X-SR0101; ZFMK.

Neoserica sexfoliata* Moser, 1915*Material examined.**

SRI LANKA • 1 ♂; Matale District, Dambulla, NIFS Arboretum; 7.86011766°N, 80.67441844°E; 187m; 18 Feb. 2019; Eberle & Ranasinghe leg.; Light sheet; X-SR0115; ZFMK.

Serica fusa* Brenske, 1898*Material examined.**

SRI LANKA • 3 ♂♂; Nuwara Eliya District, Horton Plains; 6.81278056°N, 80.80444444°E; 2147m; 26 Feb. 2019; Eberle & Ranasinghe leg.; Black light; X-SR0032 to X-SR0034; ZFMK • 3 ♂♂; Hakgala SNR, Near Kande Ela resorviour; 6.90995856°N, 80.79366605°E; 1917m; 24 Feb. 2019; Eberle & Ranasinghe leg.; Black light; X-SR0164 to X-SR0166; ZFMK • 6 ♂♂; Hakgala SNR, Near Kande Ela resorviour; 6.91085232°N, 80.79427602°E; 1914m; 23-24 Feb. 2019; Eberle & Ranasinghe leg.; Black light; X-SR0042 to X-SR0044, X-SR0072 to X-SR0074; ZFMK • 3 ♂♂, 1 ♀; Hakgala SNR, Near Kande Ela resorviour; 6.91133456°N, 80.79475087°E; 1907m; 23 Feb. 2019; Eberle & Ranasinghe leg.;

Black light; X-SR0141, X-SR0171 to X-SR0173; ZFMK• 2 ♂♂; Hakgala SNR, Near Kande Ela reservoir; 6.91179564°N, 80.79491161°E; 1882m; 23-24 Feb. 2019; Eberle & Ranasinghe leg.; Black light; X-SR0091, X-SR0152; NIFS • 2 ♂♂; Hakgala SNR, Seetha Eliya; 6.92999891°N, 80.81359713°E; 1794m; 24 Feb. 2019; Eberle & Ranasinghe leg.; Black light; X-SR0153, X-SR0154; ZFMK• 1 ♂; Hakgala SNR, Seetha Eliya; 6.93074021°N, 80.8134195°E; 1773m; 24 Feb. 2019; Eberle & Ranasinghe leg.; Black light; X-SR0068; ZFMK• 1 ♂; Galways Land NP; 6.96616216°N, 80.77744079°E; 1931m; 23 Feb. 2019; Eberle & Ranasinghe leg.; Black light; X-SR0050; ZFMK• 3 ♂♂; Nuwara Eliya District, Piduruthalagala FR_outside; 6.97845°N, 80.77944444°E; 2013m; 25 Feb. 2019; Eberle & Ranasinghe leg.; Black light; X-SR0059 to X-SR0061; ZFMK• 1 ♂; Piduruthalagala FR; 6.98955278°N, 80.77138889°E; 2192m; 25 Feb. 2019; Eberle & Ranasinghe leg.; Black light; X-SR0058; ZFMK.

***Serica lurida* Brenske, 1898**

Material examined.

SRI LANKA • 2 ♂♂; Kandy District, Deenston, Knuckles South; 7.32972685°N, 80.86098159°E; 1169m; 21 Feb. 2019; Eberle & Ranasinghe leg.; Black light; X-SR0109, X-SR0110; ZFMK• 2 ♂♂, 1 ♀; Deenston, Knuckles South; 7.32991027°N, 80.86093445°E; 1142m; 19-20 Feb. 2019; Eberle & Ranasinghe leg.; Light sheet; X-SR0098, X-SR0099, X-SR0107; ZFMK• 1 ♂; Deenston, Knuckles South; 7.33097004°N, 80.85934859°E; 1190m; 20 Feb. 2019; Eberle & Ranasinghe leg.; Black light; X-SR0056; ZFMK• 1 ♂; Deenston, Knuckles South; 7.33616555°N, 80.85907541°E; 1197m; 21 Feb. 2019; Eberle & Ranasinghe leg.; Black light; X-SR0125; NIFS.

5.4 Discussion

This first supplement to the monograph of Sericini of the Sri Lanka (Fabrizi & Ahrens, 2014), that includes the description of four new species, revealed furthermore the high amount of endemism of the subcontinent and confirmed another time, how unexplored Sri Lanka is yet. Efforts on additional and more intensive sampling with light traps closer to remnant forest areas and not yet explored areas off the so far protected areas, may reveal unknown taxa but also complete the knowledge of the fauna in a more comprehensive way, covering the entire land surface of the Island. Therefore, we plan further field work and sampling effort.

5.5 References

- Ahrens D. & Fabrizi S. (2016). A Monograph of the Sericini of India (Coleoptera: Scarabaeidae). *Bonn Zoological Bulletin* 65, 1–355.
- Fabrizi S. & Ahrens D. (2014). A Monograph of the Sericini of Sri Lanka (Coleoptera: Scarabaeidae). *Bonn Zoological Bulletin, Supplements* 61, 1–124.
- Eberle J., Fabrizi S., Lago P. & Ahrens D. (2016). A historical biogeography of megadiverse Sericini – another story “out of Africa”? *Cladistics* 33, 183–197.

Chapter 6

New species of Sericini from Sri Lanka (Coleoptera, Scarabaeidae) Part II

This chapter is published in:

Ranasinghe S., Eberle J., Athukorala, N., Benjamin S.P. & Ahrens D. (2022).
New species of Sericini from Sri Lanka (Coleoptera, Scarabaeidae).
European Journal of Taxonomy, 821, 57–101.
<https://doi.org/10.5852/ejt.2022.821.1799>

Authors' contributions to the original article:

SR, JE, NP, SB: fieldwork; SR, DA: species identification, writing-original draft; DA: identification key; DA, JE, SB, SR: manuscript review and editing.

Abstract

Here we present the results of our field survey in Sri Lanka and describe ten new Sericini species: *Selaserica fabriziae* sp. nov., *Sel. sororinitida* sp. nov., *Neoserica pophami* sp. nov., *Maladera haniel* sp. nov., *M. kishi* sp. nov., *M. windy* sp. nov., *M. karunaratnae* sp. nov., *M. hiyarensis* sp. nov., *M. dambullana* sp. nov., and *M. deenstana* sp. nov. All seven of the newly described *Maladera* species belong to the *M. fistulosa* species group, which is an endemic radiation in the island that is characterized by entirely reduced or fused parameres. An updated key to the *Maladera fistulosa* group is provided. Further, new locality records for 23 already known species are given. The genitalia and the habitus of all new species are illustrated, the distribution of the new species is shown with maps.

6.1 Introduction

The fauna of the Sericini of Sri Lanka has been recently the focus of some intensive investigations (Fabrizi & Ahrens, 2014; Ranasinghe *et al.*, 2020). Currently, the Sri Lankan fauna of Sericini comprises 81 species (Fabrizi & Ahrens, 2014; Ranasinghe *et al.*, 2020), 71 of them are endemic. For a more thorough investigation of the fauna, we carried out a series of recent field expeditions to Sri Lanka, with the aim of collecting fresh material for both morphological and molecular phylogenetic studies. While the results from the first expedition in 2019 were published in Ranasinghe *et al.* (2020), here we present the results of the three subsequent expeditions, during which we were able to discover further ten new species belonging to the genera *Maladera* Mulsant & Rey, 1871, *Neoserica* Brenske, 1894 and *Selaserica* Brenske, 1897. Furthermore, we report new locality records for twenty-three previously known species.

6.2 Material and methods

Additional field surveys were carried out in order to collect Sericini beetles (Coleoptera: Scarabaeidae) in fifteen different Sri Lankan localities (Fig. 6.1) in Kandy, Kegalle, Matale, Nuwara Eliya and Galle Districts from October to November 2019, June to August 2020 and November to December 2020. Beetles were captured using UV-light traps as explained in Ranasinghe *et al.* (2020) or by manual collecting from a white sheet (Fig. 6.2) illuminated with UV light (LepiLED, © WIF, Dr Gunnar Brehm, Jena, Germany). The preserved specimens were examined under a Wild M3Z stereomicroscope. All male genitalia were dissected and glued to a card point. Specimens were identified to species level using recent literature (Fabrizi & Ahrens 2014; Ahrens & Fabrizi, 2016; Ranasinghe *et al.*, 2020) and, in some cases, by additional comparison with previously examined type specimens.

Newly discovered species were photographed using a Zeiss AxioCam HRc camera. Multifocal images were taken using the Zeiss Axio Vision software package, and stacked using Zerene Stacker (www.zerene.com). Maps of sample sites and species distribution were prepared using Quantum GIS 3.6.2 (<https://www.qgis.org>). On the specimen labels, the terms “Forest Reserve” (FR) and “Strict Nature Reserve” (SNR) were abbreviated, respectively.

Institutional abbreviations

NIFS – National Institute of Fundamental Studies, Kandy, Sri Lanka;
ZFMK – Zoological Research Museum A. Koenig, Bonn, Germany.

6.3 Results

6.1.1 Taxonomy

Class Insecta Linnaeus, 1758
Subclass Pterygota Lang, 1888
Superfamily Scarabaeoidea Latreille, 1802
Family Scarabaeidae Latreille, 1802
Subfamily Melolonthinae Leach, 1819
Tribe Sericini Kirby, 1837

Genus *Selaserica* Brenske, 1897

***Selaserica fabriziae* sp. nov.**

Figs 6.3A–D, 6.7A, 6.8A

Diagnosis. *Selaserica fabriziae* sp. nov. is in shape of aedeagus rather similar to *Sel. sericea* (Arrow, 1916), it differs by the shiny dorsal body surface and the shape of parameres and phallobase: the median dorsoapical situation of phallobase is much narrower (than in *Sel. sericea*), the parameres are bent dorsally at apex (not bent in *Sel. sericea*).

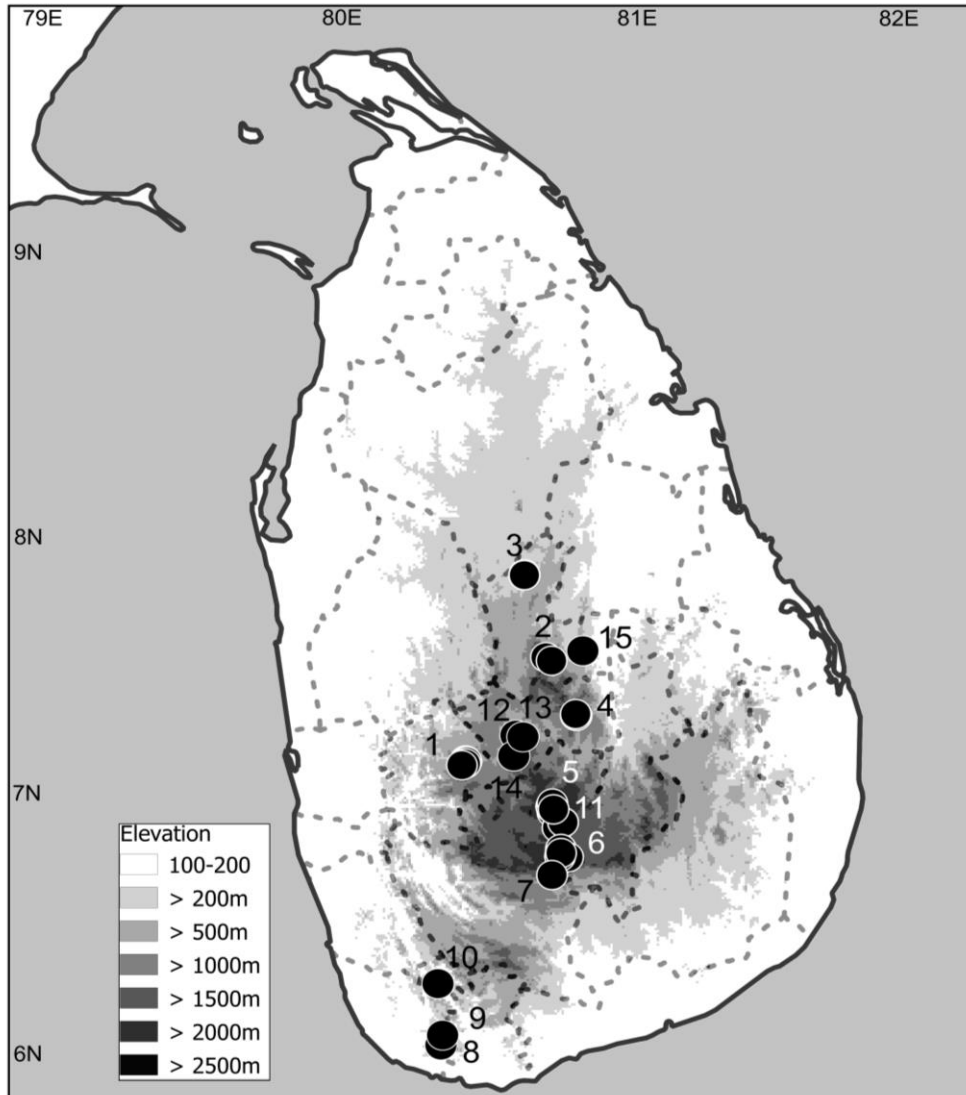


Figure 6.1. Map of Sri Lanka showing collecting sites for this study. Numbers refer to major sampling localities. 1 = Aranayake; 2 = Riverston; 3 = NIFS Arboretum; 4 = Deenston; 5 = Nuwara Eliya; 6 = Horton Plains; 7 = Belihuloya; 8 = Hiyare; 9 = Kottawa; 10 = Kanneliya; 11 = Piduruthalagala; 12 = Uda Peradeniya; 13 = Gannoruwa; 14 = Udawattakele; 15 = Sera Ella.



Figure 6.2. A. Manual collecting from a white sheet illuminated with UV light in the field. B–C. Live Sericini collected from the field. A. *Maladera bandarwelana*, male. C. *Maladera* sp., female. (Photographs: C. Jayatissa).

Etymology. The new species is dedicated to Silvia Fabrizi, who passed away too early, in memory of her and for all her efforts for Sericini taxonomy (noun in genitive singular case). - We will not forget you, Silvia!

Type material examined

Holotype

SRI LANKA • ♂; “X-SR0859, Sri Lanka, Galle District, Kottawa FR, 6.09812°N, 80.31610°E, 44m, 26-X-2019; Eberle, Bohacz & Ranasinghe, Black light”; ZFMK.

Paratypes

SRI LANKA • 1 ♂; “X-SR1948, Sri Lanka, Galle District, Kottawa FR, 6.09712°N, 80.31666°E; 46m, 29-30-VI-2020, Benjamin & Ranasinghe, Black light”; ZFMK • 1 ♂; “X-SR1956, Sri Lanka, Galle District, Kottawa FR, 6.09712°N, 80.31666°E; 46m, 29-30-VI-2020, Benjamin & Ranasinghe, Black light”; ZFMK • 1 ♂; “X-SR1957, Sri Lanka, Galle District, Kottawa FR, 6.09712°N, 80.31666°E; 46m, 29-30-VI-2020, Benjamin & Ranasinghe, Black light”; ZFMK • 1 ♂; “X-SR1958, Sri Lanka, Galle

District, Kottawa FR, 6.09712°N, 80.31666°E; 46m, 29-30-VI-2020, Benjamin & Ranasinghe, Black light”; ZFMK • 1 ♂; “X-SR1959, Sri Lanka, Galle District, Kottawa FR, 6.09712°N, 80.31666°E; 46m, 29-30-VI-2020, Benjamin & Ranasinghe, Black light”; ZFMK • 1 ♂; “X- SR1960, Sri Lanka, Galle District, Kottawa FR, 6.09712°N, 80.31666°E; 46m, 29-30-VI-2020, Benjamin & Ranasinghe, Black light”; ZFMK • 1 ♂; “X- SR2118, Sri Lanka, Galle District, Kottawa FR, 6.09812°N, 80.31610°E, 44m, 11-XII-2020; Ranasinghe & Athukorala, Black light”; ZFMK • 1 ♂; “X- SR2119, Sri Lanka, Galle District, Kottawa FR, 6.09812°N, 80.31610°E, 44m, 11-XII-2020; Ranasinghe & Athukorala, Black light”; ZFMK • 1 ♂; “X- SR2120, Sri Lanka, Galle District, Kottawa FR, 6.09812°N, 80.31610°E, 44m, 11-XII-2020; Ranasinghe & Athukorala, Black light”; ZFMK • 1 ♂; “X- SR2121, Sri Lanka, Galle District, Kottawa FR, 6.09812°N, 80.31610°E, 44m, 11-XII-2020; Ranasinghe & Athukorala, Black light”; ZFMK • 1 ♂; “X- SR2122, Sri Lanka, Galle District, Kottawa FR, 6.09812°N, 80.31610°E, 44m, 11-XII-2020; Ranasinghe & Athukorala, Black light”; ZFMK • 1 ♀; “X- SR1961, Sri Lanka, Galle District, Kottawa FR, 6.09812°N, 80.31610°E, 44m, 30-VI-2020, Benjamin & Ranasinghe, Black light”; ZFMK • 1 ♀; “X- SR2123, Sri Lanka, Galle District, Kottawa FR, 6.09812°N, 80.31610°E, 44m, 11-XII-2020; Ranasinghe & Athukorala, Black light”; ZFMK • 1 ♀; “X- SR2104, Sri Lanka, Galle District, Kottawa FR, 6.09712°N, 80.31666°E; 46m, 11-XII-2020; Ranasinghe & Athukorala, Black light”; ZFMK.

Description

MEASUREMENTS. Length: 8.9 mm, length of elytra: 6.1 mm, width: 5.2 mm.

HABITUS AND COLORATION. Body oval, dark brown, antenna yellow, dorsal surface shiny and glabrous.

HEAD. Labroclypeus subtrapezoidal, wider than long, widest at base, lateral margins weakly convex and convergent to moderately rounded anterior angles, lateral border and ocular canthus producing a blunt angle, margins weakly reflexed, anterior margin shallowly sinuate medially; surface strongly convex medially, weakly shiny, anterior half nearly impunctate, behind finely and densely punctate, distance between punctures subequal to their diameter, with a few fine setae behind anterior margin; frontoclypeal suture very feebly impressed and weakly angled medially; smooth area in front of eye approximately three times as wide as long; ocular canthus moderately long and narrow, impunctate but surface slightly concave, with a single short terminal seta. Frons with fine, moderately dense punctures, posterior half impunctate, surface

glabrous except for a few setae anteriorly beside eyes. Eyes moderately large, ratio of diameter/ interocular width: 0.7. Antenna yellowish brown, with ten antennomeres; club with four antennomeres, 1.3 times as long as remaining antennomeres combined. Mentum elevated and anteriorly flattened.

PRONOTUM. Moderately wide, widest at base, lateral margins evenly convex and narrowed to anterior angles, anterior angles strongly produced and sharp, anterior marginal line widely incomplete medially, anterior margin moderately produced medially; surface densely and coarsely punctate, glabrous; anterior and lateral borders sparsely setose, basal margin without marginal line; hypomeron ventrobasally carinate and but not produced ventrally. Scutellum wide, triangular, with fine and dense punctures, each bearing a single very minute seta.

ELYTRA. Oblong, widest in posterior third, striae indistinctly impressed, finely and densely punctate, intervals flat, with fine, moderately dense punctures concentrated along striae, punctures partly with minute setae, without longer erect setae; epipleural edge fine, ending at the convex external apical angle of elytra, epipleura densely setose, apical border membranous, apex covered with short microtrichomes.

VENTRAL SURFACE. Dull, thorax and metacoxa with large and dense punctures, sparsely finely setose, metacoxa glabrous except for numerous short setae laterally; each abdominal sternite with generally distributed fine and dense punctures, without a distinct transverse row of coarse punctures each bearing a short seta, punctures with very short or minute setae, penultimate sternite apically with a shiny smooth but very short chitinous border. Mesosternum between mesocoxae little wider than mesofemur. Ratio of length of metepisternum/ metacoxa: 1/ 1.15. Pygidium lost in holotype.

LEGS. Moderately wide; femur with two longitudinal rows of setae, finely and moderately densely punctate; metafemur dull, anterior edge acute, with adjacent continuously serrated line, anterior longitudinal row of setae complete; posterior ventral margin almost straight, weakly widened in apical half, nor ventrally nor dorsally serrated, glabrous. Metatibia moderately wide and long, widest behind middle, dorsal and ventral margins in posterior two thirds subparallel, ratio width/ length: 1/ 3.2, dorsally weakly edged, with two groups of spines, basal one at first quarter, apical one at three quarters of metatibial length, basally beside dorsal margin with a very short serrated line; lateral face longitudinally convex, with very sparse

and fine punctures, punctures glabrous; ventral margin with three strong spines equidistant from each other, medial face smooth, apex interiorly near tarsal articulation distinctly concave. Tarsomeres impunctate dorsally, ventrally with dense, fine setae; metatarsomeres ventrally with a strongly serrated ridge, beside which is no strong longitudinal carina, first metatarsomere one quarter of its length longer than dorsal tibial spur, subsequent tarsomeres lacking in holotype. Protibia moderately long, tridentate. Protarsomeres lacking in holotype.

AEDEAGUS. Fig. 6.3A–C.

HABITUS. Fig. 6.3D.

Variation. Length: 8.2-8.8 mm, length of elytra: 6.1-6.25 mm, width: 5.2-5.3 mm. Pygidium moderately convex, shiny, finely densely punctate, without smooth midline, glabrous except some longer setae along the apical margin. First metatarsomere one quarter of its length longer than dorsal tibial spur, slightly shorter than following two tarsomeres combined. Protibia moderately long, tridentate. Protarsomeres ventrally with some yellow setae, protarsal claws symmetrical, feebly curved and short, with normally developed basal tooth.

Female. Length: 8.8-9.2 mm, length of elytra: 6.2-7.0 mm, width: 5.5-5.7 mm. Eyes as large as in male; antennal club as long as remaining antennomeres combined.

Distribution. See Fig. 6.7A.

***Selaserica sororinitida* sp. nov.**

Figs 6.3E–H, 6.7B, 6.8B

Diagnosis. *Selaserica sororinitida* sp. nov. is in shape of aedeagus and external morphology similar to *Sel. nitida* (Candèze, 1861) and *Sel. knucklensis* Fabrizi & Ahrens, 2014. *Selaserica sororinitida* sp. nov. differs by the antennal club, which is longer compared to *Sel. nitida* but shorter in comparison with *Sel. knucklensis*. From both species *Sel. sororinitida* sp. nov. can be also distinguished by the shape of aedeagus: the right paramere is in the new species shorter and less narrowed before the apex (lateral view); the phallobase is not widened distally as in *Sel. knucklensis*.

Etymology. The name is derived from the Latin noun “*soror*” (sister) with “*nitida*” from the species *Sel. nitida*, with reference to the strong morphological similarity with *Sel. nitida* (noun in nominative case).

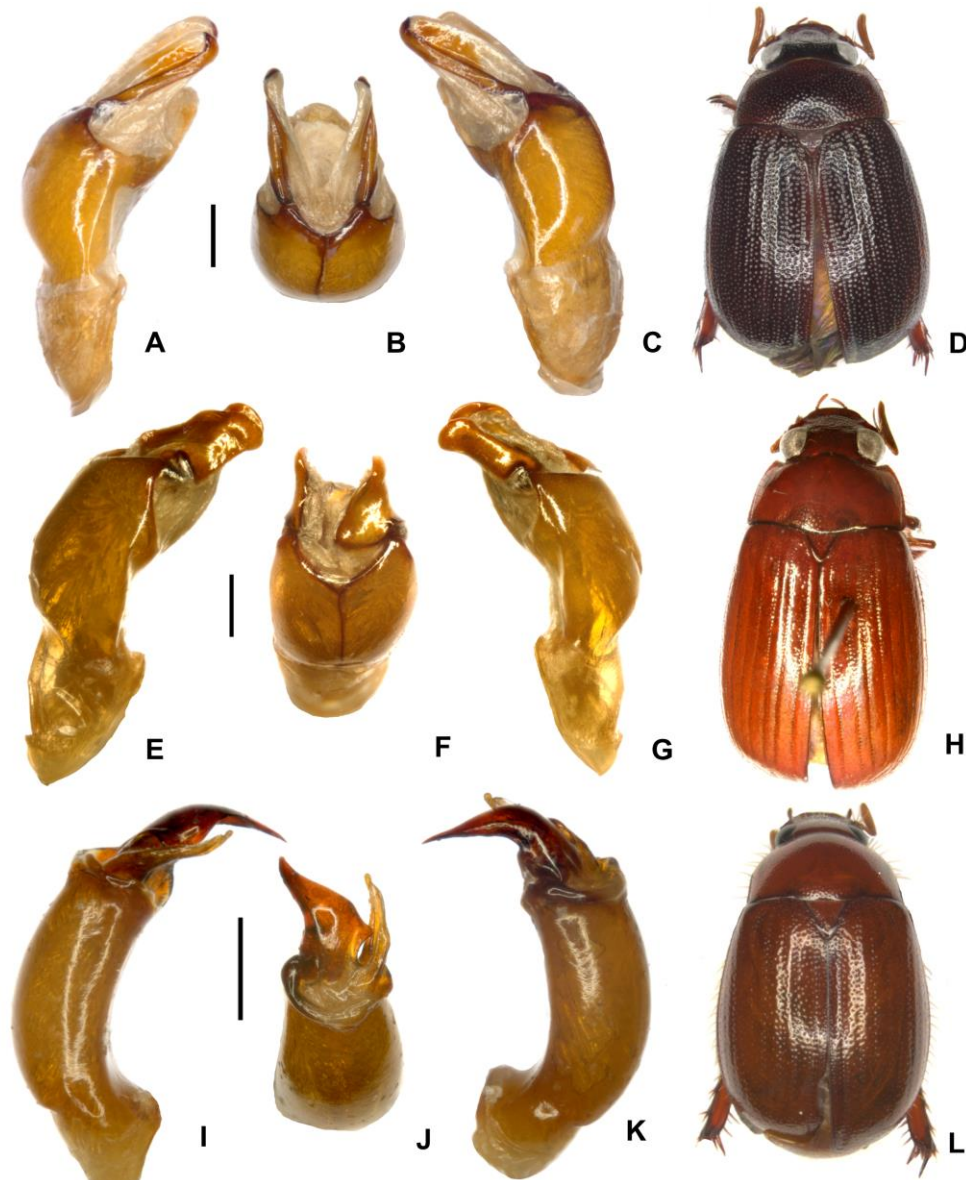


Figure 6.3. A–D *Selaserica fabriziae* sp. nov., (holotype) E–H *Selaserica sororinitida* sp. nov., (holotype) I–L *Neoserica pophami* sp. nov., (holotype) A, E, I aedeagus, left side lateral view C, G, K aedeagus, right side lateral view B, F, J parameres, dorsal view D, H, L habitus (not to scale). Scale: 0.5 mm.

Type material examined**Holotype**

SRI LANKA • ♂; “X-SR0670, Sri Lanka, Kandy District, Deanston, Knuckles South; 7.33159°N, 80.86110°E; 1139m; 17-X-2019; Eberle, Bohacz & Ranasinghe leg.; Black light”; ZFMK.

Paratypes

SRI LANKA • 1 ♂; “X-SR0224, Sri Lanka, Kandy District, Deanston, Knuckles South; 7.33082°N, 80.86203°E; 1108m; 17-18-X-2019; Eberle, Bohacz & Ranasinghe leg.; Black light”; ZFMK • 1 ♂; “X-SR0227, Sri Lanka, Kandy District, Deanston, Knuckles South; 7.33082°N, 80.86203°E; 1108m; 17-18-X-2019; Eberle, Bohacz & Ranasinghe leg.; Black light”; ZFMK • 1 ♂; “X-SR0228, Sri Lanka, Kandy District, Deanston, Knuckles South; 7.33082°N, 80.86203°E; 1108m; 17-18-X-2019; Eberle, Bohacz & Ranasinghe leg.; Black light”; ZFMK • 1 ♂; “X-SR0229, Sri Lanka, Kandy District, Deanston, Knuckles South; 7.33082°N, 80.86203°E; 1108m; 17-18-X-2019; Eberle, Bohacz & Ranasinghe leg.; Black light”; ZFMK • 1 ♂; “X-SR0230, Sri Lanka, Kandy District, Deanston, Knuckles South; 7.33082°N, 80.86203°E; 1108m; 17-18-X-2019; Eberle, Bohacz & Ranasinghe leg.; Black light”; ZFMK • 1 ♂; “X-SR0231, Sri Lanka, Kandy District, Deanston, Knuckles South; 7.33082°N, 80.86203°E; 1108m; 17-18-X-2019; Eberle, Bohacz & Ranasinghe leg.; Black light”; ZFMK • 1 ♂; “X-SR0232, Sri Lanka, Kandy District, Deanston, Knuckles South; 7.33082°N, 80.86203°E; 1108m; 17-18-X-2019; Eberle, Bohacz & Ranasinghe leg.; Black light”; ZFMK • 1 ♂; “X-SR0233, Sri Lanka, Kandy District, Deanston, Knuckles South; 7.33082°N, 80.86203°E; 1108m; 17-18-X-2019; Eberle, Bohacz & Ranasinghe leg.; Black light”; ZFMK • 1 ♂; “X-SR0234, Sri Lanka, Kandy District, Deanston, Knuckles South; 7.33082°N, 80.86203°E; 1108m; 17-18-X-2019; Eberle, Bohacz & Ranasinghe leg.; Black light”; ZFMK • 1 ♂; “X-SR0235, Sri Lanka, Kandy District, Deanston, Knuckles South; 7.33082°N, 80.86203°E; 1108m; 17-18-X-2019; Eberle, Bohacz & Ranasinghe leg.; Black light”; ZFMK • 1 ♂; “X-SR0236, Sri Lanka, Kandy District, Deanston, Knuckles South; 7.33082°N, 80.86203°E; 1108m; 17-18-X-2019; Eberle, Bohacz & Ranasinghe leg.; Black light”; ZFMK • 1 ♂; “X-SR0237, Sri Lanka, Kandy District, Deanston, Knuckles South; 7.33082°N, 80.86203°E; 1108m; 17-18-X-2019; Eberle, Bohacz & Ranasinghe leg.; Black light”; ZFMK • 1 ♂; “X-SR0240, Sri Lanka, Kandy District, Deanston, Knuckles South; 7.33082°N, 80.86203°E; 1108m; 17-18-X-2019; Eberle, Bohacz & Ranasinghe leg.; Black light”; ZFMK • 1 ♂; “X-SR0511, Sri Lanka, Kandy District, Deanston, Knuckles South; 7.33082°N, 80.86203°E; 1108m; 17-18-X-2019; Eberle, Bohacz &

Ranasinghe leg.; Black light”; ZFMK • 1 ♂; “X-SR0512, Sri Lanka, Kandy District, Deanston, Knuckles South; 7.33082°N, 80.86203°E; 1108m; 17-18-X-2019; Eberle, Bohacz & Ranasinghe leg.; Black light”; ZFMK • 1 ♂; “X-SR0513, Sri Lanka, Kandy District, Deanston, Knuckles South; 7.33082°N, 80.86203°E; 1108m; 17-18-X-2019; Eberle, Bohacz & Ranasinghe leg.; Black light”; ZFMK • 1 ♂; “X-SR0514, Sri Lanka, Kandy District, Deanston, Knuckles South; 7.33082°N, 80.86203°E; 1108m; 17-18-X-2019; Eberle, Bohacz & Ranasinghe leg.; Black light”; ZFMK • 1 ♂; “X-SR0515, Sri Lanka, Kandy District, Deanston, Knuckles South; 7.33082°N, 80.86203°E; 1108m; 17-18-X-2019; Eberle, Bohacz & Ranasinghe leg.; Black light”; ZFMK • 1 ♂; “X-SR0516, Sri Lanka, Kandy District, Deanston, Knuckles South; 7.33082°N, 80.86203°E; 1108m; 17-18-X-2019; Eberle, Bohacz & Ranasinghe leg.; Black light”; ZFMK • 1 ♂; “X-SR0517, Sri Lanka, Kandy District, Deanston, Knuckles South; 7.33082°N, 80.86203°E; 1108m; 17-18-X-2019; Eberle, Bohacz & Ranasinghe leg.; Black light”; ZFMK • 1 ♂; “X-SR0518, Sri Lanka, Kandy District, Deanston, Knuckles South; 7.33082°N, 80.86203°E; 1108m; 17-18-X-2019; Eberle, Bohacz & Ranasinghe leg.; Black light”; ZFMK • 1 ♂; “X-SR0519, Sri Lanka, Kandy District, Deanston, Knuckles South; 7.33082°N, 80.86203°E; 1108m; 17-18-X-2019; Eberle, Bohacz & Ranasinghe leg.; Black light”; ZFMK • 1 ♂; “X-SR0520, Sri Lanka, Kandy District, Deanston, Knuckles South; 7.33082°N, 80.86203°E; 1108m; 17-18-X-2019; Eberle, Bohacz & Ranasinghe leg.; Black light”; ZFMK • 1 ♂; “X-SR0521, Sri Lanka, Kandy District, Deanston, Knuckles South; 7.33082°N, 80.86203°E; 1108m; 17-18-X-2019; Eberle, Bohacz & Ranasinghe leg.; Black light”; ZFMK • 1 ♂; “X-SR0941, Sri Lanka, Kandy District, Deanston, Knuckles South; 7.33082°N, 80.86203°E; 1108m; 17-18-X-2019; Eberle, Bohacz & Ranasinghe leg.; Black light”; ZFMK • 1 ♂; “X-SR0942, Sri Lanka, Kandy District, Deanston, Knuckles South; 7.33082°N, 80.86203°E; 1108m; 17-18-X-2019; Eberle, Bohacz & Ranasinghe leg.; Black light”; ZFMK • 1 ♂; “X-SR0563, Sri Lanka, Kandy District, Deanston, Knuckles South; 7.33616°N, 80. 85907°E; 1197m; 18-X-2019; Eberle, Bohacz & Ranasinghe leg.; Black light”; ZFMK • 1 ♂; “X-SR0664, Sri Lanka, Kandy District, Deanston, Knuckles South; 7.33501°N, 80. 85966°E; 1171m; 18-X-2019; Eberle, Bohacz & Ranasinghe leg.; Black light”; ZFMK • 1 ♂; “X-SR0669, Sri Lanka, Kandy District, Deanston, Knuckles South; 7.33159°N, 80. 86110°E; 1139m; 17-X-2019; Eberle, Bohacz & Ranasinghe leg.; Black light”; ZFMK • 1 ♂; “X-SR0915, Sri Lanka, Kandy District, Deanston, Knuckles South; 7.33159°N, 80. 86110°E; 1139m; 17-X-2019; Eberle, Bohacz & Ranasinghe leg.; Black light”; ZFMK • 1 ♂; “X-SR1135, Sri Lanka, Kandy District, Deanston, Knuckles South; 7.33501°N, 80. 85966°E; 1171m; 21-II-2019; Eberle & Ranasinghe leg.; Black light”;

ZFMK • 1 ♀; “X-SR0186, Sri Lanka, Kandy District, Deanston, Knuckles South; 7.33082°N, 80.86203°E; 1108m; 20-II-2019; Eberle & Ranasinghe leg.; Black light”; ZFMK • 1 ♀; “X-SR0239, Sri Lanka, Kandy District, Deanston, Knuckles South; 7.33082°N, 80.86203°E; 1108m; 18-X-2019; Eberle, Bohacz & Ranasinghe leg.; Black light”; ZFMK • 1 ♀; “X-SR0943, Sri Lanka, Kandy District, Deanston, Knuckles South; 7.33082°N, 80.86203°E; 1108m; 17-X-2019; Eberle, Bohacz & Ranasinghe leg.; Black light”; ZFMK • 1 ♀; “X-SR2194, Sri Lanka, Kandy District, Deanston, Knuckles South; 7.33082°N, 80.86203°E; 1108m; 05-XII-2020; Ranasinghe & Athukorala leg.; Black light”; ZFMK • 1 ♀; “X-SR2184, Sri Lanka, Kandy District, Deanston, Knuckles South; 7.33159°N, 80.86110°E; 1139m; 05-XII-2020; Ranasinghe & Athukorala leg.; Black light”; ZFMK • 1 ♀; “X-SR0793, Sri Lanka, Kandy District, Deanston, Knuckles South; 7.33501°N, 80.85966°E; 1171m; 18-X-2019; Eberle, Bohacz & Ranasinghe leg.; Black light”; ZFMK • 1 ♀; “X-SR0795, Sri Lanka, Kandy District, Deanston, Knuckles South; 7.33501°N, 80.85966°E; 1171m; 18-X-2019; Eberle, Bohacz & Ranasinghe leg.; Black light”; ZFMK.

Description.

MEASUREMENTS. Length: 10.2 mm, length of elytra: 7.1 mm, width: 5.6 mm.

HABITUS AND COLORATION. Body oblong, reddish brown, antenna yellow, dorsal surface shiny and glabrous, ventral surface dull.

HEAD. Labroclypeus subtrapezoidal, distinctly wider than long, widest at base, lateral margins weakly convex and strongly convergent to strongly rounded anterior angles, lateral border and ocular canthus producing an indistinct blunt angle, margins weakly reflexed; anterior margin shallowly sinuate medially; surface almost flat, finely and densely punctate, distance between punctures subequal to their diameter, with a few robust setae anteriorly; frontoclypeal suture very feebly impressed and curved medially; smooth area in front of eye approximately three times as wide as long; ocular canthus moderately long and narrow, impunctate, with a single short terminal seta. Frons with fine, sparse punctures, posterior third impunctate, surface glabrous except for a few long setae beside eyes. Eyes large, ratio of diameter/interocular width: 0.9. Antenna yellowish brown, with nine antennomeres; club with four antennomeres, 1.2 times as long as remaining antennomeres combined. Mentum elevated and anteriorly flattened.

PRONOTUM. Moderately wide, widest at base, lateral margins in basal half almost straight and weakly convergent, in anterior half weakly convex and distinctly narrowed towards anterior angles, anterior angles moderately produced and moderately sharp; anterior margin moderately produced medially, its marginal line complete; surface moderately densely and finely punctate, glabrous; anterior and lateral borders sparsely setose; basal margin without marginal line. Hypomeron ventrobasally not carinate. Scutellum wide, triangular, with fine and dense punctures, glabrous, apical portion completely impunctate.

ELYTRA. Oblong, widest in posterior third, striae distinctly impressed, finely and densely punctate, intervals flat, with fine, sparse punctures, glabrous, only on penultimate lateral interval a few single long, erect setae; epipleural edge fine, ending well anterior to convex external apical angle of elytra; epipleura densely setose; apical border membranous, apex covered with a narrow rim of short microtrichomes.

VENTRAL SURFACE. Dull, thorax and metacoxa with large and dense punctures, with long and dense setae; metacoxa glabrous except for a few long setae laterally; each abdominal sternite with evenly distributed fine and dense punctures, and with a transverse row of coarse punctures each bearing a robust seta, other punctures with a short or minute setae, penultimate sternite apically with a shiny smooth but very short chitinous border. Mesosternum between mesocoxae little narrower than maximum width of mesofemur. Ratio of length of metepisternum/ metacoxa: 1/ 1.28. Pygidium weakly convex, shiny, finely densely punctate, with long fine setae along the apical margin, otherwise glabrous.

LEGS. Moderately wide and shiny; femur with two longitudinal rows of setae, finely and moderately densely punctate; metafemur with acute anterior edge, without an adjacent serrated line, anterior longitudinal row of setae complete; posterior ventral margin almost weakly convex, weakly widened in apical half, not serrated, glabrous; posterior dorsal margin smooth, densely shortly setose. Metatibia moderately wide and long, widest at apex, ratio width/ length: 1/ 3.3; dorsal margin longitudinally convex, with two groups of spines, basal one at first quarter, apical one at three quarters of metatibial length, without a serrated line; lateral face longitudinally convex, with very sparse and fine punctures, glabrous; ventral margin serrated, with five robust equidistant spines; medial face smooth; apex interiorly near tarsal articulation concavely emarginate. Tarsomeres dorsally impunctate and glabrous, ventrally with dense, long and robust setae; metatarsomeres ventrally with a serrated

ridge, beside it without additional strong longitudinal carina; first metatarsomere one third of its length longer than dorsal tibial spur, distinctly shorter than following two tarsomeres combined. Protibia moderately long, tridentate, basal tooth smaller than the two distal ones. Protarsomeres ventrally with long and dense yellow setae forming a setose pad, protarsal claws symmetrical, basal tooth of claws sharply pointed.

AEDEAGUS. Fig. 6.3E–G.

HABITUS. Fig. 6.3H.

Variation. Length: 9.9-12.0 mm, length of elytra: 7.1-8.1 mm, width: 5.3-5.8 mm.

Female. Length: 12.0-12.2 mm, length of elytra: 8.1-8.3 mm, width: 6.2-6.4 mm. Eyes as smaller than in male; antennal club with three antennomeres and longer than remaining antennomeres combined.

Distribution. See Fig. 6.7B.

Genus *Neoserica* Brenske, 1894

Neoserica pophami sp. nov.

Figs 6.3I–L, 6.7C, 6.8C

Diagnosis. *Neoserica pophami* sp. nov. differs from the very similar *N. kalaarensis* Fabrizi & Ahrens, 2014 in shape of parameres: the right paramere is slightly longer, medially distinctly bent (lateral view) and much wider (dorsal view).

Etymology. The new species is named after Mr. Sam Popham, founder of the NIFS Arboretum (noun in the genitive case).

Type material examined

Holotype

SRI LANKA • ♂; “X-SR0346, Sri Lanka, Matale District, Dambulla, NIFS Arboretum, 7.85783°N, 80.67391°E, 167m, 13-X-2019, Eberle, Bohacz & Ranasinghe, Black light”; ZFMK.

Paratypes

SRI LANKA • 1 ♂; “X-SR0332, Sri Lanka, Matale District, Dambulla, NIFS Arboretum; 7.85783°N, 80.67391°E; 167m; 13-X-2019; Eberle, Bohacz & Ranasinghe leg.; Black light”, ZFMK • 1 ♂; “X-SR0333, Sri Lanka, Matale District, Dambulla, NIFS Arboretum; 7.85783°N, 80.67391°E; 167m; 13-X-2019; Eberle, Bohacz & Ranasinghe leg.; Black light”, ZFMK • 1 ♂; “X-SR0348, Sri Lanka, Matale District, Dambulla, NIFS Arboretum; 7.85783°N, 80.67391°E; 167m; 13-X-2019; Eberle, Bohacz & Ranasinghe leg.; Black light”, ZFMK • 1 ♂; “X-SR0353, Sri Lanka, Matale District, Dambulla, NIFS Arboretum; 7.85783°N, 80.67391°E; 167m; 13-X-2019; Eberle, Bohacz & Ranasinghe leg.; Black light”, ZFMK • 1 ♂; “X-SR0357, Sri Lanka, Matale District, Dambulla, NIFS Arboretum; 7.85783°N, 80.67391°E; 167m; 13-X-2019; Eberle, Bohacz & Ranasinghe leg.; Black light”, ZFMK • 1 ♂; “X-SR0360, Sri Lanka, Matale District, Dambulla, NIFS Arboretum; 7.85783°N, 80.67391°E; 167m; 13-X-2019; Eberle, Bohacz & Ranasinghe leg.; Black light”, ZFMK • 1 ♂; “X-SR0365, Sri Lanka, Matale District, Dambulla, NIFS Arboretum; 7.85783°N, 80.67391°E; 167m; 13-X-2019; Eberle, Bohacz & Ranasinghe leg.; Black light”, ZFMK • 1 ♂; “X-SR0369, Sri Lanka, Matale District, Dambulla, NIFS Arboretum; 7.85783°N, 80.67391°E; 167m; 13-X-2019; Eberle, Bohacz & Ranasinghe leg.; Black light”, ZFMK • 1 ♂; “X-SR0370, Sri Lanka, Matale District, Dambulla, NIFS Arboretum; 7.85783°N, 80.67391°E; 167m; 13-X-2019; Eberle, Bohacz & Ranasinghe leg.; Black light”, ZFMK • 1 ♂; “X-SR0380, Sri Lanka, Matale District, Dambulla, NIFS Arboretum; 7.85783°N, 80.67391°E; 167m; 13-X-2019; Eberle, Bohacz & Ranasinghe leg.; Black light”, ZFMK • 1 ♂; “X-SR0383, Sri Lanka, Matale District, Dambulla, NIFS Arboretum; 7.85783°N, 80.67391°E; 167m; 13-X-2019; Eberle, Bohacz & Ranasinghe leg.; Black light”, ZFMK • 1 ♂; “X-SR0384, Sri Lanka, Matale District, Dambulla, NIFS Arboretum; 7.85783°N, 80.67391°E; 167m; 13-X-2019; Eberle, Bohacz & Ranasinghe leg.; Black light”, ZFMK • 1 ♂; “X-SR0388, Sri Lanka, Matale District, Dambulla, NIFS Arboretum; 7.85783°N, 80.67391°E; 167m; 13-X-2019; Eberle, Bohacz & Ranasinghe leg.; Black light”, ZFMK • 1 ♂; “X-SR0393, Sri Lanka, Matale District, Dambulla, NIFS Arboretum; 7.85783°N, 80.67391°E; 167m; 13-X-2019; Eberle, Bohacz & Ranasinghe leg.; Black light”, ZFMK • 1 ♂; “X-SR0394, Sri Lanka, Matale District, Dambulla, NIFS Arboretum; 7.85783°N, 80.67391°E; 167m; 13-X-2019; Eberle, Bohacz & Ranasinghe leg.; Black light”, ZFMK • 1 ♂; “X-SR0401, Sri Lanka, Matale District, Dambulla, NIFS Arboretum; 7.85783°N, 80.67391°E; 167m; 13-X-2019; Eberle, Bohacz & Ranasinghe leg.; Black light”, ZFMK • 1 ♂; “X-SR1081, Sri Lanka, Matale District, Dambulla, NIFS Arboretum; 7.85783°N,

80.67391°E; 167m; 13-X-2019; Eberle, Bohacz & Ranasinghe leg.; Black light”, ZFMK • 1 ♂; “X-SR0471, Sri Lanka, Matale District, Dambulla, NIFS Arboretum; 7.85783°N, 80.67391°E; 167m; 12-X-2019; Eberle, Bohacz & Ranasinghe leg.; Black light”, ZFMK • 1 ♂; “X-SR0473, Sri Lanka, Matale District, Dambulla, NIFS Arboretum; 7.85783°N, 80.67391°E; 167m; 12-X-2019; Eberle, Bohacz & Ranasinghe leg.; Black light”, ZFMK • 1 ♂; “X-SR0474, Sri Lanka, Matale District, Dambulla, NIFS Arboretum; 7.85783°N, 80.67391°E; 167m; 12-X-2019; Eberle, Bohacz & Ranasinghe leg.; Black light”, ZFMK • 1 ♂; “X-SR0475, Sri Lanka, Matale District, Dambulla, NIFS Arboretum; 7.85783°N, 80.67391°E; 167m; 12-X-2019; Eberle, Bohacz & Ranasinghe leg.; Black light”, ZFMK • 1 ♂; “X-SR0488, Sri Lanka, Matale District, Dambulla, NIFS Arboretum; 7.85766°N, 80.67474°E; 174m; 12-13-X_2019; Eberle, Bohacz & Ranasinghe leg.; Black light”, ZFMK • 1 ♂; “X-SR0417, Sri Lanka, Matale District, Dambulla, NIFS Arboretum; 7.85796°N, 80.67554°E; 181m; 12-13-X-2019; Eberle, Bohacz & Ranasinghe leg.; Black light”, ZFMK • 1 ♂; “X-SR0423, Sri Lanka, Matale District, Dambulla, NIFS Arboretum; 7.85796°N, 80.67554°E; 181m; 12-13-X-2019; Eberle, Bohacz & Ranasinghe leg.; Black light”, ZFMK • 1 ♂; “X-SR1014, Sri Lanka, Matale District, Dambulla, NIFS Arboretum; 7.85824°N, 182m; 80.67506°E; 13-X-2019; Eberle, Bohacz & Ranasinghe leg.; Black light” ZFMK • 1 ♀; “X-SR1042, Sri Lanka, Matale District, Dambulla, NIFS Arboretum; 7.85783°N, 80.67391°E; 174m; 12-X-2019; Eberle, Bohacz & Ranasinghe leg.; Black light”, ZFMK • 1 ♀; “X-SR1056, Sri Lanka, Matale District, Dambulla, NIFS Arboretum; 7.85783°N, 80.67391°E; 174m; 12-X-2019; Eberle, Bohacz & Ranasinghe leg.; Black light”, ZFMK • 1 ♀; “X-SR1067, Sri Lanka, Matale District, Dambulla, NIFS Arboretum; 7.85783°N, 80.67391°E; 174m; 12-X-2019; Eberle, Bohacz & Ranasinghe leg.; Black light”, ZFMK • 1 ♀; “X-SR1068, Sri Lanka, Matale District, Dambulla, NIFS Arboretum; 7.85783°N, 80.67391°E; 174m; 12-X-2019; Eberle, Bohacz & Ranasinghe leg.; Black light”, ZFMK.

Description.

MEASUREMENTS. Length: 6.1 mm, length of elytra: 4.4 mm, width: 3.5 mm.

HABITUS AND COLORATION. Body oval, light reddish brown, antenna yellow, dorsal completely shiny, except a few setae on head almost glabrous.

HEAD. Labroclypeus wide and subtrapezoidal, widest at base, lateral margins convex and convergent anteriorly, anterior angles moderately rounded, anterior margin

slightly sinuated medially, all margins moderately reflexed, lateral margins produce an indistinct angle with the ocular canthus; surface weakly convex medially, densely punctate, coarse and fine punctures mixed, with numerous erect setae; frontoclypeal suture indistinctly incised, not elevated and weakly angled medially; smooth area anterior to eye flat, three times as wide as long; ocular canthus moderately long and wide (one third of ocular diameter), finely and densely punctate, with a single terminal seta. Frons with fine, sparse punctures, with a few erect setae beside eyes. Eyes moderately large, ratio diameter/ interocular width: 0.75. Antenna with ten antennomeres; club with five antennomeres and straight, as long as the remaining antennomeres combined. Mentum elevated and slightly flattened anteriorly.

PRONOTUM. Moderately transverse, widest at base, lateral margins in basal half almost straight and moderately convergent anteriorly, in anterior half weakly convex and evenly convergent anteriorly, anterior angles distinctly produced and moderately acute, posterior angles blunt; anterior margin almost not produced medially, with a robust and complete marginal line, base of pronotum without marginal line; surface finely and densely punctate, punctures glabrous; lateral and lateral anterior margin sparsely setose; hypomeron carinate, not ventrally produced. Scutellum wide, triangular, at apex moderately pointed, with fine, moderately dense punctures, glabrous.

ELYTRA. Widest shortly behind the middle, striae weakly impressed, finely and moderately densely punctate, intervals flat, with fine and evenly moderately dense punctures, except a few short setae on lateral intervals glabrous; epipleural edge robust, ending at strongly curved external apical angle of elytra, epipleura densely setose; apical border of elytra with a fine rim of microtrichomes (100x).

VENTRAL SURFACE. In major part dull, some parts shiny, coarsely and densely punctate, metasternum sparsely covered with fine, short or very minute setae, metacoxa glabrous, with a few long setae laterally; abdominal sternites finely and densely punctate, with a transverse row of coarse punctures, each bearing a robust seta, the row of punctures on the first visible basal sternite fused to a robust transverse carina bearing the setae, before the carina the fine punctation extremely dense but glabrous. Mesosternum between mesocoxae 1.5 times as wide as the width of mesofemur. Ratio of length of metepisternum/ metacoxa: 1/ 1.65. Pygidium strongly convex and shiny, finely and moderately densely punctate, without smooth midline, glabrous except some longer setae along the apical margin.

LEGS. Wide and moderately long; femur with two longitudinal row of setae, finely and sparsely punctate; metafemur shiny, behind the posterior longitudinal row of setae punctures finer and slightly denser, anterior margin acute, without serrated line behind anterior edge, posterior margin smooth ventrally, strongly widened, posterior margin finely serrated over its entire length dorsally, with just a few short setae basally. Metatibia wide and flattened, short, widest at apical second third of metatibial length, ratio of width/ length: 1/ 2.8, sharply carinate dorsally, with two groups of spines, basal group at first third, apical group at two thirds of metatibial length, basally with a few short robust single spines, on basal quarter beside dorsal margin with a short serrated line; lateral face weakly longitudinally convex, finely, superficially and sparsely punctate, glabrous, widely smooth along the middle; ventral margin finely serrated, with four robust equidistant setae; medial face smooth and glabrous; apex finely serrated, interiorly near tarsal articulation weakly concavely sinuate. Tarsomeres dorsally smooth and glabrous, neither laterally nor dorsally carinate, ventrally robustly densely setose; metatarsomeres with a strongly serrated ridge and a smooth subventral longitudinal carina; first metatarsomere slightly shorter than following two tarsomeres combined and slightly longer than dorsal tibial spur. Protibia short, bidentate; anterior claws symmetrical, basal tooth of both claws bluntly truncate at apex.

AEDEAGUS. Fig. 6.3I–K.

HABITUS. Fig. 6.3L.

Variation. Length: 6.0-6.8 mm, length of elytra: 4.3-4.7 mm, width: 3.2-3.6 mm.

Female. Length: 6.8-7.2 mm, length of elytra: 4.6-5.0 mm, width: 3.7-4.0 mm. Eyes as large as in male; antennal club shorter little than remaining antennomeres combined, the basal joint of club equals only 1/3 of the length of the club; pygidium weakly convex.

Distribution. See Fig. 6.7C.

Genus *Maladera* Mulsant & Rey, 1871

***Maladera haniel* sp. nov.**

Figs 6.4A–D, 6.7D, 6.8D

Diagnosis. *Maladera haniel* sp. nov. is in external morphology very similar to *M. cervicornis* Ranasinghe, Eberle, Benjamin & Ahrens, 2020, both having in common the tubercle on abdominal sternite III. *Maladera haniel* sp. nov. differs in the setose pronotum, as well as the shape of parameres: the fused parameres are extremely long, as long as the rest of the basal part of the phallobase.

Etymology. The new species is named for Suresh Benjamin's son, Haniel P. Benjamin (noun in apposition).

Type material examined

Holotype

SRI LANKA • ♂; “X-SR0251, Sri Lanka, Kandy District, Deenston, Knuckles South, 7.33082°N, 80.86203°E, 1108m, 18-X-2019, Eberle, Bohacz & Ranasinghe, Black light”; ZFMK.

Paratypes

SRI LANKA • 1 ♂; “X-SR0245, Sri Lanka, Kandy District, Deenston, Knuckles South; 7.33082°N, 80.86203°E; 1108m; 18-X-2019; Eberle, Bohacz & Ranasinghe leg.; Black light”, ZFMK • 1 ♂; “X-SR0250, Sri Lanka, Kandy District, Deenston, Knuckles South; 7.33082°N, 80.86203°E; 1108m; 18-X-2019; Eberle, Bohacz & Ranasinghe leg.; Black light”, ZFMK • 1 ♂; “X-SR0947, Sri Lanka, Kandy District, Deenston, Knuckles South; 7.33082°N, 80.86203°E; 1108m; 17-X-2019; Eberle, Bohacz & Ranasinghe leg.; Black light”, ZFMK • 1 ♂; “X-SR0708, Sri Lanka, Kandy District, Deenston, Knuckles South; 7.33097°N, 80.85934°E; 1190m; 18-X-2019; Eberle, Bohacz & Ranasinghe leg.; Black light”, ZFMK • 1 ♂; “X-SR0552, Sri Lanka, Kandy District, Deenston, Knuckles South; 7.33501°N, 80.85966°E; 1171m; 18-X-2019; Eberle, Bohacz & Ranasinghe leg.; Black light”, ZFMK • 1 ♂; “X-SR0776, Sri Lanka, Kandy District, Deenston, Knuckles South; 7,3577N, 80,85006E; 980m; 17-X-2019; Eberle, Bohacz & Ranasinghe leg.; Light sheet”, ZFMK • 1 ♂; “X-SR0781, Sri Lanka, Kandy District, Deenston, Knuckles South; 7,3577N, 80,85006E; 980m; 17-X-2019; Eberle, Bohacz & Ranasinghe leg.; Light sheet”, ZFMK • 1 ♂; “X-SR0783, Sri Lanka, Kandy District, Deenston, Knuckles South;

7,3577N, 80,85006E; 980m; 17-X-2019; Eberle, Bohacz & Ranasinghe leg.; Light sheet”, ZFMK.

Description.

MEASUREMENTS. Length: 8.0 mm, length of elytra: 5.9 mm, width: 4.5 mm.

HABITUS AND COLORATION. Body short oval, dark brown, antenna yellow, dorsal surface shiny, finely densely setose.

HEAD. Labroclypeus short and trapezoidal, wider than long, widest at base, lateral margins strongly convex and convergent to widely rounded anterior angles, lateral border and ocular canthus producing an indistinct blunt angle, margins weakly reflexed, anterior margin almost weakly sinuate medially; surface slightly convex, finely and densely punctate, distance between punctures smaller than their diameter, with numerous erect setae in larger punctures; frontoclypeal suture indistinctly incised and bluntly bent medially; smooth area in front of eye approximately three times as wide as long; ocular canthus long and narrow, minutely and superficially punctate, with a single short terminal seta. Frons with fine, dense punctures, with a few long erect setae in larger punctures, setae on disc less dense. Eyes large, ratio of diameter/ interocular width: 0.79. Antenna yellow, with ten antennomeres; club with three antennomeres, as long as remaining antennomeres combined. Mentum elevated and anteriorly flattened.

PRONOTUM. Wide, widest at base, lateral margins in basal half straight and weakly convergent, in anterior half weakly convex and narrowed to anterior angles, anterior angles moderately produced and sharp, anterior marginal line fine and complete, anterior margin convexly produced medially; surface finely densely punctate, with moderately dense, short and fine setae and dense long erect setae being directed anteriorly; anterior and lateral borders sparsely setose, basal margin without marginal line; hypomeron ventrobasally carinate and slightly produced ventrally. Scutellum short and wide, triangular, with fine and dense punctures, with short, dense, fine setae.

ELYTRA. Short oval, widest shortly behind middle, striae distinctly impressed, finely and densely punctate, intervals weakly convex, with moderately fine, dense punctures and with dense, fine, short setae as well as with sparse long erect setae; epipleural edge fine, ending at the weakly convex external apical angle of elytra, epipleura

densely setose; apical border narrowly membranous, apex covered with short microtrichomes.

VENTRAL SURFACE. Shiny, thorax and metacoxa with large and dense punctures, sparsely setose, metacoxa with minute adjacent setae in the punctures except for numerous long setae laterally, apical margin weakly convex, without a wide rim of long white microtrichomes; each abdominal sternite, in addition to evenly distributed fine and dense punctures bearing each a fine seta, with a distinct transverse row of coarse punctures each bearing a long and more robust seta, 3rd sternite with a sharp median tubercle being half as high as sternite length, penultimate sternite apically with a shiny smooth chitinous border, which is a quarter as long as the sternite. Mesosternum between mesocoxae as wide as mesofemur, with a semi-circular ridge bearing robust setae. Ratio of length of metepisternum/ metacoxa: 1/ 1.93. Pygidium moderately convex, moderately finely and densely punctate, without smooth midline, punctures with short and dense, adjacent setae as well as with moderately dense, long, erect setae.

LEGS. Short and wide; femur with two longitudinal rows of setae, finely and densely punctate; metafemur shiny, anterior edge acute, lacking an adjacent serrated line, ventral surface densely punctate and setose, posterior ventral margin straight, only little widened in apical half, finely serrate apically, dorsally not serrated, glabrous. Metatibia short, widest at middle, posteriorly only very little narrowed, ratio width/ length: 1/ 2.5, dorsally sharply carinate, with two groups of spines, basal shortly behind middle, apical one at three quarters of metatibial length, basally beside dorsal margin with two single punctures with serrated margins, each bearing a single robust spine and beside them a longitudinal serrated line; lateral face almost flat, with dense, large punctures and with minute setae in the punctures; ventral margin with five strong spines equidistant from each other, medial face smooth, apex interiorly near tarsal articulation shallowly concave. Meso- and metatarsomeres finely and sparsely punctate but glabrous dorsally, ventrally with sparse, short setae; metatarsomeres ventrally with a strongly serrated ridge, beside which is a strong longitudinal carina; first metatarsomere as long as following two tarsomeres combined and as long as dorsal tibial spur. Protibia short, bidentate. All claws symmetrical, feebly curved and long, with normally developed basal tooth.

AEDEAGUS. Fig. 6.4A–C.

HABITUS. Fig. 6.4D.

Variation. Length: 8.0-8.2 mm, length of elytra: 5.5-6.1 mm, width: 4.3-4.8 mm.

Female. Unknown.

Distribution. See Fig. 6.7D.

***Maladera kishi* sp. nov.**

Figs 6.4E–H, 6.7E, 6.8D

Diagnosis. *Maladera kishi* sp. nov. is in external morphology very similar to *M. haniel* sp. nov. Differs by lack of tubercle on abdominal sternite III as well as by the shape of parameres: the fused parameres (distal aedeagal process) is simply pointed and not bifurcate, while the lateral process on left side is more robust.

Etymology. The new species is named for Suresh Benjamin's daughter, Kishi P. L. Benjamin (noun in apposition).

Type material examined

Holotype

SRI LANKA • ♂; “X-SR0724, Sri Lanka, Kandy District, Deenston, Knuckles South, 7.3389°N, 80.8510°E, 1192m, 18-X-2019, Eberle, Bohacz & Ranasinghe, Black light”; ZFMK.

Paratypes

SRI LANKA • 1 ♂; “X-SR0730, Sri Lanka, Kandy District, Deenston, Knuckles South, 7.3389°N, 80.8510°E, 1192m, 18-X-2019, Eberle, Bohacz & Ranasinghe, Black light”; ZFMK • 1 ♂; “X-SR0731, Sri Lanka, Kandy District, Deenston, Knuckles South, 7.3389°N, 80.8510°E, 1192m, 18-X-2019, Eberle, Bohacz & Ranasinghe, Black light”; ZFMK • 1 ♂; “X-SR0736, Sri Lanka, Kandy District, Deenston, Knuckles South, 7.3389°N, 80.8510°E, 1192m, 18-X-2019, Eberle, Bohacz & Ranasinghe, Black light”; ZFMK • 1 ♂; “X-SR0737, Sri Lanka, Kandy District, Deenston, Knuckles South, 7.3389°N, 80.8510°E, 1192m, 18-X-2019, Eberle, Bohacz & Ranasinghe, Black light”; ZFMK • 1 ♂; “X-SR0738, Sri Lanka, Kandy District, Deenston, Knuckles South, 7.3389°N, 80.8510°E, 1192m, 18-X-2019, Eberle, Bohacz

& Ranasinghe, Black light”; ZFMK • 1 ♂; “X-SR0739, Sri Lanka, Kandy District, Deenston, Knuckles South, 7.3389°N, 80.8510°E, 1192m, 18-X-2019, Eberle, Bohacz & Ranasinghe, Black light”; ZFMK • 1 ♂; “X-SR0740, Sri Lanka, Kandy District, Deenston, Knuckles South, 7.3389°N, 80.8510°E, 1192m, 18-X-2019, Eberle, Bohacz & Ranasinghe, Black light”; ZFMK • 1 ♂; “X-SR0741, Sri Lanka, Kandy District, Deenston, Knuckles South, 7.3389°N, 80.8510°E, 1192m, 18-X-2019, Eberle, Bohacz & Ranasinghe, Black light”; ZFMK • 1 ♂; “X-SR0742, Sri Lanka, Kandy District, Deenston, Knuckles South, 7.3389°N, 80.8510°E, 1192m, 18-X-2019, Eberle, Bohacz & Ranasinghe, Black light”; ZFMK • 1 ♂; “X-SR0743, Sri Lanka, Kandy District, Deenston, Knuckles South, 7.3389°N, 80.8510°E, 1192m, 18-X-2019, Eberle, Bohacz & Ranasinghe, Black light”; ZFMK • 1 ♂; “X-SR0749, Sri Lanka, Kandy District, Deenston, Knuckles South, 7.3389°N, 80.8510°E, 1192m, 18-X-2019, Eberle, Bohacz & Ranasinghe, Black light”; ZFMK • 1 ♂; “X-SR0750, Sri Lanka, Kandy District, Deenston, Knuckles South, 7.3389°N, 80.8510°E, 1192m, 18-X-2019, Eberle, Bohacz & Ranasinghe, Black light”; ZFMK • 1 ♂; “X-SR0697, Sri Lanka, Kandy District, Deenston, Knuckles South, 7.3389°N, 80.8510°E, 1192m, 18-X-2019, Eberle, Bohacz & Ranasinghe, Black light”; ZFMK • 1 ♂; “X-SR0701, Sri Lanka, Kandy District, Deenston, Knuckles South, 7.3389°N, 80.8510°E, 1192m, 18-X-2019, Eberle, Bohacz & Ranasinghe, Black light”; ZFMK • 1 ♂; “X-SR0924, Sri Lanka, Kandy District, Deenston, Knuckles South, 7.3389°N, 80.8510°E, 1192m, 18-X-2019, Eberle, Bohacz & Ranasinghe, Black light”; ZFMK • 1 ♂; “X-SR0925, Sri Lanka, Kandy District, Deenston, Knuckles South, 7.3389°N, 80.8510°E, 1192m, 18-X-2019, Eberle, Bohacz & Ranasinghe, Black light”; ZFMK • 1 ♂; “X-SR0926, Sri Lanka, Kandy District, Deenston, Knuckles South, 7.3389°N, 80.8510°E, 1192m, 18-X-2019, Eberle, Bohacz & Ranasinghe, Black light”; ZFMK • 1 ♂; “X-SR0927, Sri Lanka, Kandy District, Deenston, Knuckles South, 7.3389°N, 80.8510°E, 1192m, 18-X-2019, Eberle, Bohacz & Ranasinghe, Black light”; ZFMK • 1 ♂; “X-SR0929, Sri Lanka, Kandy District, Deenston, Knuckles South, 7.3389°N, 80.8510°E, 1192m, 18-X-2019, Eberle, Bohacz & Ranasinghe, Black light”; ZFMK • 1 ♂; “X-SR0565, Sri Lanka, Kandy District, Deenston, Knuckles South, 7.33616°N, 80.85907°E; 1197m; 17-18-X-2019, Eberle, Bohacz & Ranasinghe, Black light”; ZFMK • 1 ♂; “X-SR0566, Sri Lanka, Kandy District, Deenston, Knuckles South, 7.33616°N, 80.85907°E; 1197m; 17-18-X-2019, Eberle, Bohacz & Ranasinghe, Black light”; ZFMK • 1 ♂; “X-SR0936, Sri Lanka, Kandy District, Deenston, Knuckles South, 7.33616°N, 80.85907°E; 1197m; 18-X-2019, Eberle, Bohacz & Ranasinghe, Black light”; ZFMK • 1 ♂; “X-SR0546, Sri Lanka, Kandy District, Deenston, Knuckles South, 7.33501°N, 80.85966°E; 1171m; 17-18-X-2019, Eberle, Bohacz & Ranasinghe, Black light”; ZFMK • 1 ♂; “X-

SR0548, Sri Lanka, Kandy District, Deenston, Knuckles South, 7.33501°N, 80.85966°E; 1171m; 18-X-2019, Eberle, Bohacz & Ranasinghe, Black light”; ZFMK
 • 1 ♀ “X-SR0545, Sri Lanka, Kandy District, Deenston, Knuckles South, 7.33501°N, 80.85966°E; 1171m; 18-X-2019, Eberle, Bohacz & Ranasinghe, Black light”; ZFMK
 • 1 ♀ “X-SR0567, Sri Lanka, Kandy District, Deenston, Knuckles South, 7.33616°N, 80.85907°E; 1197m; 18-X-2019, Eberle, Bohacz & Ranasinghe, Black light”; ZFMK
 • 1 ♀ “X-SR0700, Sri Lanka, Kandy District, Deenston, Knuckles South, 7.3389°N, 80.8510°E, 1192m; 17-X-2019, Eberle, Bohacz & Ranasinghe, Black light”; ZFMK
 • 1 ♀ “X-SR0725, Sri Lanka, Kandy District, Deenston, Knuckles South, 7.3389°N, 80.8510°E, 1192m; 18-X-2019, Eberle, Bohacz & Ranasinghe, Black light”; ZFMK
 • 1 ♀ “X-SR0799, Sri Lanka, Kandy District, Deenston, Knuckles South, 7.33501°N, 80.85966°E; 1171m; 18-X-2019, Eberle, Bohacz & Ranasinghe, Black light”; ZFMK
 • 1 ♀ “X-SR0800, Sri Lanka, Kandy District, Deenston, Knuckles South, 7.33501°N, 80.85966°E; 1171m; 18-X-2019, Eberle, Bohacz & Ranasinghe, Black light”; ZFMK.

Description.

MEASUREMENTS. Length: 9.2 mm, length of elytra: 6.6 mm, width: 5.2 mm.

HABITUS AND COLORATION. Body short oval, dark brown, antenna yellow, dorsal surface shiny, finely densely setose.

HEAD. Labroclypeus short and trapezoidal, wider than long, widest at base, lateral margins strongly convex and convergent to widely rounded anterior angles, lateral border and ocular canthus producing an indistinct blunt angle, margins weakly reflexed, anterior margin not sinuate medially; surface slightly convex, finely and densely punctate, distance between punctures smaller than their diameter, with numerous erect setae in larger punctures; frontoclypeal suture indistinctly incised and bluntly bent medially; smooth area in front of eye approximately three times as wide as long; ocular canthus long and narrow, minutely and superficially punctate, without a short terminal seta. Frons with fine, dense punctures, with a few long erect setae in larger punctures. Eyes large, ratio of diameter/ interocular width: 0.81. Antenna yellow, with ten antennomeres; club with three antennomeres, little longer than remaining antennomeres combined. Mentum elevated and anteriorly flattened.

PRONOTUM. Wide, widest at base, lateral margins in basal half straight and weakly convergent, in anterior half weakly convex and narrowed to anterior angles, anterior angles moderately produced and sharp, anterior marginal line fine and complete,

anterior margin convexly produced medially; surface finely densely punctate, with moderately dense, short and fine setae and dense long erect setae being directed anteriorly; anterior and lateral borders sparsely setose, basal margin without marginal line; hypomeron ventrobasally carinate and slightly produced ventrally. Scutellum short and wide, triangular, with fine and dense punctures, with short, dense, fine setae.

ELYTRA. Short oval, widest shortly behind middle, striae distinctly impressed, finely and densely punctate, intervals weakly convex, with moderately fine, dense punctures and with dense, fine, short setae as well as with sparse long erect setae; epipleural edge fine, ending at the weakly convex external apical angle of elytra, epipleura densely setose; apical border narrowly membranous, apex covered with short microtrichomes.

VENTRAL SURFACE. Shiny, thorax and metacoxa with large and dense punctures, sparsely setose, metacoxa with minute adjacent setae in the punctures except for numerous long setae laterally, apical margin weakly convex, without a wide rim of long white microtrichomes; each abdominal sternite, in addition to evenly distributed fine and dense punctures bearing each a fine seta, with a distinct transverse row of coarse punctures each bearing a long and more robust seta, penultimate sternite apically with a shiny smooth chitinous border, which is a quarter as long as the sternite. Mesosternum between mesocoxae as wide as mesofemur, with a semi-circular ridge bearing robust setae. Ratio of length of metepisternum/ metacoxa: 1/ 1.8. Pygidium moderately convex, moderately finely and densely punctate, without smooth midline, punctures with short and dense, adjacent setae as well as with dense, long, erect setae.

LEGS. Short and wide; femur with two longitudinal rows of setae, finely and densely punctate; metafemur shiny, anterior edge acute, lacking an adjacent serrated line, ventral surface densely punctate and setose, posterior ventral margin straight, only little widened in apical half, finely indistinctly serrate apically, dorsally not serrated, glabrous. Metatibia short, widest at middle, posteriorly only very slightly narrowed, ratio width/ length: 1/ 2.4, dorsally sharply carinate, with two groups of spines, basal well behind middle, apical one at four fifths of metatibial length, basally beside dorsal margin with two single punctures with serrated margins, each bearing a single robust spine and beside them a longitudinal serrated line; lateral face almost flat, with dense, large punctures and with fine setae in the punctures; ventral margin with five

strong spines equidistant from each other, medial face smooth, apex interiorly near tarsal articulation shallowly concave. Meso- and metatarsomeres finely and sparsely punctate but glabrous dorsally, ventrally with sparse, short setae; metatarsomeres ventrally with a strongly serrated ridge, beside which is a strong longitudinal carina; first metatarsomere little shorter than following two tarsomeres combined and as long as dorsal tibial spur. Protibia short, bidentate. All claws symmetrical, feebly curved and long, with normally developed basal tooth.

AEDEAGUS. Fig. 6.4E–G.

HABITUS. Fig. 6.4H.

Variation. Length: 8.9-9.2 mm, length of elytra: 6.6-7.1 mm, width: 5.1-5.6 mm.

Female. Length: 9.0-9.3 mm, length of elytra: 7.0-7.5 mm, width: 5.4-5.7 mm. Eyes as large as in male; antennal club little shorter than the remaining antennomeres combined.

Distribution. See Fig. 6.7E.

***Maladera windy* sp. nov.**

Figs 6.4I–L, 6.7F, 6.8E

Diagnosis. The new species is very similar to *M. pubescens* (Arrow, 1916) and *M. dambullana* sp. nov. as well as *M. bisornata* Fabrizi & Ahrens, 2014. *Maladera windy* differs from the first two by the distal aedeagal lobe (i.e, the fused parameres) having a basal lateral lobe with grater-like surface, the ventral process of phallobase is shorter, less pointed and not mesally extended; from *M. bisornata*, *M. windy* sp. nov. differs by the longer and slightly reflexed distal aedeagal lobe (i.e, the fused parameres).

Etymology. The name of the new species is derived from “Windy Holiday Bungalow”, where the research group stayed during the second expedition in Knuckles region (noun in apposition).



Figure 6.4. A–D *Maladera haniel* sp. nov., (holotype) E–H *M. kishi* sp. nov., (holotype) I–L *M. windy* sp. nov., (holotype) A, E, I aedeagus, left side lateral view C, G, K aedeagus, right side lateral view B, F, J parameres, dorsal view D, H, L habitus (not to scale). Scale: 0.5 mm.

Type material examined**Holotype**

SRI LANKA • ♂; “X-SR0769, Sri Lanka, Deenston, Knuckles South, 7.35771°N, 80.85006°E, 980m, 17-X-2019, Eberle, Bohacz & Ranasinghe, Light sheet”; ZFMK.

Paratypes

SRI LANKA • 1 ♂; “X-SR0757, Sri Lanka, Deenston, Knuckles South, 7.35771°N, 80.85006°E, 980m, 17-X-2019, Eberle, Bohacz & Ranasinghe, Light sheet”; ZFMK • 1 ♂; “X-SR0790, Sri Lanka, Deenston, Knuckles South, 7.35771°N, 80.85006°E, 980m, 17-X-2019, Eberle, Bohacz & Ranasinghe, Light sheet” ZFMK • 1 ♂; “X-SR0580, Sri Lanka, Deenston, Knuckles South, 7.35771°N, 80.85006°E, 980m, 16-X-2019, Eberle, Bohacz & Ranasinghe, Light sheet”; ZFMK • 1 ♀; “X-SR0572, Sri Lanka, Deenston, Knuckles South, 7.35771°N, 80.85006°E, 980m, 16-X-2019, Eberle, Bohacz & Ranasinghe, Light sheet”; ZFMK • 1 ♀; “X-SR0574, Sri Lanka, Deenston, Knuckles South, 7.35771°N, 80.85006°E, 980m, 16-X-2019, Eberle, Bohacz & Ranasinghe, Light sheet”; ZFMK • 1 ♀; “X-SR0575, Sri Lanka, Deenston, Knuckles South, 7.35771°N, 80.85006°E, 980m, 16-X-2019, Eberle, Bohacz & Ranasinghe, Light sheet”; ZFMK.

Description.

MEASUREMENTS. Length: 6.0 mm, length of elytra: 4.1 mm, width: 3.4 mm.

HABITUS AND COLORATION. Body short oval, yellowish brown, antenna yellow, dorsal surface shiny, densely finely setose.

HEAD. Labroclypeus subtrapezoidal, distinctly wider than long, widest at base, lateral margins weakly convex and strongly convergent to widely rounded anterior angles, lateral border and ocular canthus producing an indistinct blunt angle, margins moderately reflexed, anteriorly distinctly sinuate medially; surface flat, finely and densely punctate, distance between punctures smaller than their diameter, with numerous erect setae in larger punctures; frontoclypeal suture fine and angled medially; smooth area in front of eye approximately twice as wide as long; ocular canthus short and narrow, finely and densely punctate, with a single short terminal seta. Frons with fine, dense punctures, with dense short and sparse long erect setae. Eyes large, ratio of diameter/ interocular width: 0.85. Antenna yellow, with ten antennomeres; club with three antennomeres, as long as remaining antennomeres combined. Mentum elevated and anteriorly flattened.

PRONOTUM. Moderately wide, widest at base, lateral margins weakly convex and evenly narrowed anteriorly, anterior angles strongly produced and sharp, anterior marginal line fine and complete, anterior margin weakly produced medially; surface finely and densely punctate, with dense moderately long setae being bent posteriorly on entire disc and with a few sparse longer setae being directed anteriorly; anterior and lateral borders setose, basal margin without marginal line; hypomeron ventrobasally carinate and slightly produced ventrally. Scutellum short and wide, triangular, with fine and dense punctures, with fine and dense adjacent setae.

ELYTRA. Short oval, widest shortly behind middle, striae indistinctly impressed, finely and densely punctate, intervals flat, with fine, very dense punctures, with a fine setae similar to those of the pronotum and a few sparser ones being longer and erect or directed anteriorly, in particular on lateral intervals; epipleural edge fine, ending at the weakly convex external apical angle of elytra, epipleura densely setose; apical border narrowly membranous, apex covered with short microtrichomes.

VENTRAL SURFACE. Moderately shiny, thorax and metacoxa with large and dense punctures, densely setose, metacoxa glabrous except for numerous long setae laterally; each abdominal sternite, in addition to evenly distributed fine and dense punctures bearing each a fine seta, with a distinct transverse row of coarse punctures each bearing a long and more robust seta, penultimate sternite apically with a shiny smooth chitinous border, which is a quarter as long as the sternite. Mesosternum between mesocoxae as wide as mesofemur, with a semi-circular ridge bearing robust setae. Ratio of length of metepisternum/ metacoxa: 1/ 1.9. Pygidium moderately convex, finely and very densely punctate, without smooth midline, punctures with short and moderately dense, adjacent setae, along the apical margin with a few long erect setae.

LEGS. Short and wide; femur with two longitudinal rows of setae, finely and densely punctate, densely setose; metafemur shiny, anterior edge acute, lacking an adjacent serrated line, ventral surface densely punctate and setose, posterior ventral margin straight, only little widened in apical half and very indistinctly serrate apically, dorsally not serrated, glabrous. Metatibia short, widest at middle, posteriorly slightly narrowed, ratio width/ length: 1/ 2.6, dorsally sharply carinate, with two groups of spines, basal one shortly behind middle, apical one at four fifths of metatibial length, basally beside dorsal margin with two single punctures with serrated margins, each bearing single spines and beside them a longitudinal serrated line; lateral face almost

flat, with dense, fine punctures and with minute setae; ventral margin with five strong spines equidistant from each other, medial face smooth, apex interiorly near tarsal articulation shallowly truncate. Meso- and metatarsomeres finely and densely punctate and setose dorsally, ventrally with sparse, short setae; metatarsomeres ventrally with a strongly serrated ridge, beside which is a strong longitudinal carina; first metatarsomere little shorter than following two tarsomeres combined and a little longer than dorsal tibial spur. Protibia short, bidentate. All claws symmetrical, feebly curved and long, with normally developed basal tooth.

AEDEAGUS. Fig. 6.4I–K.

HABITUS. Fig. 6.4L.

Variation. Length: 6.0-6.4 mm, length of elytra: 4.0-4.6 mm, width: 3.2-3.4 mm.

Female. Length: 6.5-6.8 mm, length of elytra: 4.6-5.0 mm, width: 3.6-3.7 mm. Eyes slightly smaller than in male; antennal club little shorter than the remaining antennomeres combined.

Distribution. See Fig. 6.7F.

***Maladera karunaratnae* sp. nov.**

Figs 6.5A–D, 7G, 8F

Diagnosis. *Maladera karunaratnae* sp. nov. is in external appearance similar to *M. anderssoni* Fabrizi & Ahrens, 2014 and *M. romanoi* Fabrizi & Ahrens, 2014 being, however, the aedeagus has no ventral hook (lateral view), just a distinct ventral convexity at middle.

Etymology. The new species is named after Prof. Inoka Karunaratne (University of Peradeniya), in gratitude for her kind support for this project (noun in the genitive case).

Type material examined**Holotype**

SRI LANKA • ♂; “X-SR1030, Sri Lanka, Matale District, Dambulla, NIFS Arboretum, 7.85796°N, 80.67554°E; 181m; 13-X-2019; Eberle, Bohacz & Ranasinghe leg.; Black light”; ZFMK.

Paratypes

SRI LANKA • 1 ♂; “X-SR1010, Sri Lanka, Matale District, Dambulla, NIFS Arboretum, 7.85897°N, 80.67533°E; 203m; 11-12-X-2019; Eberle, Bohacz & Ranasinghe leg.; Black light”; ZFMK • 1 ♂; “X-SR1087, Sri Lanka, Matale District, Dambulla, NIFS Arboretum, 7.85897°N, 80.67533°E; 203m; 11-X-2019; Eberle, Bohacz & Ranasinghe leg.; Black light”; ZFMK • 1 ♂; “X-SR1025, Sri Lanka, Matale District, Dambulla, NIFS Arboretum, 7.85766°N, 80.67474°E; 174m; 12-X-2019; Eberle, Bohacz & Ranasinghe leg.; Black light”; ZFMK • 1 ♂; “X-SR1029, Sri Lanka, Matale District, Dambulla, NIFS Arboretum, 7.85766°N, 80.67474°E; 174m; 12-X-2019; Eberle, Bohacz & Ranasinghe leg.; Black light”; ZFMK • 1 ♂; “X-SR1113, Sri Lanka, Matale District, Dambulla, NIFS Arboretum, 7.85796°N, 80.67554°E; 181m; 13-X-2019; Eberle, Bohacz & Ranasinghe leg.; Black light”; ZFMK • 1 ♂; “X-SR0887, Sri Lanka, Matale District, Riverston, Pitawala Pathana; 7.54976°N, 80.75212°E; 902m; 15-X-2019; Eberle, Bohacz & Ranasinghe leg.; Black light”; ZFMK • 1 ♀; “X-SR1088, Sri Lanka, Matale District, Dambulla, NIFS Arboretum, 7.85897°N, 80.67533°E; 203m; 11-X-2019; Eberle, Bohacz & Ranasinghe leg.; Black light”; ZFMK.

Description.

MEASUREMENTS. Length: 5.6 mm, length of elytra: 4.2 mm, width: 3.2 mm.

HABITUS AND COLORATION. Body oval, brown, antenna, ventral side, and legs yellowish, dorsal surface with iridescent shine, densely shortly setose, elytra with numerous single erect setae.

HEAD. Labroclypeus subtrapezoidal, wider than long, widest at base, lateral margins weakly convex and convergent to widely rounded anterior angles, lateral border and ocular canthus producing an blunt angle, margins moderately reflexed; anterior margin weakly emarginate medially; surface shiny, flat, finely and coarsely, densely punctate, with a few erect setae in larger punctures and minute setae in the remaining

punctures; frontoclypeal suture finely incised and weakly curved; smooth area in front of eye three times as wide as long; ocular canthus long and narrow, sparsely finely punctate, with a single short terminal seta. Frons with toment and iridescent shine, with fine, dense punctures and short, erect setae in punctures, with a few long, erect setae on disc and beside eyes. Eyes extremely large, ratio of diameter/interocular width: 1.1. Antenna yellow, with ten antennomeres; club with three antennomeres, straight, 1.2 times as long as remaining antennomeres combined. Mentum elevated and anteriorly flattened.

PRONOTUM. Narrow, widest at base, lateral margins weakly convex and convergent anteriorly; anterior angles moderately produced and sharp; anterior marginal line fine and complete, anterior margin weakly produced medially; surface finely and densely punctate, with short erect setae in punctures, and a numerous longer erect setae in anterior part; anterior and lateral borders sparsely setose, basal margin without marginal line; hypomerion ventrobasally carinate and slightly produced ventrally. Scutellum short and wide, triangular, with fine and dense punctures and setae as in pronotum.

ELYTRA. Short oval, widest at middle, striae indistinctly impressed, finely and densely punctate, intervals flat, with fine, dense punctures, with short setae in punctures; odd intervals with numerous longer, erect setae around which the smaller setae are lacking circularly; epipleural edge fine, ending at the weakly convex external apical angle of elytra, epipleura densely setose; apical border membranous, apex covered with a rim of short microtrichomes.

VENTRAL SURFACE. Moderately shiny, thorax and metacoxa with large and dense punctures, densely shortly setose; metacoxa with numerous long setae laterally; each abdominal sternite, in addition to evenly distributed fine and dense punctures bearing each a fine seta, with a distinct transverse row of coarse punctures each bearing a long and more robust seta, penultimate sternite apically with a narrow, shiny smooth chitinous border. Mesosternum between mesocoxae as wide as mesofemur, with a semi-circular ridge bearing robust setae. Ratio of length of metepisternum/ metacoxa: 1/ 2.28. Pygidium weakly convex, finely densely punctate, with short dense setae, and numerous long setae on apical half.

LEGS. Short and wide; femur with two longitudinal rows of setae, finely and densely punctate, densely setose; metafemur shiny, anterior edge acute, lacking an adjacent

serrated line, ventral surface densely punctate and setose; posterior ventral margin straight, strongly widened in apical half and very indistinctly serrate apically; posterior dorsal margin not serrated, densely setose. Metatibia short, widest at middle, posteriorly slightly narrowed, ratio width/ length: 1/ 2.4, dorsally sharply carinate, with two groups of spines, basal one shortly behind middle, apical one at four fifths of metatibial length, basally beside dorsal margin with two single punctures with serrated margins, each bearing single spines and a longitudinal serrated line in basal half; lateral face longitudinal convex, with dense, fine punctures and with fine white setae in punctures; ventral margin finely serrate, with five strong spines equidistant from each other; medial face smooth, apex interiorly near tarsal articulation shallowly truncate. Meso- and metatarsomeres dorsally densely and fine punctate, and densely setose, ventrally with robust, dense, short setae; metatarsomeres with a strongly serrated ventral ridge, beside it with a strong longitudinal carina; first metatarsomere as long as two following tarsomeres combined and as long as dorsal tibial spur. Protibia short, bidentate. All claws symmetrical, feebly curved and long, with normally developed basal tooth, protarsal claws asymmetric, basal tooth of inner claw widened and bluntly truncate at apex.

AEDEAGUS. Fig. 6.5A–C.

HABITUS. Fig. 6.5D.

Variation. Length: 5.6-6.0 mm, length of elytra: 4.0-4.5 mm, width: 2.8-3.4 mm.

Female. Length: 7.0 mm, length of elytra: 5.4 mm, width: 3.6 mm. Eyes as large as in male; antennal club little shorter than remaining antennomeres combined.

Distribution. See Fig. 6.7G.

***Maladera hiyarensis* sp. nov.**

Figs 6.5E–H, 6.7H, 6.8G

Diagnosis. *Maladera hiyarensis* sp. nov. is in external appearance similar to *M. anderssoni* Fabrizi & Ahrens, 2014 and *M. romanoi* Fabrizi & Ahrens, 2014 being, however, stouter in shape and larger, the aedeagus has the distal part longer and narrower. The aedeagus is also rather similar to *M. badullana* Fabrizi & Ahrens,

2014, but the ventral convexity is in this new species less pronounced and the distal portion is longer and reflexed (lateral view).

Etymology. The new species is named after its type locality “Hiyare”, (adjective in the nominative singular).

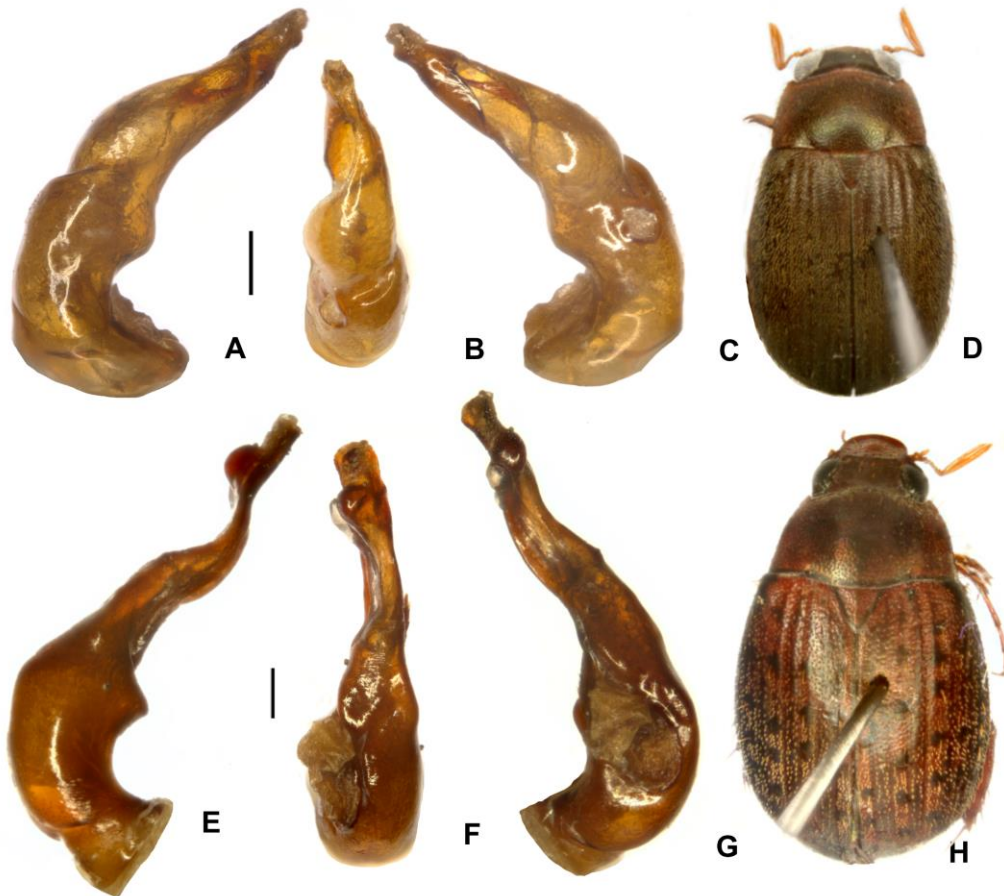


Figure 6.5. A–D *Maladera karunaratnae* sp. nov., (holotype) E–H *M. hiyarensis* sp. nov., (holotype) A, E aedeagus, left side lateral view C, G aedeagus, right side lateral view B, F parameres, dorsal view D, H habitus (not to scale). Scale: 0.5 mm.

Type material examined

Holotype

SRI LANKA • ♂; “X-SR1946, Sri Lanka, Galle District, Hiyare FR; 6.05959°N, 80.31503°E; 116m; 01-VII-2020; Benjamin & Ranasinghe leg.; Black light”; ZFMK.

Description.

MEASUREMENTS. Length: 6.8 mm, length of elytra: 4.8 mm, width: 4.1 mm.

HABITUS AND COLORATION. Body oval, reddish brown, frons, disc of pronotum and a few spots on elytra dark brown, antenna and legs yellow, dorsal surface with iridescent shine, densely and shortly setose, elytra with numerous single erect setae.

HEAD. Labroclypeus subtrapezoidal, little wider than long, widest at base, lateral margins weakly convex and strongly convergent to widely rounded anterior angles, lateral border and ocular canthus producing an indistinct blunt angle, margins moderately reflexed; anterior margin very weakly emarginate medially; surface shiny, weakly elevated medially, finely and densely punctate, distance between punctures equal their diameter, with a few erect setae in larger punctures; frontoclypeal suture fine and weakly angled medially; smooth area in front of eye approximately twice as wide as long; ocular canthus moderately long and narrow, impunctate, with a single short terminal seta. Frons with toment and iridescent shine, with fine, dense punctures and minute setae in punctures, with a few long, erect setae on disc and beside eyes. Eyes large, ratio of diameter/ interocular width: 0.79. Antenna yellow, with ten antennomeres; club with three antennomeres, straight, 1.1 times as long as remaining antennomeres combined. Mentum elevated and anteriorly flattened.

PRONOTUM. Moderately wide, widest at base, lateral margins in basal half straight and convergent, in anterior half weakly convex and convergent anteriorly; anterior angles moderately produced and sharp; anterior marginal line fine and complete, anterior margin weakly produced medially; surface finely and densely punctate, with short setae in punctures, otherwise glabrous; anterior and lateral borders sparsely setose, basal margin without marginal line; hypomeron ventrobasally carinate and slightly produced ventrally. Scutellum short and wide, triangular, with fine and dense punctures, along midline narrowly impunctate.

ELYTRA. Short oval, widest at posterior third, striae indistinctly impressed, finely and densely punctate, intervals flat, with fine, dense punctures, with short setae in punctures; odd intervals with a few impunctate dots which are darker and each bear at centre an erect seta; epipleural edge fine, ending at the weakly convex external apical angle of elytra, epipleura densely setose; apical border membranous, apex covered with a rim of short microtrichomes.

VENTRAL SURFACE. Moderately shiny, thorax and metacoxa with large and dense punctures, densely shortly setose; metacoxa with numerous long setae laterally; each abdominal sternite, in addition to evenly distributed fine and dense punctures bearing each a fine seta, with a distinct transverse row of coarse punctures each bearing a long and more robust seta, penultimate sternite apically with a narrow, shiny smooth chitinous border. Mesosternum between mesocoxae as wide as mesofemur, with a semi-circular ridge bearing robust setae. Ratio of length of metepisternum/ metacoxa: 1/ 2.24. Pygidium weakly convex, finely densely punctate, with short dense setae, and numerous long setae along apical margin.

LEGS. Short and wide; femur with two longitudinal rows of setae, finely and densely punctate, densely setose; metafemur shiny, anterior edge acute, lacking an adjacent serrated line, ventral surface densely punctate and setose; posterior ventral margin straight, strongly widened in apical half and very indistinctly serrate apically; posterior dorsal margin not serrated, densely setose. Metatibia short, widest at middle, posteriorly slightly narrowed, ratio width/ length: 1/ 2.4, dorsally sharply carinate, with two groups of spines, basal one shortly behind middle, apical one at four fifths of metatibial length, basally beside dorsal margin with two single punctures with serrated margins, each bearing single spines and beside them a longitudinal serrated line; lateral face longitudinal convex, with dense, fine punctures and with short setae in punctures; ventral margin finely serrate, with five strong spines equidistant from each other; medial face smooth, apex interiorly near tarsal articulation shallowly truncate. Meso- and metatarsomeres dorsally sparsely and very finely punctate and with minute setae in punctures, ventrally with robust, dense, short setae; metatarsomeres with a strongly serrated ventral ridge, beside it with a strong longitudinal carina; first metatarsomere as long as two following tarsomeres combined and as long as dorsal tibial spur. Protibia short, bidentate. All claws symmetrical, feebly curved and long, with normally developed basal tooth, distal protarsomeres lacking in holotype.

AEDEAGUS. Fig. 6.5E–G.

HABITUS. Fig. 6.5H.

Female. Unknown.

Distribution. See Fig. 6.7H.

***Maladera dambullana* sp. nov.**

Figs 6.6A–D, 6.7I, 6.8H

Diagnosis. The new species is very similar to *M. pubescens* (Arrow, 1916). *Maladera dambullana* sp. nov. differs from *M. pubescens* by the shape of aedeagus: the ventral distal lobe (i.e, the fused parameres) is not extended mesally but constant in width over its entire length.

Etymology. The name of the new species is derived from its type locality “Dambulla” (adjective in nominative case singular).

Type material examined**Holotype**

SRI LANKA • ♂; “X-SR0269, Sri Lanka, Matale District, Dambulla, NIFS Arboretum, 7.85766°N, 80.67474°E, 174, 13-X-2019, Eberle, Bohacz & Ranasinghe, Black light”; ZFMK.

Paratypes

SRI LANKA • 1 ♂; “X-SR0254, Sri Lanka, Matale District, Dambulla, NIFS Arboretum; 7.85766°N, 80.67474°E; 174m; 13-X-2019; Eberle, Bohacz & Ranasinghe leg.; Black light”, ZFMK • 1 ♂; “X-SR0257, Sri Lanka, Matale District, Dambulla, NIFS Arboretum; 7.85766°N, 80.67474°E; 174m; 13-X-2019; Eberle, Bohacz & Ranasinghe leg.; Black light”, ZFMK • 1 ♂; “X-SR0258, Sri Lanka, Matale District, Dambulla, NIFS Arboretum; 7.85766°N, 80.67474°E; 174m; 13-X-2019; Eberle, Bohacz & Ranasinghe leg.; Black light”, ZFMK • 1 ♂; “X-SR0259, Sri Lanka, Matale District, Dambulla, NIFS Arboretum; 7.85766°N, 80.67474°E; 174m; 13-X-2019; Eberle, Bohacz & Ranasinghe leg.; Black light”, ZFMK • 1 ♂; “X-SR0262, Sri Lanka, Matale District, Dambulla, NIFS Arboretum; 7.85766°N, 80.67474°E; 174m; 13-X-2019; Eberle, Bohacz & Ranasinghe leg.; Black light”, ZFMK • 1 ♂; “X-SR0264, Sri Lanka, Matale District, Dambulla, NIFS Arboretum; 7.85766°N, 80.67474°E; 174m; 13-X-2019; Eberle, Bohacz & Ranasinghe leg.; Black light”, ZFMK • 1 ♂; “X-SR0265, Sri Lanka, Matale District, Dambulla, NIFS Arboretum; 7.85766°N, 80.67474°E; 174m; 13-X-2019; Eberle, Bohacz & Ranasinghe leg.; Black light”, ZFMK • 1 ♂; “X-SR0266, Sri Lanka, Matale District, Dambulla, NIFS Arboretum; 7.85766°N, 80.67474°E; 174m; 13-X-2019; Eberle, Bohacz & Ranasinghe leg.; Black light”, ZFMK • 1 ♂; “X-SR0267, Sri Lanka, Matale District, Dambulla, NIFS Arboretum; 7.85766°N, 80.67474°E; 174m; 13-X-

2019; Eberle, Bohacz & Ranasinghe leg.; Black light”, ZFMK • 1 ♂; “X-SR0271, Sri Lanka, Matale District, Dambulla, NIFS Arboretum; 7.85766°N, 80.67474°E; 174m; 13-X-2019; Eberle, Bohacz & Ranasinghe leg.; Black light”, ZFMK • 1 ♂; “X-SR0272, Sri Lanka, Matale District, Dambulla, NIFS Arboretum; 7.85766°N, 80.67474°E; 174m; 13-X-2019; Eberle, Bohacz & Ranasinghe leg.; Black light”, ZFMK • 1 ♂; “X-SR0279, Sri Lanka, Matale District, Dambulla, NIFS Arboretum; 7.85766°N, 80.67474°E; 174m; 13-X-2019; Eberle, Bohacz & Ranasinghe leg.; Black light”, ZFMK • 1 ♂; “X-SR0281, Sri Lanka, Matale District, Dambulla, NIFS Arboretum; 7.85766°N, 80.67474°E; 174m; 13-X-2019; Eberle, Bohacz & Ranasinghe leg.; Black light”, ZFMK • 1 ♂; “X-SR0282, Sri Lanka, Matale District, Dambulla, NIFS Arboretum; 7.85766°N, 80.67474°E; 174m; 13-X-2019; Eberle, Bohacz & Ranasinghe leg.; Black light”, ZFMK • 1 ♂; “X-SR0283, Sri Lanka, Matale District, Dambulla, NIFS Arboretum; 7.85766°N, 80.67474°E; 174m; 13-X-2019; Eberle, Bohacz & Ranasinghe leg.; Black light”, ZFMK • 1 ♂; “X-SR0284, Sri Lanka, Matale District, Dambulla, NIFS Arboretum; 7.85766°N, 80.67474°E; 174m; 13-X-2019; Eberle, Bohacz & Ranasinghe leg.; Black light”, ZFMK • 1 ♂; “X-SR0285, Sri Lanka, Matale District, Dambulla, NIFS Arboretum; 7.85766°N, 80.67474°E; 174m; 13-X-2019; Eberle, Bohacz & Ranasinghe leg.; Black light”, ZFMK • 1 ♂; “X-SR0286, Sri Lanka, Matale District, Dambulla, NIFS Arboretum; 7.85766°N, 80.67474°E; 174m; 13-X-2019; Eberle, Bohacz & Ranasinghe leg.; Black light”, ZFMK • 1 ♂; “X-SR0292, Sri Lanka, Matale District, Dambulla, NIFS Arboretum; 7.85766°N, 80.67474°E; 174m; 13-X-2019; Eberle, Bohacz & Ranasinghe leg.; Black light”, ZFMK • 1 ♂; “X-SR0297, Sri Lanka, Matale District, Dambulla, NIFS Arboretum; 7.85766°N, 80.67474°E; 174m; 13-X-2019; Eberle, Bohacz & Ranasinghe leg.; Black light”, ZFMK • 1 ♂; “X-SR0300, Sri Lanka, Matale District, Dambulla, NIFS Arboretum; 7.85766°N, 80.67474°E; 174m; 13-X-2019; Eberle, Bohacz & Ranasinghe leg.; Black light”, ZFMK • 1 ♂; “X-SR0486, Sri Lanka, Matale District, Dambulla, NIFS Arboretum; 7.85766°N, 80.67474°E; 174m; 13-X-2019; Eberle, Bohacz & Ranasinghe leg.; Black light”, ZFMK • 1 ♂; “X-SR0489, Sri Lanka, Matale District, Dambulla, NIFS Arboretum; 7.85766°N, 80.67474°E; 174m; 13-X-2019; Eberle, Bohacz & Ranasinghe leg.; Black light”, ZFMK • 1 ♂; “X-SR0490, Sri Lanka, Matale District, Dambulla, NIFS Arboretum; 7.85766°N, 80.67474°E; 174m; 13-X-2019; Eberle, Bohacz & Ranasinghe leg.; Black light”, ZFMK • 1 ♂; “X-SR0491, Sri Lanka, Matale District, Dambulla, NIFS Arboretum; 7.85766°N, 80.67474°E; 174m; 13-X-2019; Eberle, Bohacz & Ranasinghe leg.; Black light”, ZFMK • 1 ♂; “X-SR0501, Sri Lanka, Matale District, Dambulla, NIFS Arboretum; 7.85766°N, 80.67474°E; 174m; 13-X-2019; Eberle,

Bohacz & Ranasinghe leg.; Black light”, ZFMK • 1 ♂; “X-SR0507, Sri Lanka, Matale District, Dambulla, NIFS Arboretum; 7.85766°N, 80.67474°E; 174m; 13-X-2019; Eberle, Bohacz & Ranasinghe leg.; Black light”, ZFMK • 1 ♂; “X-SR0510, Sri Lanka, Matale District, Dambulla, NIFS Arboretum; 7.85766°N, 80.67474°E; 174m; 13-X-2019; Eberle, Bohacz & Ranasinghe leg.; Black light”, ZFMK • 1 ♂ “X-SR1049, Sri Lanka, Matale District, Dambulla, NIFS Arboretum; 7.85766°N, 80.67474°E; 174m; 13-X-2019; Eberle, Bohacz & Ranasinghe leg.; Black light”, ZFMK • 1 ♂; “X-SR0341, Sri Lanka, Matale District, Dambulla, NIFS Arboretum; 7.85783°N, 80.67391°E; 167m; 12-13-X-2019; Eberle, Bohacz & Ranasinghe leg.; Black light”, ZFMK • 1 ♂; “X-SR0363, Sri Lanka, Matale District, Dambulla, NIFS Arboretum; 7.85783°N, 80.67391°E; 167m; 12-13-X-2019; Eberle, Bohacz & Ranasinghe leg.; Black light”, ZFMK • 1 ♂; “X-SR0414, Sri Lanka, Matale District, Dambulla, NIFS Arboretum; 7.85796°N, 80.67554°E; 181m; 12-13-X-2019; Eberle, Bohacz & Ranasinghe leg.; Black light”, ZFMK • 1 ♂; “SR0301, Sri Lanka, Matale District, Dambulla, NIFS Arboretum; 7.85824°N, 80.67506°E; 182m; 13-X-2019; Eberle, Bohacz & Ranasinghe leg.; Black light”, ZFMK • 1 ♂; “X-SR0985, Sri Lanka, Matale District, Dambulla, NIFS Arboretum; 7.85897°N, 80.67533°E; 203m; 11-12-X-2019; Eberle, Bohacz & Ranasinghe leg.; Black light”, ZFMK • 1 ♂; “X-SR0209, Sri Lanka, Matale District, Dambulla, NIFS Arboretum; 7.85907°N, 80.67587°E; 160m; 13-X-2019; Eberle, Bohacz & Ranasinghe leg.; Black light”, ZFMK • 1 ♂; “X-SR0210, Sri Lanka, Matale District, Dambulla, NIFS Arboretum; 7.85907°N, 80.67587°E; 160m; 13-X-2019; Eberle, Bohacz & Ranasinghe leg.; Black light”, ZFMK • 1 ♀; “X-SR0261, Sri Lanka, Matale District, Dambulla, NIFS Arboretum; 7.85766°N, 80.67474°E; 174m; 13-X-2019; Eberle, Bohacz & Ranasinghe leg.; Black light”, ZFMK • 1 ♀; “X-SR0263, Sri Lanka, Matale District, Dambulla, NIFS Arboretum; 7.85766°N, 80.67474°E; 174m; 13-X-2019; Eberle, Bohacz & Ranasinghe leg.; Black light”, ZFMK.

Description.

MEASUREMENTS. Length: 5.6 mm, length of elytra: 4.1 mm, width: 3.1 mm.

HABITUS AND COLORATION. Body short oval, yellowish brown, antenna yellow, dorsal surface shiny, densely finely setose.

HEAD. Labroclypeus subtrapezoidal, distinctly wider than long, widest at base, lateral margins weakly convex and strongly convergent to widely rounded anterior angles, lateral border and ocular canthus producing an indistinct blunt angle, margins

weakly reflexed, anteriorly shallowly sinuate medially; surface slightly convex, finely and densely punctate, distance between punctures smaller than their diameter, with numerous erect setae in larger punctures; frontoclypeal suture almost invisible and strongly angled medially; smooth area in front of eye approximately twice as wide as long; ocular canthus short and narrow, minutely and superficially punctate, with a single short terminal seta. Frons with fine, dense punctures, with long erect setae in the punctures. Eyes large, ratio of diameter/ interocular width: 0.85. Antenna yellow, with ten antennomeres; club with three antennomeres, as long as remaining antennomeres combined. Mentum elevated and anteriorly flattened.

PRONOTUM. Moderately wide, widest at base, lateral margins weakly convex and evenly narrowed to the anterior third, anteriorly stronger convex, anterior angles strongly produced and sharp, anterior marginal line fine but complete medially, anterior margin weakly produced medially; surface finely and densely punctate, with dense moderately long setae being bent posteriorly on entire disc and with a few sparse longer setae being directed anteriorly; anterior and lateral borders setose, basal margin without marginal line; hypomeron ventrobasally carinate and slightly produced ventrally. Scutellum short and wide, triangular, with fine and dense punctures, with fine and dense adjacent setae.

ELYTRA. Short oval, widest shortly behind middle, striae indistinctly impressed, finely and densely punctate, intervals flat, with fine, very dense punctures, with a fine setae similar to those of the pronotum and a few sparser ones being longer and erect or directed anteriorly, in particular on lateral intervals; epipleural edge fine, ending at the weakly convex external apical angle of elytra, epipleura densely setose; apical border narrowly membranous, apex covered with short microtrichomes.

VENTRAL SURFACE. Moderately shiny, thorax and metacoxa with large and dense punctures, densely setose, metacoxa glabrous except for numerous long setae laterally; each abdominal sternite, in addition to evenly distributed fine and dense punctures bearing each a fine seta, with a distinct transverse row of coarse punctures each bearing a long and more robust seta, penultimate sternite apically with a shiny smooth chitinous border, which is a quarter as long as the sternite. Mesosternum between mesocoxae as wide as mesofemur, with a semi-circular ridge bearing robust setae. Ratio of length of metepisternum/ metacoxa: 1/ 1.93. Pygidium moderately convex, finely and very densely punctate, without smooth midline, punctures with short and moderately dense, adjacent setae, along the apical margin with a few long erect setae.

LEGS. Short and wide; femur with two longitudinal rows of setae, finely and densely punctate, densely setose; metafemur shiny, anterior edge acute, lacking an adjacent serrated line, ventral surface densely punctate and setose, posterior ventral margin straight, only little widened in apical half and very indistinctly serrate apically, dorsally not serrated, glabrous. Metatibia short, widest at middle, posteriorly slightly narrowed, ratio width/ length: 1/ 2.18, dorsally sharply carinate, with two groups of spines, basal one at middle, apical one at three quarters of metatibial length, basally beside dorsal margin with two single punctures with serrated margins, each bearing single spines and beside them a longitudinal serrated line; lateral face almost flat, with dense, fine punctures and with minute setae in the punctures; ventral margin with five strong spines equidistant from each other, medial face smooth, apex interiorly near tarsal articulation shallowly truncate. Meso- and metatarsomeres finely and densely punctate and setose dorsally, ventrally with sparse, short setae; metatarsomeres ventrally with a strongly serrated ridge, beside which is a strong longitudinal carina; first metatarsomere as long as following two tarsomeres combined and a little longer than dorsal tibial spur. Protibia short, bidentate. All claws symmetrical, feebly curved and long, with normally developed basal tooth.

AEDEAGUS. Fig. 6.6A–C.

HABITUS. Fig. 6.6D.

Variation. Length: 5.6-6.7 mm, length of elytra: 4.1-4.6 mm, width: 3.1-3.5 mm.

Female. Length: 6.0-6.5 mm, length of elytra: 4.7-4.9 mm, width: 3.7-3.8 mm. Eyes slightly smaller than in male; antennal club little shorter than remaining antennomeres combined.

Distribution. See Fig. 6.7I.

***Maladera deenstana* sp. nov.**

Figs 6.6E–H, 6.7J, 6.8I

Diagnosis. *Maladera deenstana* sp. nov. is in external shape and shape of aedeagus similar to *M. weligamana* (Brenske, 1898). The new species differs from *M.*

weligamana by the mesally more compressed aedeagus and having the distal part less narrowed towards apex (all lateral view); the apical part is less narrowed a quarter before apex than in *M. weligamana* (dorsal view).

Etymology. The new species is named after its type locality “Deenston”, (adjective in the nominative singular).

Type material examined

Holotype

SRI LANKA • ♂; “X-SR0187, Sri Lanka, Kandy District, Deenston, Knuckles South; 7.330824°N, 80.862032°E; 1108m; 20-II-2019; Eberle and Ranasinghe leg.; Black light”; ZFMK.

Description.

MEASUREMENTS. Length: 8.2 mm, length of elytra: 6.1 mm, width: 4.9 mm.

HABITUS AND COLORATION. Body oval, dark brown, antenna yellow, dorsal surface dull, densely minutely setose, elytra with moderately dense, short setae.

HEAD. Labroclypeus subtrapezoidal, distinctly wider than long, widest at base, lateral margins weakly convex and strongly convergent to widely rounded anterior angles, lateral border and ocular canthus producing an indistinct blunt angle, margins moderately reflexed, anteriorly distinctly emarginate medially; surface shiny, convexly elevated medially, finely and densely punctate, distance between punctures equal their diameter, with a few erect setae; frontoclypeal suture fine and weakly angled medially; smooth area in front of eye approximately twice as wide as long; ocular canthus short and narrow, finely and densely punctate, with a single short terminal seta. Frons dull, with fine, irregularly sparse punctures, with a few longer, adpressed setae on disc and beside eyes. Eyes moderately large, ratio of diameter/interocular width: 0.66. Antenna yellow, with ten antennomeres; club with three antennomeres, little shorter than remaining antennomeres combined. Mentum elevated and anteriorly flattened.

PRONOTUM. Moderately wide, widest at base, lateral margins weakly convex and evenly narrowed anteriorly, anterior angles moderately produced and moderately sharp, anterior marginal line fine and complete, anterior margin weakly produced medially; surface finely and densely punctate, with minute setae in punctures,

otherwise glabrous; anterior and lateral borders sparsely setose, basal margin without marginal line; hypomerion ventrobasally carinate and slightly produced ventrally. Scutellum short and wide, triangular, with fine and dense punctures, along midline impunctate.

ELYTRA. Short oval, widest at posterior third, striae indistinctly impressed, finely and densely punctate, intervals flat, with fine, dense punctures, with a minute setae in punctures and a few moderately dense, short setae on lateral intervals and posterior half; epipleural edge fine, ending at the weakly convex external apical angle of elytra, epipleura densely setose; apical border membranous, apex covered with a rim of short microtrichomes.

VENTRAL SURFACE. Moderately shiny, thorax and metacoxa with large and dense punctures, densely minutely setose, metacoxa with numerous long setae laterally; each abdominal sternite, in addition to evenly distributed fine and dense punctures bearing each a fine seta, with a distinct transverse row of coarse punctures each bearing a long and more robust seta, penultimate sternite apically with a narrow, shiny smooth chitinous border. Mesosternum between mesocoxae as wide as mesofemur, with a semi-circular ridge bearing robust setae. Ratio of length of metepisternum/ metacoxa: 1/ 2.0. Pygidium lacking in holotype.

LEGS. Short and wide; femur with two longitudinal rows of setae, finely and densely punctate, densely setose; metafemur shiny, anterior edge acute, lacking an adjacent serrated line, ventral surface densely punctate and setose; posterior ventral margin straight, strongly widened in apical half and very indistinctly serrate apically; posterior dorsal margin not serrated, densely setose. Metatibia short, widest at middle, posteriorly slightly narrowed, ratio width/ length: 1/ 2.9, dorsally sharply carinate, with two groups of spines, basal one shortly behind middle, apical one at four fifths of metatibial length, basally beside dorsal margin with two single punctures with serrated margins, each bearing single spines; lateral face longitudinal convex, with sparse, fine punctures and with minute setae in punctures; ventral margin finely serrate, with five strong spines equidistant from each other; medial face smooth, apex interiorly near tarsal articulation shallowly truncate. Meso- and metatarsomeres impunctate and glabrous dorsally, ventrally with sparse, short setae; metatarsomeres ventrally glabrous, with a strongly serrated ridge, beside which is a strong longitudinal carina; first metatarsomere as long as two following tarsomeres combined and as long as dorsal tibial spur. Protibia short, bidentate. All claws

symmetrical, feebly curved and long, with normally developed basal tooth, distal protarsomeres lacking in holotype.

AEDEAGUS. Fig. 6.6E–G.

HABITUS. Fig. 6.6H.

Female. Unknown.

Distribution. See Fig. 6.7J.

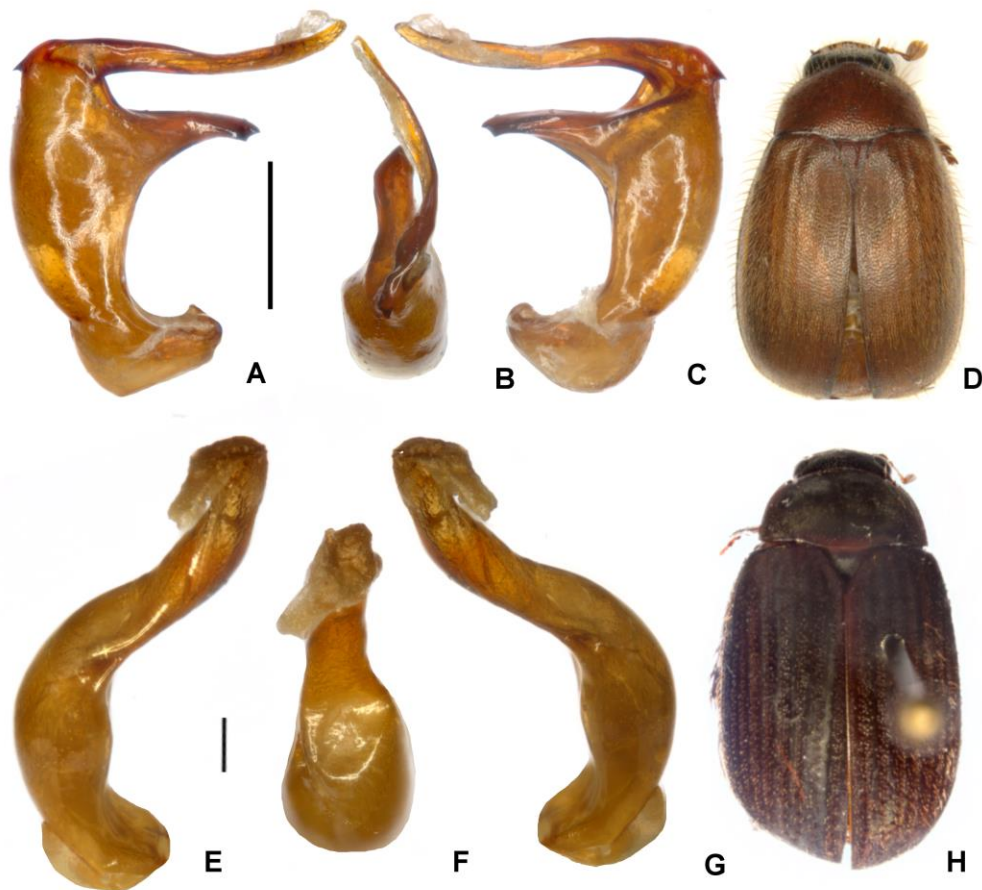


Figure 6.6. A–D *M. dambullana* sp. nov., (holotype) E–H *M. deenstana* sp. nov. (holotype) A, E aedeagus, left side lateral view C, G aedeagus, right side lateral view B, F parameres, dorsal view D, H habitus (not to scale). Scale: 0.5 mm.

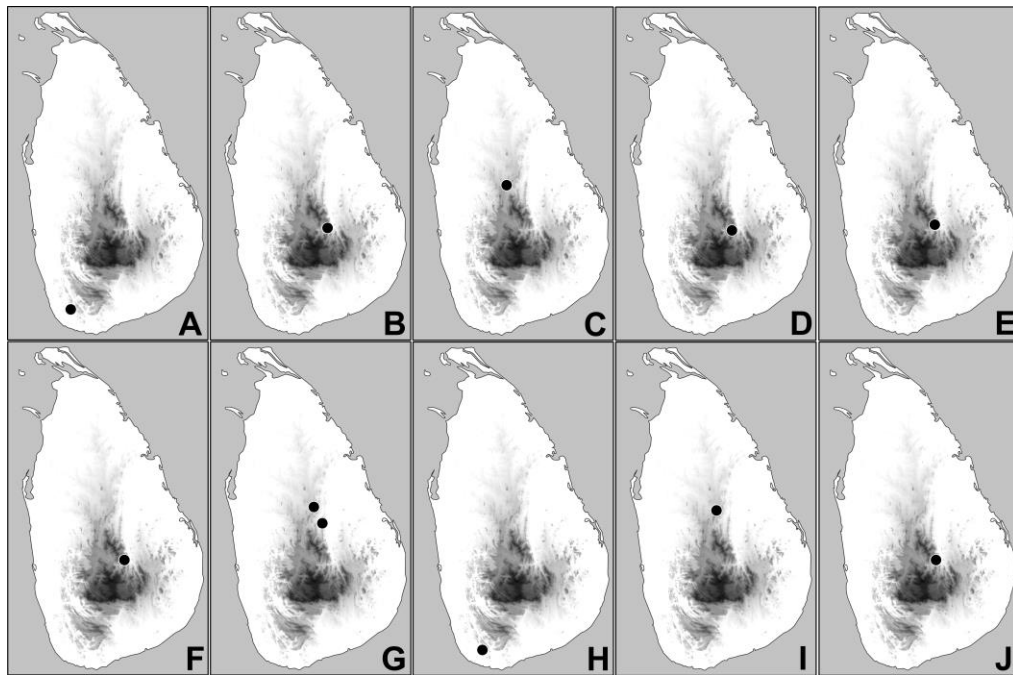


Figure 6.7. Distribution of ten new species. **A.** *Selaserica fabriziae* sp. nov., **B.** *Sel. sororinitida* sp. nov., **C.** *Neoserica pophami* sp. nov., **D.** *Maladera haniel* sp. nov., **E.** *M. kishi* sp. nov., **F.** *M. windy* sp. nov. **G.** *M. karunaratnae* sp. nov., **H.** *M. hiyarensis* sp. nov. **I.** *M. dambullana* sp. nov., **J.** *M. deenstana* sp. nov.

6.3.2 Updated and corrected key to species of the *Maladera fistulosa* group (♂♂)

- 1 Pronotum glabrous on disc, sometimes a few sparse setae on lateral pronotal disc. Anterior marginal line of pronotum widely incomplete medially.....2
- 1' Pronotum densely setose.....13
- 2 Apical margin of metacoxa slightly concave, glabrous. Metatibia basally with a longitudinal serrated line.....3
- 2' Apical margin of metacoxa straight or convex. Metatibia basally without a longitudinal serrated line.....5
- 3 Metatibia more stout (ratio width/ length > 1/ 3.2)..... 4
- 3' Metatibia more slender (ratio width/ length < 1/ 3.7). Antennal club slightly longer than the remaining antennomeres together. Apex of aedeagus more strongly narrowed apically, median hook absent ventrally..... *M. hortonensis* Fabrizi & Ahrens, 2014



Figure 6.8. Photographs of the habitats of the new species. **A.** *Selaserica fabriziae* sp. nov. **B.** *Sel. sororinitida* sp. nov., **C.** *Neoserica pophami* sp. nov., **D.** *Maladera haniel* sp. nov. and *M. kishi* sp. nov., **E.** *M. windy* sp. nov., **F.** *M. karunaratnae* sp. nov., **G.** *M. hiyarensis* sp. nov., **H.** *M. dambullana* sp. nov., **I.** *M. deenstana* sp. nov.

- 4 Metatibia ratio width/ length: 1/ 2.8. Antennal club 1.2 times as long as remaining antennomeres together. Apex of aedeagus apically evenly narrowed and dorsoventrally compressed.....*M. lindulana* Fabrizi & Ahrens, 2014
- 4' Metatibia ratio width/ length: 1/ 3.2. Antennal club 1.5 times as long as remaining antennomeres together. Apex of aedeagus apically widened (lateral view), with a median hook ventrally.....*M. dubia* (Arrow, 1916)
- 5 Basis of clypeus dull..... 6
- 5' Basis of clypeus shiny.....9
- 6 Metatibia wide (ratio width/ length: 1/ 2.4-2.6). Metacoxal apophysis with very dense, evenly short, scale-like setae.....7
- 6' Metatibia slender (ratio width/ length: 1/ 3.0). Metacoxal apophysis without scale-like setae. Aedeagus with a single narrowly extended tube.....*M. schintlmeisteri* Fabrizi & Ahrens, 2014
- 7 Body size smaller 10 mm (ca. 8.8 mm).....*M. woodi* Fabrizi & Ahrens, 2014
- 7' Body size larger 10 mm (ca. 11.8 mm).....8
- 8 Aedeagus apically deeply bifurcate.....*M. kuruwitana* Fabrizi & Ahrens, 2014
- 8' Aedeagus apically not incised.....*M. coxalis* (Moser, 1915)
- 9 Distal operculum of aedeagus enlarged apically.....10
- 9' Apex of aedeagus almost evenly narrowed, distal operculum of aedeagus not significantly enlarged apically.....11
- 10 Aedeagus ventrally with a large convex elevation at middle. Distal operculum of aedeagus moderately large, not half as wide as width of aedeagus.....*M. fistulosa* (Brenske, 1898)
- 10' Aedeagus ventrally without a large convex elevation at middle. Distal operculum of aedeagus large, as wide as width of aedeagus.....*M. poyagana* Fabrizi & Ahrens, 2014
- 11 Aedeagus ventrally with a large convex elevation at middle..... *M. badullana* Fabrizi & Ahrens, 2014
- 11' Aedeagus ventrally without a large convex elevation at middle.....12
- 12 Aedeagus strongly compressed at middle, its distal part strongly narrowed towards apex (lateral view) and distinctly narrowed a quarter before apex (dorsal view).....*M. weligamana* (Brenske, 1900)
- 12' Aedeagus moderately compressed at middle, its distal part less narrowed towards apex (lateral view) and less narrowed a quarter before apex (dorsal view).....*M. deenstana* sp. nov.

- 13 Elytra with a longitudinal row of widely separated impunctate spots each bearing at centre a coarse puncture with an erect seta.....14
- 13' Elytra without widely separated impunctate spots bearing at centre a coarse puncture with an erect seta.....17
- 14 Body shape more elongate. Distal part of aedeagus short and wide (lateral view).....15
- 14' Body shape oval. Distal part of aedeagus longer and narrower (lateral view).....*M. hiyarensis* sp. nov.
- 15 Aedeagus with a ventral hook.....16
- 15' Aedeagus without a ventral hook.*M. karunaratnae* sp. nov.
- 16 Pronotum with double pilosity composed of short adjacent and long erect setae. Aedeagus, with a sharp ventral hook before the middle.....*M. anderssoni* Fabrizi & Ahrens, 2014
- 16' Pronotum with simple pilosity composed of short adjacent setae. Aedeagus, with a sharp ventral hook before the apex.....*M. romanoi* Fabrizi & Ahrens, 2014
- 17 Pronotum and elytra with fine and significantly larger punctures.....18
- 17' Pronotum and elytra only with fine, dense punctures. Elytra unicoloured.....22
- 18 Aedeagus simple, without lobes or branches. Elytral intervals with dark stripes.*M. galdaththana* Ranasinghe et al., 2020
- 18' Aedeagus with apical or lateral lobes or branches.19
- 19 Apical margin of metacoxa without setae.....20
- 19' Apical margin of metacoxa with dense short setae.....21
- 20 Median apophysis of metacoxa with dense, evenly short setae. Ventral metatibial spur slightly longer than the basal metatarsomere.....*M. brincki* Fabrizi & Ahrens, 2014
- 20' Median apophysis of metacoxa with moderately dense, unevenly long setae. Ventral metatibial spur almost as long as the two basal metatarsomeres combined.....*M. heveli* Fabrizi & Ahrens, 2014
- 21 Ventral metatibial spur almost straight and not elongated. Median apophysis of metacoxa with moderately dense and unevenly short setae.....*M. uggalkaltotensis* Fabrizi & Ahrens, 2014
- 21' Ventral metatibial spur strongly curved and almost as long as the three basal metatarsomeres combined. Median apophysis of metacoxa with very dense and evenly short setae.....*M. diyalumana* Fabrizi & Ahrens, 2014
- 22 Apical margin of metacoxa with dense, short setae.....23
- 22' Apical margin of metacoxa without setae.....24

23	Colour reddish brown, body smaller than 7.5 mm	<i>M. tricuspidata</i> Fabrizi & Ahrens, 2014
23'	Colour dark reddish brown, body larger than 8.0 mm.....	<i>M. nilaveliensis</i> Fabrizi & Ahrens, 2014
24	Body smaller than 7 mm.....	25
24'	Body larger than 7 mm.....	28
25	Antennal club as long as remaining antennomeres combined.....	26
25'	Antennal club slightly longer than the remaining antennomeres combined.....	<i>M. bisornata</i> Fabrizi & Ahrens, 2014
26	Dorsal distal lobe of aedeagus simple.....	27
26'	Dorsal distal lobe of aedeagus with a long lobiform extension at the base.....	<i>M. windy</i> sp. nov.
27	Ventral distal lobe of aedeagus (i.e., including the fused parameres) extremely extended medially exceeding almost the maximum width of phallobase (dorsal view).....	<i>M. pubescens</i> (Arrow, 1916)
27'	Ventral distal lobe of aedeagus (i.e., including the fused parameres) not extended mesally but constant in width over its entire length and being much narrower than the phallobase (dorsal view).....	<i>M. dambullana</i> sp. nov.
28	Aedeagus with at least two apical processes.....	29
28'	Aedeagus with a single principal apical process.....	<i>M. yalaensis</i> Fabrizi & Ahrens, 2014
29	Aedeagus with at two apical processes. 3 rd abdominal sternite without median tubercle.....	31
29'	Aedeagus with at three apical processes.....	30
30	3 rd abdominal sternite with a median tubercle. Right distal lobe of aedeagus split before apex.....	34
30'	3 rd abdominal sternite without a median tubercle. Right distal lobe of aedeagus not split before apex.....	<i>M. kishi</i> sp. nov.
31	Median apophysis of metacoxa with dense, evenly short setae.....	32
31'	Median apophysis of metacoxa with moderately dense, unevenly long setae.....	<i>M. mavilluensis</i> Fabrizi & Ahrens, 2014
32	Aedeagus in lateral view strongly enlarged ventrally, with a marsupium-like excavation.....	<i>M. flinti</i> Fabrizi & Ahrens, 2014
32'	Aedeagus in lateral not enlarged ventrally.....	33
33	Right lateral process of aedeagus convex at the tip.....	<i>M. kandyensis</i> Fabrizi & Ahrens, 2014

- 33' Right lateral process of aedeagus acute at the tip.....*M. hastata* Fabrizi & Ahrens, 2014
- 34 Setae on disc of pronotum almost missing. Right distal lobe of aedeagus shorter, shorter than the rest of the basal part of the phallobase, strongly narrowed towards apex.....*M. cervicornis* Ranasinghe et al., 2020
- 34' Setae on disc of pronotum dense. Right distal lobe of aedeagus extremely long, as long as the rest of the basal part of the phallobase, equal in width over its entire length.....*M. haniel* sp. nov.

6.3.3 New distribution records

Maladera anderssoni Fabrizi & Ahrens, 2014

Material examined

SRI LANKA • 1 ♂; “X-SR0949, Sri Lanka, Kandy District, Deanston, Knuckles South; 7.33082°N, 80.86203°E; 1108m; 17-X-2019; Eberle, Bohacz & Ranasinghe leg.; Black light”; ZFMK • 1 ♂; “X-SR0950, Sri Lanka, Kandy District, Deanston, Knuckles South; 7.33082°N, 80.86203°E; 1108m; 17-X-2019; Eberle, Bohacz & Ranasinghe leg.; Black light”; ZFMK • 1 ♂; “X-SR0704, Sri Lanka, Kandy District, Deanston, Knuckles South; 7.33097°N, 80.85934°E; 1190m; 18-X-2019; Eberle, Bohacz & Ranasinghe leg.; Black light”; ZFMK • 1 ♂; “X-SR0705, Sri Lanka, Kandy District, Deanston, Knuckles South; 7.33097°N, 80.85934°E; 1190m; 18-X-2019; Eberle, Bohacz & Ranasinghe leg.; Black light”; ZFMK • 1 ♂; “X-SR0706, Sri Lanka, Kandy District, Deanston, Knuckles South; 7.33097°N, 80.85934°E; 1190m; 18-X-2019; Eberle, Bohacz & Ranasinghe leg.; Black light”; ZFMK • 1 ♂; “X-SR0707, Sri Lanka, Kandy District, Deanston, Knuckles South; 7.33097°N, 80.85934°E; 1190m; 18-X-2019; Eberle, Bohacz & Ranasinghe leg.; Black light”; ZFMK • 1 ♂; “X-SR0709, Sri Lanka, Kandy District, Deanston, Knuckles South; 7.33097°N, 80.85934°E; 1190m; 18-X-2019; Eberle, Bohacz & Ranasinghe leg.; Black light”; ZFMK • 1 ♂; “X-SR0710, Sri Lanka, Kandy District, Deanston, Knuckles South; 7.33097°N, 80.85934°E; 1190m; 18-X-2019; Eberle, Bohacz & Ranasinghe leg.; Black light”; ZFMK • 1 ♂; “X-SR0711, Sri Lanka, Kandy District, Deanston, Knuckles South; 7.33097°N, 80.85934°E; 1190m; 18-X-2019; Eberle, Bohacz & Ranasinghe leg.; Black light”; ZFMK • 1 ♂; “X-SR0922, Sri Lanka, Kandy District, Deanston, Knuckles South; 7.33159°N, 80.86110°E; 1139m; 17-X-2019; Eberle, Bohacz & Ranasinghe leg.; Black light”; ZFMK • 1 ♂; “X-SR0923, Sri

Lanka, Kandy District, Deanston, Knuckles South; 7.33159°N, 80.86110°E; 1139m; 17-X-2019; Eberle, Bohacz & Ranasinghe leg.; Black light”; ZFMK • 1 ♂; “X-SR0559, Sri Lanka, Kandy District, Deanston, Knuckles South; 7.33501°N, 80.85966°E; 1171m; 18-X-2019; Eberle, Bohacz & Ranasinghe leg.; Black light”; ZFMK.

***Maladera bandarwelana* Fabrizi & Ahrens, 2014**

Material examined

SRI LANKA • 1 ♂; “X-SR0666, Sri Lanka, Matale District, Riverston, below the Greenview lodge; 7.53830°N, 80.7511°E; 765m; 14-X-2019; Eberle, Bohacz & Ranasinghe leg.; Black light”; ZFMK • 1 ♂; “X-SR0881, Sri Lanka, Matale District, Riverston, below the Greenview lodge; 7.54976°N, 80.75212°E; 902m; 15-X-2019; Eberle, Bohacz & Ranasinghe leg.; Black light”; ZFMK • ZFMK • 1 ♀; “X-SR0882, Sri Lanka, Matale District, Riverston, below the Greenview lodge; 7.54976°N, 80.75212°E; 902m; 15-X-2019; Eberle, Bohacz & Ranasinghe leg.; Black light”; ZFMK.

***Maladera breviatella* Fabrizi & Ahrens, 2014**

Material examined.

SRI LANKA • 1 ♂; “X-SR2162, Sri Lanka, Kandy District, Udawattakele FR; 7.29590°N, 80.64224°E; 26-XI-2020; Ranasinghe & Athukorala leg.; Black light”; ZFMK.

***Maladera calcarata* (Brenske, 1898)**

Material examined.

SRI LANKA • 1 ♂; “X-SR0309, Sri Lanka, Matale District, Dambulla, NIFS Arboretum; 7.85824°N, 80.67506°E; 182m; 13-X-2019; Eberle, Bohacz & Ranasinghe leg.; Black light”; ZFMK.

***Maladera cervicornis* Ranasinghe, Eberle, Benjamin & Ahrens, 2020**

Material examined.

SRI LANKA • 1 ♂; “X-SR0621, Sri Lanka, Matale District, Riverston, Greenview lodge; 7.53827°N, 80.75°E; 782m; 14-X-2019; Eberle, Bohacz & Ranasinghe leg.;

Black light”; ZFMK • 1 ♂; “X-SR0622, Sri Lanka, Matale District, Riverston, Greenview lodge; 7.53827°N, 80.75°E; 782m; 14-X-2019; Eberle, Bohacz & Ranasinghe leg.; Black light”; ZFMK • 1 ♂; “X-SR0623, Sri Lanka, Matale District, Riverston, Greenview lodge; 7.53827°N, 80.75°E; 782m; 14-X-2019; Eberle, Bohacz & Ranasinghe leg.; Black light”; ZFMK • 1 ♂; “X-SR0624, Sri Lanka, Matale District, Riverston, Greenview lodge; 7.53827°N, 80.75°E; 782m; 14-X-2019; Eberle, Bohacz & Ranasinghe leg.; Black light”; ZFMK • 1 ♂; “X-SR0625, Sri Lanka, Matale District, Riverston, Greenview lodge; 7.53827°N, 80.75°E; 782m; 14-X-2019; Eberle, Bohacz & Ranasinghe leg.; Black light”; ZFMK • 1 ♂; “X-SR0626, Sri Lanka, Matale District, Riverston, Greenview lodge; 7.53827°N, 80.75°E; 782m; 14-X-2019; Eberle, Bohacz & Ranasinghe leg.; Black light”; ZFMK • 1 ♂, “X-SR0653, Sri Lanka, Matale District, Riverston, Pitawala Pathana; 7.5491°N, 80.75386°E; 880m; 15-X-2019; Eberle, Bohacz & Ranasinghe leg.; Black light”; ZFMK • 1 ♂, “X-SR0867, Sri Lanka, Matale District, Riverston, Pitawala Pathana; 7.5491°N, 80.75386°E; 880m; 15-X-2019; Eberle, Bohacz & Ranasinghe leg.; Black light”; ZFMK • 1 ♂, “X-SR0868, Sri Lanka, Matale District, Riverston, Pitawala Pathana; 7.5491°N, 80.75386°E; 880m; 15-X-2019; Eberle, Bohacz & Ranasinghe leg.; Black light”; ZFMK • 1 ♂, “X-SR0869, Sri Lanka, Matale District, Riverston, Pitawala Pathana; 7.5491°N, 80.75386°E; 880m; 15-X-2019; Eberle, Bohacz & Ranasinghe leg.; Black light”; ZFMK • 1 ♂, “X-SR2237, Matale District, Riverston, Thelgamu oya bungalow; 7.5363°N, 80.7723°E; 509m; 02-XII-2020; Ranasinghe & Athukorala leg.; Black light”; ZFMK.

***Maladera coxalis* (Moser, 1915)**

Material examined.

SRI LANKA • 1 ♂; “X-SR0659, Sri Lanka, Matale District, Riverston, Greenview lodge; 7.53804°N, 80.75027°E; 778m; 15-X-2019; Eberle, Bohacz & Ranasinghe leg.; Light sheet”; ZFMK • 1 ♂; “X-SR0320, Sri Lanka, Matale District, Dambulla, NIFS Arboretum; 7.85824°N, 80.67506°E; 182m, 13-X-2019; Eberle, Bohacz & Ranasinghe leg.; Black light”; ZFMK • 1 ♂; “X-SR0328, Sri Lanka, Matale District, Dambulla, NIFS Arboretum; 7.85824°N, 80.67506°E; 182m, 13-X-2019; Eberle, Bohacz & Ranasinghe leg.; Black light”; ZFMK • 1 ♂; “X-SR0329, Sri Lanka, Matale District, Dambulla, NIFS Arboretum; 7.85824°N, 80.67506°E; 182m, 13-X-2019; Eberle, Bohacz & Ranasinghe leg.; Black light”; ZFMK • 1 ♂; “X-SR0330, Sri Lanka, Matale District, Dambulla, NIFS Arboretum; 7.85824°N, 80.67506°E; 182m, 13-X-2019; Eberle, Bohacz & Ranasinghe leg.; Black light”; ZFMK • 1 ♂; “X-

SR0991, Sri Lanka, Matale District, Dambulla, NIFS Arboretum; 7.85897°N, 80.67533°E; 203, 11-12-X-2019; Eberle, Bohacz & Ranasinghe leg.; Black light”; ZFMK • 1 ♂; “X-SR0992, Sri Lanka, Matale District, Dambulla, NIFS Arboretum; 7.85897°N, 80.67533°E; 203, 11-12-X-2019; Eberle, Bohacz & Ranasinghe leg.; Black light”; ZFMK • 1 ♂; “X-SR0993, Sri Lanka, Matale District, Dambulla, NIFS Arboretum; 7.85897°N, 80.67533°E; 203, 11-12-X-2019; Eberle, Bohacz & Ranasinghe leg.; Black light”; ZFMK • 1 ♂; “X- SR1004, Sri Lanka, Matale District, Dambulla, NIFS Arboretum; 7.85897°N, 80.67533°E; 203, 11-12-X-2019; Eberle, Bohacz & Ranasinghe leg.; Black light”; ZFMK • 1 ♂; “X- SR1005, Sri Lanka, Matale District, Dambulla, NIFS Arboretum; 7.85897°N, 80.67533°E; 203, 11-12-X-2019; Eberle, Bohacz & Ranasinghe leg.; Black light”; ZFMK • 1 ♂; “X-SR1094, Sri Lanka, Matale District, Dambulla, NIFS Arboretum; 7.85897°N, 80.67533°E; 203, 11-12-X-2019; Eberle, Bohacz & Ranasinghe leg.; Black light”; ZFMK • 1 ♂; “X-SR1099, Sri Lanka, Matale District, Dambulla, NIFS Arboretum; 7.85897°N, 80.67533°E; 203, 11-12-X-2019; Eberle, Bohacz & Ranasinghe leg.; Black light”; ZFMK.

***Maladera galdaththana* Ranasinghe, Eberle, Benjamin & Ahrens, 2020**

Material examined

SRI LANKA • 1 ♂; “X-SR2048, Sri Lanka, Kandy District, Gannoruwa FR; 7.28342°N, 80.59840 °E; 592,5 m; 14-VII-2020; Ranasinghe & Athukorala leg.; Black light” ZFMK • 1 ♂; “X-SR2245, Sri Lanka, Matale District, Riverston, Thelgamu oya bangalow; 7.53635°N, 80.77234°E; 509 m; 01-XII-2020; Ranasinghe & Athukorala leg.; Black light”; ZFMK.

***Maladera kandyensis* Fabrizi & Ahrens, 2014**

Material examined

SRI LANKA • 1 ♂; “X-SR2163, Sri Lanka, Kandy District, Udawattakele FR; 7.29590°N, 80.64224 °E; 26-XI-2020; Ranasinghe & Athukorala leg.; Black light” ZFMK • 1 ♂; “X-SR2045, Sri Lanka, Kandy District, Gannoruwa FR; 7.28368°N, 80.59874 °E; 578m; 15-VII-2020; Ranasinghe & Athukorala leg.; Black light” ZFMK.

Maladera heveli* Fabrizi & Ahrens, 2014*Material examined**

SRI LANKA • 1 ♂; “X-SR0988, Sri Lanka, Matale District, Dambulla, NIFS Arboretum; 7.85897°N, 80.67533°E; 203m; 11-12-X-2019; Eberle, Bohacz & Ranasinghe leg.; Black light” ZFMK • 1 ♂; “X-SR0989, Sri Lanka, Matale District, Dambulla, NIFS Arboretum; 7.85897°N, 80.67533°E; 203m; 11-12-X-2019; Eberle, Bohacz & Ranasinghe leg.; Black light” ZFMK • 1 ♂; “X-SR0990, Sri Lanka, Matale District, Dambulla, NIFS Arboretum; 7.85897°N, 80.67533°E; 203m; 11-12-X-2019; Eberle, Bohacz & Ranasinghe leg.; Black light” ZFMK • 1 ♂; “X-SR1006, Sri Lanka, Matale District, Dambulla, NIFS Arboretum; 7.85897°N, 80.67533°E; 203m; 11-12-X-2019; Eberle, Bohacz & Ranasinghe leg.; Black light” ZFMK • 1 ♂; “X-SR1089, Sri Lanka, Matale District, Dambulla, NIFS Arboretum; 7.85897°N, 80.67533°E; 203m; 11-12-X-2019; Eberle, Bohacz & Ranasinghe leg.; Black light” ZFMK • 1 ♂; “X-SR1090, Sri Lanka, Matale District, Dambulla, NIFS Arboretum; 7.85897°N, 80.67533°E; 203m; 11-12-X-2019; Eberle, Bohacz & Ranasinghe leg.; Black light” ZFMK • 1 ♂; “X-SR1091, Sri Lanka, Matale District, Dambulla, NIFS Arboretum; 7.85897°N, 80.67533°E; 203m; 11-12-X-2019; Eberle, Bohacz & Ranasinghe leg.; Black light” ZFMK • 1 ♂; “X-SR1092, Sri Lanka, Matale District, Dambulla, NIFS Arboretum; 7.85897°N, 80.67533°E; 203m; 11-12-X-2019; Eberle, Bohacz & Ranasinghe leg.; Black light” ZFMK • 1 ♂; “X-SR0404, Sri Lanka, Matale District, Dambulla, NIFS Arboretum; 7.86011°N, 80.67441°E; 187m; 11-13-X-2019; Eberle, Bohacz & Ranasinghe leg.; Light sheet” ZFMK • 1 ♂; “X-SR0406, Sri Lanka, Matale District, Dambulla, NIFS Arboretum; 7.86011°N, 80.67441°E; 187m; 11-13-X-2019; Eberle, Bohacz & Ranasinghe leg.; Light sheet” ZFMK • 1 ♂; “X-SR1037, Sri Lanka, Matale District, Dambulla, NIFS Arboretum; 7.86011°N, 80.67441°E; 187m; 11-13-X-2019; Eberle, Bohacz & Ranasinghe leg.; Light sheet”; ZFMK.

Maladera iuga* Fabrizi & Ahrens, 2014*Material examined**

SRI LANKA • 1 ♂; “X-SR0543, Sri Lanka, Kandy District, Deenston, Knuckles South; 7.35771°N, 80.85006°E; 980m; 17-X-2019; Eberle, Bohacz & Ranasinghe leg.; Light sheet”; ZFMK • 1 ♂; “X-SR2000, Sri Lanka, Matale District, Dambulla, NIFS Arboretum; 7.58507°N, 80.74714°E; 399m; 24-VI- 2020 ; Ranasinghe &

Athukorala leg.; Black light”; ZFMK • 1 ♂; “X-SR2022, Sri Lanka, Matale District, Dambulla, NIFS Arboretum; 7.5845°N, 80.7472°E; 396m; 25-VI-2020 ; Ranasinghe, Athukorala & Jayatissa leg.; Black light”; ZFMK.

***Maladera laterita* (Moser, 1915)**

Material examined

SRI LANKA • 1 ♂; “X-SR0866, Sri Lanka, Matale District, Riverston, Pitawala Pathana; 7.54911°N, 80.75386°E; 880m; 15-X-2019; Eberle, Bohacz & Ranasinghe leg.; Black light”; ZFMK.

***Maladera mollis* (Walker, 1859)**

Material examined

SRI LANKA • 1 ♂; “X-SR2027, Sri Lanka, Matale District, Dambulla, NIFS Arboretum; 7.85783°N, 80.67391°E; 167m; 02-VII- 2020; Eberle, Ranasinghe & Athukorala leg.; Black light”; ZFMK.

***Maladera padaviyaensis* Ahrens & Fabrizi, 2016**

Material examined

SRI LANKA • 1 ♂; “X-SR1046, Sri Lanka, Matale District, Dambulla, NIFS Arboretum; 7.85766°N, 80.67474°E; 174m; 13-X-2019; Eberle, Bohacz & Ranasinghe leg.; Black light”;

ZFMK • 1 ♂; “X-SR1915, Sri Lanka, Matale District, Dambulla, NIFS Arboretum; 7.85796°N, 80.67554°E; 181m; 13-X-2019; Eberle, Bohacz & Ranasinghe leg.; Black light”; ZFMK.

***Maladera rufocuprea* (Blanchard, 1850)**

Material examined

SRI LANKA • 1 ♂; “X-SR0844, Sri Lanka, Galle District, Hiyare FR; 6.05871°N, 80.31538°E; 117m; 22-23-X-2019; Eberle, Bohacz & Ranasinghe leg.; Light sheet”;

ZFMK • 1 ♂; “X-SR0845, Sri Lanka, Galle District, Hiyare FR; 6.05871°N, 80.31538°E; 117m; 22-23-X-2019; Eberle, Bohacz & Ranasinghe leg.; Light sheet”;

ZFMK • 1 ♂; “X-SR0846, Sri Lanka, Galle District, Hiyare FR; 6.05871°N,

80.31538°E; 117m; 22-23-X-2019; Eberle, Bohacz & Ranasinghe leg.; Light sheet”; ZFMK • 1 ♂; “X-SR0847, Sri Lanka, Galle District, Hiyare FR; 6.05871°N, 80.31538°E; 117m; 22-23-X-2019; Eberle, Bohacz & Ranasinghe leg.; Light sheet”; ZFMK • 1 ♂; “X-SR0848, Sri Lanka, Galle District, Hiyare FR; 6.05871°N, 80.31538°E; 117m; 22-23-X-2019; Eberle, Bohacz & Ranasinghe leg.; Light sheet”; ZFMK • 1 ♂; “X-SR0849, Sri Lanka, Galle District, Hiyare FR; 6.05871°N, 80.31538°E; 117m; 22-23-X-2019; Eberle, Bohacz & Ranasinghe leg.; Light sheet”; ZFMK • 1 ♂; “X-SR0850, Sri Lanka, Galle District, Hiyare FR; 6.05871°N, 80.31538°E; 117m; 22-23-X-2019; Eberle, Bohacz & Ranasinghe leg.; Light sheet”; ZFMK • 1 ♂; “X-SR0851, Sri Lanka, Galle District, Hiyare FR; 6.05871°N, 80.31538°E; 117m; 22-23-X-2019; Eberle, Bohacz & Ranasinghe leg.; Light sheet”; ZFMK • 1 ♂; “X-SR0852, Sri Lanka, Galle District, Hiyare FR; 6.05871°N, 80.31538°E; 117m; 22-23-X-2019; Eberle, Bohacz & Ranasinghe leg.; Light sheet”; ZFMK • 1 ♂; “X-SR0853, Sri Lanka, Galle District, Hiyare FR; 6.05871°N, 80.31538°E; 117m; 22-23-X-2019; Eberle, Bohacz & Ranasinghe leg.; Light sheet”; ZFMK • 1 ♂; “X-SR0854, Sri Lanka, Galle District, Hiyare FR; 6.05871°N, 80.31538°E; 117m; 22-23-X-2019; Eberle, Bohacz & Ranasinghe leg.; Light sheet”; ZFMK • 1 ♂; “X-SR0529, Sri Lanka, Kandy District, Deenston, Knuckles South; 7.35771°N, 80.85006°E; 980m; 17-X-2019; Eberle, Bohacz & Ranasinghe leg.; Light sheet”; ZFMK • 1 ♂; “X-SR0530, Sri Lanka, Kandy District, Deenston, Knuckles South; 7.35771°N, 80.85006°E; 980m; 17-X-2019; Eberle, Bohacz & Ranasinghe leg.; Light sheet”; ZFMK • 1 ♂; “X-SR0531, Sri Lanka, Kandy District, Deenston, Knuckles South; 7.35771°N, 80.85006°E; 980m; 17-X-2019; Eberle, Bohacz & Ranasinghe leg.; Light sheet”; ZFMK • 1 ♂; “X-SR0532, Sri Lanka, Kandy District, Deenston, Knuckles South; 7.35771°N, 80.85006°E; 980m; 17-X-2019; Eberle, Bohacz & Ranasinghe leg.; Light sheet”; ZFMK • 1 ♂; “X-SR0533, Sri Lanka, Kandy District, Deenston, Knuckles South; 7.35771°N, 80.85006°E; 980m; 17-X-2019; Eberle, Bohacz & Ranasinghe leg.; Light sheet”; ZFMK • 1 ♂; “X-SR0569, Sri Lanka, Kandy District, Deenston, Knuckles South; 7.35771°N, 80.85006°E; 980m; 17-X-2019; Eberle, Bohacz & Ranasinghe leg.; Light sheet”; ZFMK • 1 ♂; “X-SR0570, Sri Lanka, Kandy District, Deenston, Knuckles South; 7.35771°N, 80.85006°E; 980m; 17-X-2019; Eberle, Bohacz & Ranasinghe leg.; Light sheet”; ZFMK • 1 ♂; “X-SR0571, Sri Lanka, Kandy District, Deenston, Knuckles South; 7.35771°N, 80.85006°E; 980m; 17-X-2019; Eberle, Bohacz & Ranasinghe leg.; Light sheet”; ZFMK • 1 ♂; “X-SR0752, Sri Lanka, Kandy District, Deenston, Knuckles South; 7.35771°N, 80.85006°E; 980m; 17-X-2019; Eberle, Bohacz & Ranasinghe leg.; Light sheet”; ZFMK • 1 ♂; “X-SR0753, Sri Lanka, Kandy District, Deenston,

Knuckles South; 7.35771°N, 80.85006°E; 980m; 17-X-2019; Eberle, Bohacz & Ranasinghe leg.; Light sheet”; ZFMK • 1 ♂; “X-SR0754, Sri Lanka, Kandy District, Deenston, Knuckles South; 7.35771°N, 80.85006°E; 980m; 17-X-2019; Eberle, Bohacz & Ranasinghe leg.; Light sheet”; ZFMK • 1 ♂; “X-SR0755, Sri Lanka, Kandy District, Deenston, Knuckles South; 7.35771°N, 80.85006°E; 980m; 17-X-2019; Eberle, Bohacz & Ranasinghe leg.; Light sheet”; ZFMK • 1 ♂; “X-SR0762, Sri Lanka, Kandy District, Deenston, Knuckles South; 7.35771°N, 80.85006°E; 980m; 17-X-2019; Eberle, Bohacz & Ranasinghe leg.; Light sheet”; ZFMK • 1 ♂; “X-SR0763, Sri Lanka, Kandy District, Deenston, Knuckles South; 7.35771°N, 80.85006°E; 980m; 17-X-2019; Eberle, Bohacz & Ranasinghe leg.; Light sheet”; ZFMK • 1 ♂; “X-SR0773, Sri Lanka, Kandy District, Deenston, Knuckles South; 7.35771°N, 80.85006°E; 980m; 17-X-2019; Eberle, Bohacz & Ranasinghe leg.; Light sheet”; ZFMK • 1 ♂; “X-SR0774, Sri Lanka, Kandy District, Deenston, Knuckles South; 7.35771°N, 80.85006°E; 980m; 17-X-2019; Eberle, Bohacz & Ranasinghe leg.; Light sheet”; ZFMK • 1 ♂; “X-SR0775, Sri Lanka, Kandy District, Deenston, Knuckles South; 7.35771°N, 80.85006°E; 980m; 17-X-2019; Eberle, Bohacz & Ranasinghe leg.; Light sheet”; ZFMK • 1 ♂; “X-SR0779, Sri Lanka, Kandy District, Deenston, Knuckles South; 7.35771°N, 80.85006°E; 980m; 17-X-2019; Eberle, Bohacz & Ranasinghe leg.; Light sheet”; ZFMK • 1 ♂; “X-SR0788, Sri Lanka, Kandy District, Deenston, Knuckles South; 7.35771°N, 80.85006°E; 980m; 17-X-2019; Eberle, Bohacz & Ranasinghe leg.; Light sheet”; ZFMK • 1 ♂; “X-SR0652, Sri Lanka, Matale District, Riverston, Pitawala Pathana; 7.5491115°N, 80.7538616°E; 880m; 15-X-2019; Eberle, Bohacz & Ranasinghe leg.; Black light”; ZFMK • 1 ♂; “X-SR0864, Sri Lanka, Matale District, Riverston, Pitawala Pathana; 7.5491115°N, 80.7538616°E; 880m; 15-X-2019; Eberle, Bohacz & Ranasinghe leg.; Black light”; ZFMK • 1 ♂; “X-SR0865, Sri Lanka, Matale District, Riverston, Pitawala Pathana; 7.5491115°N, 80.7538616°E; 880m; 15-X-2019; Eberle, Bohacz & Ranasinghe leg.; Black light”; ZFMK • 1 ♂; “X-SR0877, Sri Lanka, Matale District, Riverston, Pitawala Pathana; 7.54976°N, 80.75212°E; 902; 15-X-2019; Eberle, Bohacz & Ranasinghe leg.; Black light”; ZFMK • 1 ♂; “X-SR0878, Sri Lanka, Matale District, Riverston, Pitawala Pathana; 7.54976°N, 80.75212°E; 902; 15-X-2019; Eberle, Bohacz & Ranasinghe leg.; Black light”; ZFMK • 1 ♂; “X-SR1082, Sri Lanka, Matale District, Dambulla, NIFS Arboretum; 7.85783°N, 80.67391°E; 167m; 15-X-2019; Eberle, Bohacz & Ranasinghe leg.; Black light”; ZFMK.

Maladera setosa* (Brenske, 1896)*Material examined**

SRI LANKA • 1 ♂; “X-SR1024, Sri Lanka, Matale District, Dambulla, NIFS Arboretum; 7.85766°N, 80.67474°E; 174m; 12-13-X-2019; Eberle, Bohacz & Ranasinghe leg.; Black light”; ZFMK • 1 ♂; “X-SR1035, Sri Lanka, Matale District, Dambulla, NIFS Arboretum; 7.85766°N, 80.67474°E; 174m; 12-13-X-2019; Eberle, Bohacz & Ranasinghe leg.; Black light”; ZFMK • 1 ♂; “X-SR1047, Sri Lanka, Matale District, Dambulla, NIFS Arboretum; 7.85766°N, 80.67474°E; 174m; 12-13-X-2019; Eberle, Bohacz & Ranasinghe leg.; Black light”; ZFMK • 1 ♂; “X-SR0372, Sri Lanka, Matale District, Dambulla, NIFS Arboretum; 7.85783°N, 80.67391°E; 167m; 12-13-X-2019; Eberle, Bohacz & Ranasinghe leg.; Black light”; ZFMK • 1 ♂; “X-SR0457, Sri Lanka, Matale District, Dambulla, NIFS Arboretum; 7.85783°N, 80.67391°E; 167m; 12-13-X-2019; Eberle, Bohacz & Ranasinghe leg.; Black light”; ZFMK • 1 ♂; “X-SR0460, Sri Lanka, Matale District, Dambulla, NIFS Arboretum; 7.85783°N, 80.67391°E; 167m; 12-13-X-2019; Eberle, Bohacz & Ranasinghe leg.; Black light”; ZFMK • 1 ♂; “X-SR0465, Sri Lanka, Matale District, Dambulla, NIFS Arboretum; 7.85783°N, 80.67391°E; 167m; 12-13-X-2019; Eberle, Bohacz & Ranasinghe leg.; Black light”; ZFMK • 1 ♂; “X-SR1039, Sri Lanka, Matale District, Dambulla, NIFS Arboretum; 7.85783°N, 80.67391°E; 167m; 12-13-X-2019; Eberle, Bohacz & Ranasinghe leg.; Black light”; ZFMK • 1 ♂; “X-SR1052, Sri Lanka, Matale District, Dambulla, NIFS Arboretum; 7.85783°N, 80.67391°E; 167m; 12-13-X-2019; Eberle, Bohacz & Ranasinghe leg.; Black light”; ZFMK • 1 ♂; “X-SR0411, Sri Lanka, Matale District, Dambulla, NIFS Arboretum; 7.85796°N, 80.67554°E; 181m; 12-X-2019; Eberle, Bohacz & Ranasinghe leg.; Black light”; ZFMK • 1 ♂; “X-SR0450, Sri Lanka, Matale District, Dambulla, NIFS Arboretum; 7.85796°N, 80.67554°E; 181m; 12-X-2019; Eberle, Bohacz & Ranasinghe leg.; Black light”; ZFMK • 1 ♂; “X-SR1013, Sri Lanka, Matale District, Dambulla, NIFS Arboretum; 7.85824°N, 80.67506°E; 182m; 13-X-2019; Eberle, Bohacz & Ranasinghe leg.; Black light”; ZFMK • 1 ♂; “X-SR0405, Sri Lanka, Matale District, Dambulla, NIFS Arboretum; 7.86011766°N, 80.67441844°E; 187m; 11-X-2019; Eberle, Bohacz & Ranasinghe leg.; Black light”; ZFMK.

Maladera tricuspidata* Fabrizi & Ahrens, 2014*Material examined**

SRI LANKA • 1 ♂; “X-SR0326, Sri Lanka, Matale District, Dambulla, NIFS Arboretum; 7.85824°N, 80.67506°E; 182m; 13-X-2019; Eberle, Bohacz & Ranasinghe leg.; Black light”; ZFMK.

Maladera weligamana* (Brenske, 1900)*Material examined**

SRI LANKA • 1 ♂; “X-SR0815, Sri Lanka, Nuwara Eliya District, Hakgala SNR, Seetha Eliya; 6.9307°N, 80.8134°E; 1773m; 20-XI-2019; Ranasinghe & Athukorala leg.; Black light”; ZFMK • 1 ♂; “X-SR0835, Sri Lanka, Nuwara Eliya District, Hakgala SNR, Seetha Eliya; 6.93045°N, 80.81356°E; 1789m; 20-XI-2019; Ranasinghe & Athukorala leg.; Black light”; ZFMK.

Selaserica convexiuscula* Fabrizi & Ahrens, 2014*Material examined**

SRI LANKA • 1 ♂; “X-SR0858, Sri Lanka, Galle District, Kottawa FR; 6.09712°N, 80.3166°E; 49m; 26-X-2019; Eberle, Bohacz & Ranasinghe leg.; Black light”; ZFMK • 1 ♂; “X-SR2074, Sri Lanka, Galle District, Kottawa FR; 6.09712°N, 80.3166°E; 49m; 11-XII-2020; Ranasinghe & Athukorala leg.; Black light”; ZFMK.

Selaserica impexa* Fabrizi & Ahrens, 2014*Material examined**

SRI LANKA • 1 ♂; “X-SR0855, Sri Lanka, Galle District, Hiyare FR; 6.0587°N, 80.3153°E; 117m; 22-X-2019; Eberle, Bohacz & Ranasinghe leg.; Light sheet”; ZFMK • 1 ♂; “X-SR0856, Sri Lanka, Galle District, Kanneliya FR; 6.2509°N, 80.340130°E; 56m; 26-X-2019; Eberle, Bohacz & Ranasinghe leg.; Black light”; ZFMK • 1 ♂; “X-SR0857, Sri Lanka, Galle District, Kanneliya FR; 6.25013°N, 80.338°E; 42m; 26-X-2019; Eberle, Bohacz & Ranasinghe leg.; Black light”; ZFMK.

Selaserica nuwarana* Fabrizi & Ahrens, 2014*Material examined**

SRI LANKA • 1 ♂; “X-SR2058, Sri Lanka, Nuwara Eliya District, Hakgala SNR, Seetha Eliya; 6.9299°N, 80.81359°E; 1789m; 21-XII-2020; Ranasinghe & Athukorala leg.; Black light”; ZFMK • 1 ♂; “X-SR2099, Sri Lanka, Nuwara Eliya District, Hakgala SNR, Seetha Eliya; 6.93074°N, 80.81341°E; 1773m; 21-XII-2020; Ranasinghe & Athukorala leg.; Black light”; ZFMK.

Selaserica praetexta* Fabrizi & Ahrens, 2014*Material examined**

SRI LANKA • 1 ♂; “X-SR1973, Sri Lanka, Kandy District, Gannoruwa FR; 7.28329°N, 80.59819 °E; 528 m; 16-VII-2020; Ranasinghe & Athukorala leg.; Black light” ZFMK • 1 ♂; “X-SR1974, Sri Lanka, Kandy District, Gannoruwa FR; 7.28329°N, 80.59819 °E; 528 m; 16-VII-2020; Ranasinghe & Athukorala leg.; Black light” ZFMK • 1 ♂; “X-SR1975, Sri Lanka, Kandy District, Gannoruwa FR; 7.28329°N, 80.59819 °E; 528 m; 16-VII-2020; Ranasinghe & Athukorala leg.; Black light” ZFMK • 1 ♂; “X-SR2042, Sri Lanka, Kandy District, Gannoruwa FR; 7.28329°N, 80.59819 °E; 528 m; 15-VII-2020; Ranasinghe & Athukorala leg.; Black light” ZFMK • 1 ♂; “X-SR2208, Sri Lanka, Kandy District, Gannoruwa FR; 7.28329°N, 80.59819 °E; 528 m; 25-XI-2020; Ranasinghe & Athukorala leg.; Black light” ZFMK • 1 ♂; “X-SR2209, Sri Lanka, Kandy District, Gannoruwa FR; 7.28329°N, 80.59819 °E; 528 m; 25 Nov. 2020; Ranasinghe & Athukorala leg.; Black light” ZFMK • 1 ♂; “X-SR1972, Sri Lanka, Kandy District, Gannoruwa FR; 7.28342°N, 80.59840 °E; 592.5 m; 16-VII-2020; Ranasinghe & Athukorala leg.; Black light” ZFMK • 1 ♂; “X-SR2046, Sri Lanka, Kandy District, Gannoruwa FR; 7.28342°N, 80.59840 °E; 592.5 m; 14-VII-2020; Ranasinghe & Athukorala leg.; Black light” ZFMK • 1 ♂; “X-SR1970, Sri Lanka, Kandy District, Udawattakele FR; 7.29590°N, 80.64224°E; 16-VII-2020; Ranasinghe & Athukorala leg.; Black light”; ZFMK • 1 ♂; “X-SR2159, Sri Lanka, Kandy District, Udawattakele FR; 7.29690°N, 80.6448°E; 26-XI-2020; Ranasinghe & Athukorala leg.; Black light”; ZFMK • 1 ♂; “X-SR2160, Sri Lanka, Kandy District, Udawattakele FR; 7.29690°N, 80.6448°E; 27-XI-2020; Ranasinghe & Athukorala leg.; Black light”; ZFMK • 1 ♂; “X-SR2017, Sri Lanka, Matale District, Riverston, Pitawala Pathana, 7°55223°N, 80.75293°E, 888m; 24-VII-2020; Ranasinghe & Athukorala leg.; Black light”; ZFMK • 1 ♂; “X-SR2025,

Sri Lanka, Matale District, Riverston, Pitawala Pathana, 7°55223°N, 80.75293°E, 888m; 23 -VII-2020; Ranasinghe & Athukorala leg.; Black light”; ZFMK.

***Selaserica pusilla* Arrow, 1916**

Material examined

SRI LANKA • 1 ♂; “X-SR0654, Sri Lanka, Matale District, Riverston, Greenview lodge; 7.53804°N, 80.75027°E; 778m; 15-X-2019; Eberle, Bohacz & Ranasinghe leg.; Light sheet” ZFMK • 1 ♂; “X-SR0655, Sri Lanka, Matale District, Riverston, Greenview lodge; 7.53804°N, 80.75027°E; 778m; 15-X-2019; Eberle, Bohacz & Ranasinghe leg.; Light sheet” ZFMK • 1 ♂; “X-SR0656, Sri Lanka, Matale District, Riverston, Greenview lodge; 7.53804°N, 80.75027°E; 778m; 15-X-2019; Eberle, Bohacz & Ranasinghe leg.; Light sheet” ZFMK • 1 ♂; “X-SR0627, Sri Lanka, Matale District, Riverston, Pitawala Pathana; 7.54911N, 80.75386E; 880m; 15-X-2019; Eberle, Bohacz & Ranasinghe leg.; Black light” ZFMK • 1 ♂; “X-SR0631, Sri Lanka, Matale District, Riverston, Pitawala Pathana; 7.54911N, 80,75386E; 880m; 15-X-2019; Eberle, Bohacz & Ranasinghe leg.; Black light” ZFMK • 1 ♂; “X-SR0634, Sri Lanka, Matale District, Riverston, Pitawala Pathana; 7.54911N, 80.75386E; 880m; 15-X-2019; Eberle, Bohacz & Ranasinghe leg.; Black light” ZFMK • 1 ♂; “X-SR0635, Sri Lanka, Matale District, Riverston, Pitawala Pathana; 7.54911N, 80.75386E; 880m; 778m; 15-X-2019; Eberle, Bohacz & Ranasinghe leg.; Black light” ZFMK • 1 ♂; “X-SR0636, Sri Lanka, Matale District, Riverston, Pitawala Pathana; 7.54911N, 80.75386E; 880m; 778m; 15-X-2019; Eberle, Bohacz & Ranasinghe leg.; Black light” ZFMK • 1 ♂; “X-SR0637, Sri Lanka, Matale District, Riverston, Pitawala Pathana; 7.54911N, 80.75386E; 880m; 15-X-2019; Eberle, Bohacz & Ranasinghe leg.; Black light” ZFMK • 1 ♂; “X-SR0638, Sri Lanka, Matale District, Riverston, Pitawala Pathana; 7.54911N, 80.75386E; 880m; 15-X-2019; Eberle, Bohacz & Ranasinghe leg.; Black light” ZFMK • 1 ♂; “X-SR0639, Sri Lanka, Matale District, Riverston, Pitawala Pathana; 7.54911N, 80.75386E; 880m15-X-2019; Eberle, Bohacz & Ranasinghe leg.; Black light” ZFMK • 1 ♂; “X-SR0640, Sri Lanka, Matale District, Riverston, Pitawala Pathana; 7.54911N, 80.75386E; 880m; 15-X-2019; Eberle, Bohacz & Ranasinghe leg.; Black light” ZFMK • 1 ♂; “X-SR0641, Sri Lanka, Matale District, Riverston, Pitawala Pathana; 7,54911N, 80,75386E; 880m; 15-X-2019; Eberle, Bohacz & Ranasinghe leg.; Black light” ZFMK • 1 ♂; “X-SR0642, Sri Lanka, Matale District, Riverston, Pitawala Pathana; 7,54911N, 80,75386E; 880m; 15-X-2019; Eberle, Bohacz & Ranasinghe leg.; Black light” ZFMK • 1 ♂; “X-SR0643, Sri Lanka, Matale District, Riverston, Pitawala

Pathana; 7,54911N, 80,75386E; 880m; 15-X-2019; Eberle, Bohacz & Ranasinghe leg.; Black light” ZFMK • 1 ♂; “X-SR0644, Sri Lanka, Matale District, Riverston, Pitawala Pathana; 7,54911N, 80,75386E; 880m; 15-X-2019; Eberle, Bohacz & Ranasinghe leg.; Black light” ZFMK • 1 ♂; “X-SR0645, Sri Lanka, Matale District, Riverston, Pitawala Pathana; 7,54911N, 80,75386E; 880m; 15-X-2019; Eberle, Bohacz & Ranasinghe leg.; Black light” ZFMK • 1 ♂; “X-SR0650, Sri Lanka, Matale District, Riverston, Pitawala Pathana; 7,54911N, 80,75386E; 880m; 15-X-2019; Eberle, Bohacz & Ranasinghe leg.; Black light” ZFMK • 1 ♂; “X-SR0651, Sri Lanka, Matale District, Riverston, Pitawala Pathana; 7,54911N, 80,75386E; 880m; 15-X-2019; Eberle, Bohacz & Ranasinghe leg.; Black light” ZFMK • 1 ♂; “X-SR0671, Sri Lanka, Matale District, Riverston, Pitawala Pathana; 7,54911N, 80,75386E; 880m; 15-X-2019; Eberle, Bohacz & Ranasinghe leg.; Black light” ZFMK • 1 ♂; “X-SR0672, Sri Lanka, Matale District, Riverston, Pitawala Pathana; 7,54911N, 80,75386E; 880m; 15-X-2019; Eberle, Bohacz & Ranasinghe leg.; Black light” ZFMK • 1 ♂; “X-SR0673, Sri Lanka, Matale District, Riverston, Pitawala Pathana; 7,54911N, 80,75386E; 880m; 15-X-2019; Eberle, Bohacz & Ranasinghe leg.; Black light” ZFMK • 1 ♂; “X-SR0252, Sri Lanka, Matale District, Dambulla, NIFS Arboretum; 7.85766°N, 80.67474°E; 174m; 12-13-X-2019; Eberle, Bohacz & Ranasinghe leg.; Black light” ZFMK • 1 ♂; “X-SR0253, Sri Lanka, Matale District, Dambulla, NIFS Arboretum; 7.85766°N, 80.67474°E; 174m; 12-13-X-2019; Eberle, Bohacz & Ranasinghe leg.; Black light” ZFMK • 1 ♂; “X-SR0256, Sri Lanka, Matale District, Dambulla, NIFS Arboretum; 7.85766°N, 80.67474°E; 174m; 12-13-X-2019; Eberle, Bohacz & Ranasinghe leg.; Black light” ZFMK • 1 ♂; “X-SR0287, Sri Lanka, Matale District, Dambulla, NIFS Arboretum; 7.85766°N, 80.67474°E; 174m; 12-13-X-2019; Eberle, Bohacz & Ranasinghe leg.; Black light” ZFMK • 1 ♂; “X-SR0295, Sri Lanka, Matale District, Dambulla, NIFS Arboretum; 7.85766°N, 80.67474°E; 174m; 12-13-X-2019; Eberle, Bohacz & Ranasinghe leg.; Black light” ZFMK • 1 ♂; “X-SR0296, Sri Lanka, Matale District, Dambulla, NIFS Arboretum; 7.85766°N, 80.67474°E; 174m; 12-13-X-2019; Eberle, Bohacz & Ranasinghe leg.; Black light” ZFMK • 1 ♂; “X-SR0298, Sri Lanka, Matale District, Dambulla, NIFS Arboretum; 7.85766°N, 80.67474°E; 174m; 12-13-X-2019; Eberle, Bohacz & Ranasinghe leg.; Black light” ZFMK • 1 ♂; “X-SR0299, Sri Lanka, Matale District, Dambulla, NIFS Arboretum; 7.85766°N, 80.67474°E; 174m; 12-13-X-2019; Eberle, Bohacz & Ranasinghe leg.; Black light” ZFMK • 1 ♂; “X-SR0485, Sri Lanka, Matale District, Dambulla, NIFS Arboretum; 7.85766°N, 80.67474°E; 174m; 12-13-X-2019; Eberle, Bohacz & Ranasinghe leg.; Black light” ZFMK • 1 ♂; “X-SR0487, Sri Lanka, Matale District, Dambulla, NIFS Arboretum; 7.85766°N, 80.67474°E; 174m; 12-13-X-2019;

Eberle, Bohacz & Ranasinghe leg.; Black light” ZFMK • 1 ♂; “X-SR0504, Sri Lanka, Matale District, Dambulla, NIFS Arboretum; 7.85766°N, 80.67474°E; 174m; 12-13-X-2019; Eberle, Bohacz & Ranasinghe leg.; Black light” ZFMK • 1 ♂; “X-SR0505, Sri Lanka, Matale District, Dambulla, NIFS Arboretum; 7.85766°N, 80.67474°E; 174m; 12-13-X-2019; Eberle, Bohacz & Ranasinghe leg.; Black light” ZFMK • 1 ♂; “X-SR0506, Sri Lanka, Matale District, Dambulla, NIFS Arboretum; 7.85766°N, 80.67474°E; 174m; 12-13-X-2019; Eberle, Bohacz & Ranasinghe leg.; Black light” ZFMK • 1 ♂; “X-SR0507, Sri Lanka, Matale District, Dambulla, NIFS Arboretum; 7.85766°N, 80.67474°E; 174m; 12-13-X-2019; Eberle, Bohacz & Ranasinghe leg.; Black light” ZFMK • 1 ♂; “X-SR0508, Sri Lanka, Matale District, Dambulla, NIFS Arboretum; 7.85766°N, 80.67474°E; 174m; 12-13-X-2019; Eberle, Bohacz & Ranasinghe leg.; Black light” ZFMK • 1 ♂; “X-SR0509, Sri Lanka, Matale District, Dambulla, NIFS Arboretum; 7.85766°N, 80.67474°E; 174m; 12-13-X-2019; Eberle, Bohacz & Ranasinghe leg.; Black light” ZFMK • 1 ♂; “X-SR0998, Sri Lanka, Matale District, Dambulla, NIFS Arboretum; 7.85766°N, 80.67474°E; 174m; 12-13-X-2019; Eberle, Bohacz & Ranasinghe leg.; Black light” ZFMK • 1 ♂; “X-SR0999, Sri Lanka, Matale District, Dambulla, NIFS Arboretum; 7.85766°N, 80.67474°E; 174m; 12-13-X-2019; Eberle, Bohacz & Ranasinghe leg.; Black light” ZFMK • 1 ♂; “X-SR1021, Sri Lanka, Matale District, Dambulla, NIFS Arboretum; 7.85766°N, 80.67474°E; 174m; 12-13-X-2019; Eberle, Bohacz & Ranasinghe leg.; Black light” ZFMK • 1 ♂; “X-SR1033, Sri Lanka, Matale District, Dambulla, NIFS Arboretum; 7.85766°N, 80.67474°E; 174m; 12-13-X-2019; Eberle, Bohacz & Ranasinghe leg.; Black light” ZFMK • 1 ♂; “X-SR1048, Sri Lanka, Matale District, Dambulla, NIFS Arboretum; 7.85766°N, 80.67474°E; 174m; 12-13-X-2019; Eberle, Bohacz & Ranasinghe leg.; Black light”; ZFMK.

***Serica lurida* Brenske, 1898**

Material examined

SRI LANKA • 1 ♂; “X-SR0591, Sri Lanka, Matale District, Riverston, Pitawala Pathana, 7°55223°N, 80.75293°E, 888m; 15-X-2019; Eberle, Bohacz & Ranasinghe leg.; Black light”; ZFMK • 1 ♂; “X-SR0615, Sri Lanka, Matale District, Riverston, Pitawala Pathana, 7°55223°N, 80.75293°E, 888m; 15-X-2019; Eberle, Bohacz & Ranasinghe leg.; Black light”; ZFMK • 1 ♂; “X-SR0616, Sri Lanka, Matale District, Riverston, Pitawala Pathana, 7°55223°N, 80.75293°E, 888m; 15-X-2019; Eberle, Bohacz & Ranasinghe leg.; Black light”; ZFMK • 1 ♂; “X-SR0617, Sri Lanka, Matale District, Riverston, Pitawala Pathana, 7°55223°N, 80.75293°E, 888m; 15-X-

light”; ZFMK • 1 ♂; “X-SR0913, Sri Lanka, Matale District, Riverston, Pitawala Pathana, 7°55223°N, 80.75293°E, 888m; 15-X-2019; Eberle, Bohacz & Ranasinghe leg.; Black light”; ZFMK • 1 ♂; “X-SR0914, Sri Lanka, Matale District, Riverston, Pitawala Pathana, 7°55223°N, 80.75293°E, 888m; 15-X-2019; Eberle, Bohacz & Ranasinghe leg.; Black light”; ZFMK.

6.4 Discussion

Although the sampling was mainly carried out at the same sites as in the first expedition (Ranasinghe *et al.*, 2020), we still found different species within the assemblages, that had not been previously collected at the same site. This might be due to seasonal change, as sampling was performed in both dry and wet seasons. However, more thorough conclusions regarding temporal turnover of Sericini assemblages would need long-term observation, and these data are analysed in a separate paper, focussing particularly on the synecology of the species in relation to their habitat. The study once more revealed a large amount of endemism, confirmed that Sri Lanka remains unexplored, and that night active chafers are still rather poorly represented in material from occasional, non-specialized field surveys.

Acknowledgements

Fieldwork for this study was fully funded by institutional funds of the ZFMK and by the German Academic Exchange Service (DAAD). S.R. was funded by the DAAD; N.A. and S.P.B. were funded by the NIFS. We are thanking to C. Bohacz (ZFMK), D. Boppearachchi, A. Sathkunanathan, M. Tharmarajan, C. Jayatissa and S. Wijesundara of the NIFS for their support in the field and lab. Further, we are grateful to Prof. S. Wijesundara and Mr. C. Lekamge for providing facility in the NIFS Arboretum. Thanks to Mr. Madhura de Silva and Mr. Sampath for providing facility in the Hiyare Conservation Center. Furthermore, we are thankful to all Wildlife Rangers (Nuwara Eliya, Hiyare, Horton Plains), Regional forest officers (Kandy, Knuckles, Nuwara

Eliya, Kottawa, Kanneliya) who helped us to conduct fieldwork. S.P.B. thanks to the Department of Wildlife Conservation, Sri Lanka (permit no: WL/3/2/61/18), the Department of Forest Conservation, Sri Lanka (permit no: R&E/RES/NFSRCM/2019-01 & R&E/RES/NFSRCM/EXTENSION/2020), the Divisional Forest Office, Kandy, Sri Lanka (permit no: K/G/01/06/03) for providing research and collection permits.

6.5 References

- Ahrens, D. & Fabrizi, S. (2016). A Monograph of the Sericini of India (Coleoptera: Scarabaeidae). *Bonn Zoological Bulletin*, 65, 1–355.
- Fabrizi, S. & Ahrens, D. (2014). A Monograph of the Sericini of Sri Lanka (Coleoptera: Scarabaeidae). *Bonn Zoological Bulletin, Supplements*, 61, 1–124.
- Ranasinghe, S., Eberle, J., Benjamin, S.P. & Ahrens, D. (2020). New species of Sericini from Sri Lanka (Coleoptera, Scarabaeidae). *European Journal of Taxonomy*, 621, 1–20.

Chapter 7

Chorological scale and lineage shape the correlation between morphospace disparity and species diversity in phytophagous scarab beetles

This chapter is submitted to *Journal of Biogeography*

Ranasinghe U.G.S.L., Eberle J, Benjamin S.P., Ahrens D. (submitted).
Chorological scale and lineage shape the correlation between disparity and diversity in phytophagous scarab beetles. JBI-22-0296

Authors' contributions to the original article:

SR, JE, SB: fieldwork collections; SR: morphometric measurements and analyses,
SR, DA: writing-original draft; DA, JE, SB, SR: manuscript review and editing.

Abstract

Evolutionary success of lineages becomes visible by species diversity or morphological disparity, but the link between both phenomena is poorly investigated for invertebrates, particularly considering various ecochorological scales. Here, we explore multiple tropical assemblages of phytophagous scarab beetles (Coleoptera: Scarabaeidae) in Sri Lanka and infer their pattern of morphospace and species diversity along forest types, elevation zones, and collection sites. Morphospace including disparity was analysed using linear distances measurements partitioned for three major lineages: 1) the entire assemblage, and two sister subclades, 2) Sericini, and 3) Pleurostictis excluding Sericini. The relation disparity versus species diversity followed two distinctive patterns, one for the entire assemblage and Pleurostictis excluding Sericini, and one for Sericini. For the first we found a significant correlation between diversity and disparity between different forest types and elevation zone with size-corrected data. The opposite was the case for the different sampling locations in which Sericini showed significance, however, the other two lineages not. For uncorrected raw data this tendency was similar, but less pronounced. These patterns were corroborated by body size variation of the entire assemblage which was observed to shrink towards higher altitudes with the general decrease of species diversity and morphological disparity.

7.1 Introduction

Evolutionary success of lineages becomes visible by species diversity or morphological disparity (Guillerme et al., 2020). However, the two phenomena are not necessarily correlated (Ricklefs, 2012; Hopkins, 2013). High diversity may be associated with high or low morphological disparity (Minelli, 2016; Simões et al., 2016), as can be low diversity. The informative value of disparity on the evolutionary performance of organisms has been frequently investigated in palaeontology (Heard & Hauser, 1995; Romano et al., 2017; Deline et al., 2018; Romano, 2019), since discordance between taxonomic and morphological diversity is also apparent over evolutionary timescales (Roy et al., 2004). Recent studies of disparity specifically captured factors that affect morphological evolution (Guillerme et al., 2020). Recognizing morphological differentiation in

response to adaptation or in relation to rates of molecular evolution helps to understand macroevolution of lineages, e.g., in respect of morphological key innovations (Heard & Hauser, 1995; Eberle et al., 2014; Simões et al., 2016; Hopkins and Gerber, 2017; Nel et al., 2018). It has been shown that phylogenetic sampling affects the evolutionary patterns of morphological disparity, at least when being based on cladistic character matrices (Smith et al., 2021). Macroevolutionary patterns are expected to be expressed in species assemblies at various geographical scales (Jönsson et al., 2015) and particularly at community level (Ribera et al., 2001; Inward et al., 2011), where direct competition and stress occur. At different chorological scales, patterns are not necessarily the same (Ricklefs, 2012). Due to “environmental filtering”, co-occurring species are likely to share traits that enable them to persist in a defined environment. On the other hand, disparity in key ecological traits between sympatric species allows them to coexist (Cardillo et al., 2008, García-Navas, 2019).

Species richness is likely to increase the density of morphospace occupation (Jönsson et al., 2015; Triantis et al., 2016). Observed diversity across spatial scales is the result of speciation and local interactions between species, primarily of competition for shared resources (Ricklefs, 2012). Tropical regions harbour many more species than temperate regions. Diverse rainforests with high structural complexity possess a high number and variety of available niches allowing the extensive co-existence of taxa with divergent functional traits (García-Navas, 2019). Studies on vertebrates suggest a general tendency for the morphospace volume to increase with taxonomic diversity, while disparity within defined lineages tends not to vary with richness, even for tropical-temperate comparisons (Shepherd, 1998; Roy et al., 2004). However, there have been few studies on this to date, and these focused on large-scale spatial patterns of taxonomic richness vs morphological diversity, with only sparse reference to local phenomena (Ricklefs, 2012).

Extant invertebrates have been rarely studied in this context, especially in tropical regions (Triantis et al., 2016) and in the context of disparity vs. diversity, and if so, often only body size rather than disparity was investigated (Brehm et al., 2019; Salomão et al., 2021). Since their diversity is by several dimensions higher, invertebrates are particularly suitable to test findings so far reported, mainly from vertebrates. Therefore, we explore here multiple assemblages of tropical phytophagous scarab beetles (Coleoptera: Scarabaeidae) and infer their pattern of morphospace and species diversity along various spatial and ecological scales. Phytophagous scarabs are a monophyletic clade (Ahrens et al., 2014; McKenna et al., 2019) which so far is referred to as "pleurostict chafers" or Pleurostictics (Ritcher, 1958; Ahrens et al., 2014). Pleurostictics are a very diverse group of some

30,000 species, which rapidly diversified during the Late Cretaceous – Early Paleogene. Adults feed unspecifically on leaves of angiosperm plants (Ahrens et al., 2014), while larvae feed on humus and roots (Ritcher 1958). The causes for their high diversity are yet poorly understood (Ahrens et al., 2014; Eberle et al., 2014).

Body size and shape variation (i.e., morphospace) are assumed to reflect differences in the species ecology and behaviour (Inward et al., 2011; Eberle et al., 2014). Morphospace reflects at global scale the general niche occupation of phytophagous scarab lineages (Pleurosticti) according to their different microhabitats and foraging behaviour (Eberle et al., 2014). However, since single lineages showed only little divergence and sampling was not yet considering local assemblages, it remained obscure whether direct competition between species occurred (Eberle et al., 2014). We addressed this by investigating the morphospace, disparity, and species diversity in 14 different local assemblages in Sri Lanka along an altitudinal and ecological gradient in the light of chorological scale. At three major levels of chorological and landscape partition from regional to local scale, represented by forest types, elevation zones, and collection sites, we attempt to quantify the effect of direct competition among species by investigating local-scale vs. higher spatial scale patterns of the assemblages. We expect the morphospace of the co-occurring species to generally not overlap when competition occurs. In absence of direct competition, we expect a link between disparity and species diversity and thus a positive correlation at chorological and ecological levels.

7.2 Materials and Methods

Specimens sampling

The studied species assemblage included all pleurostict chafers (Coleoptera: Scarabaeidae) that were sampled during four field campaigns in Sri Lanka. This tropical island is a highly suitable study area, with its topographic, climatic, and vegetational diversity. Standardized sampling at 14 localities (L1–L14) covered almost all major biomes, altitudinal zones (0–2500m) and different forest types (Table S7.1, Figure 7.1). One locality (L7) was excluded from final analysis, as it could not be sampled with the same frequency. We operated six UV-light traps per locality. In total, 60–72 sampling events were conducted in each location during both rainy and dry seasons. Specimens were sorted to morphospecies based

on genital morphology using available taxonomic literature (Fabrizi & Ahrens, 2014; Ranasinghe et al., 2020).

Morphometric analysis and morphological disparity

Disparity may be assessed by qualitative characters or quantitative approaches (body shape / morphospace) (Nel et al., 2018; Guillerme et al., 2020). For compatibility with Eberle et al. (2014), we measured twenty linear distances (Figure 7.2) of 384 adult specimens from 105 species (Table S7.2). Measurements were taken directly from specimens using an ocular grid on a Wild M3Z stereomicroscope.—Generally, the major component of variance in distance measurements is explained through size (Jolicoeur, 1963; Eberle et al., 2014). Therefore, we have done additional analyses that were corrected for size by log₁₀ transformation (Mosimann & James, 1979) to render more linear relations among variables and to obtain a similar dimension of variance (Ricklefs et al., 1981; Klingenberg, 1996). Patterns of morphometric covariation were analysed with principal component analysis (PCA) on raw and log-normalized data. Morphospace disparity was calculated using PC loadings which represent >95% cumulative variation.

Morphospace and disparity were analysed separately for three different monophyletic lineages: 1) the entire assemblage (i.e., all Pleurostictids), 2) for Sericini only, and 3) for Pleurostictids excluding Sericini (i.e., other Pleurostictids). The latter two lineages are sister clades (Ahrens et al., 2014; McKenna et al., 2019) being treated here separately to explore the impact of lineage choice (Smith et al., 2021). Analyses were partitioned for three major chorological and landscape entities (from regional to local scale) based on 1) forest type, 2) elevation zone, and 3) sampling locality. Forest types included four entities: a) evergreen wet lowland forests, b) evergreen dry lowland forests, c) sub-montane forests, and d) montane forests. Elevation was partitioned in five units: EZ1: 0–500m, EZ2: 501–1000m, EZ3: 1001–1500m, EZ4: 1501–2000m, and EZ5: 2001–2500m. At locality-level, morphospace occupation referred to actually co-occurring species. Disparity was calculated as the mean and median of pairwise Euclidean distances among species from resulting PC axes representing 95% of cumulative morphospace variation for each of the three landscape partitions. The outcome was compared with species' total body length (sum of pronotal and elytral length).

Finally, MANOVA was performed on principal components that explained 95% of total variation of subsets for each partition applying sequential Bonferroni

correction. All analyses were done in PAST v. 3.25 (Hammer et al., 2001). Finally, we assessed the Pearson coefficient between mean disparity and species diversity for lineages and landscape partitions.

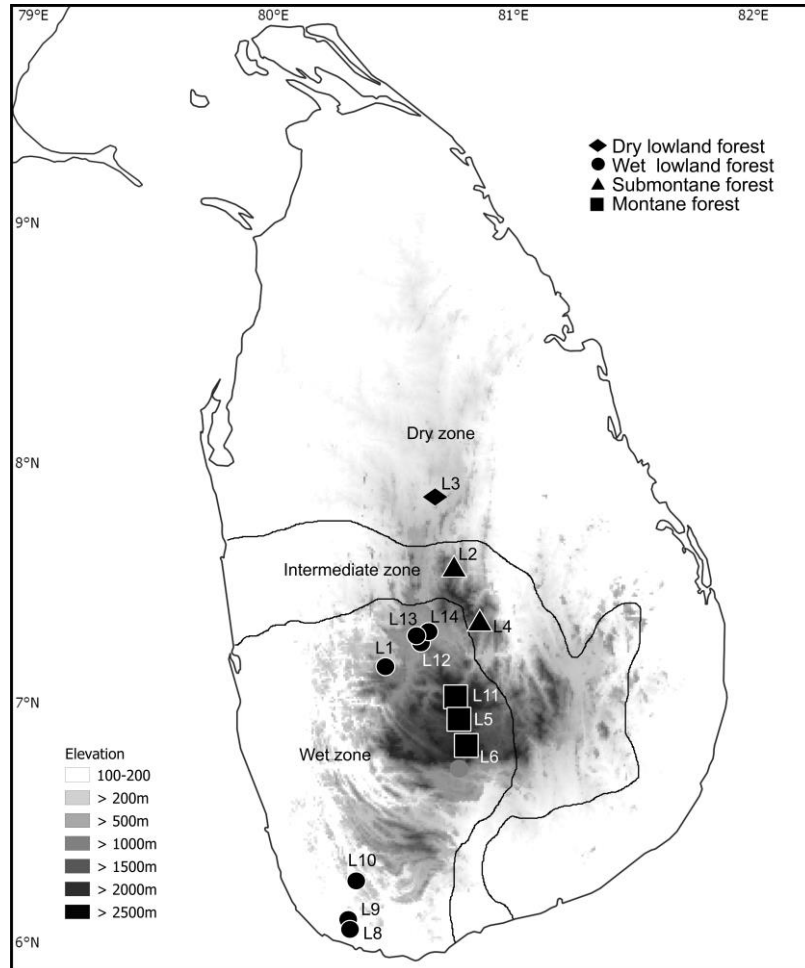


Figure 7.1. Map illustrating the location of sampling sites. L1: Aranayake; L2: Riverston; L3: NIFS Arboretum; L4: Deenston; L5: Nuwara Eliya; L6: Horton Plains; L8: Hiyare; L9: Kottawa; L10: Kanneliya; L11: Pidurutalagala; L12: Uda Peradeniya; L13: Gannoruwa; L14: Udawattakele. Symbols represent different forest types; evergreen wet lowland forest, evergreen dry lowland forest, sub-montane, montane forests.

7.3 Results

Species diversity strongly varied among localities but generally declined from wet lowland forest to montane forest and from the lowest elevation zone to the highest (Figure 7.3). All assemblages included herbivore Rutelinae, Melolonthinae and Dynastinae (Table S7.2) but not floricolous diurnal species (e.g., Cetoniinae).

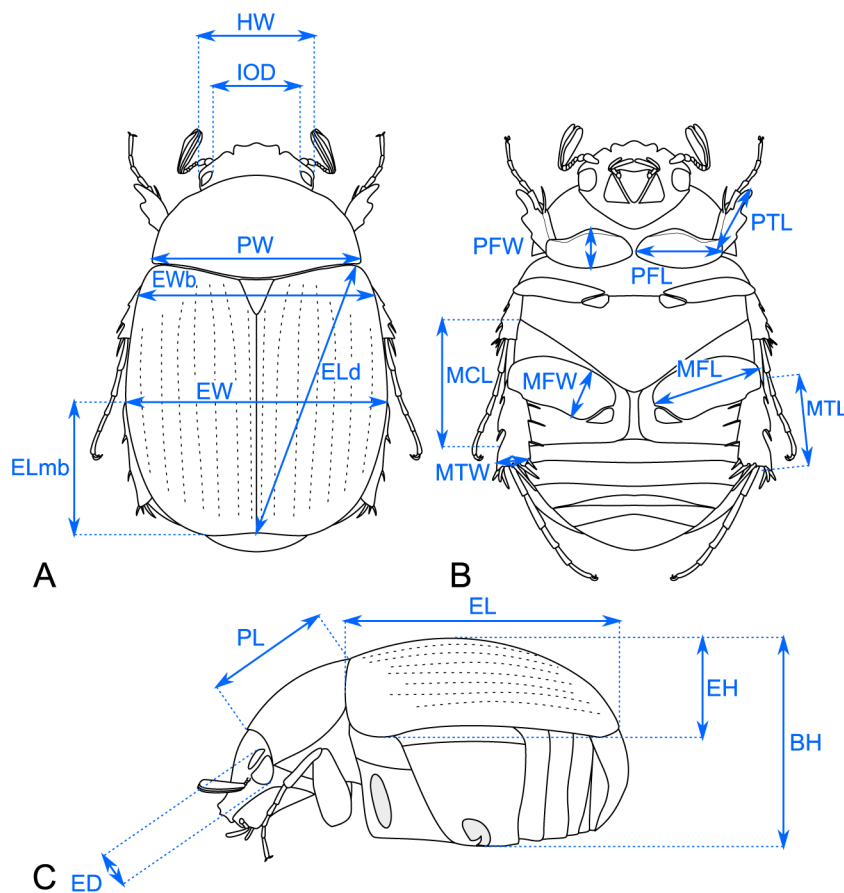


Figure 7.2. Illustration of the measured morphological traits (after Eberle et al., 2014). Schematic drawings of a Sericini beetle, in (A) dorsal, (B) ventral, and (C) lateral aspect. Body: BH - maximal body height, EH - maximal elytra height, EL - maximal elytra length, ELd - maximal diagonal elytra length, ELmb - length from maximal body width to elytral apex, EW - maximal elytra width, EWb - elytral width at middle of scutellum, PL - maximal pronotum length, PW - maximal pronotum width; Head: ED - maximal eye diameter, HW - maximal head with including eyes, IOD - minimal interocular distance (dorsal view); Legs: MCL - maximal length of metacoxa, MFL - maximal length of metafemur, MFW - maximal width of metafemur, MTL - maximal length of metatibia, MTW - maximal width of metatibia, PFL - maximal length of profemur, PFW - maximal width of profemur, PTL - maximal length of protibia.

A minimum of 95% of the cumulative variation was represented by PC axis 1 (96.9%) for raw data, and by PC 1 and 2 for log-normalized data (86.8% and 7.18%, respectively) (Table S7.3). Plots of PC 1 and 2 confirmed major morphospace divergence between principal pleurostict lineages while species of diverse groups (Sericini, Adoretini) overlapped. Among all traits, particularly body length and size of metacoxa contributed to divergence of morphospace (Figure S7.3). Body length variation considerably differed between localities, among generally smaller Sericini (4–13 mm) it was rather constant. It was higher in wet lowland forests than any other forest type (Figure 7.3) and slightly diminishing with increasing elevation except in Sericini.

Morphospace divergence and morphospace occupancy followed two distinctive patterns, one for the entire assemblage and Pleurosticts excluding Sericini, and one for Sericini. Divergence between species was generally reduced with size-corrected data (Figures 7.3, S7.4), for Sericini it was the opposite. The morphospace volume of the assemblages decreased from wet lowland forests, to dry lowland forest, submontane forest, and montane forest (Figures 7.4A, S7.4A). Montane forest species occupied less than a quarter of the entire morphospace. The speciose Sericini again contrasted these patterns for forest types and elevation zones. Their morphospace was more restricted and species of different forest types and elevation zones partly overlapped considerably (Figure 7.4B, E). Overlap was more pronounced with raw data (Figure 7.4B, E). Pleurosticts without Sericini showed similar patterns for forest types and elevation zones as all Pleurosticts (Figure 7.4C, F vs. 7.4A, D). No differences were observed between the highest elevation zones (EZ4, EZ5) representing montane forest. Individual localities (Figure S7.5a) revealed for the entire assemblage a generally limited overlap in species' morphospace, while strong overlap occurred, also in Sericini (Figure S7.5b), in some species-rich localities. Disparity for all lineages, except Sericini, was similar between raw and log-normalized data, with highest mean and median values for the wet lowland forest (Figure 7.3A; Tables S7.4, S7.5), and a general drop from lowland to montane forest and/or higher elevations. In Sericini disparity was almost constant but rather low.

MANOVAs on partitioned PC scores of entire assemblages showed significant differences for log-normalized data, but differences were not significant between sub-montane and wet lowland forest, and between dry lowland and montane forest. Also highest elevation zones (EZ 4 vs 5) and lower elevation zones (EZ 1 vs 2/3, EZ 2 vs 3) showed no significant morphospace differences (Table S7.8). Sericini and Pleurosticts excluding Sericini showed no significance (Table S7, S8); the morphospace of the latter only significantly differed in EZ 5 from all other elevation zones.

Disparity partitioned by localities (Table S7.6, Figure 7.3C, F), revealed again outstanding patterns of Sericini, where localities of montane forest (L5, L6, L11) were distinct from all other. Here, MANOVA revealed maximal 25% of pairwise locality comparisons of normalized morphospace data to be significant (Tables S7.9, S7.10), for raw data even 50-90% less (and no significance for Pleurosticts excluding Sericini).

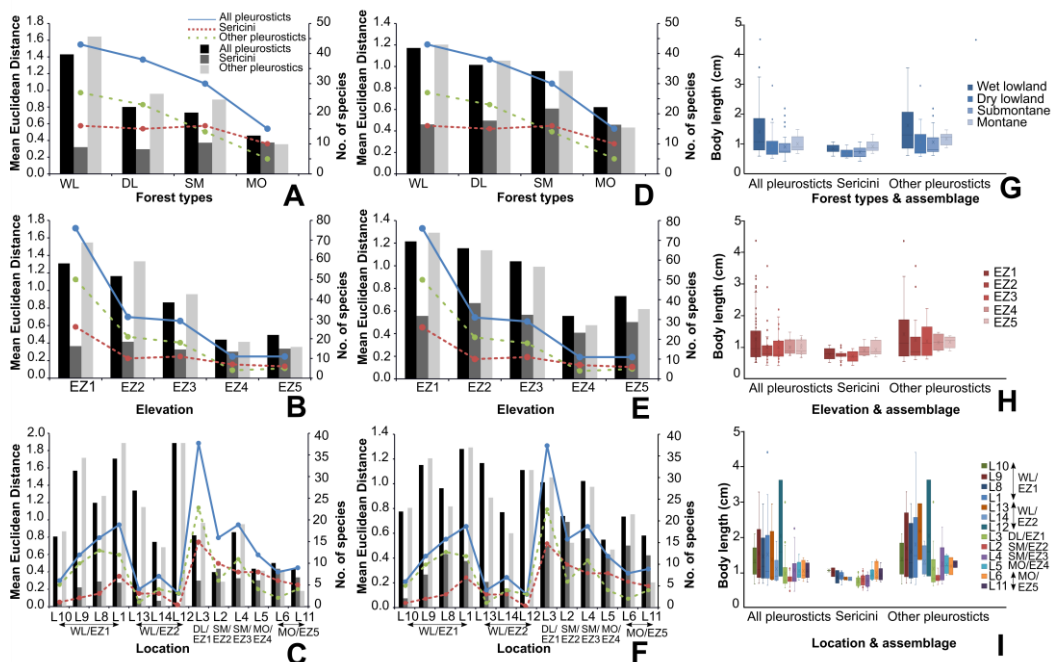


Figure 7.3. Lineage-specific disparity (A-F; mean Euclidean distances) and body size variation (G-I) for the entire assemblages (all Pleurosticts), Sericini, and other Pleurosticts (excluding Sericini) partitioned by forest type (A,D,G), elevation (B, E, H), and location (C, F, I) based on raw data (A, B, C) or log-normalized data (D, E, F). Species numbers of lineages are shown by line graphs (A-F).

The relation of disparity versus species diversity followed again two distinctive patterns, one for the entire assemblage and Pleurosticts excluding Sericini, and another one for Sericini. For log-normalized data we found a significant correlation between diversity and disparity between different forest types and elevation zones, for all Pleurosticts and for Pleurosticts excluding Sericini, for elevation zones only for the latter (Table 7.1). The opposite was observed for sampling locations, for which only Sericini showed significant correlation. For uncorrected raw data this tendency was similar, but less pronounced, and generally not sufficiently clear to result significant.

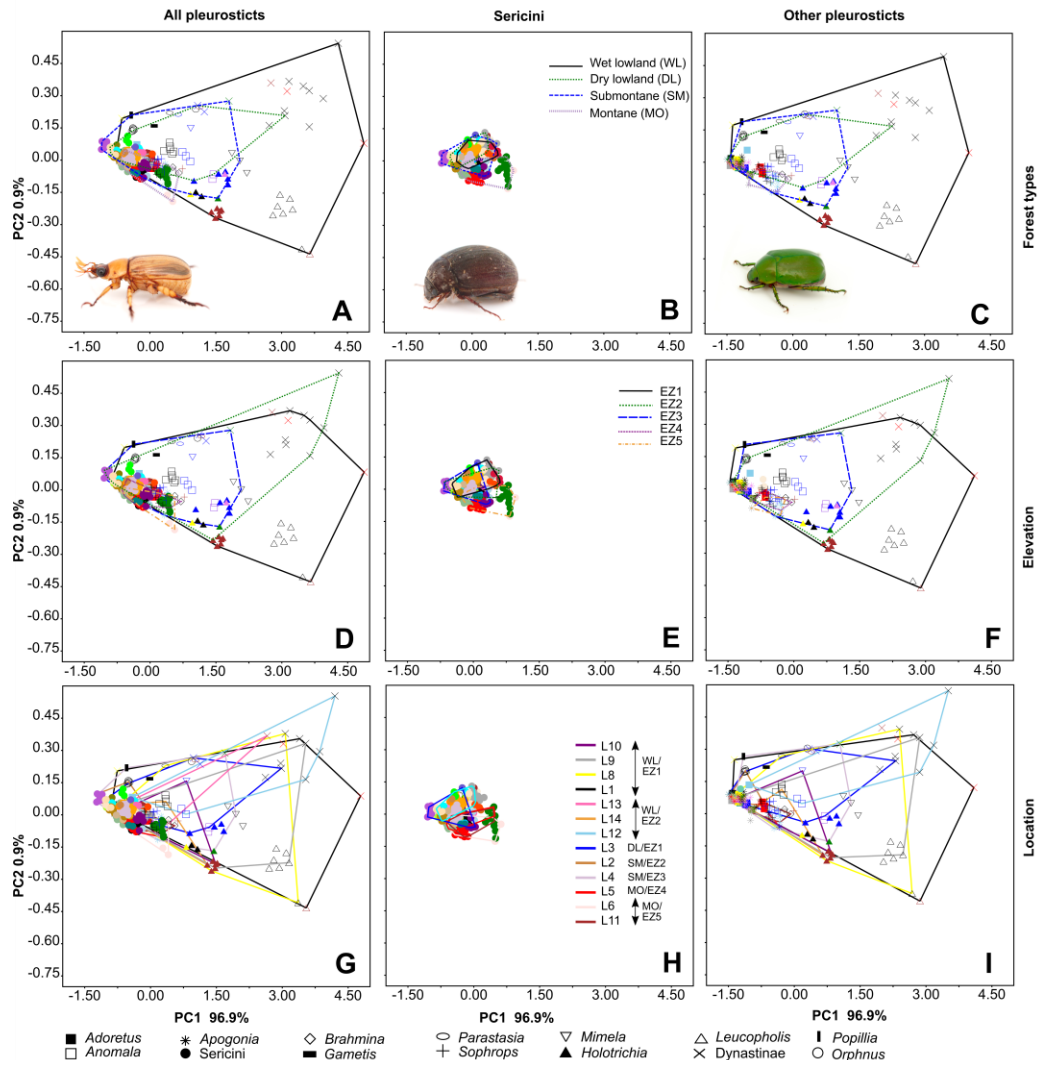


Figure 7.4. Patterns of morphospace disparity (plots of PC1 and 2) derived from raw measurements of pleurostict chafer assemblages (all Pleurosticts (A, D, G), Sericini (B, E, H), other Pleurosticts (C, F, I)) partitioned for forest types (A, B, C), elevation (D, E, F), and localities (G, H, I). Symbols represent genus or other family-group level, colour of symbols single species, outlines group points according to unique forest types, elevation zones or localities.

Table 7.1 Pearson correlation between the mean disparity (derived from raw and size reduced data) and species diversity for the entire assemblage (Pleurostictids all), Sericini, and Pleurostictids excluding Sericini* (partitioned by forest types, elevation zones, and localities). Significant correlation coefficients ($p < 0.05$) are printed in bold.

	Raw data		Log-normal data	
	r	p	r	p
Forest type				
<i>Pleurostictids (All)</i>	0.828	0.172	0.992	0.008
<i>Sericini</i>	-0.267	0.734	0.841	0.159
<i>Pleurostictids (part)*</i>	0.915	0.085	0.984	0.016
Elevation zone				
<i>Pleurostictids (All)</i>	0.875	0.052	0.810	0.097
<i>Sericini</i>	-0.099	0.874	0.261	0.672
<i>Pleurostictids (part)*</i>	0.902	0.036	0.890	0.043
Location				
<i>Pleurostictids (All)</i>	-0.127	0.680	0.164	0.592
<i>Sericini</i>	0.651	0.016	0.774	0.002
<i>Pleurostictids (part)*</i>	0.280	0.355	0.445	0.128

7.4 Discussion

Our results, for the first time, corroborated a general correlation between morphological disparity and species richness among phytophagous chafers at different ecochorological scales showing contrasting patterns of lineages at different geographical scale. The volume of morphospace that is occupied by lineages is supposed to mirror the heterogeneity of the species' ecological niches and may thus indicate resource partitioning and competition (Inward et al., 2011). While at larger geographical scales the relation of species diversity vs. disparity is determined by the historical integration of a multitude of species or lineages, at local scale assembled species compete for space and resources. If competition occurs, we may expect an alteration between higher-scale chorological patterns (i.e., regional) versus local patterns which is what we observed here with the phytophagous chafer assemblages.

We interpret the decreasing variation of morphospace and body size with increasing elevation along associated forest types as reduced ecological niche space in which generally less species co-occur (Figure 7.3). However, in contrast to other Pleurostictids, Sericini showed almost constant size of morphospace clusters across all landscape partitions, as well as almost constant disparity and less pronounced altitude-related decrease of diversity (Figures 7.3, 7.4). Sericini together with their Afrotropical sister lineage Ablaberini form the sister clade to all other Pleurostictids (Ahrens et al., 2014; Eberle et al., 2017; McKenna et al., 2019), therefore, the lineage incongruity in morphospace disparity cannot be explained by different group ages. High species numbers of Sericini in particular also at higher elevations reflect their evolutionary success (Ahrens, 2004) in contrast to most other phytophagous Pleurostictids. This success might be linked to adaptation to lower temperatures, for example by reduced size or optimized digging mechanics and behaviour, which is reflected also in morphospace (Eberle et al., 2014). This is linked with similar body size contrasts of lineages along the elevational gradients which extends Horne et al.'s (2018) hypothesis that temperature–body size trends of insect across altitudes are not stringent (but sometimes present). Increased size in scarab chafers is generally linked with significantly longer larval development: smaller species may have bivoltine cycles (Ahrens et al., 2009), whereas larger species may have a 2- or 3-year life cycle (Ritcher, 1958). Deviation from highly successful adaptations like faster development is likely to result in reduced fitness of the species. Therefore, body shape and size can become conserved, resulting in a narrow and constant morphospace occupation. Consequently, local scale patterns of disparity among Sericini (Figure S7.5b) go hand in hand with higher species diversity. On the other hand, evolutionary key innovations in Sericini such as the metacoxal enlargement or the modification of the elytral base (Eberle et al., 2014; Pacheco et al., 2022), might have catalysed evolutionary change in other traits such as weight reduction in Sericini (Ahrens, 2006; Eberle et al., 2014), so that directed selection and competition would be triggered in multiple dimensions along a complex evolutionary pathway.

Polyphagous herbivory and virtually unlimited food resources in a tropical forest are supposed to exclude interspecific competition and to facilitate a similar ecology of many species, particularly in Sericini (Eberle et al., 2014). Thus, competition for food seems unsuited to explain divergence in morphospace of Pleurostictids discussed here or earlier (Eberle et al., 2014). However, striking morphospace divergence between pairs of sister lineages of Pleurostictids with divergent feeding habits revealed that strong directed selection on morphospace was linked with resource partitioning although being catalysed principally by

other factors such as feeding related locomotion behaviour (Eberle et al., 2014). This is also known from dung beetles for which resource competition and partitioning is very well documented (Inward et al., 2011), also in connection with parental care and reported parallelisms are a major indicator for selection pressure (Emlen & Philips, 2006). Thus, from the shift of disparity patterns in assemblages between local and regional scales, we may deduct resource competition and partitioning also for Sericini.

Landscapes with high productivity and a multitude of ecological niches allow to be populated by lineages with different ecological attributes. Since ecological properties of species are reflected in their morphology (Wainwright and Reilly 1994), an increasing number of ecological niches also leads to increasing morphological differentiation. Assemblages studied here showed higher species richness and higher disparity in wet lowland forests and at low elevations.

However, morphological disparity can also be triggered when abiotic selective constraints are weaker and biotic interaction and/or niche partitioning are more important (Chartier et al., 2021). Areas with harsh environments like at higher altitudes, with less resources and little habitat structure, allow only certain well adapted species to survive (García-Navas, 2019). Therefore, highest elevations typically harbour the least species (McCoy, 1990), although the complexity of climatic conditions, biogeographical history, focal taxon, as well as the elevational and geographical extend of the mountains (Mani, 1968) are important influencing factors. Yet, many studies report a significant decline of diversity with increased elevation (García-Lopez et al., 2012; Salomão et al., 2021), as reported here. Decreasing disparity in our chafer assemblages was caused by the absence of many unrelated species at higher elevations that were present in lower altitudes. Factors that might explain reduced species richness in higher altitudes are lower temperature and in result the reduced vegetation height. The first would not favour larger species with long larval development. The latter reduces ecological niches and increases interspecific competition. Non-overlapping clusters of montane Sericini species in morphospace (Figure S7.5b) supported this theory by suggesting interspecific competition. However, lowland species' clusters were also generally distinct (Figures 7.3, 7.4), but overlap between a few species occurred, particularly in species rich assemblages. Thus, competition might exist also in less harsh environments but its impact is likely less stringent due to more ecological vacancies. It fits into this context that most closely related (and morphologically most similar) species tend to not co-occur with each other (Ahrens 2004; Fabrizi & Ahrens 2014) since diversification of Sericini in Asian mountains seems to be particularly triggered by geography-driven speciation (Ahrens, 2007; Eberle et al., 2017).

However, in contrast to adults that may occupy the huge three-dimensional angiosperm food space, very little is known about larval coexistence in the two-dimensional soil layers, which might be more restrictive for coexistence of species (Ahrens et al., 2009). Therefore, studies are needed that investigate larvae in combination with adults in the framework of molecular phylogenies. We need to explore more rigorously community composition at different landscape scales to disentangle the driving forces of diversity vs disparity in the context of assemblage evolution among pleurostict chafers. Furthermore, future studies might consider in this point phylogenetic correction in disparity analysis (Brusatte et al., 2011) to investigate more in detail the genealogic component of morphospace divergence, particularly when comparing different systematic levels (see also Eberle et al., 2014).

Acknowledgments

This work was funded by German Academic Exchange Service (DAAD), Alexander Koenig Stiftung, and ZFMK institutional funding. For providing research and collection permits we thank the Department of Wildlife Conservation, the Department of Forest Conservation, the Divisional Forest Office Kandy and Galle.

7.5 References

- Ahrens, D. (2004). Monographie der Sericini des Himalaya (Coleoptera, Scarabaeidae). Dissertation.de - Verlag im Internet GmbH, Berlin, 534pp.
- Ahrens, D. (2006). The phylogeny of Sericini and their position within the Scarabaeidae based on morphological characters (Coleoptera: Scarabaeidae). *Systematic Entomology*, 31, 113–144.
- Ahrens, D. (2007). Beetle evolution in the Asian highlands: insight from a phylogeny of the scarabaeid subgenus *Serica* (Coleoptera, Scarabaeidae). *Systematic Entomology*, 32, 450–476.
- Ahrens, D., Dhoj, G.C.Y., Lago, P.K., & Nagel, P. (2009). Seasonal fluctuation, phenology and turnover of chafer assemblages - insight to the structural plasticity of insect communities in tropical farmland (Coleoptera: Scarabaeidae). *Agricultural and Forest Entomology*, 11, 265–274.

- Ahrens, D., Schwarzer, J., & Vogler, A.P. (2014). The evolution of scarab beetles tracks the sequential rise of angiosperms and mammals. *Proceedings of the Royal Society B*, 281, 20141470.
- Brehm, G., Zeuss, D., & Colwell, R.K. (2019). Moth body size increases with elevation along a complete tropical elevational gradient for two hyperdiverse clades. *Ecography*, 42, 632–642.
- Brusatte, S.L., Montanari, S., Yi, H., & Norell, M.A. (2011). Phylogenetic corrections for morphological disparity analysis: new methodology and case studies, *Paleobiology*, 37, 1–22.
- Cardillo, M., Gittleman, J.L., & Purvis, A. (2008). Global patterns in the phylogenetic structure of island mammal assemblages. *Proceedings of the Royal Society B*, 275, 1549–1556.
- Chartier, M., von Balthazar, M., Sontag, S., Lofstrand, S., Palme, T., Jabbour, F., Sauquet, H., & Schonenberger, J. (2021). Global patterns and a latitudinal gradient of flower disparity: perspectives from the angiosperm order Ericales. *New Phytologist*, 230, 821–831.
- Deline, B., Greenwood, J.M., Clark, J.W., Puttick, M.N., Peterson, K.J., & Donoghue, P.C.J. (2018). Evolution of metazoan morphological disparity. *The Proceedings of the National Academy of Sciences*, 115 (38), E8909–E8918.
- Eberle, J., Myburgh, R., & Ahrens, D. (2014). The Evolution of morphospace in phytophagous scarab chafers: no competition - no divergence? *PLoS ONE*, 9(5), e98536
- Eberle, J., Fabrizi, S., Lago, P., & Ahrens, D. (2016). A historical biogeography of megadiverse Sericini – another story out of Africa? *Cladistics*, 33, 183–197.
- Emlen, D.J., & Philips, T.K. (2006). Phylogenetic evidence for an association between tunneling behavior and the evolution of horns in dung beetles (Coleoptera: Scarabaeidae: Scarabaeinae). *Coleopterists Society Monograph*, 60, 47–56.
- Fabrizi, S. & Ahrens, D. (2014). A Monograph of the Sericini of Sri Lanka (Coleoptera: Scarabaeidae). *Bonn Zoological Bulletin Supplements*, 61, 1–124.
- García-Lopez, A., Mico, E., & Galante, E. (2012). From lowlands to highlands: searching for elevational patterns of species richness and distribution of scarab beetles in Costa Rica. *Diversity and Distribution*, 18, 543–553.
- García-Navas, V. (2019). Phylogenetic and functional diversity of African muroid rodents at different spatial scales. *Organisms Diversity and Evolution*, 19, 637–650.
- Guillerme, T. et al. (2020). Disparities in the analysis of morphological disparity. *Biology Letters*, 16, 20200199

- Hammer, O., Harper, D.A.T. & Ryan, P.D. (2001). PAST: paleontological statistics software package for education and data analysis. *Palaeontologia Electronica*, 4, 1–9.
- Heard, S.B., & Hauser, D.L. (1995). Key innovations and their ecological mechanisms. *Historical Biology*, 10, 151–173.
- Hopkins, M.J. (2013). Decoupling of taxonomic diversity and morphological disparity during decline of the Cambrian trilobite family Pteroccephaliidae. *Journal of Evolutionary Biology*, 26, 1665–1676.
- Hopkins, M.J., & Gerber, S. (2017). Morphological disparity. In: Nuno de la Rosa L., Müller G. (eds) *Evolutionary developmental biology*. Springer, Cham. https://doi.org/10.1007/978-3-319-33038-9_132-1.
- Horne, C.R., Hirst, A.G., & Atkinson, D. (2018). Insect temperature–body size trends common to laboratory, latitudinal and seasonal gradients are not found across altitudes. *Functional Ecology*, 32, 948–957.
- Inward, D.J.G., Davies, R.G., Pergande, C., Denham, A.J., & Vogler, A.P. (2011). Local and regional ecological morphology of dung beetle assemblages across four biogeographic regions. *Journal of Biogeography*, 38, 1668–1682.
- Jolicoeur, P. (1963). The multivariate generalization of the allometry equation. *Biometrics*, 19, 497–499.
- Jønsson, K.A., Lessard, J.P., & Ricklefs, R.E. (2015). The evolution of morphological diversity in continental assemblages of passerine birds. *Evolution*, 69, 879–889.
- Klingenberg, C.P. (1996). Multivariate allometry. In: Marcus et al., *Advances in Morphometrics*. New York: Plenum Press. pp. 23–49.
- Mani, M.S. (1968). *Ecology and biogeography of high altitude insects*. Junk, The Hague, 527pp.
- McCoy, E.D. (1990). The distribution of insects along elevational gradients. *Oikos*, 58, 313–322.
- McKenna, D.D., Shin, S., Ahrens, D., Balke, M., Beza, C., Clarke, D.J., Donath, A., Escalona, H.E., Friedrich, F., Letsch, H., Liu, S., Maddison, D., Mayer, C., Misof, B., Murin, P. J., Niehuis, O., Peters, R.S., Podsiadlowski, L., Pohl, H., Scully, E.D., Yan, E.V., Zhou, X., Ślipiński, A., Beutel, R.G. (2019). The evolution and genomic basis of beetle diversity. *Proceedings of the National Academy of Sciences*, 116(49), 24729–24737.
- Minelli, A. (2016). Species diversity vs. morphological disparity in the light of evolutionary developmental biology. *Annals of Botany*, 117, 781–794
- Mosiman, J.E., & James, F.C. (1979). New statistical methods for allometry with application to Florida Red-winged Blackbirds. *Evolution*, 33, 444–459.

- Nel, P., Bertrand, S., & Nel, A. (2018). Diversification of insects since the Devonian: a new approach based on morphological disparity of mouthparts. *Scientific Reports*, 8, 3516
- Pacheco, T.L., Monné, M.L., & Ahrens, D. (2022). Comparative analysis of morphospace of Neotropical Sericini (Coleoptera: Scarabaeidae): disparity in the light of species diversity and activity patterns. *Organisms Diversity and Evolution*, 22, 177–188.
- Ranasinghe, S., Eberle, J., Benjamin, S.P. & Ahrens, D. (2020). New species of Sericini from Sri Lanka (Coleoptera, Scarabaeidae). *European Journal of Taxonomy*, 621, 1–20.
- Ribera, I., Dolédec, S., Downie, I.S., & Foster, G.N. (2001). Effect of land disturbance and stress on species traits of ground beetle assemblages. *Ecology*, 82, 1112–1129.
- Ricklefs, R.E. (2012). Species richness and morphological diversity of passerine birds. *The Proceedings of the National Academy of Sciences*, 109, 14482–14487.
- Ricklefs, R.E., Cochran, D., & Pianka, E.R. (1981). A morphological analysis of the structure of communities of lizards in desert habitats. *Ecology*, 62, 1474–1483.
- Ritcher, P.O. (1958). Biology of Scarabaeidae. *Annual Review of Entomology*, 3, 311–334.
- Romano, M. (2019). Disparity vs. diversity in Stegosauria (Dinosauria, Ornithischia): cranial and post-cranial sub-dataset provide different signals. *Historical Biology*, 31, 857–865
- Romano, M., Brocklehurst, N., & Fröbisch, J. (2017). Discrete and continuous character-based disparity analyses converge to the same macroevolutionary signal: a case study from captorhinids. *Scientific Reports*, 7, 17531.
- Roy, K., Jablonski, D., & Valentine, J.W. (2004). Beyond species richness: biogeographic patterns and biodiversity dynamics using other metrics of diversity. In: M. V. Lomolino and L. R. Heaney, eds., *Frontiers of Biogeography: New Directions in the Geography of Nature*. Sunderland, MA: Sinauer, 151–170.
- Salomão, R.P., Arriaga-Jiménez, A., & Kohlmann, B. (2021). The relationship between altitudinal gradients, diversity, and body size in a dung beetle (Coleoptera: Scarabaeinae: Onthophagus) model system. *Canadian journal of zoology*, 99, 33–43.
- Shepherd, U.L. (1998). A comparison of species diversity and morphological diversity across the North American latitudinal gradient. *Journal of Biogeography*, 25, 19–29.

- Simões, M., Breitzkreuz, L., Alvarado, M., Baca, S., Cooper, J.C., Heins, L., Herzog, K., & Lieberman, B.S. (2016). The evolving theory of evolutionary radiations. *TREE*, 31, 27–34.
- Smith, T.J., Puttick, M.N., O'Reilly, J.E., Pisani, D., & Donoghue, P.C.J. (2021). Phylogenetic sampling affects evolutionary patterns of morphological disparity. *Palaeontology*, 64, 765–787.
- Triantis, K.A., Rigal, F., Parent, C.E., Cameron, R.A.D., Lenzner, B., Parmakelis, A., Yeung, N.W., Alonso, M.R., Ibáñez, M., de Frias, Martins, A.M., Teixeira, D.N.F., Griffiths, O.L., Yanes, Y., Hayes, K.A., Preece, R.C., & Cowie, R.H. (2016). Discordance between morphological and taxonomic diversity: land snails of oceanic archipelagos. *Journal of Biogeography*, 43, 2050–2061.
- Wainwright, P.C., & Reilly, S.M. eds. (1994). *Ecological morphology: integrative organismal biology*. University of Chicago Press, Chicago, 367 pp.

7.6 Supplementary Figures

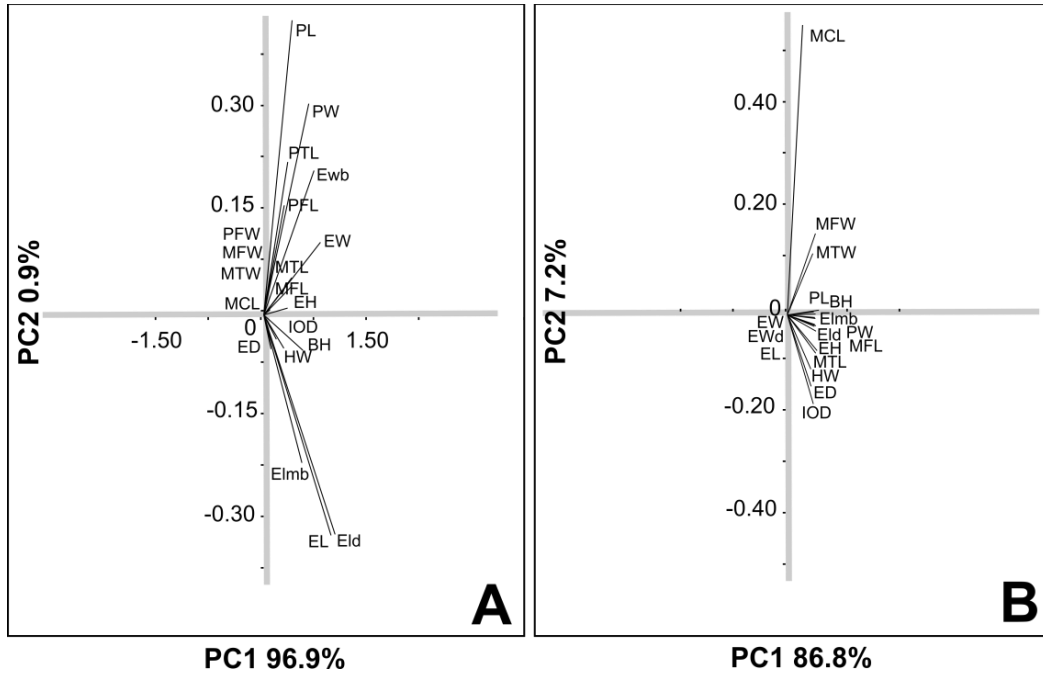


Figure S7.3. Biplots of PC1 and 2 from principal components analysis, illustrating trait contribution to the principal patterns of morphospace. **A:** raw measurements; **B:** log-normalized measurements. Trait abbreviations are explained in Figure S2.

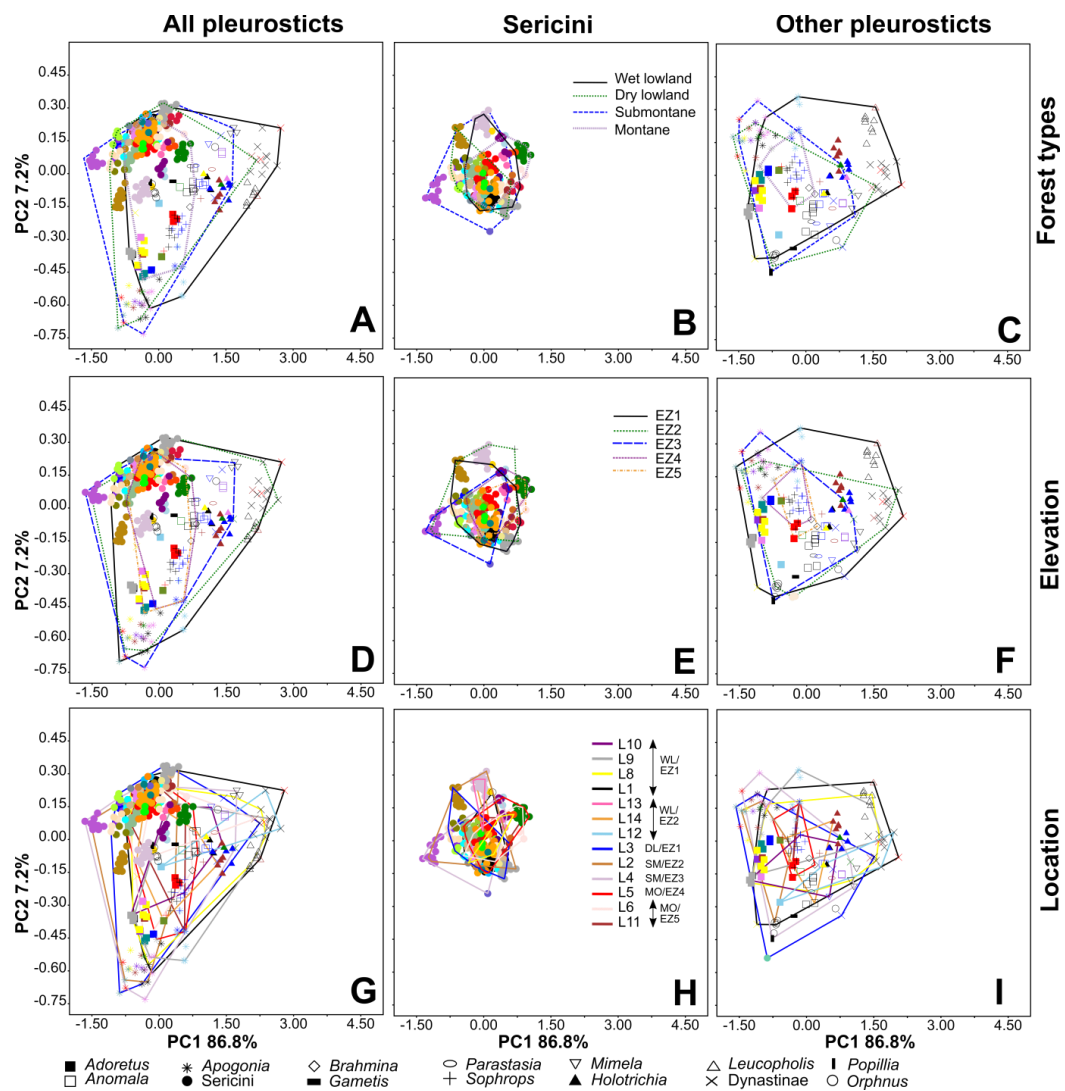


Figure S7.4. Patterns of morphospace disparity derived from log-normalized data of pleurostict chafer assemblages (All Pleurosticts, Sericini, other pleurostict chafers) partitioned for forest types, elevation zones, localities. Principal components analysis (PCA) plots of PC1 and PC2. **A, D, G:** All Pleurosticts; **B, E, H:** Sericini chafers; **C, F, I:** other pleurostict chafers; **A, B, C:** partitioned for forest types; **D, E, F:** elevation zones; **G, H, I:** localities. Symbols represent genus or other family-group level, colour of symbols single species, outlines grouping according to forest types, elevation zones or localities.

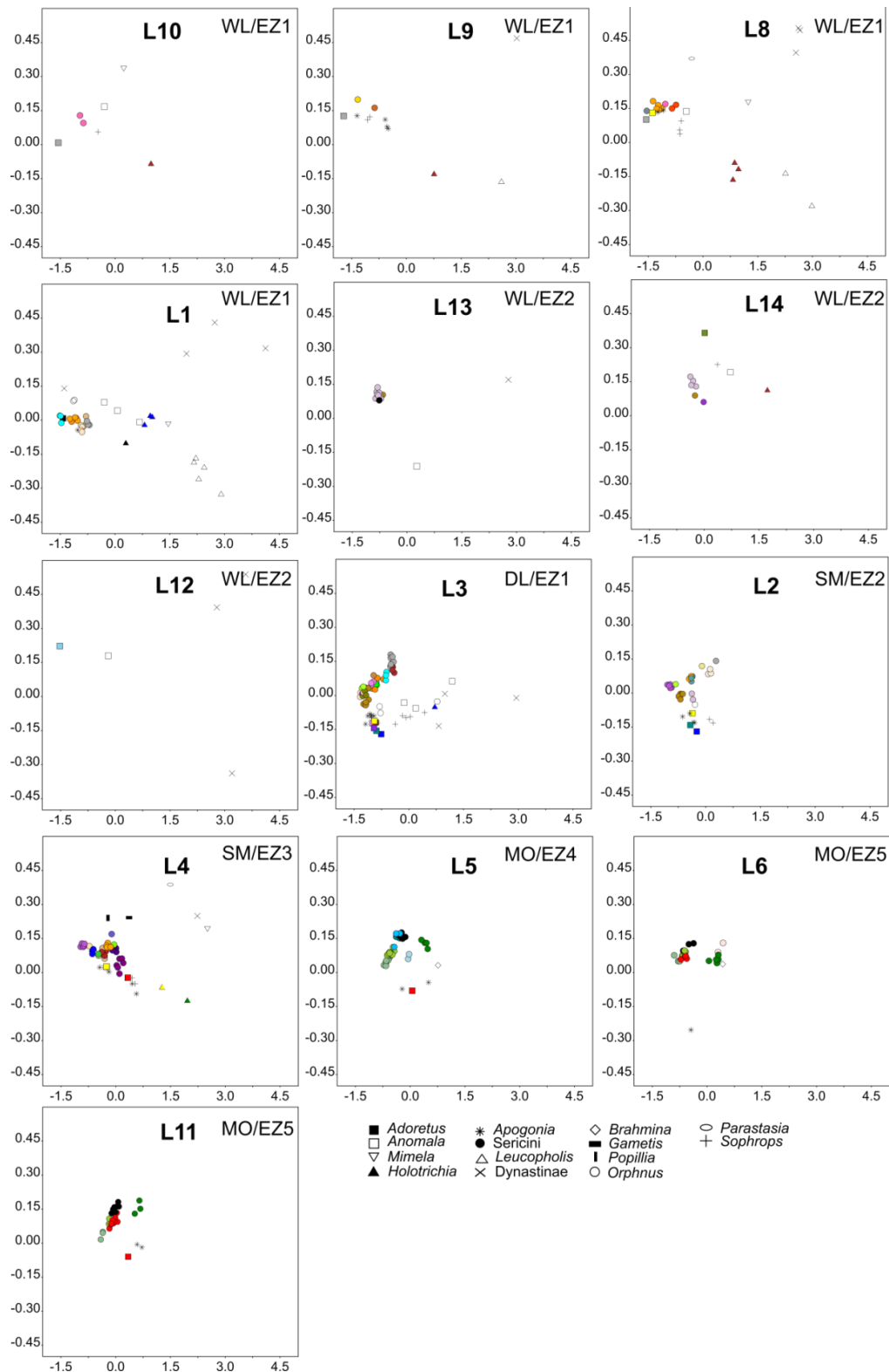


Figure S7.5a. Patterns of morphospace disparity of all Pleurostictids derived from raw measurements in individual localities. Symbols represent genus or other family-group level, colour of symbols single species.

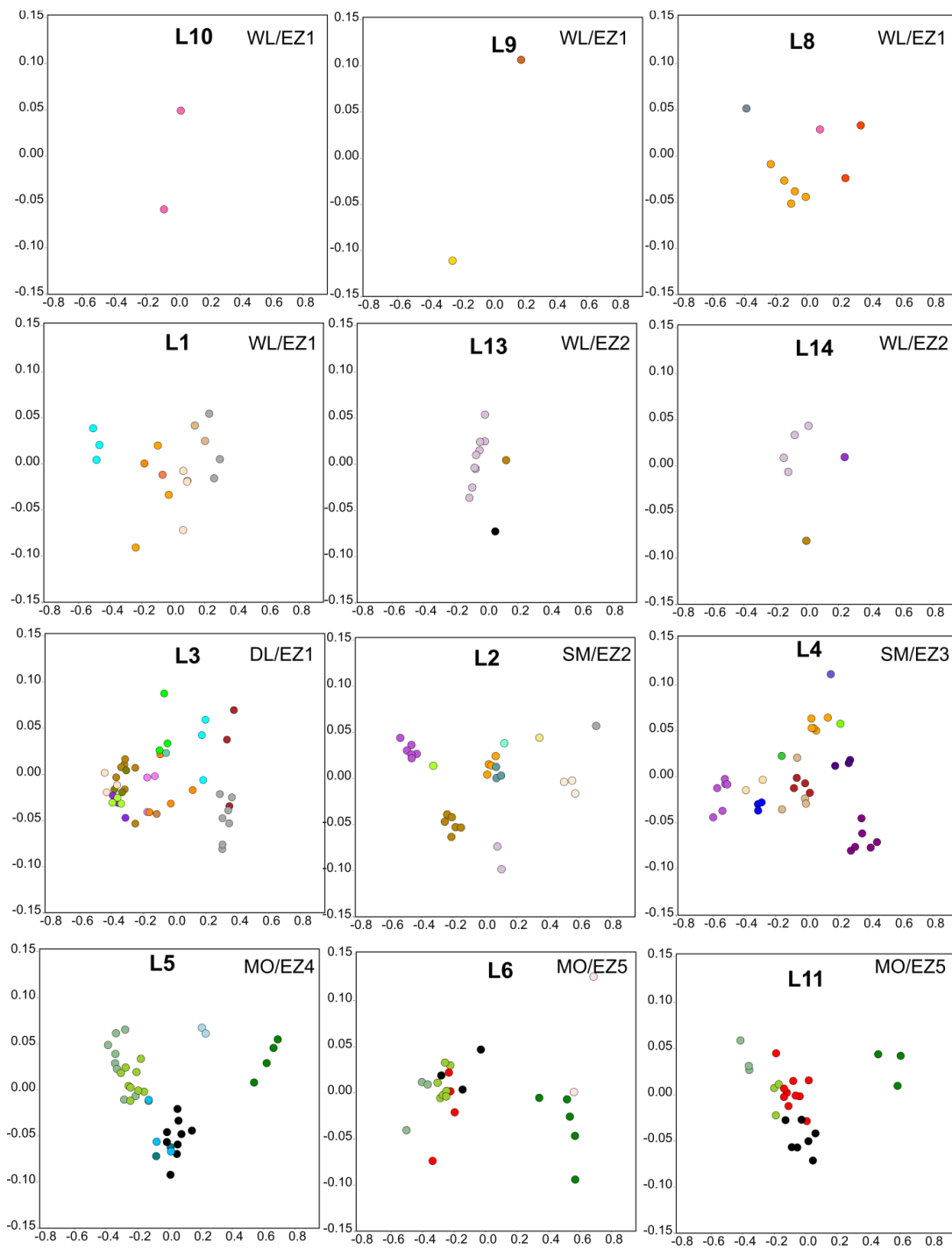


Figure S7.5b. Patterns of morphospace disparity of Sericini derived from raw measurements in individual localities. Coloured dots represent single species. Locality L12 had no Sericini recorded.

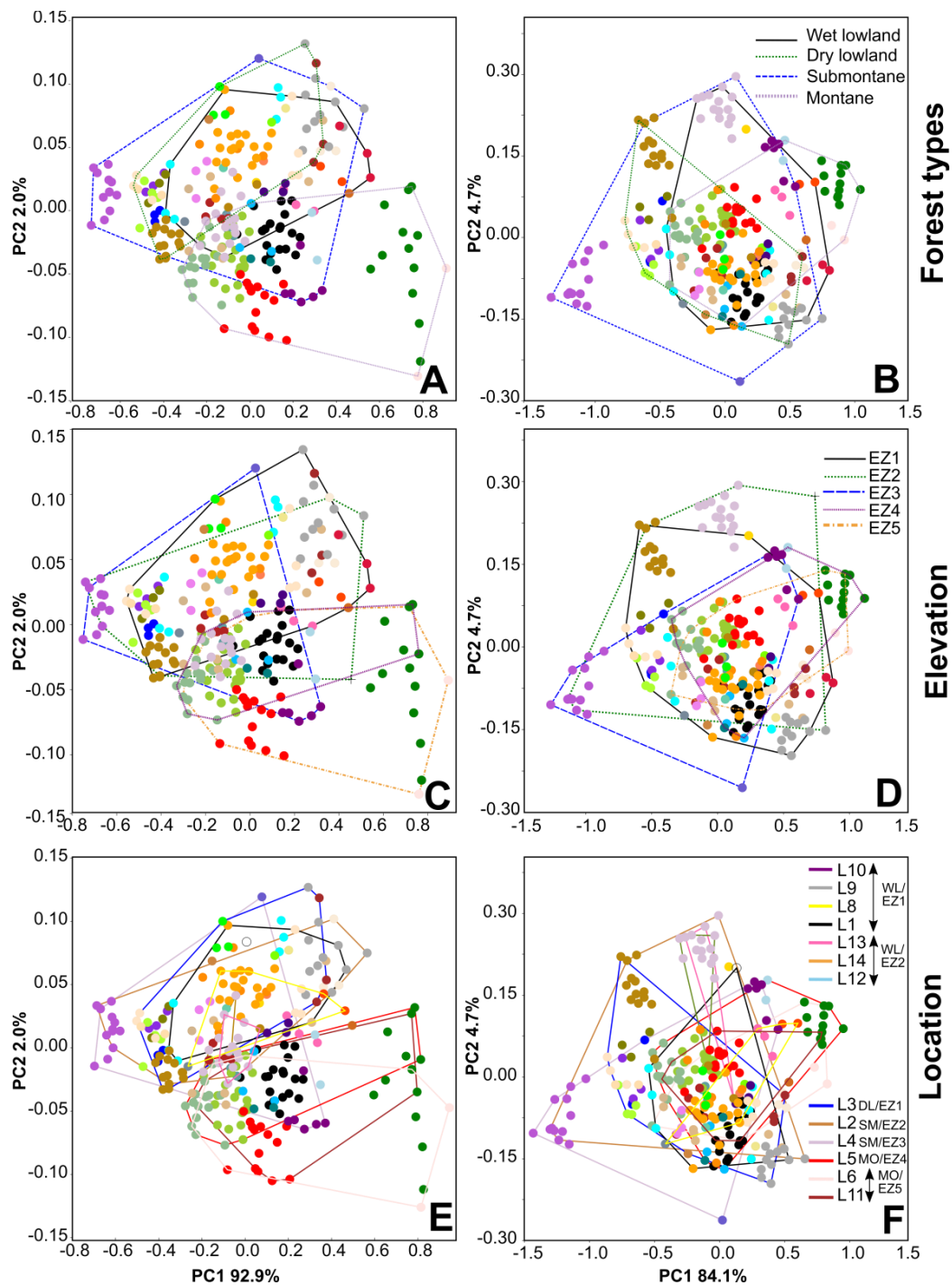


Figure S7.6. Patterns of morphospace disparity (PCA plots of PC1 and PC2) derived from raw and log-normalized measurements of Sericini chafer species partitioned for forest types, elevation zones, localities (enlarged visualization from Fig. 2). **A, B:** partitioned for forest types; **C, D:** elevation zones; **E, F:** localities. **A, C, E:** from raw measurements **B, D, F:** log-normalized measurements. Coloured dots represent single species, outlines grouping according to forest types, elevation zones or localities.

Chapter 8

Local stochasticity and ecoclimatic situation shape phytophagous chafer assemblage composition

This chapter is intended for publication in *Ecography*:

Ranasinghe U.G.S.L., Eberle J, Benjamin S.P., Ahrens D. (in-prep).
Local stochasticity and ecoclimatic situation shape phytophagous chafer
assemblage composition

Authors' contributions to the original article:

SR, JE, SB: fieldwork collections; SR: analyses, SR, DA: writing-original draft;
DA, JE, SB, SR: manuscript review and editing.

Abstract

Very little is known about factors determining the structure of megadiverse tropical assemblages of polyphagous-herbivore scarab chafer (Coleoptera: Scarabaeidae). Here, we examined factors determining chafer assemblage composition, comparing the influence of ecoclimatic situation and macrohabitat with determinants of the locality. We also explored the influence of lineage membership and body size. Case study was the Sri Lankan fauna, which was examined with field surveys during dry and wet seasons. We examined 4847 chafer individuals of 105 species sampled using multiple UV-light traps in 11 localities covering different forest types and altitudinal zones. Assemblages were assessed for compositional similarity, species diversity and abundance for four major eco-spatial partitions: forest types, elevational zones, localities, and macrohabitats. Results revealed that assemblages were shaped mainly by locality stochasticity, and to minor extent by ecoclimatic conditions. Macrohabitat had little effect on the assemblage composition. This was true for the entire chafer assemblage but also for all single lineages or different body size classes. However, in medium and large specimens contrasts between localities were less pronounced, which was not the case for the lineages. Contrasts of assemblage similarity between localities were much more evident than those of forest types and elevation zones. Significant correlation between species composition and geographic distance was found only for the assemblage of small-bodied specimens. Seasonal change (dry-wet) in species composition was minor and only measurable in a few localities.

8.1 Introduction

Describing and analysing biodiversity and its major patterns is a key for understanding the underlying processes and causes of diversification (Holt et al., 2013). Taxonomy, ecology, and distribution of arthropods are, compared to plants and vertebrates, only fragmentarily known and comprehensive data are rare (Decaëns, 2010; Beck & Kitching, 2007; Stork et al., 2015; Nielsen, 2019). This is particularly true for biodiversity hotspots (Myers et al., 2000). In most cases they only rely on museum's collection specimens and thus suffer largely from sampling bias (Santos & Quicke 2011; Echevarría et al., 2019). Nevertheless, their often restricted dispersal capacities and their occurrence in micro-niches

results in high endemism, fine scale and still unknown patterns (Buckley and Jets 2007; Daru et al., 2020; Baselga et al., 2022). This includes even large-bodied taxa such as phytophagous beetles.

Diversity patterns of phytophagous beetles are known to be linked to species turnover of their host plants (Ødegaard, 2006; Kemp et al., 2017; Luo et al., 2021) and their distribution is correlated with the region and forest type (Yotkham et al., 2021). Other guilds, such as dung feeding beetles, respond to shade cover rather than plant species composition, while their occurrence and relative abundance varies according to their responses to microclimate (light intensity, temperature, humidity) (Davis et al., 2013) or different factors (rainfall, temperature, and host density/diversity) varying from regional to local scale as well as by responses to current local functional ecological conditions (Tshikae et al., 2013). Such correlation with environmental conditions, suggest that a strong role of lineage- or species-specific traits such as dispersal capabilities or body size determines local community composition (Murria et al., 2017). It was shown that insect body size is affected by many climatic conditions along species ranges, especially when they are distributed across climatic gradients at large spatial scales (Lira et al., 2021; Romero et al., 2016; Brehm et al., 2019; Salomão et al., 2021). Changes in body size may affect fertility, lifespan, population dynamics, and species composition (Garcia-Robledo et al., 2020).

In contrast to most other herbivore insects being very host-specific, phytophagous scarab chafers (Coleoptera: Scarabaeidae) feed unspecifically on leaves of a variety of angiosperm plants and have had with worldwide ca. 30,000 extant species a very successful follow-up evolution with angiosperms (Ahrens et al., 2014). They spend in larval stage most of their lifetime on feeding soil humus or roots (Ritcher, 1958). However, knowledge about their actual assemblages, differences between habitats is even rarer (Ahrens et al., 2009; García Lopez et al., 2010, 2013). Most available studies on chafer assemblages include either mostly only a part of the assemblage (Ahrens et al., 2007), or assemblages from a single or a few distant localities (Ahrens et al., 2009; García-Lopez et al., 2013), despite chafers were found to be very suitable proxies for habitat conditions (Eberle et al., 2017). Factors determining their assemblage composition so far never have been explored.

Consequently, we investigate here the patterns of species diversity and turnover in tropical phytophagous chafers in Sri Lanka, a global biodiversity hotspot (Myers, 2000), across different forest types, elevation zones, localities, and habitats. We compared larger scale entities (such as forest type and elevation) versus smaller

scale entities (such as localities and macrohabitats). We were interested in which spatial component determines the assemblage composition, and at which extent. In this context, we also assessed the influence of lineage membership and body size in shaping the species composition. If body size (as proxy of dispersal capability) had an impact assemblage composition, we would expect contrasting patterns between entities of different spatial scales between smaller and larger species assemblies, also in respect to phylogenetically partitioned assemblages. This way, we expect to elucidate the dynamics of community assembly and differentiation and to get insight to explain the high species richness and local endemism in tropical chafers.

8.2 Materials and Methods

Study area and sampling

Four field expeditions were conducted during 2019 and 2020 (in February-March/October-November and June-July/ November-December, respectively) during rainy and dry seasons. Specimens were sampled using UV-light traps (Ranasinghe et al., 2020) in 11 localities covering different forest types and altitudinal zones of Sri Lanka (Figure S8.1). Sites were situated in evergreen wet lowland forests (below 500m: L1, L8, L9; or above 500m: L12, L13, L14), in the evergreen dry lowland forest (L3), in sub-montane forests (L2, L4), or in montane forests (L5, L11) (Figure S8.1, Table S8.1). Six traps were placed in each locality at different subsites (i.e., macrohabitats) at approximately 2 m above ground (Table S8.1). They were positioned at the same spot for 2–3 consecutive days and ran from 6 pm to 11 pm. All traps (traps A-F) were separated by at least 100–500m distance depending on the landscape of the locality to not influence each other. Beetles were trapped in a sampling container with preservation liquid (96% ethanol) (for trap design, see Ranasinghe et al., 2020; 2022). Specimens were stored in 96% ethanol for identification and/or DNA sequencing. In total, we performed 10-12 trapping events per expedition and site, resulting in 60-72 tapping events in each location.

Phytophagous chafers (Coleoptera: Scarabaeidae) in Sri Lanka include Dynastinae, Melolonthinae, and Rutelinae. Specimens were identified to morphospecies based on external and genital morphology using recent literature (Fabrizi & Ahrens, 2014; Ranasinghe et al., 2020), some being subsequently

examined by a specialist. Specimens are deposited in the Zoological Research Museum A. Koenig, Bonn (ZFMK) and in the National Institute of Fundamental Studies, Kandy, Sri Lanka (NIFS).

Assemblage characterization

Species richness and abundance was assessed by the mean number of individuals or species per trapping event and site (i.e., total number of specimens per species of a particular trap divided by number of used traps). This measure helped to smooth out sampling biases due to electric failures and weather problems. Species presence and absence data were used for the assessment of species composition and assemblage similarity. Species accumulation curves were plotted for each trap with the cumulative number of recorded species vs. number of cumulative trapping events to assess sampling adequacy and comparability of the results. Inventory completeness in each sampling locality was measured by observed species in respect to the number of species predicted by the Chao1 richness estimator, i.e., the total number of species in each locality with lower and upper limits (Chao & Lee, 1992; Zou & Axmacher, 2021). Sampling data (i.e., specimens per trap) were pooled for each trap from all four sampling campaigns (2019 I, 2019 II, 2020 I, 2020 II). Later, data of each of the six traps were pooled for a complete locality. A two-way cluster analysis (species vs locality) was performed based on presence absence data using the Jaccard similarity index (Jaccard, 1912) using PAST v. 3.25 (Hammer et al., 2001).

The alpha diversity was measured using Shannon index, Simpson index and Evenness for each locality (Shannon, 1948; Simpson, 1949; Hill, 1973) being calculated in PAST v. 3.25. Approximate confidence intervals for all these indices were computed with a bootstrap procedure (number of random samples (default 9999) with 95 % confidence interval).

Partitioned assemblage assessment by body size and lineages

Differences in body size may reflect divergences in species ecology and behaviour (Inward et al., 2011; Eberle et al., 2014; Lira et al., 2021). Thus, size related differences in assemblage composition across different spatial scales may provide insight to the causalities of these pattern. Therefore, observed specimens were analysed according to these groupings: according to their body size, in three groups: 1) smaller 7 mm; 2) 7-15 mm; 3) larger 15 mm. The respective total body length was calculated using the sum of pronotal and elytral length (PL+EL). The mean total body length of a species was determined by taking the mean value of

3-5 individuals of the same species. Alternatively, species were grouped according to their membership to phylogenetic lineages (following McKenna et al. 2021): Dynastinae, Rutelinae, Melolonthinae (excluding Sericini), and Sericini to explore also phylogenetic patterns of differences in assemblage composition (Smith et al., 2021), also for comparison with body size classes.

Spatial turnover analysis

Non-metric multidimensional scaling analyses (NMDS) based on presence/absence data (using Jaccard similarity indices) were performed for four major spatial components i.e. (forest types, elevational zones, localities, and habitats). For this purpose, each single trap was assigned for a particular spatial component (Table S8.1). Forest types included four entities: a) evergreen wet lowland forests, b) evergreen dry lowland forests, c) sub-montane forests, and d) montane forests. Elevation was partitioned in five units: EZ1: 0–500 m, EZ2: 501–1000 m, EZ3: 1001–1500 m, EZ4: 1501–2000 m, and EZ5: 2001–2500 m. Localities included the individual sampling localities. Habitat types included seven entities: abandoned plantation, grassland, rock outcrop, hilltop, forest edges, central forest, and disturbed forest. NMDS ordination was performed on the full data set. Entities of spatial components (i.e., forest types, elevational zones, localities, and habitats) were subsequently mapped on the ordination results. Spatial turnover analysis was performed for the full assemblage and assemblage partitions based on body-size and phylogenetic lineage membership (see above). In this context, also the association between qualitative species composition similarity and geographic distances of sampling sites was estimated by linear regression using PAST. The relation was measured for both body size groups, and for separate phylogenetic lineages.

Seasonal turnover analysis

Seasonality can strongly impact assemblage composition. Therefore, we assessed the seasonal turnover for single traps and localities using NMDS ordinations based on Jaccard indices from species presence-absence data. The turnover of species composition in time was also evaluated for the localities through ANOVA and Kruskal-Wallis tests as implemented in PAST. Finally, we compared also seasonal turnover for lineage- and body-size partitioned assemblage data. Additionally, seasonal emergence patterns of Sericini were evaluated using their total evidence presence-absence data for each month. For this group there were available all-year collection data based on revised museum specimens (Fabrizi

and Ahrens, 2014), and on specimens of this work. This approach of comparison was useful to identify and compare highly seasonal and/or rare species versus common species.

8.3 Results

A total of 4847 specimens of 105 chafer species belonging to Rutelinae, Melolonthinae, and Dynastinae were recorded (Table S8.2). Species richness estimators suggested >89% of total species inventory had been captured. While 82% of the individual locality assemblages showed more than 84% of sampling completeness (in terms of species composition), in two cases sampling completeness was, with less than 50%, quite low (L9, L14) (Table S8.3). Species accumulation curves for individual localities showed that about 80% of its local assemblage has been captured in less than half of the total trapping events (before 34th trapping event) (Figure S8.2). Similarly, species accumulation curves for individual traps showed that about 80% or slightly more of the expected species has been captured before its sixth trapping event (i.e., half of the total trapping events for individual trap).

Melolonthinae was the most speciose subfamily (n=79), for which the highest number of individuals was recorded (n=2504). Dynastinae had the lowest number of species (n=8) and individuals (n=38), for Rutelinae we recorded 18 species in 531 exemplars. Among the Melolonthinae, Sericini was the most speciose accounting 44.7% of all species (Figure 8.1). Many species were geographically restricted, 67 species out of 105 (64% of total assemblage) were found exclusively at just one site. L3 showed the highest alpha diversity and L13 showed the lowest (Table S8.3). These patterns are also reflected by the results of the two-way cluster analysis, once for the species occurring in different localities, and for the different localities being encountered for the different species (Figure 8.2). This way we could identify species with similar occurrence pattern.

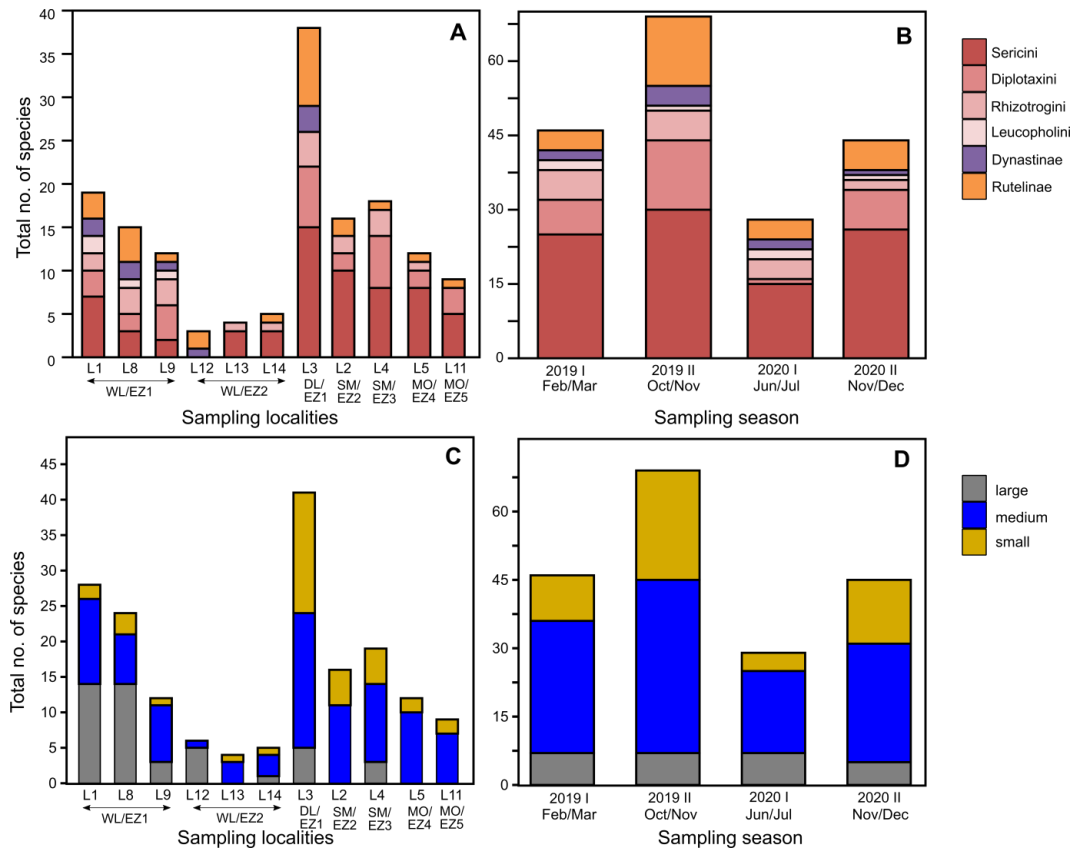


Figure 8.1. Total number of species (species richness) in different locations and in four field campaigns; **A,B.** based on subfamily level/separate lineages; **C,D.** assemblage sorted for body size.

Spatial turnover

Ordination analysis on species presence/absence data (NMDS) of the full chafer assemblage showed generally different patterns between the different spatial components (Figure 8.3A,F,K,P). The largest overlap of the clusters of entities was observed for the macrohabitats, while overlap in forest types, elevation and localities was limited to a few single entities. Here, most entities were well-separated, the distances between them almost similar between entities of the same spatial component, and similar patterns were also observed for single lineages, but differences between the single entities (e.g., elevation zones or forest types) were less pronounced with slightly larger overlaps. For Dynastinae, patterns were not robust due to low representation (Figure 8.3). Species composition in the localities of montane forests (L5, L11) resulted generally more similar (Figure 8.3), while

assemblages of dry lowland forest were dissimilar for single lineages while there was an overlap for the full assemblage analysis.

NMDS on species presence/absence data for the three different body size classes showed similar overall patterns: large overlap for all partitions in macrohabitats, and moderate to clear distinction for ecoclimatic zones (elevation, forest type) and localities. Small and medium-sized assemblages showed somewhat contrasting patterns for assemblages of large-bodied specimens for forest types, elevation zones and localities (Figure 8.4), particularly because the latter was more poorly sampled in terms of species and recorded localities. Again, spatial entities (e.g., elevation zones, or forest types) in partitioned analyses were less different than for the full assemblage data (Figure. 8.4).

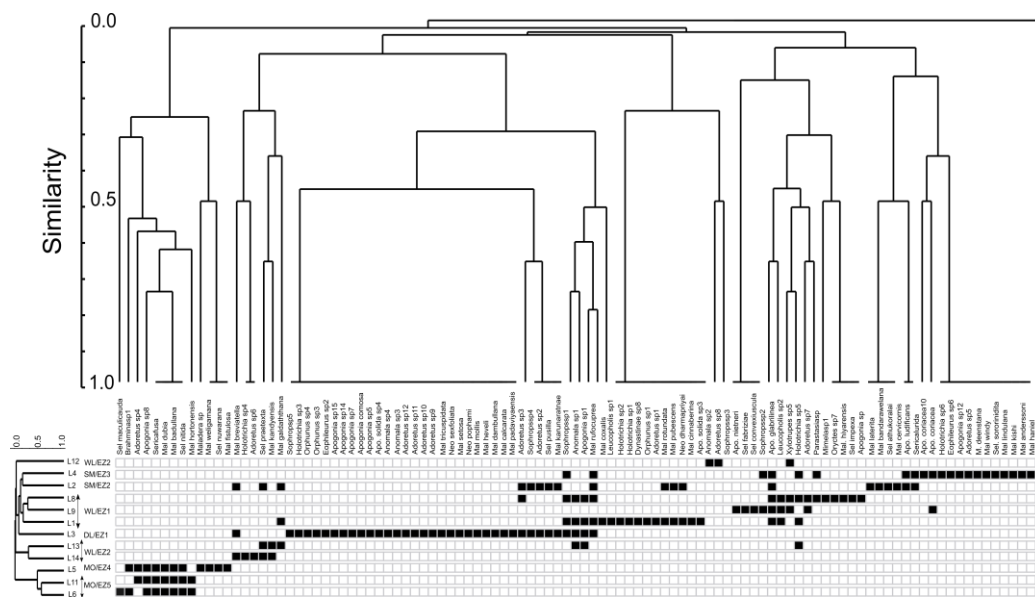


Figure 8.2. Dendrogram from species presence data. Results of a UPGMA clustering of localities is shown at the lower left of the figure, with 1000 bootstraps. Black square: Presence; White square: Absence.

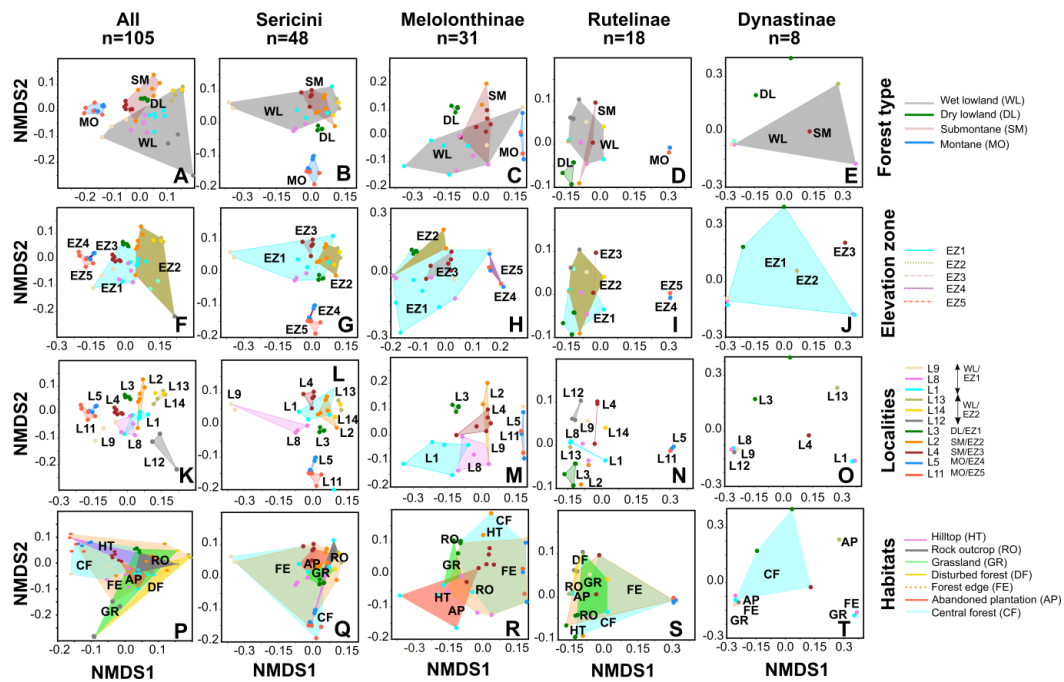


Figure 8.3 NMDS analyses of assemblages from single trapping events separated by taxa and different spatial and eco-spatial partitions; forest types (**A-E**), elevation zones (**F-J**), localities (**K-O**) and habitats (**P-T**). Partitions are enclosed by convex hulls. Multiple traps from one locality have the same colour and colours correspond to Figure S8.1. The ordination was based on presence/absence data (Jaccard index).

A linear regression analysis showed overall no significant correlation ($r = -0.029$, $p = 0.831$), between species composition similarity and geographic distance among localities (Figure 8.5). The relation was also tested for the assemblage partitioned by body size and lineages (Table S8.4), but a significant dependence between species composition and geographic distance was found only for the assemblage of small-bodied specimens ($r = -0.344$, $p = 0.02$).

Seasonal turnover

Species richness and abundance varied significantly between four field campaigns (ANOVA, $p < 0.01$) (Figure 8.1B). Species turnover among single traps between four campaigns was not showing any difference in species composition (Figure 8.6). When data from each of the six traps were pooled for single locality and field campaign, seasonal species turnover of localities varied between 19–61% (Table S8.5). Kruskal-Wallis test for individual localities showed that L1, L2, L3,

L9 had significantly different seasonal species turnover, while other localities did not show any significant species turnover with the season (Table S8.5). Among four studied campaigns, February (2019I) and December (2020II) campaigns showed the highest faunal similarity (i.e., 49.2%) and lowest similarity (17%) was found between October (2019II) and June (2020I) campaigns (Table S8.6). Species turnover among four campaigns varied for lineage and body size partitioned assemblage data, which showed significant difference except for large-bodied and Dynastinae (Table S8.6).

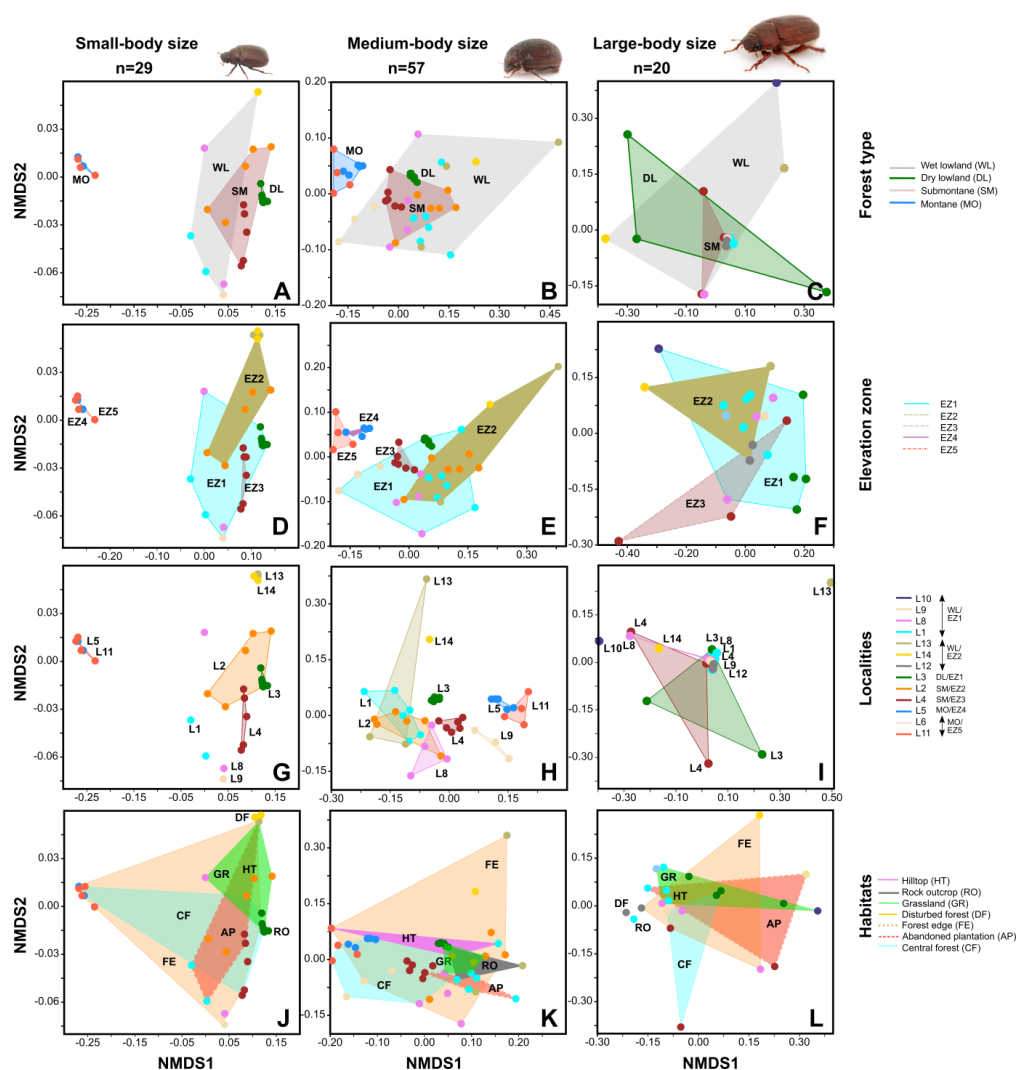


Figure 8.4. NMDS analyses assemblages separated by body size classes and different spatial and eco-spatial partitions; forest types (A-C), elevation zones (D-F), localities (G-I) and habitats (J-L). Partitions are enclosed by convex hulls. Multiple traps from one locality have the same colour and colours correspond to Figure S8.1. The ordination was based on presence/absence data (Jaccard index).

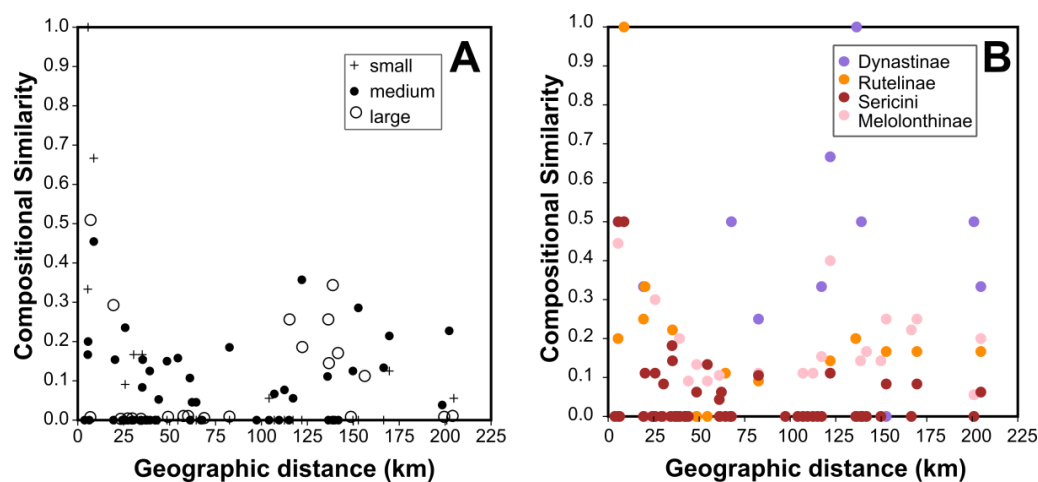


Figure 8.5. Correlation between species compositional similarity (based on presence-absence data) and pairwise geographic distance. **A.** assemblage sorted for body size; **B.** assemblage sorted for lineages.

The comparison of our seasonal distribution data with the detailed seasonal occurrence of Sericini of Fabrizi and Ahrens (2014) and Ranasinghe et al. (2020, 2020), revealed that some species were found to be highly seasonal, particularly the rare species recorded with one or two individual's occurrences only, while some species were found all over the year (Table S8.7). Species diversity and overall abundance of Sericini, varied greatly between months as two peaks were observed in March and October in terms of both number of species and individuals. In contrast to that, overall low species and individual numbers during monsoon period (June–July) were low (Figure S8.3).

8.4 Discussion

In this study, we investigated for the first time the components determining chafer assemblage composition, comparing the impact of the ecoclimatic situation with macrohabitat and locality stochasticity on the similarity of investigated entities. Locality stochasticity represents a not further investigated multi-factor ensemble that includes all environmental conditions at local scale such as macrohabitat, biogeography, edaphic conditions, land use, local climate and exposition to rain and radiation. We also explored the influence of lineage membership and body size on assemblage composition across larger scale entities (such as forest type and elevation) versus smaller scale entities (such as localities and macrohabitats).

The comparison of chafer assemblage composition using different spatial and ecological scales revealed that assemblages were shaped mainly by locality stochasticity, and to a minor extent to the ecoclimatic conditions rather than by macrohabitat. This was true for the entire chafer assemblage but also for all single lineages or different body size classes. NMDS plots of faunal similarity had the largest overlaps among macrohabitat entities. In contrast to that overlap for forest types, elevation zones, and localities was limited. However, in medium and large specimens, contrasts between localities were less pronounced, which was not the case for the lineages.

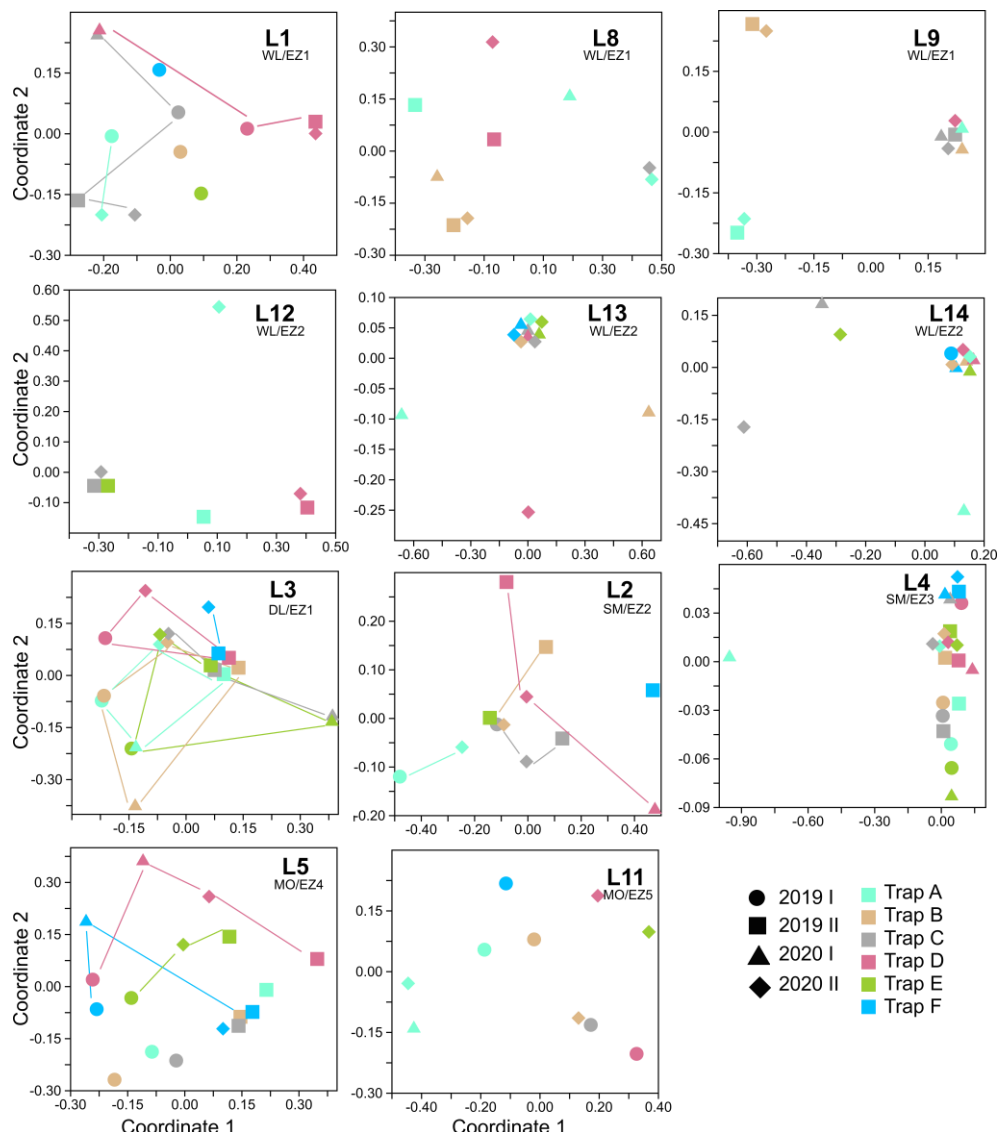


Figure 8.6. NMDS analyses of assemblages from single trapping events separated by sampling locality in the course of four field campaigns (2019 I, 2019 II, 2020 I, 2020 II).

Although investigated macrohabitats were highly diverse, from ‘forest’ to ‘grassland’ to ‘abandoned plantation’, and they are known to provide multiple niches (Bosc et al., 2019) for chafer species, only a few species were recorded for specific habitats. Most species sorted rather by their locality rather than by macrohabitat. This could be partly explained by the trapping method used, as fully winged chafer beetles can arrive from other habitats over certain distances within the same locality or even to adjacent localities. However, there was no relation between species composition (for total assemblage) and geographic distance (Figure 8.5), even for adjacent localities situated in the same forest type also in the same mountain range (e.g., L2, L4). This observation is not surprising as previous studies have also shown high turnover rates of assemblage composition at higher elevations independently from geographical distance (García Lopez et al., 2010). The resulting significant correlation reported here for the assemblage of small-bodied specimens is definitively linked to their limited dispersal capacity. Additionally, influence from biogeographical factors should also be considered in this context (Kemp et al., 2017) as several sampling localities are situated in the central highlands within complex mountain systems (escarpments, ridges, or peaks) which can act as geographical barriers (Meegaskumbura et al., 2015) for dispersal (Perez et al., 2018).

Some of the divergent similarity patterns retrieved for the full assemblage (Figure 8.3A, F), for example between wet lowland forest and submontane forest or between elevation zone 1 and 2, which are in turn not encountered for any of the single lineages, reveal that occurrences of entire lineage members may also impact on the apparent differentiation. The latter case is merely just caused by a lack of Dynastinae and/or larger-bodied species in higher elevations/ submontane forests since low temperatures do not favour larger species with long larval development. In fact, even in mountain ranges with larger amplitudes of elevations, the altitudinal differentiation of the fauna and assemblages in phytophagous chafers is rather poor (Ahrens, 2004) compared to other insects (Mani, 1968).

The strong divergence revealed for localities is in line with the rather high degree of endemism in many phytophagous lineages (Ahrens & Fabrizi, 2016), despite their rather large body size. Their assemblage pattern across local spatial scales can be explained not only by poor dispersal capacities, but also because emergence times are short compared to the entire life span, while endogenous larvae do not disperse; and emergence during early night time often falls together with heavy monsoon rains which narrow down the time window for potential dispersal flights.

Other lineages composed of larger species, such as Dynastinae, have greater dispersal ability compared to smaller Rutelinae and Melolonthinae (García Lopez et al., 2013), and this has an impact on the faunal divergence pattern of assemblages as shown as pronounced larger overlaps across different spatial scales. However, we should not neglect lineage-specific sampling bias with the used UV-light traps regarding the poorly sampled Dynastinae, in terms of species and recorded localities.

Seasonality and weather patterns may strongly impact the patterns of assemblage composition in ecofaunistic analyses (Gonçalves, 2020; De Oliveira et al., 2021). However, due to the tropical climate as well as with minor dry-wet seasonal change together with monsoon effect in Sri Lanka (de Costa, 2008), rainy seasons and dry seasons are alternating in shorter intervals, and quite constant temperature and humidity throughout the year with continuously available food resources, thus minor fluctuations of species numbers may have an influence even in the tropical ecosystems. Many of our localities (except L1-L3, L9) did not show a significant seasonal species turnover. Most of these exceptional localities experience stronger dry-wet fluctuations than other localities according to their position in the island. Similarly, short term meteorological events (Ahrens et al., 2009) also influence capture rates and hence species composition in short-term surveys. In this context, the record of rare species, which of course are expectedly linked to the amount of collection efforts, might strongly influence the outcome.

Acknowledgments

This work was funded by German Academic Exchange Service (DAAD), Alexander Koenig Stiftung, and ZFMK institutional funding. For providing research and collection permits we thank the Department of Wildlife Conservation, the Department of Forest Conservation, the Divisional Forest Office Kandy and Galle.

8.5 References

- Ahrens, D. (2004). Monographie der Sericini des Himalaya (Coleoptera, Scarabaeidae). Dissertation.de - Verlag im Internet GmbH, Berlin, 534pp.
- Ahrens, D. & Fabrizi, S. (2016). A Monograph of the Sericini of India (Coleoptera: Scarabaeidae). *Bonn Zoological Bulletin*, 65, 1–355.
- Ahrens, D., Monaghan, M.T. & Vogler, A.P. (2007). DNA-based taxonomy for associating adults and larvae in multi-species assemblages of chafers (Coleoptera: Scarabaeidae). *Molecular Phylogenetics and Evolution*, 44, 436–449.
- Ahrens, D., Dhoj Gc, Y., Lago, P. K. & Nagel, P. (2009). Seasonal fluctuation, phenology and turnover of chafer assemblages - insight to the structural plasticity of insect communities in tropical farmland (Coleoptera: Scarabaeidae). *Agricultural and Forest Entomology*, 11, 265–274.
- Ahrens, D., Schwarzer, J. & Vogler, A.P. (2014). The evolution of scarab beetles tracks the sequential rise of angiosperms and mammals. *Proceedings of the Royal Society B*, 281, 20141470.
- Arribas, P., Andujar, C., Salces-Castellano, A., Emerson, B.C., & Vogler, A.P. (2020). The limited spatial scale of dispersal in soil arthropods revealed with whole-community haplotype-level metabarcoding. *Molecular Ecology*, 1–14.
- Baselga, A., Gómez-Rodríguez, C., Araújo, M.B., Castro-Insua, A., Arenas, M., Posada, D. & Vogler, A.P. (2022). Joint analysis of species and genetic variation to quantify the role of dispersal and environmental constraints in community turnover. *Ecography*, e05808. <https://doi.org/10.1111/ecog.05808>
- Beck, J. & Kitching, I.J. (2007). Estimating regional species richness of tropical insects from museum data: a comparison of a geography-based and sample-based methods. *Journal of Applied Ecology*, 44, 672–681.
- Bosc, C. Hui, C., Roets, F., & Pauw, A. (2019). Importance of biotic niches versus drift in a plant-inhabiting arthropod community depends on rarity and trophic group. *Ecography*, 42, 1926–1935.
- Brehm, G., Zeuss, D., & Colwell, R.K. (2019). Moth body size increases with elevation along a complete tropical elevational gradient for two hyperdiverse clades. *Ecography*, 42(4), 632–642.
- Buckley, L.B., & Jetz, W. (2007). Environmental and historical constraints on global patterns of amphibian richness. *Proceedings of the Royal Society B*, 274, 1167–1173.
- Chao, A. & Lee, S.M. (1992). Estimating the number of classes via sample

- coverage. *Journal of the American Statistical Association*, 87, 210–217.
- Creedy, T. J., Ng, W. S., & Vogler, A. P. (2019). Toward accurate species-level metabarcoding of arthropod communities from the tropical forest canopy. *Ecology and Evolution*, 9 (6), 3105–3116.
- Daru, B.H., Farooq, H., Antonelli, A. & Faurby, S., (2020). Endemism patterns are scale dependent. *Nature Communications*, 11, 2115
- Davis, A.L.V., van Aarde, R.J., Scholtz, C.H., Guldmond, R.A.R., Fourie, J. & Deschodt, C.M., (2013). Is microclimate-driven turnover of dung beetle assemblage structure in regenerating coastal vegetation a precursor to re-establishment of a forest fauna? *Journal of Insect Conservation*, 17, 565–576. doi 10.1007/s10841-012-9542-8
- Danks, H.V. (1992). Long life cycles in insects. *The Canadian Entomologist*, 124(1), 167–187. doi:10.4039/ent124167-1
- Decaëns, T. (2010). Macroecological patterns in soil communities. *Global Ecology and Biogeography*, 19, 287–302.
- De Costa, W.A.J.M. (2008). Climate change in Sri Lanka: myth or reality? Evidence from long-term meteorological data. *Journal of National Science Foundation*, 36, 63–88
- De Oliveira, C.P., De Oliveira, C.M., Specht, A., & Frizzas, M.R. (2021). Seasonality and distribution of Coleoptera families (Arthropoda, Insecta) in the Cerrado of Central Brazil. *Revista Brasileira de Entomologia*, 65(3), e20210025.
- Eberle, J., Myburgh, R., & Ahrens, D. (2014). The Evolution of morphospace in phytophagous scarab chafers: no competition - no divergence? *PLoS ONE*, 9(5), e98536.
- Eberle, J., Fabrizi, S., Lago, P. & Ahrens, D. (2016). A historical biogeography of megadiverse Sericini – another story “out of Africa”? *Cladistics*, 33, 183–197.
- Eberle, J., Rödder, D., Beckett, M. & Ahrens, D. (2017). Landscape genetics indicate recently increased habitat fragmentation in African forest-associated chafers. *Global Change Biology*, 23, 1988–2004.
- Echevarría Ramos, M., & Hulshof, C.M. (2019). Using digitized museum collections to understand the effects of habitat on wing coloration in the Puerto Rican monarch. *Biotropica*, 51, 477–483.
- Fabrizi, S., & Ahrens, D. (2014). A Monograph of the Sericini of Sri Lanka (Coleoptera: Scarabaeidae). *Bonn Zoological Bulletin*, 61, 1–124.
- Gálvez-Reyes, N., Arribas, P., Andujar, C., Emerson, B., Píñero, D., & Mastretta-Yanes, A. (2020). Local-scale dispersal constraints promote spatial structure and arthropod diversity within a tropical sky-island. Preprint, *Authorea*. DOI: 10.22541/au.160193334.45224582/v1

- García-López, A., Micó, E., Numa, C. & Galante, E. (2010). Spatiotemporal variation of scarab beetle assemblages (Coleoptera: Scarabaeidae: Dynastinae, Melolonthinae, Rutelinae Rutelinae) in the premontane rain forest in Costa Rica: a question of scale. *Annals of the Entomological Society of America*, 103, 956–964.
- García-Lopez, A., Mico, E., Murria, C., Galante, E. & Vogler, A.P. (2013). Beta diversity at multiple hierarchical levels: explaining the high diversity of scarab beetles in tropical montane forests. *Journal of Biogeography*, 40, 2134–2145.
- Garcia-Robledo, C., Baer, C.S., Lippert, K., & Sarathy, V. (2020). Evolutionary history, not ecogeographic rules, explains size variation of tropical insects along elevational gradients. *Functional Ecology*, 34, 2513–2523.
- Gonçalves, M.P.G. (2020). Beetles and meteorological conditions: A case study. In: Meena, R. S., editor. *Agrometeorology*. London: IntechOpen. <https://www.intechopen.com/chapters/73943> doi: 10.5772/intechopen.94517
- Hammer, O., Harper, D.A.T. & Ryan, P.D. (2001). PAST: paleontological statistics software package for education and data analysis. *Palaeontologia Electronica*, 4, 1–9.
- Hill, M.O. (1973). Diversity and evenness: a unifying notation and its Consequences. *Ecology*, 54 (2), 427–432. doi:10.2307/1934352.
- Holt, B.G., Lessard, J.P., Borregaard, M.K., Fritz, S., Arajo, M.B., Dimitrov, D., Fabre, P.H., Graham, C.H., Graves, G.R., Jonsson, K., Nogués-Bravo, D., Wang, Z., Whittaker, R.J., Fjelds., J. & Rahbek, C. (2013). An update of Wallace’s zoogeographic regions of the world. *Science*, 339, 74–78.
- Inward, D.J.G., Davies, R.G., Pergande, C., Denham, A.J., & Vogler, A.P. (2011). Local and regional ecological morphology of dung beetle assemblages across four biogeographic regions. *Journal of Biogeography*, 38, 1668–1682.
- Jaccard, P. (1912). The distribution of the flora In the Alpine zone. *New Phytologist*. 11 (2), 37–50.
- Kemp, J.E., Linder, H.P. & Ellis, A.G. (2017). Beta diversity of herbivorous insects is coupled to high species and phylogenetic turnover of plant communities across short spatial scales in the Cape Floristic Region. *Journal of Biogeography*, 44, 1813–1823.
- Lira, A.F.A., Foerster, S.I.A., Albuquerque, C.M.R., & Moura, G.J.B. (2021). Contrasting patterns at interspecific and intraspecific levels in scorpion body size across a climatic gradient from rainforest to dryland vegetation. *Zoology (Jena)*, 146:125908. doi: 10.1016/j.zool.2021.125908.

- Luo, F., Meng, L., Aluthwattha, S.T., Lin, M., Weigel, A., Zhang, W., Qi, J. & Chen, J., (2021). Scale-dependent contribution of host-specificity and environmental factors to wood-boring longhorn beetle community assemblage in SW China, *Scientific Reports*, 11, 1. 10.1038/s41598-021-84511-3.
- Mani, M.S. (1968). Ecology and biogeography of high altitude insects. Junk, The Hague, 527pp.
- McKenna, D.D., Shin, S., Ahrens, D., Balke, M., Beza, C., Clarke, D.J., Donath, A., Escalona, H.E., Friedrich, F., Letsch, H., Liu, S., Maddison, D., Mayer, C., Misof, B., Murin, P. J., Niehuis, O., Peters, R.S., Podsiadlowski, L., Pohl, H., Scully, E.D., Yan, E.V., Zhou, X., Ślipiński, A., & Beutel, R.G. (2019). The evolution and genomic basis of beetle diversity. *Proceedings of the National Academy of Sciences*, 116(49), 24729–24737.
- Meegaskumbura, M., Wijayathilaka, N., Abayalath, N., & Senevirathne G. (2015). Realities of rarity: climatically and ecologically restricted, critically endangered Kandian Torrent Toads (*Adenomus kandianus*) breed en masse. PeerJ, *PrePrints*, <https://doi.org/10.7287/peerj>.
- Múrria, C., Bonada, N., Vellend, M., Zamora-Muñoz, C., Alba-Tercedor, J., Sainz-Cantero, C.E., Garrido, J., Acosta, R., El Alami, M., Barquín, J., Derka, T., Álvarez-Cabria, M., Sáinz-Bariain, M., Filipe, A.F., & Vogler, A.P. (2017). Local environment rather than past climate determines community composition of mountain stream macroinvertebrates across Europe. *Molecular Ecology*, 26, 6085–6099.
- Myers, N., Mittermeier, R., Mittermeier, C., da Fonseca, G. A. B., & Kent, J. (2000). Biodiversity hotspots for conservation priorities. *Nature*, 403, 853–858.
- Nielsen, U.N. (2019). Soil Fauna Assemblages. Global to local scales. Cambridge University Press, Cambridge, New York, Port Melbourne, 365pp.
- Novotny, V., Miller, S.E., Hulcr, J., Drew, R.A.I., Basset, Y., Janda, M. & Setliff, G.P. (2007). Low beta diversity of herbivorous insects in tropical forests. *Nature*, 448, 692–697.
- Numa, C. Verdú, J.R., Sánchez, A., & Galante, E. (2009). Effect of landscape structure on the spatial distribution of Mediterranean dung beetle diversity. *Diversity and Distribution*, 15, 489–501.
- Ødegaard, F. (2006). Host specificity, alpha- and beta-diversity of phytophagous beetles in two tropical forests in Panama. *Biodiversity and Conservation*, 15, 83–105.
- Perez, M.F., Franco, F.F., Bombonato, J.R., Bonatelli, I.S.A., Khan, G., Romeiro-Brito, M., Fegies, A.C., Ribeiro, P.M., Silva, G.A.R., & Moraes, E.M. (2018). Assessing population structure in the face of isolation by distance:

- Are we neglecting the problem? *Diversity and Distribution*, 24, 1883–1889.
- Ranasinghe, S., Eberle, J., Benjamin, S.P. & Ahrens, D. (2020). New species of Sericini from Sri Lanka (Coleoptera, Scarabaeidae). *European Journal of Taxonomy*, 621, 1–20.
- Ranasinghe, S., Eberle, J., Athukorala, N., Benjamin, S.P. & Ahrens, D. (2022). New species of Sericini from Sri Lanka (Coleoptera, Scarabaeidae). Part II. *European Journal of Taxonomy*, 821, 57–101.
- Ritcher, P.O. (1958). Biology of Scarabaeidae. *Annual Review of Entomology*, 3, 311–334.
- Romero, G.Q. (2016). Food web structure shaped by habitat size and climate across a latitudinal gradient. *Ecology*, 97, 2705–2715.
- Salomão, R.P., Arriaga-Jiménez, A., & Kohlmann, B. (2021). The relationship between altitudinal gradients, diversity, and body size in a dung beetle (Coleoptera: Scarabaeinae: Onthophagus) model system. *Canadian journal of zoology*, 99, 33–43. [dx.doi.org/10.1139/cjz-2020-0072](https://doi.org/10.1139/cjz-2020-0072). www.nrcresearchpress.com/cjz
- Santos, A.M.C. & Quicke, D. (2011). Large-scale diversity patterns of parasitoid insects. *Insect Science*, 14, 371–382.
- Schroeder, P.J. & Jenkins, D.G. (2018). How robust are popular beta diversity indices to sampling error? *Ecosphere*, 9(2), e02100.
- Shannon, C.E. (1948). A mathematical theory of communication. *Bell Labs Technical Journal*, 27, 379–423 and 623–656.
- Simpson, E.H. (1949). Measurement of diversity. *Nature*, 163 (4148), 688.
- Smith, T.J., Puttick, M.N., O'Reilly, J.E., Pisani, D., & Donoghue, P.C.J. (2021). Phylogenetic sampling affects evolutionary patterns of morphological disparity. *Palaeontology*, 64, 765–787.
- Stork, N.E., McBroom, J, Gely, C. & Hamilton, A.J. (2015). New approaches narrow global species estimates for beetles, insects, and terrestrial arthropods. *Proceedings of the National Academy of Sciences*, 112, 201502408.
- Tshikae, B.P., Davis, A.L.V. & Scholtz, C.H. (2013). Dung beetle assemblage structure across the aridity and trophic resource gradient of the Botswana Kalahari: patterns and drivers at regional and local scales, *Journal of Insect Conservation*, 17, 623–636.
- Yotkham, S., Suttiprapan, P., Likhitrakarn, N., Sulin, C. & Srisuka, W. (2021). Biodiversity and spatiotemporal variation of longhorn beetles (Coleoptera: Cerambycidae) in tropical forest of Thailand. *Insects*, 12, 45.
- Zou, Y. & Axmacher, J.C. (2021). Estimating the number of species shared by incompletely sampled communities. *Ecography*, 44, 1–11.

8.6 Supplementary Figures

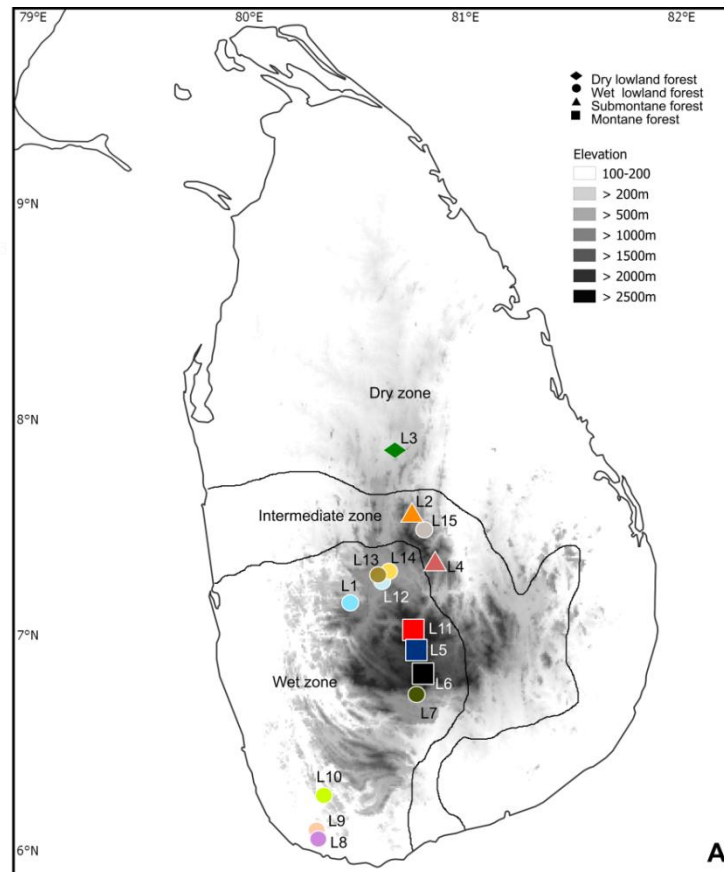


Figure S8.1. Map of Sri Lanka showing sampling sites. L1: Aranayake; L2: Riverston; L3: NIFS Arboretum; L4: Deenston; L5: Nuwara Eliya; L6: Horton Plains; L7: Belihuloya; L8: Hiyare; L9: Kottawa; L10: Kanneliya; L11: Piduruthalagala; L12: Uda Peradeniya; L13: Gannoruwa; L14: Udawattakele. Symbols represent different forest types.

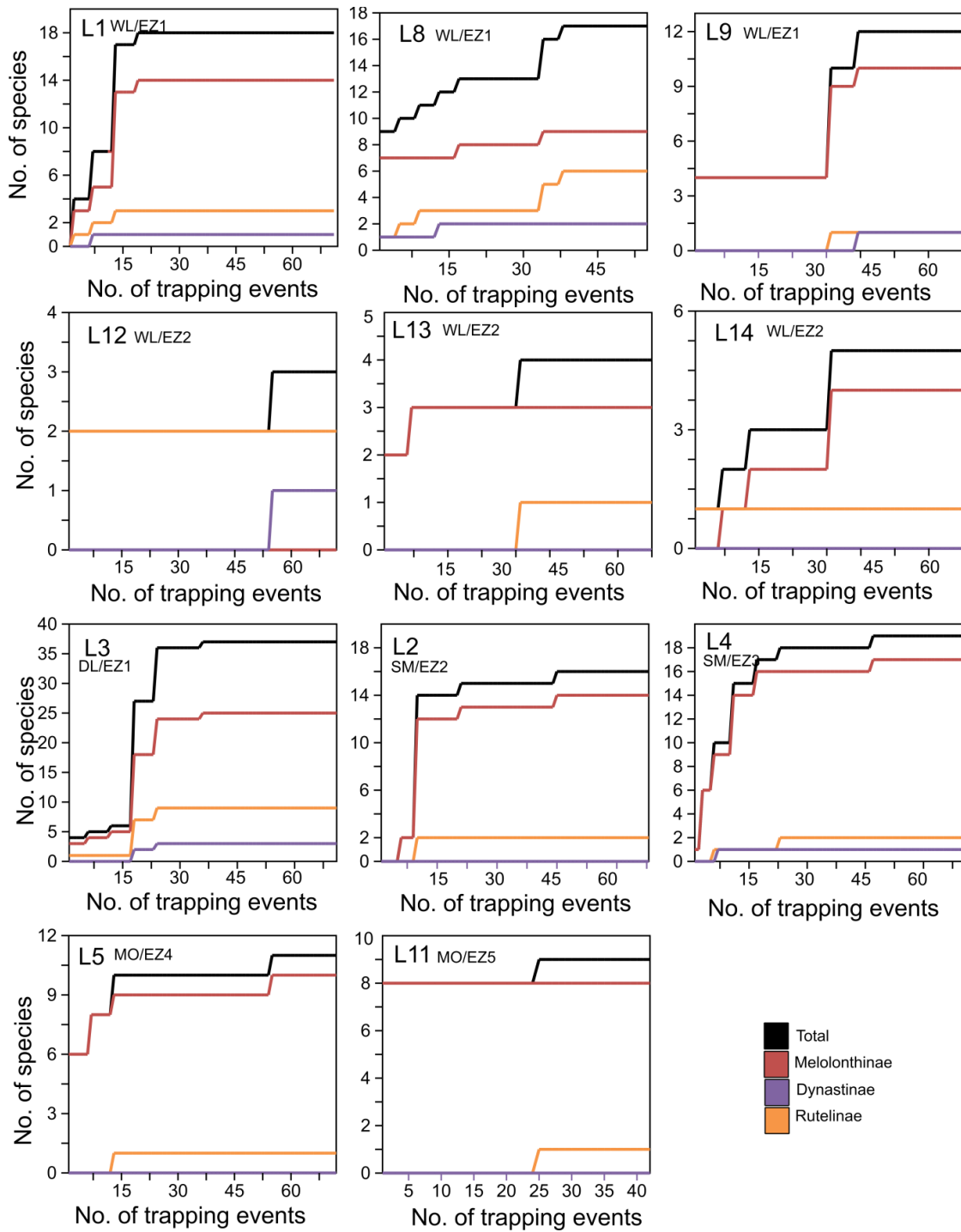


Figure S8.2. Species accumulation curves for each sampling locality for total species and subfamily level.

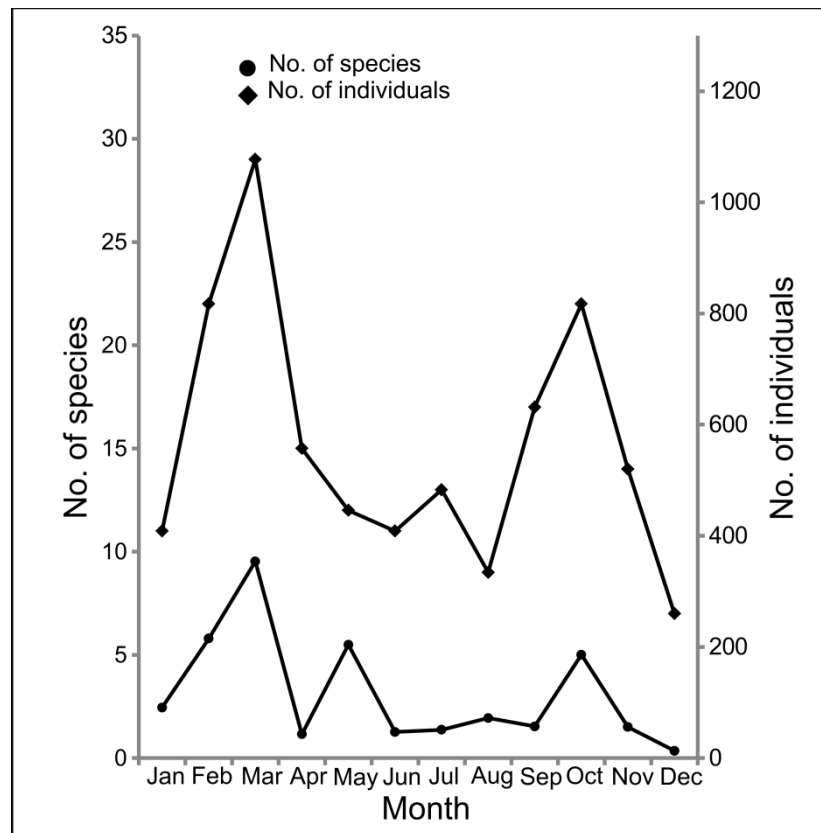


Figure S8.3. No. of species and no. of individuals of Sericini chafers among twelve months, based on data raised by Fabrizi and Ahrens, 2014; Ranasinghe et al., 2020.

Chapter 9

General discussion and conclusions

The study contributed considerably to the knowledge of scarab chafer biology, including their diversity, morphology, morphospace disparity, factors determining assemblage composition and synecology.

The standardized six-UV light trap sampling design allowed a detailed research on chafer assemblage diversity, turnover and their ecology. Standardized sampling encompassed 15 localities (L1–L15), covering different forest types (evergreen wet lowland forests, evergreen dry lowland forest, sub-montane forests and montane forests) along an elevational gradient (0–2500m). In total, 60–72 sampling events were conducted in most localities during both the rainy and dry seasons. Therefore, a quantitatively comparable sample which sufficiently represents the entire locality was obtained for subsequent analyses.

The extensive fieldwork revealed the high amount of endemism and confirmed how unexplored Sri Lanka is yet. Although the sampling was mainly carried out at the same sites repeatedly during four expeditions, different species within the assemblages were found that had not been previously collected. This might be due to seasonal change, as sampling was performed in both dry and wet seasons. Hence ‘new or rare’ species were reported in each expedition. Efforts on additional and more intensive sampling with light traps closer to remnant forest areas and not yet explored areas off the so far protected areas, may reveal further unknown taxa but also complete the knowledge of the fauna in a more comprehensive way, covering the entire land surface and landscape diversity of the Island.

During the study, fourteen new species of the Sericini were described. Consequently, the Sri Lankan fauna of Sericini now comprises 91 species, of which 81 are endemic. The study once more revealed a large amount of endemism, confirming that Sri Lanka remains unexplored, and that night active chafers are still rather poorly represented in material from occasional, non-specialized field surveys. Especially, most of the northern and eastern regions of

the country, located in the dry zone, have received limited sampling coverage, and that future surveys should focus on these regions.

The study confirmed that *COI* barcode data alone are unlikely to correctly delimit all species, in particular, when using only a single delimitation approach. The study showed that different delimitation methods (i.e., PTP, TCS, ABGD, ASAP and BIN assignments) resulted in different numbers of MOTUs and the congruence of delimitation between MOTUs and morphospecies expressed by the match ratio was low. A comparison of the outcome of all DNA-based species delimitation methods using Principal Coordinate Analysis (PCoA) based on pairwise match ratios, in which no method neither matched the other nor the morphospecies, confirmed this further.

Our study strongly discouraged approaches of a minimalist taxonomic procedure (Sharkey et al., 2021a, b) defining (new) species based on *COI* barcode data alone, using a single species delimitation approach only and without morphological reference diagnoses. A stable and robust nomenclature is the basis of clear communication and scientific discussion about biodiversity. In this manner, species entities and names provide the ‘anchor’ to which all taxonomic, ecological, molecular and conservation data are attached (International Trust for Zoological Nomenclature, 2008), also in legal protection and policy making strategies.

Moreover, due to incongruent outcomes from various species delimitation methods, particularly when researchers follow an integrative taxonomic approach provide certain ambiguities for synecological studies. The study showed that such method-related ambiguity of DNA-based species estimates severely affected the patterns of faunal similarity and thus, the certainty of biodiversity patterns at different spatial scales such as elevations, forest types, or sampling localities. Nevertheless, even more contrasting patterns results from individual clade-wise analyses of faunal similarity or even from cumulated species inventories from individual clade-wise species delimitation analysis. In this context, the study underlines the need of awareness when synecological observations from different studies are integrated which use different species delimitation methods for their biodiversity assessment. At the same time, the study showed why searching for proper species boundaries should be the ultimate goal of biodiversity assessment to place the trust in species delimitations to give an enduring meaning to biodiversity research and its sustainable application. In this even morphospecies, especially due to its globally complete and enormous reference system, remain a valid variable for biodiversity research.

In this context we discovered that almost all haplotypes were unique at any spatial entity, except in a few rare cases. Therefore, clustering of haplotype composition (based on shared characteristics, i.e., haplotypes) resulted almost meaningless due to missing of shared haplotypes. Therefore, the basis for an ordination was the amount of divergence alone. This resulted in hierarchical clustering often in unresolved polytomy of entities (see Figures 4.3, S4.4) which makes haplotypes a poor proxy for compositional comparison of species diversity, at least in hyperdiverse and ancient tropical habitats (Rodríguez et al., 2015; Cruz-Salazar et al., 2021).

The results of this study showed that phytophagous chafer assemblages were shaped mainly by locality stochastics, and to minor extent by ecoclimatic conditions. Locality stochastics represent a not further investigated multi-factor ensemble that includes all environmental conditions at local scale such as macrohabitat, biogeography, edaphic conditions, land use, local climate and exposition to rain and radiation. Macrohabitat had little effect on the assemblage composition. The significant correlation between species composition and geographic distance for the assemblage of small-bodied specimens is definitively linked to their limited dispersal capacity. Nevertheless, the study showed that seasonal change (dry-wet) in species composition was minor and only measurable in a few localities. Although seasonality and weather patterns may strongly impact patterns of assemblage composition in ecofaunistic analyses (Gonçalves, 2020), due to the tropical climate as well as with minor dry-wet seasonal change (rainy seasons and dry seasons are alternating in shorter intervals) together with the monsoon effect in Sri Lanka, and quite constant temperature and humidity throughout the year with continuously available food resources, thus minor fluctuations of species numbers may have an influence even in the tropical ecosystems.

The study for the first time, corroborated a general correlation between morphological disparity and species richness among phytophagous chafers at different ecochorological scales showing contrasting patterns of lineages at different geographical scales. The study showed the volume of morphospace that is occupied by lineages is supposed to mirror the heterogeneity of the species' ecological niches and may thus indicate resource partitioning and competition (Eberle et al., 2014). While at larger geographical scales the relation of species diversity vs. disparity is determined by the historical integration of a multitude of species or lineages, at local scale assembled species compete for space and resources. However, future studies need to explore more rigorously community composition at different landscape scales to disentangle the driving forces of

diversity vs disparity in the context of assemblage evolution among pleurostict chafers.

References

- Cruz-Salazar, B., Ruiz-Montoya, L., Ramírez-Marcial, N., & García-Bautista, M., (2021). Relationship between genetic variation and diversity of tree species in tropical forests in the El Ocote Biosphere Reserve, Chiapas, Mexico. *Tropical Conservation Science*, 14(1), <https://doi.org/10.1177/1940082920978143>
- Eberle, J., Myburgh, R., & Ahrens, D. (2014). The Evolution of morphospace in phytophagous scarab chafers: no competition - no divergence? *PLoS ONE*, 9(5), e98536.
- Gonçalves, M.P.G. (2020). Beetles and meteorological conditions: A case study. In: Meena, R. S., editor. *Agrometeorology*. London: IntechOpen. <https://www.intechopen.com/chapters/73943> doi: 10.5772/intechopen.94517
- International Trust for Zoological Nomenclature. (2008). Memorandum. House of Lords –Science and Technology –Writte evidence. <https://publications.parliament.uk/pa/ld200708/ldselect/ldsctech/162/162we25.htm>
- Rodríguez, A., Börner, M., Pabijan, M., Gehara, M., Haddad, C.F.B., & Vences, M. (2015). Genetic divergence in tropical anurans: deeper phylogeographic structure in forest specialists and in topographically complex regions. *Evolutionary ecology*, 29, 765–785.
- Sharkey, M.J., Janzen, D.H., Hallwachs, W., Chapman, E.G., Smith, M.A., Dapkey, T., Brown, A., Ratnasingham, S., Naik, S., Manjunath, R., Perez, K., Milton, M., Hebert, P., Shaw, S.R., Kittel, R.N., Solis, M.A., Metz, M.A., Goldstein, P.Z., Brown, J.W., Quicke, D.L.J., van Achterberg, C., Brown, B.V., & Burns, J.M. (2021a). Minimalist revision and description of 403 new species in 11 subfamilies of Costa Rican braconid parasitoid wasps, including host records for 219 species. *ZooKeys*, 1013, 1–665.
- Sharkey, M., Brown, B., Baker, A. & Mutanen, M. (2021b). Response to Zamani *et al.* (2020). The omission of critical data in the pursuit of “revolutionary” methods to accelerate the description of species. *ZooKeys*, 1033, 191–201.

Chapter 10

Supplement Tables

Table S3.1. Details of species; Voucher numbers, Species identification, sampling location (Sri Lanka) details with L numbers, Barcode Index Number (BIN) assignments and GenBank accession numbers.

Voucher ID	Species	District	Location	L Number	BIN	GenBank
X-SR0002	<i>Maladera fistulosa</i>	Nuwara Eliya District	Hakgala SNR	L5	BOLD:AEH7081	MW698428
X-SR0004	<i>Maladera badullana</i>	Nuwara Eliya District	Hakgala SNR	L5	BOLD:AEH7081	MW698377
X-SR0006	<i>Maladera badullana</i>	Nuwara Eliya District	Hakgala SNR	L5	BOLD:AEH7081	MW698281
X-SR0007	<i>Maladera hortonensis</i>	Nuwara Eliya District	Horton Plains	L6	BOLD:AEH5976	MW698406
X-SR0008	<i>Maladera hortonensis</i>	Nuwara Eliya District	Horton Plains	L6	BOLD:AEH5976	MW698437
X-SR0022	<i>Maladera badullana</i>	Nuwara Eliya District	Piduruthalagala FR	L11	BOLD:AEH7081	MW698340
X-SR0023	<i>Maladera badullana</i>	Nuwara Eliya District	Piduruthalagala FR	L11	BOLD:AEH7081	MW698379
X-SR0025	<i>Maladera dubia</i>	Nuwara Eliya District	Hakgala SNR	L5	BOLD:AEH6135	MW698210
X-SR0030	<i>Maladera breviatella</i>	Matale District	Dambulla	L3	BOLD:AEH4423	MW698320
X-SR0032	<i>Serica fusa</i>	Nuwara Eliya District	Horton Plains	L6	BOLD:AEH5844	MW698451
X-SR0033	<i>Serica fusa</i>	Nuwara Eliya District	Horton Plains	L6	BOLD:AEH5844	MW698455
X-SR0034	<i>Serica fusa</i>	Nuwara Eliya District	Horton Plains	L6	BOLD:AEH5844	MW698351
X-SR0035	<i>N. dharmapriyai</i>	Kegalle District	Aranayake	L1	BOLD:AEH7083	MW698308
X-SR0036	<i>M. galdaththana</i>	Kegalle District	Aranayake	L1	BOLD:AEH4344	MW698332
X-SR0037	<i>Maladera pubescens</i>	Kegalle District	Aranayake	L1	BOLD:AEH3996	MW698417
X-SR0040	<i>Maladera hortonensis</i>	Nuwara Eliya District	Piduruthalagala FR	L11	BOLD:AEH5976	MW698234

X-SR0042	<i>Serica fusa</i>	Nuwara Eliya District	Hakgala SNR	L5	BOLD:AEH5844	MW698355
X-SR0043	<i>Serica fusa</i>	Nuwara Eliya District	Hakgala SNR	L5	BOLD:AEH5844	MW698368
X-SR0044	<i>Serica fusa</i>	Nuwara Eliya District	Hakgala SNR	L5	BOLD:AEH5844	MW698253
X-SR0045	<i>Maladera badullana</i>	Nuwara Eliya District	Horton Plains	L6	BOLD:AEH7081	MW698260
X-SR0046	<i>Maladera dubia</i>	Nuwara Eliya District	Horton Plains	L6	BOLD:AEH6135	MW698245
X-SR0047	<i>Maladera dubia</i>	Nuwara Eliya District	Horton Plains	L6	BOLD:AEH6135	MW698391
X-SR0048	<i>Maladera badullana</i>	Nuwara Eliya District	Galways Land NP	L5	BOLD:AEH7081	MW698432
X-SR0049	<i>Maladera badullana</i>	Nuwara Eliya District	Galways Land NP	L5	BOLD:AEH7081	MW698330
X-SR0050	<i>Serica fusa</i>	Nuwara Eliya District	Galways Land NP	L5	BOLD:AEH5844	MW698229
X-SR0051	<i>Maladera breviatella</i>	Matale District	Dambulla	L3	BOLD:AEH4423	MW698362
X-SR0052	<i>Maladera breviatella</i>	Matale District	Dambulla	L3	BOLD:AEH4423	MW698285
X-SR0055	<i>Maladera lindulana</i>	Kandy District	Deenston	L4	BOLD:AEH5722	MW698359
X-SR0056	<i>Serica lurida</i>	Kandy District	Deenston	L4	BOLD:AEH5425	MW698214
X-SR0058	<i>Serica fusa</i>	Nuwara Eliya District	Piduruthalagala FR	L11	BOLD:AEH5844	MW698387
X-SR0059	<i>Serica fusa</i>	Nuwara Eliya District	Piduruthalagala FR	L11	BOLD:AEH5844	MW698354
X-SR0060	<i>Serica fusa</i>	Nuwara Eliya District	Piduruthalagala FR	L11	BOLD:AEH5844	MW698381
X-SR0062	<i>Maladera rufocuprea</i>	Kegalle District	Aranayake	L1	BOLD:AEH5150	MW698220
X-SR0063	<i>Maladera dubia</i>	Nuwara Eliya District	Horton Plains	L6	BOLD:AEH6135	MW698468
X-SR0064	<i>Maladera dubia</i>	Nuwara Eliya District	Horton Plains	L6	BOLD:AEH6135	MW698257
X-SR0068	<i>Serica fusa</i>	Nuwara Eliya District	Hakgala SNR	L5	BOLD:AEH5844	MW698321
X-SR0070	<i>Maladera badullana</i>	Nuwara Eliya District	Horton Plains	L6	BOLD:AEH7081	MW698326
X-SR0080	<i>Maladera rufocuprea</i>	Kegalle District	Aranayake	L1	BOLD:AEH5150	MW698336
X-SR0081	<i>Maladera rufocuprea</i>	Kegalle District	Aranayake	L1	BOLD:AEH5150	MW698353
X-SR0083	<i>Maladera hortonensis</i>	Nuwara Eliya District	Piduruthalagala FR	L11	BOLD:AEH5976	MW698408
X-SR0085	<i>Maladera hortonensis</i>	Nuwara Eliya District	Piduruthalagala FR	L11	BOLD:AEH5976	MW698211
X-SR0086	<i>Maladera calcarata</i>	Matale District	Dambulla	L3	BOLD:AEH6472	MW698448

X-SR0088	<i>Selaserica sp</i>	Matale District	Dambulla	L3	BOLD:AEH5331	MW698227
X-SR0089	<i>Maladera sp</i>	Matale District	Dambulla	L3	BOLD:AEH7067	MW698383
X-SR0090	<i>Maladera heveli</i>	Matale District	Dambulla	L3	BOLD:AEH8286	MW698205
X-SR0093	<i>M. galdathhana</i>	Kegalle District	Aranayake	L1	BOLD:AEH4344	MW698404
X-SR0094	<i>Maladera cinnaberina</i>	Kegalle District	Aranayake	L1	BOLD:AEH7181	MW698389
X-SR0095	<i>Apogonia sp</i>	Kegalle District	Aranayake	L1	BOLD:AEH3418	MW698424
X-SR0096	<i>Maladera coxalis</i>	Kegalle District	Aranayake	L1	BOLD:AEH6262	MW698392
X-SR0097	<i>Maladera pubescens</i>	Kegalle District	Aranayake	L1	BOLD:AEH3996	MW698233
X-SR0098	<i>Serica lurida</i>	Kandy District	Deenston	L4	BOLD:AEH5425	MW698366
X-SR0099	<i>Serica lurida</i>	Kandy District	Deenston	L4	BOLD:AEH5425	MW698446
X-SR0100	<i>Maladera calcarata</i>	Matale District	Dambulla	L3	BOLD:AEH6472	MW698277
X-SR0101	<i>Selaserica pusilla</i>	Matale District	Dambulla	L3	BOLD:AEH5010	MW698291
X-SR0106	<i>Maladera lindulana</i>	Kandy District	Deenston	L4	BOLD:AEH5722	MW698415
X-SR0108	<i>Maladera lindulana</i>	Kandy District	Deenston	L4	BOLD:AEH5722	MW698370
X-SR0115	<i>Neoserica sexfoliata</i>	Matale District	Dambulla	L3	BOLD:AEH7100	MW698293
X-SR0118	<i>Selaserica sp</i>	Nuwara Eliya District	Hakgala SNR	L5	BOLD:AEH6994	MW698467
X-SR0119	<i>Selaserica nitida</i>	Nuwara Eliya District	Hakgala SNR	L5	BOLD:AEH6994	MW698331
X-SR0121	<i>Maladera badullana</i>	Nuwara Eliya District	Horton Plains	L6	BOLD:AEH7081	MW698243
X-SR0126	<i>Maladera badullana</i>	Nuwara Eliya District	Piduruthalagala FR	L11	BOLD:AEH7081	MW698375
X-SR0127	<i>Maladera dubia</i>	Nuwara Eliya District	Piduruthalagala FR	L11	BOLD:AEH6135	MW698235
X-SR0130	<i>Maladera dubia</i>	Nuwara Eliya District	Hakgala SNR	L5	BOLD:AEH6135	MW698419
X-SR0132	<i>Maladera coxalis</i>	Kegalle District	Aranayake	L1	BOLD:AEH6264	MW698334
X-SR0133	<i>Maladera coxalis</i>	Kegalle District	Aranayake	L1	BOLD:AEH6264	MW698426
X-SR0134	<i>Maladera rotundata</i>	Kegalle District	Aranayake	L1	BOLD:AEH5377	MW698276
X-SR0142	<i>Maladera calcarata</i>	Matale District	Dambulla	L3	BOLD:AEH6472	MW698454
X-SR0145	<i>Sel. maculicauda</i>	Nuwara Eliya District	Horton Plains	L6	BOLD:AEH4591	MW698462

X-SR0147	<i>Maladera badullana</i>	Nuwara Eliya District	Galways Land NP	L5	BOLD:AEH7081	MW698342
X-SR0149	<i>Maladera dubia</i>	Nuwara Eliya District	Piduruthalagala FR	L11	BOLD:AEH6135	MW698259
X-SR0153	<i>Serica fusa</i>	Nuwara Eliya District	Hakgala SNR	L5	BOLD:AEH5844	MW698294
X-SR0154	<i>Serica fusa</i>	Nuwara Eliya District	Hakgala SNR	L5	BOLD:AEH5844	MW698439
X-SR0155	<i>Maladera cinnaberina</i>	Kegalle District	Aranayake	L1	BOLD:AEH7181	MW698317
X-SR0158	<i>Maladera rufocuprea</i>	Ratnapura District	Belihuloya	L7	BOLD:AEH5150	MW698263
X-SR0160	<i>Maladera fistulosa</i>	Nuwara Eliya District	Hakgala SNR	L5	BOLD:AEH7081	MW698398
X-SR0161	<i>Maladera dubia</i>	Nuwara Eliya District	Hakgala SNR	L5	BOLD:AEH6135	MW698322
X-SR0162	<i>Maladera fistulosa</i>	Nuwara Eliya District	Hakgala SNR	L5	BOLD:AEH7081	MW698266
X-SR0167	<i>Maladera hortonensis</i>	Nuwara Eliya District	Piduruthalagala FR	L11	BOLD:AEH5976	MW698206
X-SR0170	<i>Maladera hortonensis</i>	Nuwara Eliya District	Horton Plains	L6	BOLD:AEH5976	MW698367
X-SR0174	<i>Maladera lindulana</i>	Kandy District	Deenston	L4	BOLD:AEH5722	MW698345
X-SR0175	<i>Selaserica athukoralai</i>	Matale District	Riverston	L2	BOLD:AEH8417	MW698298
X-SR0177	<i>Maladera dubia</i>	Nuwara Eliya District	Hakgala SNR	L5	BOLD:AEH6135	MW698420
X-SR0184	<i>Maladera dubia</i>	Nuwara Eliya District	Piduruthalagala FR	L11	BOLD:AEH6135	MW698403
X-SR0186	<i>Selaserica sp</i>	Kandy District	Deenston	L4	BOLD:AEH7391	MW698445
X-SR0187	<i>Maladera deenstana</i>	Kandy District	Deenston	L4	BOLD:AEH7198	MW698230
X-SR0188	<i>Maladera cervicornis</i>	Matale District	Riverston	L2	BOLD:AEH8443	MW698244
X-SR0189	<i>Maladera cervicornis</i>	Matale District	Riverston	L2	BOLD:AEH8443	MW698453
X-SR0190	<i>Periserica sp</i>	Kandy District	Deenston	L4	BOLD:AEH6212	MW698382
X-SR0202	<i>Maladera coxalis</i>	Matale District	Dambulla	L3	BOLD:AEH8752	MW698443
X-SR0206	<i>Selaserica pusilla</i>	Matale District	Dambulla	L3	BOLD:AEH5010	MW698231
X-SR0209	<i>Maladera dambullana</i>	Matale District	Dambulla	L3	BOLD:AEH7262	MW698226
X-SR0210	<i>Maladera dambullana</i>	Matale District	Dambulla	L3	BOLD:AEH3995	MW698315
X-SR0224	<i>Sel. sororinitida</i>	Kandy District	Deenston	L4	BOLD:AEH7391	MW698223
X-SR0227	<i>Sel. sororinitida</i>	Kandy District	Deenston	L4	BOLD:AEH7391	MW698349

X-SR0245	<i>Maladera haniel</i>	Kandy District	Deenston	L4	BOLD:AEH8443	MW698440
X-SR0251	<i>Maladera haniel</i>	Kandy District	Deenston	L4	BOLD:AEH8443	MW698254
X-SR0252	<i>Selaserica pusilla</i>	Matale District	Dambulla	L3	BOLD:AEH5010	MW698221
X-SR0269	<i>Maladera dambullana</i>	Matale District	Dambulla	L3	BOLD:AEH7262	MW698449
X-SR0290	<i>Maladera coxalis</i>	Matale District	Dambulla	L3	BOLD:AEH8752	MW698288
X-SR0301	<i>Maladera dambullana</i>	Matale District	Dambulla	L3	BOLD:AEH7262	MW698361
X-SR0309	<i>Maladera calcarata</i>	Matale District	Dambulla	L3	BOLD:AEH6472	MW698438
X-SR0319	<i>Neoserica sexfoliata</i>	Matale District	Dambulla	L3	BOLD:AEH7100	MW698452
X-SR0320	<i>Maladera coxalis</i>	Matale District	Dambulla	L3	BOLD:AEH8752	MW698337
X-SR0326	<i>Maladera tricuspidata</i>	Matale District	Dambulla	L3	BOLD:AEH5496	MW698225
X-SR0327	<i>Neoserica sexfoliata</i>	Matale District	Dambulla	L3	BOLD:AEH7100	MW698251
X-SR0333	<i>Neoserica pophami</i>	Matale District	Dambulla	L3	BOLD:AEH4365	MW698239
X-SR0341	<i>Maladera dambullana</i>	Matale District	Dambulla	L3	BOLD:AEH7262	MW698447
X-SR0346	<i>Neoserica pophami</i>	Matale District	Dambulla	L3	BOLD:AEH4366	MW698287
X-SR0349	<i>Maladera breviatella</i>	Matale District	Dambulla	L3	BOLD:AEH4423	MW698397
X-SR0350	<i>Maladera breviatella</i>	Matale District	Dambulla	L3	BOLD:AEH4423	MW698215
X-SR0363	<i>Maladera dambullana</i>	Matale District	Dambulla	L3	BOLD:AEH7262	MW698289
X-SR0372	<i>Maladera setosa</i>	Matale District	Dambulla	L3	BOLD:AEH6169	MW698402
X-SR0392	<i>Maladera coxalis</i>	Matale District	Dambulla	L3	BOLD:AEH6964	MW698255
X-SR0404	<i>Maladera heveli</i>	Matale District	Dambulla	L3	BOLD:AEH4245	MW698459
X-SR0405	<i>Maladera setosa</i>	Matale District	Dambulla	L3	BOLD:AEH6169	MW698358
X-SR0406	<i>Maladera heveli</i>	Matale District	Dambulla	L3	BOLD:AEH4245	MW698297
X-SR0413	<i>Selaserica pusilla</i>	Matale District	Dambulla	L3	BOLD:AEH5010	MW698457
X-SR0414	<i>Maladera dambullana</i>	Matale District	Dambulla	L3	BOLD:AEH7262	MW698363
X-SR0417	<i>Neoserica pophami</i>	Matale District	Dambulla	L3	BOLD:AEH4365	MW698378
X-SR0423	<i>Neoserica pophami</i>	Matale District	Dambulla	L3	BOLD:AEH4365	MW698280

X-SR0452	<i>Maladera coxalis</i>	Matale District	Dambulla	L3	BOLD:AEH8752	MW698463
X-SR0457	<i>Maladera setosa</i>	Matale District	Dambulla	L3	BOLD:AEH6169	MW698286
X-SR0471	<i>Neoserica pophami</i>	Matale District	Dambulla	L3	BOLD:AEH4365	MW698212
X-SR0488	<i>Neoserica pophami</i>	Matale District	Dambulla	L3	BOLD:AEH4366	MW698373
X-SR0500	<i>Maladera heveli</i>	Matale District	Dambulla	L3	BOLD:AEH4244	MW698319
X-SR0504	<i>Selaserica pusilla</i>	Matale District	Dambulla	L3	BOLD:AEH5010	MW698312
X-SR0505	<i>Selaserica pusilla</i>	Matale District	Dambulla	L3	BOLD:AEH5010	MW698344
X-SR0529	<i>Maladera rufocuprea</i>	Kandy District	Deenston	L4	BOLD:AEH5150	MW698301
X-SR0530	<i>Maladera rufocuprea</i>	Kandy District	Deenston	L4	BOLD:AEH5150	MW698328
X-SR0531	<i>Maladera rufocuprea</i>	Kandy District	Deenston	L4	BOLD:AEH5150	MW698461
X-SR0534	<i>Maladera anderssoni</i>	Kandy District	Deenston	L4	BOLD:AEH8444	MW698299
X-SR0535	<i>Maladera anderssoni</i>	Kandy District	Deenston	L4	BOLD:AEH8444	MW698284
X-SR0543	<i>Maladera igua</i>	Kandy District	Deenston	L4	BOLD:AEH8370	MW698441
X-SR0546	<i>Maladera kishi</i>	Kandy District	Deenston	L4	BOLD:AEH4589	MW698265
X-SR0548	<i>Maladera kishi</i>	Kandy District	Deenston	L4	BOLD:AEH4589	MW698218
X-SR0552	<i>Maladera haniel</i>	Kandy District	Deenston	L4	BOLD:AEH8443	MW698219
X-SR0559	<i>Maladera anderssoni</i>	Kandy District	Deenston	L4	BOLD:AEH8444	MW698216
X-SR0560	<i>Serica lurida</i>	Kandy District	Deenston	L4	BOLD:AEH5425	MW698249
X-SR0563	<i>Sel. sororinitida</i>	Kandy District	Deenston	L4	BOLD:AEH7391	MW698335
X-SR0565	<i>Maladera kishi</i>	Kandy District	Deenston	L4	BOLD:AEH4589	MW698264
X-SR0566	<i>Maladera kishi</i>	Kandy District	Deenston	L4	BOLD:AEH4589	MW698460
X-SR0580	<i>Maladera windy</i>	Kandy District	Deenston	L4	BOLD:AEH5536	MW698303
X-SR0583	<i>Maladera cervicornis</i>	Matale District	Riverston	L2	BOLD:AEH8443	MW698271
X-SR0589	<i>Selaserica pusilla</i>	Matale District	Riverston	L2	BOLD:AEH5009	MW698365
X-SR0591	<i>Serica lurida</i>	Matale District	Riverston	L2	BOLD:AEH5425	MW698425
X-SR0621	<i>Maladera cervicornis</i>	Matale District	Riverston	L2	BOLD:AEH8443	MW698341

X-SR0627	<i>Selaserica pusilla</i>	Matale District	Riverston	L2	BOLD:AEH5008	MW698393
X-SR0631	<i>Selaserica pusilla</i>	Matale District	Riverston	L2	BOLD:AEH5008	MW698302
X-SR0652	<i>Maladera rufocuprea</i>	Matale District	Riverston	L2	BOLD:AEH5150	MW698390
X-SR0653	<i>Maladera cervicornis</i>	Matale District	Riverston	L2	BOLD:AEH8443	MW698405
X-SR0654	<i>Selaserica pusilla</i>	Matale District	Riverston	L2	BOLD:AEH5009	MW698343
X-SR0655	<i>Selaserica pusilla</i>	Matale District	Riverston	L2	BOLD:AEH5009	MW698217
X-SR0659	<i>Maladera coxalis</i>	Matale District	Riverston	L2	BOLD:AEH6236	MW698427
X-SR0660	<i>Maladera cervicornis</i>	Matale District	Riverston	L2	BOLD:AEH8443	MW698246
X-SR0664	<i>Sel.a sororinitida</i>	Kandy District	Deenston	L4	BOLD:AEH7391	MW698433
X-SR0666	<i>M.bandarawelana</i>	Matale District	Riverston	L2	BOLD:AEH5956	MW698309
X-SR0669	<i>Sel. sororinitida</i>	Kandy District	Deenston	L4	BOLD:AEH7391	MW698292
X-SR0670	<i>Sel. sororinitida</i>	Kandy District	Deenston	L4	BOLD:AEH7391	MW698395
X-SR0672	<i>Maladera cervicornis</i>	Matale District	Riverston	L2	BOLD:AEH8443	MW698327
X-SR0707	<i>Maladera anderssoni</i>	Kandy District	Deenston	L4	BOLD:AEH8445	MW698348
X-SR0708	<i>Maladera haniel</i>	Kandy District	Deenston	L4	BOLD:AEH8443	MW698307
X-SR0709	<i>Maladera anderssoni</i>	Kandy District	Deenston	L4	BOLD:AEH8444	MW698305
X-SR0713	<i>Serica fusa</i>	Nuwara Eliya District	Hakgala SNR	L5	BOLD:AEH5844	MW698296
X-SR0714	<i>Serica fusa</i>	Nuwara Eliya District	Hakgala SNR	L5	BOLD:AEH5844	MW698385
X-SR0717	<i>Serica fusa</i>	Nuwara Eliya District	Hakgala SNR	L5	BOLD:AEH5844	MW698372
X-SR0720	<i>Maladera dubia</i>	Nuwara Eliya District	Hakgala SNR	L5	BOLD:AEH6135	MW698431
X-SR0721	<i>Maladera dubia</i>	Nuwara Eliya District	Hakgala SNR	L5	BOLD:AEH6135	MW698418
X-SR0722	<i>Maladera dubia</i>	Nuwara Eliya District	Hakgala SNR	L5	BOLD:AEH6135	MW698273
X-SR0723	<i>Maladera dubia</i>	Nuwara Eliya District	Hakgala SNR	L5	BOLD:AEH6135	MW698252
X-SR0724	<i>Maladera kishi</i>	Kandy District	Deenston	L4	BOLD:AEH4589	MW698283
X-SR0730	<i>Maladera kishi</i>	Kandy District	Deenston	L4	BOLD:AEH4589	MW698436
X-SR0757	<i>Maladera windy</i>	Kandy District	Deenston	L4	BOLD:AEH3994	MW698369

X-SR0769	<i>Maladera windy</i>	Kandy District	Deenston	L4	BOLD:AEH3994	MW698347
X-SR0773	<i>Maladera rufocuprea</i>	Kandy District	Deenston	L4	BOLD:AEH5150	MW698400
X-SR0774	<i>Maladera rufocuprea</i>	Kandy District	Deenston	L4	BOLD:AEH5150	MW698429
X-SR0776	<i>Maladera haniel</i>	Kandy District	Deenston	L4	BOLD:AEH8443	MW698421
X-SR0781	<i>Maladera haniel</i>	Kandy District	Deenston	L4	BOLD:AEH8443	MW698414
X-SR0790	<i>Maladera windy</i>	Kandy District	Deenston	L4	BOLD:AEH3994	MW698456
X-SR0808	<i>Serica lurida</i>	Kandy District	Deenston	L4	BOLD:AEH5425	MW698300
X-SR0810	<i>Serica lurida</i>	Kandy District	Deenston	L4	BOLD:AEH5425	MW698236
X-SR0815	<i>Maladera weligamana</i>	Nuwara Eliya District	Hakgala SNR	L5	BOLD:AEH7197	MW698339
X-SR0819	<i>Maladera dubia</i>	Nuwara Eliya District	Hakgala SNR	L5	BOLD:AEH6135	MW698222
X-SR0820	<i>Maladera dubia</i>	Nuwara Eliya District	Hakgala SNR	L5	BOLD:AEH6135	MW698356
X-SR0830	<i>Maladera dubia</i>	Nuwara Eliya District	Hakgala SNR	L5	BOLD:AEH6135	MW698401
X-SR0833	<i>Maladera dubia</i>	Nuwara Eliya District	Hakgala SNR	L5	BOLD:AEH6135	MW698469
X-SR0835	<i>Maladera weligamana</i>	Nuwara Eliya District	Hakgala SNR	L5	BOLD:AEH7197	MW698310
X-SR0837	<i>Maladera dubia</i>	Nuwara Eliya District	Hakgala SNR	L5	BOLD:AEH6135	MW698325
X-SR0839	<i>Maladera rufocuprea</i>	Galle District	Hiyare FR	L8	BOLD:AEH5150	MW698306
X-SR0840	<i>Maladera rufocuprea</i>	Galle District	Hiyare FR	L8	BOLD:AEH5150	MW698338
X-SR0841	<i>Maladera rufocuprea</i>	Galle District	Hiyare FR	L8	BOLD:AEH5150	MW698399
X-SR0843	<i>Maladera rufocuprea</i>	Galle District	Hiyare FR	L8	BOLD:AEH5150	MW698407
X-SR0847	<i>Maladera rufocuprea</i>	Galle District	Hiyare FR	L8	BOLD:AEH5150	MW698275
X-SR0855	<i>Selaserica impexa</i>	Galle District	Hiyare FR	L8	BOLD:AEH7222	MW698290
X-SR0856	<i>Selaserica impexa</i>	Galle District	Kanneliya FR	L10	BOLD:AEH7223	MW698413
X-SR0857	<i>Selaserica impexa</i>	Galle District	Kanneliya FR	L10	BOLD:AEH7223	MW698333
X-SR0858	<i>Sel. convexiuscula</i>	Galle District	Kottawa FR	L9	BOLD:AEH6645	MW698268
X-SR0859	<i>Selaserica fabriziae</i>	Galle District	Kottawa FR	L9	BOLD:AEH6644	MW698316
X-SR0862	<i>Maladera pubescens</i>	Kegalle District	Aranayake	L1	BOLD:AEH3996	MW698272

X-SR0864	<i>Maladera rufocuprea</i>	Matale District	Riverston	L2	BOLD:AEH5150	MW698282
X-SR0865	<i>Maladera rufocuprea</i>	Matale District	Riverston	L2	BOLD:AEH5150	MW698444
X-SR0866	<i>Maladera laterita</i>	Matale District	Riverston	L2	BOLD:AEH6029	MW698465
X-SR0877	<i>Maladera rufocuprea</i>	Matale District	Riverston	L2	BOLD:AEH5150	MW698207
X-SR0881	<i>M. bandarawelana</i>	Matale District	Riverston	L2	BOLD:AEH5956	MW698374
X-SR0882	<i>M. bandarawelana</i>	Matale District	Riverston	L2	BOLD:AEH5956	MW698466
X-SR0887	<i>M. karunaratnae</i>	Matale District	Riverston	L2	BOLD:AEH8445	MW698237
X-SR0889	<i>Serica lurida</i>	Matale District	Riverston	L2	BOLD:AEH5425	MW698422
X-SR0895	<i>Selaserica pusilla</i>	Matale District	Riverston	L2	BOLD:AEH5009	MW698208
X-SR0898	<i>Serica lurida</i>	Matale District	Riverston	L2	BOLD:AEH5425	MW698240
X-SR0901	<i>Serica lurida</i>	Matale District	Riverston	L2	BOLD:AEH5425	MW698371
X-SR0902	<i>Serica lurida</i>	Matale District	Riverston	L2	BOLD:AEH5425	MW698270
X-SR0906	<i>Serica lurida</i>	Matale District	Riverston	L2	BOLD:AEH5425	MW698304
X-SR0915	<i>Sel. sororinitida</i>	Kandy District	Deenston	L4	BOLD:AEH7391	MW698278
X-SR0922	<i>Maladera anderssoni</i>	Kandy District	Deenston	L4	BOLD:AEH8444	MW698450
X-SR0936	<i>Maladera kishi</i>	Kandy District	Deenston	L4	BOLD:AEH4589	MW698213
X-SR0949	<i>Maladera anderssoni</i>	Kandy District	Deenston	L4	BOLD:AEH8444	MW698396
X-SR0975	<i>Maladera coxalis</i>	Matale District	Dambulla	L3	BOLD:AEH6964	MW698311
X-SR0985	<i>Maladera dambullana</i>	Matale District	Dambulla	L3	BOLD:AEH7262	MW698380
X-SR0988	<i>Maladera heveli</i>	Matale District	Dambulla	L3	BOLD:AEH5052	MW698410
X-SR0989	<i>Maladera heveli</i>	Matale District	Dambulla	L3	BOLD:AEH5052	MW698224
X-SR0992	<i>Maladera coxalis</i>	Matale District	Dambulla	L3	BOLD:AEH6263	MW698241
X-SR1010	<i>M. karunaratnae</i>	Matale District	Dambulla	L3	BOLD:AEH8445	MW698232
X-SR1013	<i>Maladera setosa</i>	Matale District	Dambulla	L3	BOLD:AEH6169	MW698238
X-SR1014	<i>Neoserica pophami</i>	Matale District	Dambulla	L3	BOLD:AEH4365	MW698256
X-SR1029	<i>M. karunaratnae</i>	Matale District	Dambulla	L3	BOLD:AEH8445	MW698394

X-SR1030	<i>M. karunaratnae</i>	Matale District	Dambulla	L3	BOLD:AEH8445	MW698247
X-SR1046	<i>M. padaviyaensis</i>	Matale District	Dambulla	L3	BOLD:AEH6028	MW698209
X-SR1047	<i>Maladera setosa</i>	Matale District	Dambulla	L3	BOLD:AEH6169	MW698423
X-SR1087	<i>M.karunaratnae</i>	Matale District	Dambulla	L3	BOLD:AEH8445	MW698258
X-SR1093	<i>Neoserica sexfoliata</i>	Matale District	Dambulla	L3	BOLD:AEH7100	MW698435
X-SR1100	<i>Maladera heveli</i>	Matale District	Dambulla	L3	BOLD:AEH8286	MW698204
X-SR1101	<i>Maladera heveli</i>	Matale District	Dambulla	L3	BOLD:AEH8287	MW698248
X-SR1109	<i>Neoserica sexfoliata</i>	Matale District	Dambulla	L3	BOLD:AEH7101	MW698458
X-SR1110	<i>Neoserica sexfoliata</i>	Matale District	Dambulla	L3	BOLD:AEH7101	MW698411
X-SR1113	<i>M. karunaratnae</i>	Matale District	Dambulla	L3	BOLD:AEH8445	MW698442
X-SR1129	<i>N. dharmapriyai</i>	Kegalle District	Aranayake	L1	BOLD:AEH7083	MW698360
X-SR1130	<i>Maladera rotundata</i>	Kegalle District	Aranayake	L1	BOLD:AEH5377	MW698262
X-SR1132	<i>Maladera rotundata</i>	Kegalle District	Aranayake	L1	BOLD:AEH5377	MW698329
X-SR1133	<i>Maladera rotundata</i>	Kegalle District	Aranayake	L1	BOLD:AEH5377	MW698388
X-SR1135	<i>Sel. sororinitida</i>	Kandy District	Deenston	L4	BOLD:AEH7391	MW698324
X-SR1154	<i>Maladera badullana</i>	Nuwara Eliya District	Hakgala SNR	L5	BOLD:AEH7081	MW698416
X-SR1155	<i>Maladera badullana</i>	Nuwara Eliya District	Hakgala SNR	L5	BOLD:AEH7081	MW698228
X-SR1158	<i>Maladera fistulosa</i>	Nuwara Eliya District	Hakgala SNR	L5	BOLD:AEH7081	MW698350
X-SR1166	<i>Maladera hortonensis</i>	Nuwara Eliya District	Piduruthalagala FR	L11	BOLD:AEH5976	MW698267
X-SR1167	<i>Maladera hortonensis</i>	Nuwara Eliya District	Piduruthalagala FR	L11	BOLD:AEH5976	MW698314
X-SR1172	<i>Maladera hortonensis</i>	Nuwara Eliya District	Piduruthalagala FR	L11	BOLD:AEH5976	MW698430
X-SR1173	<i>Maladera hortonensis</i>	Nuwara Eliya District	Piduruthalagala FR	L11	BOLD:AEH5976	MW698242
X-SR1183	<i>Maladera hortonensis</i>	Nuwara Eliya District	Piduruthalagala FR	L11	BOLD:AEH5976	MW698376
X-SR1185	<i>Maladera badullana</i>	Nuwara Eliya District	Piduruthalagala FR	L11	BOLD:AEH7081	MW698346
X-SR1189	<i>Maladera badullana</i>	Nuwara Eliya District	Piduruthalagala FR	L11	BOLD:AEH7081	MW698357
X-SR1191	<i>Maladera badullana</i>	Nuwara Eliya District	Piduruthalagala FR	L11	BOLD:AEH7081	MW698386

X-SR1192	<i>Maladera hortonensis</i>	Nuwara Eliya District	Piduruthalagala FR	L11	BOLD:AEH5976	MW698318
X-SR1193	<i>Maladera badullana</i>	Nuwara Eliya District	Piduruthalagala FR	L11	BOLD:AEH7081	MW698279
X-SR1195	<i>Selaserica nitida</i>	Nuwara Eliya District	Piduruthalagala FR	L11	BOLD:AEH6994	MW698261
X-SR1197	<i>Selaserica nitida</i>	Nuwara Eliya District	Piduruthalagala FR	L11	BOLD:AEH6994	MW698384
X-SR1210	<i>Selaserica nitida</i>	Nuwara Eliya District	Horton Plains	L6	BOLD:AEH6993	MW698364
X-SR1211	<i>Sel. maculicauda</i>	Nuwara Eliya District	Horton Plains	L6	BOLD:AEH4591	MW698313
X-SR1212	<i>Selaserica nitida</i>	Nuwara Eliya District	Horton Plains	L6	BOLD:AEH6993	MW698434
X-SR1213	<i>Selaserica nitida</i>	Nuwara Eliya District	Horton Plains	L6	BOLD:AEH6993	MW698409
X-SR1218	<i>Maladera hortonensis</i>	Nuwara Eliya District	Horton Plains	L6	BOLD:AEH5976	MW698352
X-SR1223	<i>Selaserica nitida</i>	Nuwara Eliya District	Horton Plains	L6	BOLD:AEH6993	MW698412
X-SR1228	<i>Maladera dubia</i>	Nuwara Eliya District	Horton Plains	L6	BOLD:AEH6135	MW698295
X-SR1229	<i>Maladera dubia</i>	Nuwara Eliya District	Horton Plains	L6	BOLD:AEH6135	MW698323
X-SR1230	<i>Maladera dubia</i>	Nuwara Eliya District	Horton Plains	L6	BOLD:AEH6135	MW698274
X-SR1232	<i>Selaserica nitida</i>	Nuwara Eliya District	Horton Plains	L6	BOLD:AEH6993	MW698464

Table S4.1. Sample details: voucher number, species identification, locality id (Sri Lanka), barcode index number (BIN) assignments and GenBank accession numbers.

Voucher ID	Species	District	Location	Locality id	BIN	GenBank	Elevation zone	Forest
X-SR0002	<i>Maladera fistulosa</i>	Nuwara Eliya	Hakgala SNR	L5	BOLD:AEH7081	MW698428	EZ4	MO
X-SR0004	<i>Maladera badullana</i>	Nuwara Eliya	Hakgala SNR	L5	BOLD:AEH7081	MW698377	EZ4	MO
X-SR0006	<i>Maladera badullana</i>	Nuwara Eliya	Hakgala SNR	L5	BOLD:AEH7081	MW698281	EZ4	MO
X-SR0007	<i>Maladera hortonensis</i>	Nuwara Eliya	Horton Plains	L6	BOLD:AEH5976	MW698406	EZ5	MO
X-SR0008	<i>Maladera hortonensis</i>	Nuwara Eliya	Horton Plains	L6	BOLD:AEH5976	MW698437	EZ5	MO
X-SR0022	<i>Maladera badullana</i>	Nuwara Eliya	Piduruthalagala FR	L11	BOLD:AEH7081	MW698340	EZ5	LW1
X-SR0023	<i>Maladera badullana</i>	Nuwara Eliya	Piduruthalagala FR	L11	BOLD:AEH7081	MW698379	EZ5	LW1
X-SR0025	<i>Maladera dubia</i>	Nuwara Eliya	Hakgala SNR	L5	BOLD:AEH6135	MW698210	EZ4	MO
X-SR0030	<i>Maladera breviatella</i>	Matale	Dambulla	L3	BOLD:AEH4423	MW698320	EZ1	LD
X-SR0032	<i>Serica fusa</i>	Nuwara Eliya	Horton Plains	L6	BOLD:AEH5844	MW698451	EZ5	MO
X-SR0033	<i>Serica fusa</i>	Nuwara Eliya	Horton Plains	L6	BOLD:AEH5844	MW698455	EZ5	MO
X-SR0034	<i>Serica fusa</i>	Nuwara Eliya	Horton Plains	L6	BOLD:AEH5844	MW698351	EZ5	MO
X-SR0035	<i>Neoserica dharmapriyai</i>	Kegalle	Aranayake	L1	BOLD:AEH7083	MW698308	EZ1	LW
X-SR0036	<i>Maladera galdathhana</i>	Kegalle	Aranayake	L1	BOLD:AEH4344	MW698332	EZ1	LW
X-SR0037	<i>Maladera pubescens</i>	Kegalle	Aranayake	L1	BOLD:AEH3996	MW698417	EZ1	LW
X-SR0040	<i>Maladera hortonensis</i>	Nuwara Eliya	Piduruthalagala FR	L11	BOLD:AEH5976	MW698234	EZ5	MO
X-SR0042	<i>Serica fusa</i>	Nuwara Eliya	Hakgala SNR	L5	BOLD:AEH5844	MW698355	EZ4	MO
X-SR0043	<i>Serica fusa</i>	Nuwara Eliya	Hakgala SNR	L5	BOLD:AEH5844	MW698368	EZ4	MO
X-SR0044	<i>Serica fusa</i>	Nuwara Eliya	Hakgala SNR	L5	BOLD:AEH5844	MW698253	EZ4	MO
X-SR0045	<i>Maladera badullana</i>	Nuwara Eliya	Horton Plains	L6	BOLD:AEH7081	MW698260	EZ5	MO
X-SR0046	<i>Maladera dubia</i>	Nuwara Eliya	Horton Plains	L6	BOLD:AEH6135	MW698245	EZ5	MO

X-SR0047	<i>Maladera dubia</i>	Nuwara Eliya	Horton Plains	L6	BOLD:AEH6135	MW698391	EZ5	MO
X-SR0048	<i>Maladera badullana</i>	Nuwara Eliya	Galways Land NP	L5	BOLD:AEH7081	MW698432	EZ4	MO
X-SR0049	<i>Maladera badullana</i>	Nuwara Eliya	Galways Land NP	L5	BOLD:AEH7081	MW698330	EZ4	MO
X-SR0050	<i>Serica fusa</i>	Nuwara Eliya	Galways Land NP	L5	BOLD:AEH5844	MW698229	EZ4	MO
X-SR0051	<i>Maladera breviatella</i>	Matale	Dambulla	L3	BOLD:AEH4423	MW698362	EZ1	LD
X-SR0052	<i>Maladera breviatella</i>	Matale	Dambulla	L3	BOLD:AEH4423	MW698285	EZ1	LD
X-SR0055	<i>Maladera lindulana</i>	Kandy	Deenston	L4	BOLD:AEH5722	MW698359	EZ3	SM
X-SR0056	<i>Serica lurida</i>	Kandy	Deenston	L4	BOLD:AEH5425	MW698214	EZ3	SM
X-SR0058	<i>Serica fusa</i>	Nuwara Eliya	Piduruthalagala FR	L11	BOLD:AEH5844	MW698387	EZ5	MO
X-SR0059	<i>Serica fusa</i>	Nuwara Eliya	Piduruthalagala FR	L11	BOLD:AEH5844	MW698354	EZ5	MO
X-SR0060	<i>Serica fusa</i>	Nuwara Eliya	Piduruthalagala FR	L11	BOLD:AEH5844	MW698381	EZ5	MO
X-SR0062	<i>Maladera rufocuprea</i>	Kegalle	Aranayake	L1	BOLD:AEH5150	MW698220	EZ1	LW
X-SR0063	<i>Maladera dubia</i>	Nuwara Eliya	Horton Plains	L6	BOLD:AEH6135	MW698468	EZ5	MO
X-SR0064	<i>Maladera dubia</i>	Nuwara Eliya	Horton Plains	L6	BOLD:AEH6135	MW698257	EZ5	MO
X-SR0068	<i>Serica fusa</i>	Nuwara Eliya	Hakgala SNR	L5	BOLD:AEH5844	MW698321	EZ4	MO
X-SR0070	<i>Maladera badullana</i>	Nuwara Eliya	Horton Plains	L6	BOLD:AEH7081	MW698326	EZ5	MO
X-SR0080	<i>Maladera rufocuprea</i>	Kegalle	Aranayake	L1	BOLD:AEH5150	MW698336	EZ1	LW
X-SR0081	<i>Maladera rufocuprea</i>	Kegalle	Aranayake	L1	BOLD:AEH5150	MW698353	EZ1	LW
X-SR0083	<i>Maladera hortonensis</i>	Nuwara Eliya	Piduruthalagala FR	L11	BOLD:AEH5976	MW698408	EZ5	MO
X-SR0085	<i>Maladera hortonensis</i>	Nuwara Eliya	Piduruthalagala FR	L11	BOLD:AEH5976	MW698211	EZ5	MO
X-SR0086	<i>Maladera calcarata</i>	Matale	Dambulla	L3	BOLD:AEH6472	MW698448	EZ1	LD
X-SR0088	<i>Selaserica pusilla</i>	Matale	Dambulla	L3	BOLD:AEH5331	MW698227	EZ1	LD
X-SR0089	<i>Maladera mollis</i>	Matale	Dambulla	L3	BOLD:AEH7067	MW698383	EZ1	LD
X-SR0090	<i>Maladera heveli</i>	Matale	Dambulla	L3	BOLD:AEH8286	MW698205	EZ1	LD
X-SR0093	<i>Maladera galdaththana</i>	Kegalle	Aranayake	L1	BOLD:AEH4344	MW698404	EZ1	LW
X-SR0094	<i>Maladera cinnaberina</i>	Kegalle	Aranayake	L1	BOLD:AEH7181	MW698389	EZ1	LW

X-SR0095	<i>Apogonia solida</i>	Kegalle	Aranayake	L1	BOLD:AEH3418	MW698424	EZ1	LW
X-SR0096	<i>Maladera coxalis</i>	Kegalle	Aranayake	L1	BOLD:AEH6262	MW698392	EZ1	LW
X-SR0097	<i>Maladera pubescens</i>	Kegalle	Aranayake	L1	BOLD:AEH3996	MW698233	EZ1	LW
X-SR0098	<i>Serica lurida</i>	Kandy	Deenston	L4	BOLD:AEH5425	MW698366	EZ3	SM
X-SR0099	<i>Serica lurida</i>	Kandy	Deenston	L4	BOLD:AEH5425	MW698446	EZ3	SM
X-SR0100	<i>Maladera calcarata</i>	Matale	Dambulla	L3	BOLD:AEH6472	MW698277	EZ1	LD
X-SR0101	<i>Selaserica pusilla</i>	Matale	Dambulla	L3	BOLD:AEH5010	MW698291	EZ1	LD
X-SR0106	<i>Maladera lindulana</i>	Kandy	Deenston	L4	BOLD:AEH5722	MW698415	EZ3	SM
X-SR0108	<i>Maladera lindulana</i>	Kandy	Deenston	L4	BOLD:AEH5722	MW698370	EZ3	SM
X-SR0115	<i>Neoserica sexfoliata</i>	Matale	Dambulla	L3	BOLD:AEH7100	MW698293	EZ1	LD
X-SR0118	<i>Selaserica nitida</i>	Nuwara Eliya	Hakgala SNR	L5	BOLD:AEH6994	MW698467	EZ4	MO
X-SR0119	<i>Selaserica nitida</i>	Nuwara Eliya	Hakgala SNR	L5	BOLD:AEH6994	MW698331	EZ4	MO
X-SR0121	<i>Maladera badullana</i>	Nuwara Eliya	Horton Plains	L6	BOLD:AEH7081	MW698243	EZ5	MO
X-SR0126	<i>Maladera badullana</i>	Nuwara Eliya	Piduruthalagala FR	L11	BOLD:AEH7081	MW698375	EZ5	MO
X-SR0127	<i>Maladera dubia</i>	Nuwara Eliya	Piduruthalagala FR	L11	BOLD:AEH6135	MW698235	EZ5	MO
X-SR0130	<i>Maladera dubia</i>	Nuwara Eliya	Hakgala SNR	L5	BOLD:AEH6135	MW698419	EZ4	MO
X-SR0132	<i>Maladera coxalis</i>	Kegalle	Aranayake	L1	BOLD:AEH6264	MW698334	EZ1	LW
X-SR0133	<i>Maladera coxalis</i>	Kegalle	Aranayake	L1	BOLD:AEH6264	MW698426	EZ1	LW
X-SR0134	<i>Maladera rotundata</i>	Kegalle	Aranayake	L1	BOLD:AEH5377	MW698276	EZ1	LW
X-SR0142	<i>Maladera calcarata</i>	Matale	Dambulla	L3	BOLD:AEH6472	MW698454	EZ1	LD
X-SR0145	<i>Selaserica maculicauda</i>	Nuwara Eliya	Horton Plains	L6	BOLD:AEH4591	MW698462	EZ5	MO
X-SR0147	<i>Maladera badullana</i>	Nuwara Eliya	Galways Land NP	L5	BOLD:AEH7081	MW698342	EZ4	MO
X-SR0149	<i>Maladera dubia</i>	Nuwara Eliya	Piduruthalagala FR	L11	BOLD:AEH6135	MW698259	EZ5	MO
X-SR0153	<i>Serica fusa</i>	Nuwara Eliya	Hakgala SNR	L5	BOLD:AEH5844	MW698294	EZ4	MO
X-SR0154	<i>Serica fusa</i>	Nuwara Eliya	Hakgala SNR	L5	BOLD:AEH5844	MW698439	EZ4	MO
X-SR0155	<i>Maladera cinnaberina</i>	Kegalle	Aranayake	L1	BOLD:AEH7181	MW698317	EZ1	LW

X-SR0158	<i>Maladera rufocuprea</i>	Ratnapura	Belihuloya	L7	BOLD:AEH5150	MW698263	L7	LW
X-SR0160	<i>Maladera fistulosa</i>	Nuwara Eliya	Hakgala SNR	L5	BOLD:AEH7081	MW698398	EZ4	MO
X-SR0161	<i>Maladera dubia</i>	Nuwara Eliya	Hakgala SNR	L5	BOLD:AEH6135	MW698322	EZ4	MO
X-SR0162	<i>Maladera fistulosa</i>	Nuwara Eliya	Hakgala SNR	L5	BOLD:AEH7081	MW698266	EZ4	MO
X-SR0167	<i>Maladera hortonensis</i>	Nuwara Eliya	Piduruthalagala FR	L11	BOLD:AEH5976	MW698206	EZ5	MO
X-SR0170	<i>Maladera hortonensis</i>	Nuwara Eliya	Horton Plains	L6	BOLD:AEH5976	MW698367	EZ5	MO
X-SR0174	<i>Maladera lindulana</i>	Kandy	Deenston	L4	BOLD:AEH5722	MW698345	EZ3	SM
X-SR0175	<i>Selaserica athukoralai</i>	Matale	Riverston	L2	BOLD:AEH8417	MW698298	EZ2	SM
X-SR0177	<i>Maladera dubia</i>	Nuwara Eliya	Hakgala SNR	L5	BOLD:AEH6135	MW698420	EZ4	MO
X-SR0184	<i>Maladera dubia</i>	Nuwara Eliya	Piduruthalagala FR	L11	BOLD:AEH6135	MW698403	EZ5	LW1
X-SR0186	<i>Selaserica sororinitida</i>	Kandy	Deenston	L4	BOLD:AEH7391	MW698445	EZ3	SM
X-SR0187	<i>Maladera deenstana</i>	Kandy	Deenston	L4	BOLD:AEH7198	MW698230	EZ3	SM
X-SR0188	<i>Maladera cervicornis</i>	Matale	Riverston	L2	BOLD:AEH8443	MW698244	EZ2	SM
X-SR0189	<i>Maladera cervicornis</i>	Matale	Riverston	L2	BOLD:AEH8443	MW698453	EZ2	SM
X-SR0190	<i>Periserica sp</i>	Kandy	Deenston	L4	BOLD:AEH6212	MW698382	EZ3	SM
X-SR0202	<i>Maladera coxalis</i>	Matale	Dambulla	L3	BOLD:AEH8752	MW698443	EZ1	LD
X-SR0206	<i>Selaserica pusilla</i>	Matale	Dambulla	L3	BOLD:AEH5010	MW698231	EZ1	LD
X-SR0209	<i>Maladera dambullana</i>	Matale	Dambulla	L3	BOLD:AEH7262	MW698226	EZ1	LD
X-SR0210	<i>Maladera dambullana</i>	Matale	Dambulla	L3	BOLD:AEH3995	MW698315	EZ1	LD
X-SR0224	<i>Selaserica sororinitida</i>	Kandy	Deenston	L4	BOLD:AEH7391	MW698223	EZ3	SM
X-SR0227	<i>Selaserica sororinitida</i>	Kandy	Deenston	L4	BOLD:AEH7391	MW698349	EZ3	SM
X-SR0245	<i>Maladera haniel</i>	Kandy	Deenston	L4	BOLD:AEH8443	MW698440	EZ3	SM
X-SR0251	<i>Maladera haniel</i>	Kandy	Deenston	L4	BOLD:AEH8443	MW698254	EZ3	SM
X-SR0252	<i>Selaserica pusilla</i>	Matale	Dambulla	L3	BOLD:AEH5010	MW698221	EZ1	LD
X-SR0269	<i>Maladera dambullana</i>	Matale	Dambulla	L3	BOLD:AEH7262	MW698449	EZ1	LD
X-SR0290	<i>Maladera coxalis</i>	Matale	Dambulla	L3	BOLD:AEH8752	MW698288	EZ1	LD

X-SR0301	<i>Maladera dambullana</i>	Matale	Dambulla	L3	BOLD:AEH7262	MW698361	EZ1	LD
X-SR0309	<i>Maladera calcarata</i>	Matale	Dambulla	L3	BOLD:AEH6472	MW698438	EZ1	LD
X-SR0319	<i>Neoserica sexfoliata</i>	Matale	Dambulla	L3	BOLD:AEH7100	MW698452	EZ1	LD
X-SR0320	<i>Maladera coxalis</i>	Matale	Dambulla	L3	BOLD:AEH8752	MW698337	EZ1	LD
X-SR0326	<i>Maladera tricuspadata</i>	Matale	Dambulla	L3	BOLD:AEH5496	MW698225	EZ1	LD
X-SR0327	<i>Neoserica sexfoliata</i>	Matale	Dambulla	L3	BOLD:AEH7100	MW698251	EZ1	LD
X-SR0333	<i>Neoserica pophami</i>	Matale	Dambulla	L3	BOLD:AEH4365	MW698239	EZ1	LD
X-SR0341	<i>Maladera dambullana</i>	Matale	Dambulla	L3	BOLD:AEH7262	MW698447	EZ1	LD
X-SR0346	<i>Neoserica pophami</i>	Matale	Dambulla	L3	BOLD:AEH4366	MW698287	EZ1	LD
X-SR0349	<i>Maladera breviatella</i>	Matale	Dambulla	L3	BOLD:AEH4423	MW698397	EZ1	LD
X-SR0350	<i>Maladera breviatella</i>	Matale	Dambulla	L3	BOLD:AEH4423	MW698215	EZ1	LD
X-SR0363	<i>Maladera dambullana</i>	Matale	Dambulla	L3	BOLD:AEH7262	MW698289	EZ1	LD
X-SR0372	<i>Maladera setosa</i>	Matale	Dambulla	L3	BOLD:AEH6169	MW698402	EZ1	LD
X-SR0392	<i>Maladera coxalis</i>	Matale	Dambulla	L3	BOLD:AEH6964	MW698255	EZ1	LD
X-SR0404	<i>Maladera heveli</i>	Matale	Dambulla	L3	BOLD:AEH4245	MW698459	EZ1	LD
X-SR0405	<i>Maladera setosa</i>	Matale	Dambulla	L3	BOLD:AEH6169	MW698358	EZ1	LD
X-SR0406	<i>Maladera heveli</i>	Matale	Dambulla	L3	BOLD:AEH4245	MW698297	EZ1	LD
X-SR0413	<i>Selaserica pusilla</i>	Matale	Dambulla	L3	BOLD:AEH5010	MW698457	EZ1	LD
X-SR0414	<i>Maladera dambullana</i>	Matale	Dambulla	L3	BOLD:AEH7262	MW698363	EZ1	LD
X-SR0417	<i>Neoserica pophami</i>	Matale	Dambulla	L3	BOLD:AEH4365	MW698378	EZ1	LD
X-SR0423	<i>Neoserica pophami</i>	Matale	Dambulla	L3	BOLD:AEH4365	MW698280	EZ1	LD
X-SR0452	<i>Maladera coxalis</i>	Matale	Dambulla	L3	BOLD:AEH8752	MW698463	EZ1	LD
X-SR0457	<i>Maladera setosa</i>	Matale	Dambulla	L3	BOLD:AEH6169	MW698286	EZ1	LD
X-SR0471	<i>Neoserica pophami</i>	Matale	Dambulla	L3	BOLD:AEH4365	MW698212	EZ1	LD
X-SR0488	<i>Neoserica pophami</i>	Matale	Dambulla	L3	BOLD:AEH4366	MW698373	EZ1	LD
X-SR0500	<i>Maladera heveli</i>	Matale	Dambulla	L3	BOLD:AEH4244	MW698319	EZ1	LD

X-SR0504	<i>Selaserica pusilla</i>	Matale	Dambulla	L3	BOLD:AEH5010	MW698312	EZ1	LD
X-SR0505	<i>Selaserica pusilla</i>	Matale	Dambulla	L3	BOLD:AEH5010	MW698344	EZ1	LD
X-SR0529	<i>Maladera rufocuprea</i>	Kandy	Deenston	L4	BOLD:AEH5150	MW698301	EZ3	SM
X-SR0530	<i>Maladera rufocuprea</i>	Kandy	Deenston	L4	BOLD:AEH5150	MW698328	EZ3	SM
X-SR0531	<i>Maladera rufocuprea</i>	Kandy	Deenston	L4	BOLD:AEH5150	MW698461	EZ3	SM
X-SR0534	<i>Maladera anderssoni</i>	Kandy	Deenston	L4	BOLD:AEH8444	MW698299	EZ3	SM
X-SR0535	<i>Maladera anderssoni</i>	Kandy	Deenston	L4	BOLD:AEH8444	MW698284	EZ3	SM
X-SR0543	<i>Maladera iuga</i>	Kandy	Deenston	L4	BOLD:AEH8370	MW698441	EZ3	SM
X-SR0546	<i>Maladera kishi</i>	Kandy	Deenston	L4	BOLD:AEH4589	MW698265	EZ3	SM
X-SR0548	<i>Maladera kishi</i>	Kandy	Deenston	L4	BOLD:AEH4589	MW698218	EZ3	SM
X-SR0552	<i>Maladera haniel</i>	Kandy	Deenston	L4	BOLD:AEH8443	MW698219	EZ3	SM
X-SR0559	<i>Maladera anderssoni</i>	Kandy	Deenston	L4	BOLD:AEH8444	MW698216	EZ3	SM
X-SR0560	<i>Serica lurida</i>	Kandy	Deenston	L4	BOLD:AEH5425	MW698249	EZ3	SM
X-SR0563	<i>Selaserica sororinitida</i>	Kandy	Deenston	L4	BOLD:AEH7391	MW698335	EZ3	SM
X-SR0565	<i>Maladera kishi</i>	Kandy	Deenston	L4	BOLD:AEH4589	MW698264	EZ3	SM
X-SR0566	<i>Maladera kishi</i>	Kandy	Deenston	L4	BOLD:AEH4589	MW698460	EZ3	SM
X-SR0580	<i>Maladera windy</i>	Kandy	Deenston	L4	BOLD:AEH5536	MW698303	EZ3	SM
X-SR0583	<i>Maladera cervicornis</i>	Matale	Riverston	L2	BOLD:AEH8443	MW698271	EZ2	SM
X-SR0589	<i>Selaserica pusilla</i>	Matale	Riverston	L2	BOLD:AEH5009	MW698365	EZ2	SM
X-SR0591	<i>Serica lurida</i>	Matale	Riverston	L2	BOLD:AEH5425	MW698425	EZ2	SM
X-SR0621	<i>Maladera cervicornis</i>	Matale	Riverston	L2	BOLD:AEH8443	MW698341	EZ2	SM
X-SR0627	<i>Selaserica pusilla</i>	Matale	Riverston	L2	BOLD:AEH5008	MW698393	EZ2	SM
X-SR0631	<i>Selaserica pusilla</i>	Matale	Riverston	L2	BOLD:AEH5008	MW698302	EZ2	SM
X-SR0652	<i>Maladera rufocuprea</i>	Matale	Riverston	L2	BOLD:AEH5150	MW698390	EZ2	SM
X-SR0653	<i>Maladera cervicornis</i>	Matale	Riverston	L2	BOLD:AEH8443	MW698405	EZ2	SM
X-SR0654	<i>Selaserica pusilla</i>	Matale	Riverston	L2	BOLD:AEH5009	MW698343	EZ2	SM

X-SR0655	<i>Selaserica pusilla</i>	Matale	Riverston	L2	BOLD:AEH5009	MW698217	EZ2	SM
X-SR0659	<i>Maladera coxalis</i>	Matale	Riverston	L2	BOLD:AEH6236	MW698427	EZ2	SM
X-SR0660	<i>Maladera cervicornis</i>	Matale	Riverston	L2	BOLD:AEH8443	MW698246	EZ2	SM
X-SR0664	<i>Selaserica sororinitida</i>	Kandy	Deenston	L4	BOLD:AEH7391	MW698433	EZ3	SM
X-SR0666	<i>M. bandarawelana</i>	Matale	Riverston	L2	BOLD:AEH5956	MW698309	EZ2	SM
X-SR0669	<i>Selaserica sororinitida</i>	Kandy	Deenston	L4	BOLD:AEH7391	MW698292	EZ3	SM
X-SR0670	<i>Selaserica sororinitida</i>	Kandy	Deenston	L4	BOLD:AEH7391	MW698395	EZ3	SM
X-SR0672	<i>Maladera cervicornis</i>	Matale	Riverston	L2	BOLD:AEH8443	MW698327	EZ2	SM
X-SR0707	<i>Maladera anderssoni</i>	Kandy	Deenston	L4	BOLD:AEH8445	MW698348	EZ3	SM
X-SR0708	<i>Maladera haniel</i>	Kandy	Deenston	L4	BOLD:AEH8443	MW698307	EZ3	SM
X-SR0709	<i>Maladera anderssoni</i>	Kandy	Deenston	L4	BOLD:AEH8444	MW698305	EZ3	SM
X-SR0713	<i>Serica fusa</i>	Nuwara Eliya	Hakgala SNR	L5	BOLD:AEH5844	MW698296	EZ4	MO
X-SR0714	<i>Serica fusa</i>	Nuwara Eliya	Hakgala SNR	L5	BOLD:AEH5844	MW698385	EZ4	MO
X-SR0717	<i>Serica fusa</i>	Nuwara Eliya	Hakgala SNR	L5	BOLD:AEH5844	MW698372	EZ4	MO
X-SR0720	<i>Maladera dubia</i>	Nuwara Eliya	Hakgala SNR	L5	BOLD:AEH6135	MW698431	EZ4	MO
X-SR0721	<i>Maladera dubia</i>	Nuwara Eliya	Hakgala SNR	L5	BOLD:AEH6135	MW698418	EZ4	MO
X-SR0722	<i>Maladera dubia</i>	Nuwara Eliya	Hakgala SNR	L5	BOLD:AEH6135	MW698273	EZ4	MO
X-SR0723	<i>Maladera dubia</i>	Nuwara Eliya	Hakgala SNR	L5	BOLD:AEH6135	MW698252	EZ4	MO
X-SR0724	<i>Maladera kishi</i>	Kandy	Deenston	L4	BOLD:AEH4589	MW698283	EZ3	SM
X-SR0730	<i>Maladera kishi</i>	Kandy	Deenston	L4	BOLD:AEH4589	MW698436	EZ3	SM
X-SR0757	<i>Maladera windy</i>	Kandy	Deenston	L4	BOLD:AEH3994	MW698369	EZ3	SM
X-SR0769	<i>Maladera windy</i>	Kandy	Deenston	L4	BOLD:AEH3994	MW698347	EZ3	SM
X-SR0773	<i>Maladera rufocuprea</i>	Kandy	Deenston	L4	BOLD:AEH5150	MW698400	EZ3	SM
X-SR0774	<i>Maladera rufocuprea</i>	Kandy	Deenston	L4	BOLD:AEH5150	MW698429	EZ3	SM
X-SR0776	<i>Maladera haniel</i>	Kandy	Deenston	L4	BOLD:AEH8443	MW698421	EZ3	SM
X-SR0781	<i>Maladera haniel</i>	Kandy	Deenston	L4	BOLD:AEH8443	MW698414	EZ3	SM

X-SR0790	<i>Maladera windy</i>	Kandy	Deenston	L4	BOLD:AEH3994	MW698456	EZ3	SM
X-SR0808	<i>Serica lurida</i>	Kandy	Deenston	L4	BOLD:AEH5425	MW698300	EZ3	SM
X-SR0810	<i>Serica lurida</i>	Kandy	Deenston	L4	BOLD:AEH5425	MW698236	EZ3	SM
X-SR0815	<i>Maladera weligamana</i>	Nuwara Eliya	Hakgala SNR	L5	BOLD:AEH7197	MW698339	EZ4	MO
X-SR0819	<i>Maladera dubia</i>	Nuwara Eliya	Hakgala SNR	L5	BOLD:AEH6135	MW698222	EZ4	MO
X-SR0820	<i>Maladera dubia</i>	Nuwara Eliya	Hakgala SNR	L5	BOLD:AEH6135	MW698356	EZ4	MO
X-SR0830	<i>Maladera dubia</i>	Nuwara Eliya	Hakgala SNR	L5	BOLD:AEH6135	MW698401	EZ4	MO
X-SR0833	<i>Maladera dubia</i>	Nuwara Eliya	Hakgala SNR	L5	BOLD:AEH6135	MW698469	EZ4	MO
X-SR0835	<i>Maladera weligamana</i>	Nuwara Eliya	Hakgala SNR	L5	BOLD:AEH7197	MW698310	EZ4	MO
X-SR0837	<i>Maladera dubia</i>	Nuwara Eliya	Hakgala SNR	L5	BOLD:AEH6135	MW698325	EZ4	MO
X-SR0839	<i>Maladera rufocuprea</i>	Galle	Hiyare FR	L8	BOLD:AEH5150	MW698306	EZ1	LW
X-SR0840	<i>Maladera rufocuprea</i>	Galle	Hiyare FR	L8	BOLD:AEH5150	MW698338	EZ1	LW
X-SR0841	<i>Maladera rufocuprea</i>	Galle	Hiyare FR	L8	BOLD:AEH5150	MW698399	EZ1	LW
X-SR0843	<i>Maladera rufocuprea</i>	Galle	Hiyare FR	L8	BOLD:AEH5150	MW698407	EZ1	LW
X-SR0847	<i>Maladera rufocuprea</i>	Galle	Hiyare FR	L8	BOLD:AEH5150	MW698275	EZ1	LW
X-SR0855	<i>Selaserica impexa</i>	Galle	Hiyare FR	L8	BOLD:AEH7222	MW698290	EZ1	LW
X-SR0856	<i>Selaserica impexa</i>	Galle	Kanneliya FR	L10	BOLD:AEH7223	MW698413	EZ1	LW
X-SR0857	<i>Selaserica impexa</i>	Galle	Kanneliya FR	L10	BOLD:AEH7223	MW698333	EZ1	LW
X-SR0858	<i>Selaserica convexiuscula</i>	Galle	Kottawa FR	L9	BOLD:AEH6645	MW698268	EZ1	LW
X-SR0859	<i>Selaserica fabriziae</i>	Galle	Kottawa FR	L9	BOLD:AEH6644	MW698316	EZ1	LW
X-SR0862	<i>Maladera pubescens</i>	Kegalle	Aranayake	L1	BOLD:AEH3996	MW698272	EZ1	LW
X-SR0864	<i>Maladera rufocuprea</i>	Matale	Riverston	L2	BOLD:AEH5150	MW698282	EZ2	SM
X-SR0865	<i>Maladera rufocuprea</i>	Matale	Riverston	L2	BOLD:AEH5150	MW698444	EZ2	SM
X-SR0866	<i>Maladera laterita</i>	Matale	Riverston	L2	BOLD:AEH6029	MW698465	EZ2	SM
X-SR0877	<i>Maladera rufocuprea</i>	Matale	Riverston	L2	BOLD:AEH5150	MW698207	EZ2	SM
X-SR0881	<i>M. bandarawelana</i>	Matale	Riverston	L2	BOLD:AEH5956	MW698374	EZ2	SM

X-SR0882	<i>M. bandarawelana</i>	Matale	Riverston	L2	BOLD:AEH5956	MW698466	EZ2	SM
X-SR0887	<i>Maladera karunaratnae</i>	Matale	Riverston	L2	BOLD:AEH8445	MW698237	EZ2	SM
X-SR0889	<i>Serica lurida</i>	Matale	Riverston	L2	BOLD:AEH5425	MW698422	EZ2	SM
X-SR0895	<i>Selaserica pusilla</i>	Matale	Riverston	L2	BOLD:AEH5009	MW698208	EZ2	SM
X-SR0898	<i>Serica lurida</i>	Matale	Riverston	L2	BOLD:AEH5425	MW698240	EZ2	SM
X-SR0901	<i>Serica lurida</i>	Matale	Riverston	L2	BOLD:AEH5425	MW698371	EZ2	SM
X-SR0902	<i>Serica lurida</i>	Matale	Riverston	L2	BOLD:AEH5425	MW698270	EZ2	SM
X-SR0906	<i>Serica lurida</i>	Matale	Riverston	L2	BOLD:AEH5425	MW698304	EZ2	SM
X-SR0915	<i>Selaserica sororinitida</i>	Kandy	Deenston	L4	BOLD:AEH7391	MW698278	EZ3	SM
X-SR0922	<i>Maladera anderssoni</i>	Kandy	Deenston	L4	BOLD:AEH8444	MW698450	EZ3	SM
X-SR0936	<i>Maladera kishi</i>	Kandy	Deenston	L4	BOLD:AEH4589	MW698213	EZ3	SM
X-SR0949	<i>Maladera anderssoni</i>	Kandy	Deenston	L4	BOLD:AEH8444	MW698396	EZ3	SM
X-SR0975	<i>Maladera coxalis</i>	Matale	Dambulla	L3	BOLD:AEH6964	MW698311	EZ1	LD
X-SR0985	<i>Maladera dambullana</i>	Matale	Dambulla	L3	BOLD:AEH7262	MW698380	EZ1	LD
X-SR0988	<i>Maladera heveli</i>	Matale	Dambulla	L3	BOLD:AEH5052	MW698410	EZ1	LD
X-SR0989	<i>Maladera heveli</i>	Matale	Dambulla	L3	BOLD:AEH5052	MW698224	EZ1	LD
X-SR0992	<i>Maladera coxalis</i>	Matale	Dambulla	L3	BOLD:AEH6263	MW698241	EZ1	LD
X-SR1010	<i>Maladera karunaratnae</i>	Matale	Dambulla	L3	BOLD:AEH8445	MW698232	EZ1	LD
X-SR1013	<i>Maladera setosa</i>	Matale	Dambulla	L3	BOLD:AEH6169	MW698238	EZ1	LD
X-SR1014	<i>Neoserica pophami</i>	Matale	Dambulla	L3	BOLD:AEH4365	MW698256	EZ1	LD
X-SR1029	<i>Maladera karunaratnae</i>	Matale	Dambulla	L3	BOLD:AEH8445	MW698394	EZ1	LD
X-SR1030	<i>Maladera karunaratnae</i>	Matale	Dambulla	L3	BOLD:AEH8445	MW698247	EZ1	LD
X-SR1046	<i>Maladera padaviyaensis</i>	Matale	Dambulla	L3	BOLD:AEH6028	MW698209	EZ1	LD
X-SR1047	<i>Maladera setosa</i>	Matale	Dambulla	L3	BOLD:AEH6169	MW698423	EZ1	LD
X-SR1087	<i>Maladera karunaratnae</i>	Matale	Dambulla	L3	BOLD:AEH8445	MW698258	EZ1	LD
X-SR1093	<i>Neoserica sexfoliata</i>	Matale	Dambulla	L3	BOLD:AEH7100	MW698435	EZ1	LD

X-SR1100	<i>Maladera heveli</i>	Matale	Dambulla	L3	BOLD:AEH8286	MW698204	EZ1	LD
X-SR1101	<i>Maladera heveli</i>	Matale	Dambulla	L3	BOLD:AEH8287	MW698248	EZ1	LD
X-SR1109	<i>Neoserica sexfoliata</i>	Matale	Dambulla	L3	BOLD:AEH7101	MW698458	EZ1	LD
X-SR1110	<i>Neoserica sexfoliata</i>	Matale	Dambulla	L3	BOLD:AEH7101	MW698411	EZ1	LD
X-SR1113	<i>Maladera karunaratnae</i>	Matale	Dambulla	L3	BOLD:AEH8445	MW698442	EZ1	LD
X-SR1129	<i>Neoserica dharmapriyai</i>	Kegalle	Aranayake	L1	BOLD:AEH7083	MW698360	EZ1	LW
X-SR1130	<i>Maladera rotundata</i>	Kegalle	Aranayake	L1	BOLD:AEH5377	MW698262	EZ1	LW
X-SR1132	<i>Maladera rotundata</i>	Kegalle	Aranayake	L1	BOLD:AEH5377	MW698329	EZ1	LW
X-SR1133	<i>Maladera rotundata</i>	Kegalle	Aranayake	L1	BOLD:AEH5377	MW698388	EZ1	LW
X-SR1135	<i>Selaserica sororinitida</i>	Kandy	Deenston	L4	BOLD:AEH7391	MW698324	EZ3	SM
X-SR1154	<i>Maladera badullana</i>	Nuwara Eliya	Hakgala SNR	L5	BOLD:AEH7081	MW698416	EZ4	MO
X-SR1155	<i>Maladera badullana</i>	Nuwara Eliya	Hakgala SNR	L5	BOLD:AEH7081	MW698228	EZ4	MO
X-SR1158	<i>Maladera fistulosa</i>	Nuwara Eliya	Hakgala SNR	L5	BOLD:AEH7081	MW698350	EZ4	MO
X-SR1166	<i>Maladera hortonensis</i>	Nuwara Eliya	Piduruthalagala FR	L11	BOLD:AEH5976	MW698267	EZ5	MO
X-SR1167	<i>Maladera hortonensis</i>	Nuwara Eliya	Piduruthalagala FR	L11	BOLD:AEH5976	MW698314	EZ5	MO
X-SR1172	<i>Maladera hortonensis</i>	Nuwara Eliya	Piduruthalagala FR	L11	BOLD:AEH5976	MW698430	EZ5	MO
X-SR1173	<i>Maladera hortonensis</i>	Nuwara Eliya	Piduruthalagala FR	L11	BOLD:AEH5976	MW698242	EZ5	MO
X-SR1183	<i>Maladera hortonensis</i>	Nuwara Eliya	Piduruthalagala FR	L11	BOLD:AEH5976	MW698376	EZ5	MO
X-SR1185	<i>Maladera badullana</i>	Nuwara Eliya	Piduruthalagala FR	L11	BOLD:AEH7081	MW698346	EZ5	MO
X-SR1189	<i>Maladera badullana</i>	Nuwara Eliya	Piduruthalagala FR	L11	BOLD:AEH7081	MW698357	EZ5	MO
X-SR1191	<i>Maladera badullana</i>	Nuwara Eliya	Piduruthalagala FR	L11	BOLD:AEH7081	MW698386	EZ5	MO
X-SR1192	<i>Maladera hortonensis</i>	Nuwara Eliya	Piduruthalagala FR	L11	BOLD:AEH5976	MW698318	EZ5	MO
X-SR1193	<i>Maladera badullana</i>	Nuwara Eliya	Piduruthalagala FR	L11	BOLD:AEH7081	MW698279	EZ5	MO
X-SR1195	<i>Selaserica nitida</i>	Nuwara Eliya	Piduruthalagala FR	L11	BOLD:AEH6994	MW698261	EZ5	MO
X-SR1197	<i>Selaserica nitida</i>	Nuwara Eliya	Piduruthalagala FR	L11	BOLD:AEH6994	MW698384	EZ5	MO
X-SR1210	<i>Selaserica nitida</i>	Nuwara Eliya	Horton Plains	L6	BOLD:AEH6993	MW698364	EZ5	MO

X-SR1211	<i>Selaserica maculicauda</i>	Nuwara Eliya	Horton Plains	L6	BOLD:AEH4591	MW698313	EZ5	MO
X-SR1212	<i>Selaserica nitida</i>	Nuwara Eliya	Horton Plains	L6	BOLD:AEH6993	MW698434	EZ5	MO
X-SR1213	<i>Selaserica nitida</i>	Nuwara Eliya	Horton Plains	L6	BOLD:AEH6993	MW698409	EZ5	MO
X-SR1218	<i>Maladera hortonensis</i>	Nuwara Eliya	Horton Plains	L6	BOLD:AEH5976	MW698352	EZ5	MO
X-SR1223	<i>Selaserica nitida</i>	Nuwara Eliya	Horton Plains	L6	BOLD:AEH6993	MW698412	EZ5	MO
X-SR1228	<i>Maladera dubia</i>	Nuwara Eliya	Horton Plains	L6	BOLD:AEH6135	MW698295	EZ5	MO
X-SR1229	<i>Maladera dubia</i>	Nuwara Eliya	Horton Plains	L6	BOLD:AEH6135	MW698323	EZ5	MO
X-SR1230	<i>Maladera dubia</i>	Nuwara Eliya	Horton Plains	L6	BOLD:AEH6135	MW698274	EZ5	MO
X-SR1232	<i>Selaserica nitida</i>	Nuwara Eliya	Horton Plains	L6	BOLD:AEH6993	MW698464	EZ5	MO
X-SR1236	<i>Phileurus</i> sp2	Matale	Dambulla	L3			EZ1	LD
X-SR1237	<i>Anomala</i> sp1	Matale	Dambulla	L3			EZ1	LD
X-SR1240	<i>Adoretus</i> sp6	Kandy	Udawattakele FR	L14			EZ2	LW
X-SR1247	<i>Holotrichia</i> sp4	Kandy	Udawattakele FR	L14			EZ2	LW
X-SR1248	<i>Apogonia coriacea</i>	Kandy	Deenston	L4			EZ3	SM
X-SR1249	<i>Sophrops</i> sp2	Kandy	Deenston	L4			EZ3	SM
X-SR1250	<i>Adoretus</i> sp5	Kandy	Deenston	L4			EZ3	SM
X-SR1251	<i>Apogonia</i> sp8	Nuwara Eliya	Hakgala SNR	L5			EZ4	MO
X-SR1252	<i>Apogonia</i> sp8	Nuwara Eliya	Hakgala SNR	L5			EZ4	MO
X-SR1253	<i>Apogonia</i> sp8	Nuwara Eliya	Galways Land NP	L5			EZ4	MO
X-SR1254	<i>Apogonia coriacea</i>	Nuwara Eliya	Hakgala SNR	L5			EZ4	MO
X-SR1255	<i>Apogonia coriacea</i>	Nuwara Eliya	Hakgala SNR	L5			EZ4	MO
X-SR1257	<i>Apogonia</i> sp1	Kegalle	Aranayake	L1			EZ1	LW
X-SR1258	<i>Apogonia glabrilinea</i>	Kegalle	Aranayake	L1			EZ1	LW
X-SR1259	<i>Anomala</i> sp1	Kegalle	Aranayake	L1			EZ1	LW
X-SR1260	<i>Anomala</i> sp1	Kegalle	Aranayake	L1			EZ1	LW
X-SR1261	<i>Anomala</i> sp1	Kegalle	Aranayake	L1			EZ1	LW

X-SR1263	Anomala sp2	Kegalle	Aranayake	L1	EZ1	LW
X-SR1264	Anomala sp2	Kegalle	Aranayake	L1	EZ1	LW
X-SR1265	Anomala sp2	Kegalle	Aranayake	L1	EZ1	LW
X-SR1266	Leucopholis sp1	Kegalle	Aranayake	L1	EZ1	LW
X-SR1267	Adoretus sp4	Nuwara Eliya	Hakgala SNR	L5	EZ4	MO
X-SR1281	Adoretus sp4	Nuwara Eliya	Hakgala SNR	L5	EZ4	MO
X-SR1282	Adoretus sp4	Nuwara Eliya	Hakgala SNR	L5	EZ4	MO
X-SR1291	Adoretus sp4	Nuwara Eliya	Hakgala SNR	L5	EZ4	MO
X-SR1306	Sophrops sp1	Galle	Hiyare FR	L8	EZ1	LW
X-SR1307	Mimela sp1	Galle	Hiyare FR	L8	EZ1	LW
X-SR1309	Anomala sp1	Matale	Dambulla	L3	EZ1	LD
X-SR1311	Anomala sp1	Matale	Dambulla	L3	EZ1	LD
X-SR1315	Adoretus sp7	Galle	Hiyare FR	L8	EZ1	LW
X-SR1318	Adoretus sp8	Kandy	UdaPeradeniya	L12	EZ2	LW
X-SR1319	Anomala sp2	Kandy	UdaPeradeniya	L12	EZ2	LW
X-SR1322	Apogonia sp12	Kandy	Deenston	L4	EZ3	SM
X-SR1323	Apogonia sp12	Kandy	Deenston	L4	EZ3	SM
X-SR1328	<i>Apogonia solida</i>	Kegalle	Aranayake	L1	EZ1	LW
X-SR1331	Anomala sp1	Kegalle	Aranayake	L1	EZ1	LW
X-SR1334	Holotrichia sp1	Kegalle	Aranayake	L1	EZ1	LW
X-SR1336	<i>Apogonia solida</i>	Matale	Dambulla	L3	EZ1	LD
X-SR1337	<i>Apogonia solida</i>	Matale	Dambulla	L3	EZ1	LD
X-SR1342	<i>Apogonia solida</i>	Matale	Dambulla	L3	EZ1	LD
X-SR1345	Holotrichia sp3	Matale	Dambulla	L3	EZ1	LD
X-SR1359	<i>Xylotrupes</i> sp5	Matale	Dambulla	L3	EZ1	LD
X-SR1360	Sophrops sp2	Kandy	Deenston	L4	EZ3	SM

X-SR1363	Sophrops sp2	Kandy	Deenston	L4	EZ3	SM
X-SR1369	Apogonia sp1	Matale	Riverston	L2	EZ2	SM
X-SR1375	Anomala sp3	Kegalle	Aranayake	L1	EZ1	LW
X-SR1376	Anomala sp3	Kegalle	Aranayake	L1	EZ1	LW
X-SR1377	Anomala sp3	Kegalle	Aranayake	L1	EZ1	LW
X-SR1386	<i>Apogonia ludificans</i>	Kandy	Deenston	L4	EZ3	SM
X-SR1392	Adoretus sp5	Kandy	Deenston	L4	EZ3	SM
X-SR1393	Popillia sp1	Kandy	Deenston	L4	EZ3	SM
X-SR1394	Popillia sp1	Kandy	Deenston	L4	EZ3	SM
X-SR1395	Popillia sp1	Kandy	Deenston	L4	EZ3	SM
X-SR1399	Gametis sp	Kandy	Deenston	L4	EZ3	SM
X-SR1400	Adoretus sp5	Kandy	Deenston	L4	EZ3	SM
X-SR1405	Holotrichia sp5	Kandy	Deenston	L4	EZ3	SM
X-SR1406	<i>Eophileurus</i> sp6	Kandy	Deenston	L4	EZ3	SM
X-SR1407	Mimela sp1	Kandy	Deenston	L4	EZ3	SM
X-SR1410	Holotrichia sp6	Kandy	Deenston	L4	EZ3	SM
X-SR1412	Apogonia sp10	Kandy	Deenston	L4	EZ3	SM
X-SR1418	Sophrops sp1	Kegalle	Aranayake	L1	EZ1	LW
X-SR1420	Adoretus sp1	Kegalle	Aranayake	L1	EZ1	LW
X-SR1422	Apogonia sp1	Kegalle	Aranayake	L1	EZ1	LW
X-SR1423	<i>Orphnus</i> sp1	Kegalle	Aranayake	L1	EZ1	LW
X-SR1427	<i>Orphnus</i> sp1	Kegalle	Aranayake	L1	EZ1	LW
X-SR1428	<i>Orphnus</i> sp1	Kegalle	Aranayake	L1	EZ1	LW
X-SR1429	Holotrichia sp2	Kegalle	Aranayake	L1	EZ1	LW
X-SR1430	Holotrichia sp2	Kegalle	Aranayake	L1	EZ1	LW
X-SR1431	Holotrichia sp2	Kegalle	Aranayake	L1	EZ1	LW

X-SR1432	Leucopholis sp2	Kegalle	Aranayake	L1	EZ1	LW
X-SR1433	Apogonia sp12	Kandy	Deenston	L4	EZ3	SM
X-SR1435	Brahmina sp1	Nuwara Eliya	Hakgala SNR	L5	EZ4	MO
X-SR1438	<i>Apogonia coriacea</i>	Galle	Kottawa FR	L9	EZ1	LW
X-SR1439	Adoretus sp8	Kandy	UdaPeradeniya	L12	EZ2	LW
X-SR1440	Adoretus sp8	Kandy	UdaPeradeniya	L12	EZ2	LW
X-SR1443	Adoretus sp3	Galle	Hiyare FR	L8	EZ1	LW
X-SR1444	Sophrops sp2	Galle	Hiyare FR	L8	EZ1	LW
X-SR1455	Apogonia sp1	Galle	Hiyare FR	L8	EZ1	LW
X-SR1456	Apogonia sp1	Galle	Hiyare FR	L8	EZ1	LW
X-SR1459	Sophrops sp3	Galle	Kottawa FR	L9	EZ1	LW
X-SR1460	<i>Apogonia coriacea</i>	Kandy	Deenston	L4	EZ3	SM
X-SR1461	<i>Apogonia glabrilinea</i>	Kandy	Deenston	L4	EZ3	SM
X-SR1462	<i>Apogonia glabrilinea</i>	Kandy	Deenston	L4	EZ3	SM
X-SR1467	<i>Apogonia ludificans</i>	Kandy	Deenston	L4	EZ3	SM
X-SR1469	<i>Apogonia glabrilinea</i>	Kandy	Deenston	L4	EZ3	SM
X-SR1470	Apogonia sp1	Kandy	Deenston	L4	EZ3	SM
X-SR1474	<i>Apogonia ludificans</i>	Kandy	Deenston	L4	EZ3	SM
X-SR1475	<i>Apogonia ludificans</i>	Kandy	Deenston	L4	EZ3	SM
X-SR1477	Sophrops sp1	Galle	Hiyare FR	L8	EZ1	LW
X-SR1478	Sophrops sp1	Galle	Hiyare FR	L8	EZ1	LW
X-SR1480	Sophrops sp2	Galle	Hiyare FR	L8	EZ1	LW
X-SR1485	Apogonia sp1	Galle	Hiyare FR	L8	EZ1	LW
X-SR1489	Leucopholis sp2	Galle	Hiyare FR	L8	EZ1	LW
X-SR1490	<i>Xylotrupes</i> sp5	Galle	Hiyare FR	L8	EZ1	LW
X-SR1492	Leucopholis sp2	Kegalle	Galdaththa	L1	EZ1	LW

X-SR1493	Leucopholis sp2	Kegalle	Aranayake	L1	EZ1	LW
X-SR1494	Anomala sp4	Matale	Dambulla	L3	EZ1	LD
X-SR1497	Sophrops sp1	Matale	Dambulla	L3	EZ1	LD
X-SR1498	Sophrops sp1	Matale	Dambulla	L3	EZ1	LD
X-SR1499	Sophrops sp2	Matale	Dambulla	L3	EZ1	LD
X-SR1503	Apogonia sp1	Matale	Dambulla	L3	EZ1	LD
X-SR1504	Apogonia sp1	Matale	Dambulla	L3	EZ1	LD
X-SR1505	Apogonia sp1	Matale	Dambulla	L3	EZ1	LD
X-SR1510	Anomala sp4	Matale	Dambulla	L3	EZ1	LD
X-SR1511	Anomala sp4	Matale	Dambulla	L3	EZ1	LD
X-SR1520	Sophrops sp1	Matale	Dambulla	L3	EZ1	LD
X-SR1523	Apogonia sp5	Matale	Dambulla	L3	EZ1	LD
X-SR1524	Apogonia sp7	Matale	Dambulla	L3	EZ1	LD
X-SR1525	Apogonia sp7	Matale	Dambulla	L3	EZ1	LD
X-SR1526	Apogonia sp5	Matale	Dambulla	L3	EZ1	LD
X-SR1527	Apogonia sp7	Matale	Dambulla	L3	EZ1	LD
X-SR1528	<i>Apogonia comosa</i>	Matale	Dambulla	L3	EZ1	LD
X-SR1537	<i>Eophileurus</i> sp2	Matale	Dambulla	L3	EZ1	LD
X-SR1541	Adoretus sp3	Matale	Riverston	L2	EZ2	SM
X-SR1542	<i>Apogonia glabrilinea</i>	Matale	Riverston	L2	EZ2	SM
X-SR1543	<i>Apogonia glabrilinea</i>	Matale	Riverston	L2	EZ2	SM
X-SR1545	Adoretus sp2	Matale	Dambulla	L3	EZ1	LD
X-SR1547	Sophrops sp2	Matale	Dambulla	L3	EZ1	LD
X-SR1548	Sophrops sp2	Matale	Dambulla	L3	EZ1	LD
X-SR1550	<i>Orphunus</i> sp1	Matale	Dambulla	L3	EZ1	LD
X-SR1551	<i>Orphunus</i> sp1	Matale	Dambulla	L3	EZ1	LD

X-SR1561	<i>Orphunus</i> sp1	Matale	Dambulla	L3	EZ1	LD
X-SR1564	<i>Apogonia comosa</i>	Matale	Dambulla	L3	EZ1	LD
X-SR1565	<i>Apogonia</i> sp5	Matale	Dambulla	L3	EZ1	LD
X-SR1578	<i>Adoretus</i> sp2	Matale	Dambulla	L3	EZ1	LD
X-SR1580	<i>Xylotrupes</i> sp5	Kegalle	Aranayake	L1	EZ1	LW
X-SR1583	<i>Leucopholis</i> sp2	Galle	Hiyare FR	L8	EZ1	LW
X-SR1588	<i>Orphunus</i> sp1	Matale	Riverston	L2	EZ2	SM
X-SR1590	<i>Apogonia ludificans</i>	Matale	Riverston	L2	EZ2	SM
X-SR1591	<i>Adoretus</i> sp2	Matale	Riverston	L2	EZ2	SM
X-SR1593	<i>Sophrops</i> sp4	Matale	Riverston	L2	EZ2	SM
X-SR1594	<i>Sophrops</i> sp2	Matale	Riverston	L2	EZ2	SM
X-SR1595	<i>Sophrops</i> sp2	Matale	Riverston	L2	EZ2	SM
X-SR1596	<i>Sophrops</i> sp2	Matale	Riverston	L2	EZ2	SM
X-SR1599	<i>Sophrops</i> sp4	Matale	Dambulla	L3	EZ1	LD
X-SR1603	<i>Adoretus</i> sp3	Matale	Dambulla	L3	EZ1	LD
X-SR1611	<i>Oryctes</i> sp7	Galle	Hiyare FR	L8	EZ1	LW
X-SR1616	<i>Anomala</i> sp3	Matale	Dambulla	L3	EZ1	LD
X-SR1621	<i>Sophrops</i> sp4	Matale	Dambulla	L3	EZ1	LD
X-SR1624	<i>Adoretus</i> sp9	Matale	Dambulla	L3	EZ1	LD
X-SR1625	<i>Adoretus</i> sp9	Matale	Dambulla	L3	EZ1	LD
X-SR1626	<i>Adoretus</i> sp10	Matale	Dambulla	L3	EZ1	LD
X-SR1638	<i>Orphunus</i> sp1	Matale	Dambulla	L3	EZ1	LD
X-SR1641	<i>Adoretus</i> sp11	Matale	Dambulla	L3	EZ1	LD
X-SR1647	<i>Eophileurus</i> sp2	Matale	Dambulla	L3	EZ1	LD
X-SR1655	<i>Orphunus</i> sp1	Matale	Dambulla	L3	EZ1	LD
X-SR1661	<i>Sophrops</i> sp5	Matale	Dambulla	L3	EZ1	LD

X-SR1662	Sophrops sp5	Matale	Dambulla	L3	EZ1	LD
X-SR1668	Sophrops sp2	Ratnapura	Belihuloya	L7	EZ1	L7
X-SR1669	Anomala sp2	Ratnapura	Weddagala	L16	EZ1	LW6
X-SR1674	Adoretus sp7	Galle	Kanneliya FR	L10	EZ1	LW
X-SR1677	Holotrichia sp5	Galle	Kanneliya FR	L10	EZ1	LW
X-SR1680	Sophrops sp1	Galle	Kanneliya FR	L10	EZ1	LW
X-SR1681	Sophrops sp1	Galle	Kanneliya FR	L10	EZ1	LW
X-SR1682	Anomala sp1	Galle	Kanneliya FR	L10	EZ1	LW
X-SR1684	Sophrops sp1	Galle	Kanneliya FR	L10	EZ1	LW
X-SR1686	Mimela sp2	Galle	Kanneliya FR	L10	EZ1	LW
X-SR1688	Leucopholis sp2	Kegalle	Aranayake	L1	EZ1	LW
X-SR1692	Anomala sp1	Kandy	Kadugannawa	L17	EZ2	LW
X-SR1693	Holotrichia sp7	Kandy	Kadugannawa	L17	EZ2	LW
X-SR1694	Holotrichia sp2	Kandy	Kadugannawa	L17	EZ2	LW
X-SR1695	Holotrichia sp1	Kandy	Kadugannawa	L17	EZ2	LW
X-SR1697	Apogonia sp8	Nuwara Eliya	Horton Plains	L6	EZ5	MO
X-SR1698	Apogonia sp8	Nuwara Eliya	Horton Plains	L6	EZ5	MO
X-SR1699	Apogonia sp8	Nuwara Eliya	Horton Plains	L6	EZ5	MO
X-SR1702	Brahmina sp1	Nuwara Eliya	Horton Plains	L6	EZ5	MO
X-SR1703	Brahmina sp1	Nuwara Eliya	Horton Plains	L6	EZ5	MO
X-SR1704	Brahmina sp1	Nuwara Eliya	Horton Plains	L6	EZ5	MO
X-SR1708	<i>Apogonia coriacea</i>	Nuwara Eliya	Piduruthalagala FR	L11	EZ5	MO
X-SR1709	Apogonia sp10	Nuwara Eliya	Piduruthalagala FR	L11	EZ5	MO
X-SR1710	<i>Apogonia coriacea</i>	Nuwara Eliya	Piduruthalagala FR	L11	EZ5	MO
X-SR1713	Adoretus sp10	Matale	Riverston	L2	EZ2	SM
X-SR1720	<i>Apogonia glabrilinea</i>	Matale	Riverston	L2	EZ2	SM

X-SR1722	Sophrups sp4	Kandy	Deenston	L4	EZ3	SM
X-SR1728	Adoretus sp3	Kandy	Deenston	L4	EZ3	SM
X-SR1729	Apogonia sp1	Kandy	Deenston	L4	EZ3	SM
X-SR1734	Sophrups sp4	Kandy	Deenston	L4	EZ3	SM
X-SR1737	<i>Apogonia comosa</i>	Kandy	Deenston	L4	EZ3	SM
X-SR1738	Apogonia sp1	Kandy	Deenston	L4	EZ3	SM
X-SR1746	Apogonia sp1	Kegalle	Aranayake	L1	EZ1	LW
X-SR1749	<i>Phyllognathus</i> sp8	Kegalle	Aranayake	L1	EZ1	LW
X-SR1753	Mimela sp1	Kegalle	Aranayake	L1	EZ1	LW
X-SR1754	<i>Oryctes</i> sp7	Kegalle	Aranayake	L1	EZ1	LW
X-SR1761	<i>Xylotrupes</i> sp5	Kegalle	Aranayake	L1	EZ1	LW
X-SR1765	<i>Apogonia comosa</i>	Matale	Dambulla	L3	EZ1	LD
X-SR1773	Adoretus sp12	Matale	Dambulla	L3	EZ1	LD
X-SR1774	Adoretus sp12	Matale	Dambulla	L3	EZ1	LD
X-SR1789	Apogonia sp5	Matale	Dambulla	L3	EZ1	LD
X-SR1802	Apogonia sp15	Matale	Dambulla	L3	EZ1	LD
X-SR1840	<i>Sophrups</i> sp2	Kandy	Udawattakele FR	L14	EZ2	LW
X-SR1865	<i>Selaserica nitida</i>	Nuwara Eliya	Piduruthalagala FR	L11	EZ5	MO
X-SR1869	<i>Selaserica impexa</i>	Galle	Hiyare FR	L8	EZ1	LW
X-SR1889	Apogonia sp5	Matale	Dambulla	L3	EZ1	LD
X-SR1893	<i>Maladera karunaratnae</i>	Matale	Dambulla	L3	EZ1	LD
X-SR1895	<i>Selaserica nitida</i>	Nuwara Eliya	Hakgala SNR	L5	EZ4	MO
X-SR1896	<i>Selaserica nitida</i>	Nuwara Eliya	Hakgala SNR	L5	EZ4	MO
X-SR1904	<i>Maladera calcarata</i>	Matale	Dambulla	L3	EZ1	LD
X-SR1915	<i>Maladera padaviyaensis</i>	Matale	Dambulla	L3	EZ1	LD
X-SR1921	<i>Neoserica sexfoliata</i>	Matale	Dambulla	L3	EZ1	LD

X-SR1924	Parastasia sp	Kurunagala	Muttetugala Road	L19	EZ1	LW
X-SR1930	Parastasia sp	Kandy	Deenston	L4	EZ3	SM
X-SR1935	Maladera lindulana	Kandy	Deenston	L4	EZ3	SM
X-SR1943	Maladera fistulosa	Nuwara Eliya	Hakgala SNR	L5	EZ4	MO
X-SR1946	<i>Maladera hiyarensis</i>	Galle	Hiyare FR	L8	EZ1	LW
X-SR1947	Selaserica fabriziae	Galle	Kottawa FR	L9	EZ1	LW
X-SR1955	Selaserica impexa	Galle	Hiyare FR	L8	EZ1	LW
X-SR1962	Selaserica fabriziae	Galle	Kottawa FR	L9	EZ1	LW
X-SR1963	Selaserica fabriziae	Galle	Kottawa FR	L9	EZ1	LW
X-SR1964	Selaserica fabriziae	Galle	Kottawa FR	L9	EZ1	LW
X-SR1970	Selaserica praetexta	Kandy	Udawattakele FR	L14	EZ2	LW
X-SR1972	Selaserica praetexta	Kandy	Gannoruwa FR	L13	EZ2	LW
X-SR1973	Selaserica praetexta	Kandy	Gannoruwa FR	L13	EZ2	LW
X-SR1974	Selaserica praetexta	Kandy	Gannoruwa FR	L13	EZ2	LW
X-SR1975	Selaserica praetexta	Kandy	Gannoruwa FR	L13	EZ2	LW
X-SR1976	Anomala sp	Kandy	Udawattakele FR	L14	EZ2	LW
X-SR1984	M. bandarawelana	Matale	Riverston	L2	EZ2	SM
X-SR1985	M. bandarawelana	Matale	Riverston	L2	EZ2	SM
X-SR1986	M. bandarawelana	Matale	Riverston	L2	EZ2	SM
X-SR2000	Maladera iuga	Matale	Riverston	L2	EZ2	SM
X-SR2017	Selaserica praetexta	Matale	Riverston	L2	EZ2	SM
X-SR2022	Maladera iuga	Matale	Riverston	L2	EZ2	SM
X-SR2025	Selaserica praetexta	Matale	Riverston	L2	EZ2	SM
X-SR2027	Maladera mollis	Matale	Dambulla	L3	EZ1	LD
X-SR2030	Maladera rufocuprea	Matale	Dambulla	L3	EZ1	LD
X-SR2032	Maladera rufocuprea	Matale	Dambulla	L3	EZ1	LD

X-SR2034	<i>Maladera lindulana</i>	Kandy	Deenston	L4	EZ3	SM
X-SR2041	<i>Apogonia coriacea</i>	Kandy	Deenston	L4	EZ3	SM
X-SR2042	<i>Selaserica praetexta</i>	Kandy	Gannoruwa FR	L13	EZ2	LW
X-SR2043	<i>Selaserica praetexta</i>	Kandy	Gannoruwa FR	L13	EZ2	LW
X-SR2045	<i>Maladera kandyensis</i>	Kandy	Gannoruwa FR	L13	EZ2	LW
X-SR2046	<i>Selaserica praetexta</i>	Kandy	Gannoruwa FR	L13	EZ2	LW
X-SR2048	<i>Maladera galdaththana</i>	Kandy	Gannoruwa FR	L13	EZ2	LW
X-SR2052	<i>Adoretus</i> sp4	Nuwara Eliya	Piduruthalagala FR	L11	EZ5	LW1
X-SR2058	<i>Selaserica nuwarana</i>	Nuwara Eliya	Hakgala SNR	L5	EZ4	MO
X-SR2074	<i>Sel. convexiuscula</i>	Galle	Kottawa FR	L9	EZ1	LW
X-SR2075	<i>Sophrops</i> sp2	Galle	Kottawa FR	L9	EZ1	LW
X-SR2076	<i>Apogonia glabrilinea</i>	Galle	Kottawa FR	L9	EZ1	LW
X-SR2077	<i>Apogonia glabrilinea</i>	Galle	Kottawa FR	L9	EZ1	LW
X-SR2078	<i>Apogonia nietneri</i>	Galle	Kottawa FR	L9	EZ1	LW
X-SR2087	<i>Apogonia</i> sp8	Nuwara Eliya	Piduruthalagala FR	L11	EZ5	MO
X-SR2088	<i>Apogonia</i> sp8	Nuwara Eliya	Piduruthalagala FR	L11	EZ5	MO
X-SR2089	<i>Apogonia</i> sp8	Nuwara Eliya	Piduruthalagala FR	L11	EZ5	MO
X-SR2099	<i>Selaserica nuwarana</i>	Nuwara Eliya	Hakgala SNR	L5	EZ4	MO
X-SR2111	<i>Apogonia nietneri</i>	Galle	Kottawa FR	L9	EZ1	LW
X-SR2113	<i>Adoretus</i> sp7	Galle	Kottawa FR	L9	EZ1	LW
X-SR2125	<i>Anomala</i> sp1	Galle	Hiyare FR	L8	EZ1	LW
X-SR2126	<i>Apogonia glabrilinea</i>	Galle	Hiyare FR	L8	EZ1	LW
X-SR2129	<i>Apogonia glabrilinea</i>	Galle	Hiyare FR	L8	EZ1	LW
X-SR2135	<i>Anomala</i> sp1	Galle	Hiyare FR	L8	EZ1	LW
X-SR2136	<i>Parastasia</i> sp	Galle	Hiyare FR	L8	EZ1	LW
X-SR2146	<i>Holotrichia</i> sp5	Galle	Hiyare FR	L8	EZ1	LW

X-SR2147	<i>Maladera cinnaberina</i>	Kegalle	Aranayake	L1	EZ1	LW
X-SR2148	<i>Maladera cinnaberina</i>	Kegalle	Aranayake	L1	EZ1	LW
X-SR2153	<i>Maladera pubescens</i>	Kegalle	Galdaththa	L1	EZ1	LW
X-SR2154	<i>Maladera pubescens</i>	Kegalle	Galdaththa	L1	EZ1	LW
X-SR2156	<i>Apogonia solida</i>	Kegalle	Aranayake	L1	EZ1	LW
X-SR2157	<i>Apogonia solida</i>	Kegalle	Aranayake	L1	EZ1	LW
X-SR2159	<i>Selaserica praetexta</i>	Kandy	Udawattakele FR	L14	EZ2	LW
X-SR2160	<i>Selaserica praetexta</i>	Kandy	Udawattakele FR	L14	EZ2	LW
X-SR2162	<i>Maladera breviatella</i>	Kandy	Udawattakele FR	L14	EZ2	LW
X-SR2163	<i>Maladera kandyensis</i>	Kandy	Udawattakele FR	L14	EZ2	LW
X-SR2164	<i>Selaserica praetexta</i>	Kandy	Udawattakele FR	L14	EZ2	LW
X-SR2208	<i>Selaserica praetexta</i>	Kandy	Gannoruwa FR	L13	EZ2	LW
X-SR2209	<i>Selaserica praetexta</i>	Kandy	Gannoruwa FR	L13	EZ2	LW
X-SR2210	<i>Selaserica praetexta</i>	Kandy	Gannoruwa FR	L13	EZ2	LW
X-SR2214	<i>Anomala</i> sp1	Kandy	Gannoruwa FR	L13	EZ2	LW
X-SR2215	<i>Anomala</i> sp1	Kandy	Gannoruwa FR	L13	EZ2	LW
X-SR2233	<i>Adoretus</i> sp8	Kandy	UdaPeradeniya	L12	EZ2	LW
X-SR2236	<i>Anomala</i> sp2	Kandy	UdaPeradeniya	L12	EZ2	LW
X-SR2245	<i>Maladera galdaththana</i>	Matale	Riverston	L2	EZ2	SM
X-SR2246	<i>Maladera galdaththana</i>	Matale	Riverston	L2	EZ2	SM
X-SR2247	<i>Maladera athukoralai</i>	Matale	Riverston	L2	EZ2	SM
X-SR2251	<i>Apogonia ludificans</i>	Matale	Riverston	L2	EZ2	SM
X-SR2253	<i>Apogonia ludificans</i>	Matale	Riverston	L2	EZ2	SM
X-SR2262	<i>Apogonia</i> sp15	Matale	Riverston	L2	EZ2	SM
X-SR2350	<i>Xylotrupes</i> sp5	Kandy	UdaPeradeniya	L12	EZ2	LW
X-SR2354	<i>Xylotrupes</i> sp5	Kandy	UdaPeradeniya	L12	EZ2	LW

X-SR2355	<i>Xylotrupes</i> sp5	Kandy	UdaPeradeniya	L12	EZ2	LW
X-SR2357	<i>Alissonotum</i> sp9	Kandy	Gannoruwa FR	L13	EZ2	LW
X-SR2358	<i>Xylotrupes</i> sp5	Galle	Hiyare FR	L8	EZ1	LW
X-SR2360	<i>Holotrichia</i> sp5	Galle	Hiyare FR	L8	EZ1	LW
X-SR2361	<i>Holotrichia</i> sp5	Galle	Hiyare FR	L8	EZ1	LW
X-SR2362	<i>Leucopholis</i> sp2	Galle	Kottawa FR	L9	EZ1	LW
X-SR2364	<i>Xylotrupes</i> sp5	Galle	Kottawa FR	L9	EZ1	LW
X-SR2365	<i>Holotrichia</i> sp5	Galle	Kottawa FR	L9	EZ1	LW

Table S4.2. Number of MOTUs, number of matches between MOTUs and morphospecies (in parenthesis), and match ratios (Ahrens et al. 2016) of DNA-based species delimitation methods. Numers are given for the total dataset, individual clades, and cumulative subclades. Match ratio = $2 \times N_{\text{match}} / (N_{\text{mol}} + N_{\text{morph}})$.

	PTP	ASAP	TCS	3%	2%	bPTP	mlPTP	ABGD
Total dataset								
N motu	85 (64)	82 (64)	129 (67)	107 (72)	126(65)	139(64)	107(72)	104(70)
Match ratio	0,69	0,70	0,58	0,70	0,58	0,54	0,69	0,67
Cumulative subclade dataset								
N motu	80 (55)	92 (66)	126 (60)	107 (72)	125(65)			
Match ratio	0,62	0,69	0,54	0,70	0,58			
Clade1	11 (7)	9 (6)	21 (6)	19 (7)	22(5)			
Match ratio	0,61	0,57	0,36	0,45	0,29			
Clade2	13 (8)	15 (9)	18 (8)	16 (12)	17(10)			
Match ratio	0,62	0,64	0,52	0,83	0,67			
Clade3	40 (28)	44 (28)	60 (32)	48 (31)	58(31)			
Match ratio	0,64	0,61	0,59	0,65	0,58			
Clade4	16 (12)	24 (23)	27 (14)	23 (21)	28(19)			
Match ratio	0,59	0,94	0,54	0,88	0,72			

Table S4.3. Species similarity among different forest types and elevation zones among morphospecies, haplotypes and MOTUs. LW: wet lowland; LD: dry lowland; SM: sub-montane; MO: montane. EZ1: 0–500 m, EZ2: 501–1000 m, EZ3: 1001–1500 m, EZ4: 1501–2000 m, EZ5: 2001–2500 m.

Morphospecies	LW	LD	SM	MO	EZ1	EZ2	EZ3	EZ4	EZ5	
LW	1				EZ1	1				
LD	0,11	1			EZ2	0,19	1			
SM	0,15	0,13	1		EZ3	0,07	0,12	1		
MO	0	0,02	0,04	1	EZ4	0,01	0	0,03	1	
					EZ5	0	0	0,07	0,53	1
Haplotype										
LW	1				EZ1	1				
LD	0,006				EZ2	0,014	1			
SM	0,005	0,006	1		EZ3	0	0,018	1		
MO	0	0	0	1	EZ4	0	0	0	1	
					EZ5	0	0	0	0,076	1
mPTP MOTU										
LW	1				EZ1	1				
LD	0,27	1			EZ2	0,28	1			
SM	0,26	0,22	1		EZ3	0,18	0,2	1		
MO	0	0	0	1	EZ4	0	0	0	1	
TCS MOTU										
LW	1				EZ1	1				
LD	0,13	1			EZ2	0,14	1			
SM	0,10	0,06	1		EZ3	0,06	0,17	1		
MO	0	0	0	1	EZ4	0	0	0	1	
					EZ5	0	0	0	0,38	1

ASAP	LW	1				EZ1	1							
	LD	0,22	1			EZ2	0,31	1						
	SM	0,23	0,19	1		EZ3	0,19	0,24	1					
	MO	0	0	0,02	1	EZ4	0,00	0,00	0,03	1,00				
						EZ5	0	0	0,03	0,56	1			
3% clustering	LW	1				EZ1	1							
	LD	0,183	1			EZ2	0,177	1						
	SM	0,105	0,125	1		EZ3	0,099	0,184	1					
	MO	0	0	0	1	EZ4	0	0	0	1				
						EZ5	0	0	0	0,5	1			
2% clustering	LW	1				EZ1	1,00							
	LD	0,14	1			EZ2	0,12	1						
	SM	0,11	0,08	1		EZ3	0,06	0,18	1,00					
	MO	0	0	0	1	EZ4	0,00	0,00	0,00	1				
						EZ5	0	0	0	0,38	1			

Table S7.1: Details of sampling sites (Sri Lanka); L number, coordinates, elevation, elevation zone and forest types. Elevation zones; EZ1: 0-500m, EZ2: 501-1000m, EZ3: 1001-1500m, EZ4: 1501-2000m, EZ5; 2001-2500m. Forest types; WL: evergreen wet lowland forests, DL: evergreen dry lowland forests, SM: sub-montane forests, MO: montane forests.

Permit no: WL/3/2/61/18, R&E/RES/NFSRCM/2019-01,

R&E/RES/NFSRCM/EXTENSION/2020, K/G/01/06/03, M/0/03/2019.

Site	L Number	Latitude	Longitude	Elevation (m)	Elevation zone	Forest type
Aranayake	L1	7.1519	80.4638	245	EZ1	WL
Riverston	L2	7.5491	80.7539	882	EZ2	SM
Dambulla	L3	7.8578	80.6739	167	EZ1	DL
Deenston	L4	7.3299	80.8609	1142	EZ3	SM
Nuwara Eliya	L5	6.9118	80.7949	1882	EZ4	MO
Horton Plains	L6	6.8073	80.8047	2154	EZ5	MO
Belihuloya	L7	6.7317	80.7740	750	EZ2	WL
Hiyare FR	L8	6.0596	80.3150	116	EZ1	WL
Kottawa FR	L9	6.0971	80.3167	49	EZ1	WL
Kanneliya FR	L10	6.2501	80.3380	42	EZ1	WL
Piduruthalagala FR	L11	7.0003	80.7753	2483	EZ5	MO
Uda peradeniya	L12	7.2470	80.6149	788	EZ2	WL
Gannoruwa FR	L13	7.2834	80.5984	592.5	EZ2	WL
Udawattakele FR	L14	7.2969	80.6448	616	EZ2	WL

<i>Sophraps sp4</i>	L3	EZ1	LD	0,5625	0,325	0,9625	0,2875	0,125	0,9875	0,5125	0,73125	0,6125	0,55625	0,3625	0,26875	0,13125	0,4	0,125	0,41875	0,08125	0,28125	0,0875	0,3
<i>Sophraps sp4</i>	L3	EZ1	LD	0,5125	0,34375	0,84375	0,29375	0,13125	0,95	0,5	0,70625	0,59375	0,54375	0,3625	0,25	0,125	0,3875	0,1125	0,39375	0,075	0,26875	0,06875	0,29375
<i>Sophraps sp4</i>	L4	EZ3	SM	0,46875	0,2875	0,875	0,2625	0,1375	0,8875	0,46875	0,68125	0,55	0,5125	0,33125	0,25	0,1	0,375	0,10625	0,40625	0,075	0,25	0,06875	0,2625
<i>Sophraps sp5</i>	L3	EZ1	LD	0,66	0,37	1,11	0,38	0,13	1,15	0,6	0,84	0,71	0,65	0,45	0,34	0,19	0,47	0,15	0,5	0,1	0,32	0,1	0,35
<i>Sel. pusilla</i>	L3	EZ1	LD	0,28125	0,13125	0,5	0,125	0,05	0,4375	0,21875	0,375	0,2875	0,25	0,16875	0,1	0,09375	0,1875	0,06875	0,1625	0,0375	0,11875	0,04375	0,125
<i>M. mollis</i>	L3	EZ1	LD	0,3625	0,21875	0,5	0,14375	0,0625	0,54375	0,25	0,40625	0,33125	0,3125	0,1875	0,11875	0,16875	0,21875	0,0875	0,1875	0,0625	0,15625	0,0625	0,125
<i>Sel. nitida</i>	L5	EZ4	MO	0,575	0,34375	0,93818	0,30625	0,10625	1,01508	0,6152	0,73125	0,59375	0,5625	0,3625	0,1875	0,25	0,4125	0,18125	0,36875	0,125	0,25	0,10625	0,31875
<i>Sel. sororinitida</i>	L4	EZ3	SM	0,375	0,1875	0,7625	0,23125	0,1	0,79976	0,4375	0,6375	0,4875	0,4625	0,3	0,1625	0,19375	0,2875	0,125	0,2625	0,075	0,16875	0,075	0,21875
<i>Sel. sororinitida</i>	L4	EZ3	SM	0,4375	0,2375	0,59375	0,21875	0,05	0,61875	0,34375	0,55625	0,45	0,40625	0,2125	0,15625	0,21875	0,275	0,11875	0,2375	0,075	0,13125	0,03125	0,125
<i>Sel. sororinitida</i>	L4	EZ3	SM	0,425	0,25	0,775	0,1875	0,1	0,78	0,4375	0,53125	0,45	0,425	0,2875	0,1625	0,18125	0,28125	0,10625	0,2375	0,0625	0,175	0,06875	0,2125
<i>Sel. sororinitida</i>	L4	EZ3	SM	0,4	0,25	0,71875	0,21875	0,1125	0,775	0,40625	0,5875	0,46875	0,45	0,3	0,13125	0,19375	0,275	0,1125	0,25	0,06875	0,1875	0,075	0,2
<i>Sel. sororinitida</i>	L4	EZ3	SM	0,375	0,19375	0,7375	0,1875	0,10625	0,71875	0,375	0,5625	0,4375	0,41875	0,30625	0,13125	0,1875	0,28125	0,10625	0,25	0,0625	0,20625	0,06875	0,1875
<i>Sel. sororinitida</i>	L4	EZ3	SM	0,3875	0,2375	0,7375	0,19375	0,1	0,75	0,40625	0,53125	0,45	0,425	0,29375	0,125	0,1875	0,275	0,1125	0,2625	0,0625	0,2	0,075	0,20625
<i>Sel. sororinitida</i>	L4	EZ3	SM	0,40625	0,25	0,8	0,2375	0,11875	0,81	0,46875	0,56875	0,5	0,46875	0,30625	0,1375	0,25625	0,2875	0,11875	0,275	0,08125	0,21875	0,06875	0,20625
<i>M. tricuspidata</i>	L3	EZ1	LD	0,375	0,2	0,5125	0,175	0,0625	0,55625	0,26875	0,4375	0,35	0,325	0,18125	0,1125	0,21875	0,23125	0,09375	0,19375	0,0625	0,125	0,04375	0,1125
<i>M. deenstana</i>	L4	EZ3	SM	0,3625	0,16875	0,50625	0,125	0,05625	0,5125	0,28125	0,39375	0,3125	0,26875	0,1625	0,1	0,1875	0,1875	0,06875	0,175	0,05625	0,125	0,05	0,125
<i>M. weligamana</i>	L5	EZ4	MO	0,38125	0,14375	0,64375	0,16875	0,0625	0,65625	0,40625	0,50625	0,39375	0,34375	0,2	0,1125	0,24375	0,25625	0,0875	0,21875	0,05625	0,15	0,04375	0,125
<i>M. weligamana</i>	L5	EZ4	MO	0,41875	0,15625	0,7	0,18125	0,06875	0,69375	0,40625	0,55625	0,40625	0,35625	0,2125	0,125	0,2375	0,26875	0,0875	0,21875	0,0625	0,175	0,05	0,15625
<i>M. windy</i>	L4	EZ3	SM	0,25	0,125	0,38125	0,125	0,05625	0,40625	0,1875	0,325	0,25	0,2375	0,15	0,075	0,14375	0,175	0,075	0,15	0,04375	0,11875	0,0375	0,1
<i>M. windy</i>	L4	EZ3	SM	0,3	0,15625	0,4375	0,13125	0,0625	0,46875	0,23125	0,33125	0,28125	0,25625	0,1625	0,08125	0,1625	0,1875	0,075	0,1625	0,04375	0,125	0,0375	0,10625

Table S7.3: Variance explained by principal component analysis for the complete sampling (derived from raw and size reduced data).

PC	% variance	
	raw	log
PC1	96.96	86.80
PC2	0.91	7.17
PC3	0.64	1.11
PC4	0.27	1.03
PC5	0.24	0.84
PC6	0.20	0.64
PC7	0.16	0.44
PC8	0.12	0.43
PC9	0.10	0.33
PC10	0.09	0.28
PC11	0.07	0.23
PC12	0.06	0.18
PC13	0.04	0.16
PC14	0.04	0.11
PC15	0.03	0.09
PC16	0.02	0.05
PC17	0.02	0.04
PC18	0.01	0.02
PC19	0.01	0.02
PC20	0.01	0.02

Table S7.4: Euclidean distances of species disparity (mean/median/maximum) partitioned by forest types and lineages (all Pleurosticts, Sericini only, and Pleurosticts excluding Sericini (*)) based on raw data and log-normalized data.

WL: Wet lowland; DL: Dry lowland; SM: Sub-montane; MO: Montane.

	raw				log				
	Lineage	WL	DL	SM	MO	WL	DL	SM	MO
Mean									
<i>All Pleurosticts</i>	1.424	0.778	0.721	0.458	1.131	0.995	0.929	0.616	
<i>Sericini</i>	0.313	0.281	0.358	0.366	0.455	0.492	0.596	0.445	
<i>Pleurosticts (part)*</i>	1.613	0.933	0.843	0.556	1.171	1.038	0.937	0.436	
Median									
<i>All Pleurosticts</i>	0.943	0.449	0.479	0.393	0.928	0.837	0.808	0.662	
<i>Sericini</i>	0.279	0.257	0.310	0.265	0.448	0.465	0.526	0.388	
<i>Pleurosticts (part)*</i>	1.287	0.748	0.608	0.380	1.031	0.912	0.786	0.435	
Maximum									
<i>All Pleurosticts</i>	5.623	3.959	3.092	1.201	3.483	3.237	3.134	1.420	
<i>Sericini</i>	0.878	0.823	1.201	1.077	1.156	1.257	1.870	1.183	
<i>Pleurosticts (part)*</i>	5.577	3.855	2.761	1.201	3.417	3.195	2.627	1.038	

Table S7.5: Euclidean distances of species disparity (mean/median/maximum) partitioned by elevational zones and lineages (all Pleurosticts, Sericini only, and Pleurosticts excluding Sericini (*)) based on raw data and log-normalized data. EZ1: 0-500m. EZ2: 501-1000m. EZ3: 1001-1500m. EZ4: 1501-2000m. EZ5: 2001-2500m.

Lineage	raw					log				
	EZ1	EZ2	EZ3	EZ4	EZ5	EZ1	EZ2	EZ3	EZ4	EZ5
<i>Mean</i>										
<i>All Pleurosticts</i>	1.259	1.115	0.807	0.441	0.481	1.160	1.105	1.003	0.609	0.703
<i>Sericini</i>	0.347	0.400	0.320	0.286	0.413	0.536	0.644	0.551	0.396	0.488
<i>Pleurosticts (part)*</i>	1.512	1.293	0.926	0.407	0.339	1.238	1.084	0.962	0.474	0.611
<i>Median</i>										
<i>All Pleurosticts</i>	0.758	0.584	0.576	0.364	0.452	0.939	0.900	0.882	0.615	0.710
<i>Sericini</i>	0.313	0.377	0.283	0.184	0.288	0.492	0.600	0.460	0.338	0.424
<i>Pleurosticts (part)*</i>	1.164	0.885	0.697	0.369	0.262	1.085	0.911	0.872	0.534	0.389
<i>Maximum</i>										
<i>All Pleurosticts</i>	5.756	5.167	3.100	1.187	1.124	3.781	3.982	3.160	1.309	1.522
<i>Sericini</i>	1.013	1.194	0.925	0.840	1.030	1.445	1.847	1.580	1.000	1.164
<i>Pleurosticts (part)*</i>	5.654	4.842	2.697	0.916	0.812	3.760	3.432	2.632	1.002	1.531

Table S7.6: Euclidean distances of species disparity (mean/median/maximum) partitioned by localities (L1-14), and lineages (all Pleurostictids, Sericini only, and Pleurostictids excluding Sericini (*)) based on raw data and log-normalized data.

Mean	raw													
Lineage	L1	L2	L3	L4	L5	L6	L8	L9	L10	L11	L12	L13	L14	
<i>All Pleurostictids</i>	1.675	0.385	0.778	0.807	0.441	0.487	1.165	1.543	0.783	0.432	1.897	1.320	0.716	
<i>Sericini</i>	0.265	0.424	0.281	0.320	0.286	0.427	0.283	0.222	0.055	0.329	0.000	0.094	0.065	
<i>Pleurostictids (part)*</i>	1.857	0.273	0.933	0.926	0.407	0.426	1.228	1.698	0.840	0.175	1.897	1.157	0.588	
	log													
	L1	L2	L3	L4	L5	L6	L8	L9	L10	L11	L12	L13	L14	
<i>All Pleurostictids</i>	1.255	0.729	0.995	1.004	0.609	0.730	0.947	1.145	0.762	0.580	1.124	1.187	0.761	
<i>Sericini</i>	0.363	0.683	0.492	0.551	0.396	0.491	0.430	0.270	0.074	0.411	0.000	0.209	0.155	
<i>Pleurostictids (part)*</i>	1.274	0.509	1.038	0.963	0.474	0.765	0.824	1.190	0.802	0.205	1.124	0.903	0.609	
Median	raw													
Lineage	L1	L2	L3	L4	L5	L6	L8	L9	L10	L11	L12	L13	L14	
<i>All Pleurostictids</i>	1.248	0.338	0.449	0.576	0.364	0.408	0.650	1.255	0.623	0.382	1.206	0.894	0.613	
<i>Sericini</i>	0.245	0.374	0.257	0.283	0.184	0.226	0.247	0.222	0.055	0.196	0.000	0.094	0.065	
<i>Pleurostictids (part)*</i>	1.578	0.235	0.748	0.697	0.369	0.426	1.292	1.634	0.678	0.118	1.206	1.157	0.325	
	log													
	L1	L2	L3	L4	L5	L6	L8	L9	L10	L11	L12	L13	L14	
<i>All Pleurostictids</i>	1.018	0.678	0.837	0.882	0.616	0.849	0.769	0.997	0.673	0.606	1.052	1.297	0.789	
<i>Sericini</i>	0.313	0.604	0.465	0.460	0.339	0.350	0.414	0.270	0.074	0.377	0.000	0.209	0.155	
<i>Pleurostictids (part)*</i>	1.133	0.530	0.912	0.872	0.534	0.765	0.618	1.057	0.638	0.173	1.052	0.903	0.616	

Maximum		raw													
Lineage	L1	L2	L3	L4	L5	L6	L8	L9	L10	L11	L12	L13	L14		
<i>All Pleurosticts</i>	5.623	1.195	3.959	3.100	1.187	1.109	3.828	4.319	2.303	1.039	4.269	3.240	1.955		
<i>Sericini</i>	0.772	1.194	0.823	0.925	0.840	1.054	0.690	0.444	0.110	0.947	0.000	0.187	0.130		
<i>Pleurosticts (part)*</i>	5.563	0.790	3.855	2.697	0.916	0.851	2.998	4.322	2.304	0.393	4.269	2.314	1.322		
		log													
	L1	L2	L3	L4	L5	L6	L8	L9	L10	L11	L12	L13	L14		
<i>All Pleurosticts</i>	3.477	1.844	3.237	3.161	1.310	1.531	2.772	3.041	2.059	1.272	2.529	2.435	1.694		
<i>Sericini</i>	1.012	1.847	1.257	1.581	1.000	1.150	1.011	0.539	0.147	1.157	0.000	0.418	0.309		
<i>Pleurosticts (part)*</i>	3.381	1.190	3.195	2.633	1.002	1.531	1.708	3.042	2.062	0.429	2.529	1.805	1.269		

Table S7.7: Pairwise p-values from non-parametric MANOVA on PCA loadings representing 95% of variation and partitioned for forest types and lineages (all Pleurosticts, Sericini only, and Pleurosticts excluding Sericini (*)). Significant correlations (p value <0.05) are shown in bold italics. WL: Wet lowland; DL: Dry lowland; SM: Sub-montane; MO: Montane.

Lineage	Forest	raw				log			
		WL	SM	DL	MO	WL	SM	DL	MO
<i>All Pleurosticts</i>	WL								
	SM	0.602				0.972			
	DL	0.575	0.964			0.014	0.003		
	MO	0.190	0.620	0.979		0.033	0.007	0.963	
<i>Sericini</i>	WL								
	SM	0.979				0.389			
	DL	0.971	0.964			0.714	0.750		
	MO	0.990	0.844	0.990		0.993	0.419	0.864	
<i>Pleurosticts (part)*</i>	WL								
	SM	0.950				0.829			
	DL	0.889	0.867			0.855	0.875		
	MO	0.857	0.716	0.669		0.752	0.837	0.891	

Table S7.8: Pairwise p-values from non-parametric MANOVA on PCA loadings representing 95% of variation and partitioned for elevational zones and lineages (all Pleurosticts, Sericini only, and Pleurosticts excluding Sericini (*)). Significant correlations (p value <0.05) are shown in bold italics. EZ1: 0-500m. EZ2: 501-1000m. EZ3: 1001-1500m. EZ4: 1501-2000m. EZ5: 2001-2500m.

Lineage	raw					log				
	EZ1	EZ2	EZ3	EZ4	EZ5	EZ1	EZ2	EZ3	EZ4	EZ5
<i>All Pleurosticts</i>										
EZ1										
EZ2	0.813					0.999				
EZ3	0.926	0.974				0.998	0.994			
EZ4	0.371	0.695	0.796			0.012	0.008	0.006		
EZ5	0.104	0.519	0.463	0.870		0.0001	0.0001	0.0001	0.118	
<i>Sericini</i>										
EZ1										
EZ2	0.987					0.983				
EZ3	0.848	0.837				0.133	0.068			
EZ4	0.801	0.861	0.889			0.841	0.635	0.106		
EZ5	0.171	0.175	0.722	0.797		0.831	0.848	0.295	0.423	
<i>Pleurosticts (part)*</i>										
EZ1										
EZ2	0.793					0.993				
EZ3	0.913	0.942				0.896	0.517			
EZ4	0.854	0.363	0.574			0.959	0.982	0.545		
EZ5	0.418	0.554	0.727	0.387		0.008	0.001	0.018	0.017	

Table S7.9: Pairwise p-values from non-parametric MANOVA on PCA loadings representing 95% of variation and partitioned for localities and lineages from raw data (all Pleurostictis, Sericini only, and Pleurostictis excluding Sericini (*)). Significant correlations (p value <0.05) are shown in bold italics.

<i>All</i>	L1	L2	L3	L4	L5	L6	L8	L9	L10	L11	L12	L13	L14
<i>Pleurostictis</i>													
L1													
L2	0.180												
L3	0.562	0.988											
L4	0.880	0.558	0.945										
L5	0.302	0.997	0.999	0.791									
L6	0.059	0.703	0.505	0.316	0.639								
L8	0.979	0.150	0.495	0.960	0.344	0.046							
L9	0.921	0.278	0.652	0.949	0.521	0.117	0.897						
L10	0.983	0.034	0.192	0.582	0.101	0.009	0.965	0.859					
L11	0.354	0.978	0.999	0.844	0.999	0.529	0.376	0.481	0.126				
L12	0.941	0.429	0.821	0.830	0.719	0.208	0.771	0.907	0.747	0.792			
L13	0.142	0.983	0.939	0.616	0.957	0.967	0.150	0.336	0.035	0.943	0.348		
L14	0.890	0.434	0.783	0.906	0.597	0.215	0.824	0.787	0.431	0.593	0.694	0.346	
<i>Sericini</i>													
L1													
L2	0.868												
L3	0.937	0.984											
L4	0.916	0.993	0.996										
L5	0.928	0.988	0.996	0.999									
L6	0.983	0.778	0.863	0.839	0.856								
L8	0.880	1.000	0.989	0.995	0.991	0.792							
L9	0.099	0.032	0.048	0.041	0.044	0.136	0.034						
L10	0.116	0.041	0.057	0.053	0.058	0.163	0.043	0.578					
L11	0.900	0.992	0.986	0.997	0.997	0.824	0.993	0.038	0.052				
L13	0.120	0.042	0.059	0.054	0.059	0.169	0.044	0.655	0.992	0.052			
L14	0.078	0.030	0.039	0.038	0.042	0.110	0.031	0.242	0.803	0.039	0.733		

<i>Pleurostictis (part)*</i>	L1	L2	L3	L4	L5	L6	L8	L9	L10	L11	L12	L13	L14
L1													
L2	0.927												
L3	0.852	0.984											
L4	0.850	0.983	0.998										
L5	0.987	0.907	0.829	0.834									
L6	0.235	0.119	0.084	0.083	0.237								
L8	0.926	0.983	0.959	0.967	0.933	0.124							
L9	0.938	0.998	0.976	0.977	0.925	0.126	0.991						
L10	0.993	0.921	0.844	0.847	0.999	0.231	0.938	0.936					
L11	0.543	0.464	0.408	0.430	0.638	0.167	0.565	0.495	0.610				
L12	0.879	0.992	0.997	0.998	0.862	0.094	0.977	0.988	0.875	0.445			
L13	0.186	0.092	0.064	0.063	0.182	0.971	0.092	0.096	0.179	0.110	0.071		
L14	0.866	0.936	0.919	0.936	0.897	0.106	0.982	0.950	0.896	0.637	0.941	0.077	

Table S7.10: Pairwise p-values from non-parametric MANOVA on PCA loadings representing 95% of variation and partitioned for localities and lineages from log normalized data (all Pleurosticts, Sericini only, and Pleurosticts excluding Sericini (*)). Significant correlations (p value <0.05) are shown in bold italics.

<i>All</i>	L1	L2	L3	L4	L5	L6	L8	L9	L10	L11	L12	L13	L14
<i>Pleurosticts</i>													
L1													
L2	0.0003												
L3	0.004	0.990											
L4	0.997	0.0002	0.003										
L5	0.006	0.495	0.901	0.007									
L6	0.0001	0.009	0.006	0.0001	0.004								
L8	0.141	0.098	0.289	0.163	0.303	0.0002							
L9	0.001	0.924	0.975	0.001	0.858	0.005	0.314						
L10	0.028	0.472	0.889	0.019	0.853	0.003	0.550	0.718					
L11	0.0003	0.728	0.862	0.001	0.909	0.045	0.055	0.811	0.467				
L12	0.212	0.028	0.100	0.169	0.121	0.0001	0.671	0.071	0.410	0.027			
L13	0.589	0.0001	0.0002	0.696	0.001	0.0002	0.006	0.000	0.001	0.0001	0.012		
L14	0.016	0.531	0.673	0.008	0.310	0.003	0.644	0.760	0.751	0.240	0.403	0.0001	
<i>Sericini</i>													
L1													
L2	0.986												
L3	0.974	0.995											
L4	0.984	0.972	0.947										
L5	0.835	0.877	0.917	0.761									
L6	0.995	0.997	0.990	0.978	0.867								
L8	0.738	0.770	0.819	0.645	0.971	0.766							
L9	0.013	0.016	0.020	0.009	0.052	0.015	0.076						
L10	0.001	0.001	0.001	0.000	0.002	0.001	0.004	0.032					
L11	0.984	0.997	0.999	0.958	0.904	0.996	0.807	0.019	0.001				
L13	0.003	0.003	0.003	0.002	0.009	0.003	0.016	0.145	0.762	0.003			
L14	0.0005	0.0004	0.001	0.0005	0.001	0.000	0.003	0.018	0.969	0.001	0.617		

Table S8.1: Details of sampling sites, habitat types

L	Site	Latitude	Longitude	FR	EZ	Habitat	Trap
L1	Aranayake	7,1507	80,4629	WL	EZ1	Abandon plantation	1B
L1	Aranayake	7,1505	80,4624	WL	EZ1	Grassland	1C
L1	Aranayake	7,1615	80,4639	WL	EZ1	Hilltop	1D
L1	Aranayake	7,1509	80,4629	WL	EZ1	Plantation	1A
L1	Aranayake	7,1583	80,4667	WL	EZ1	Plantation	1E
L1	Aranayake	7,1442	80,4503	WL	EZ1	Rock outcrop	1F
L11	Piduruthlagala	6,9896	80,7713	MO	EZ5	Central forest	11B
L11	Piduruthlagala	6,9988	80,7764	MO	EZ5	Central forest	11C
L11	Piduruthlagala	7,0003	80,7753	MO	EZ5	Central forest	11D
L11	Piduruthlagala	6,9785	80,7794	MO	EZ5	Forest Edge	11E
L11	Piduruthlagala	6,9787	80,7920	MO	EZ5	Forest Edge	11F
L11	Piduruthlagala	6,9830	80,7731	MO	EZ5	Hilltop	11A
L12	UdaPeradeniya	7,2480	80,6152	WL	EZ2	Disturbed forest	12B
L12	UdaPeradeniya	7,2487	80,6145	WL	EZ2	Disturbed forest	12C
L12	UdaPeradeniya	7,2475	80,6146	WL	EZ2	Disturbed forest	12D
L12	UdaPeradeniya	7,2506	80,6129	WL	EZ2	Forest Edge	12A
L12	UdaPeradeniya	7,2454	80,6140	WL	EZ2	Forest Edge	12F
L12	UdaPeradeniya	7,2470	80,6149	WL	EZ2	Grassland	12E
L13	Gannoruwa	7,2833	80,5982	WL	EZ2	Abandon plantation	13C
L13	Gannoruwa	7,2837	80,5983	WL	EZ2	Disturbed forest	13D
L13	Gannoruwa	7,2840	80,5983	WL	EZ2	Disturbed forest	13E
L13	Gannoruwa	7,2834	80,5990	WL	EZ2	Disturbed forest	13F
L13	Gannoruwa	7,2837	80,5987	WL	EZ2	Forest Edge	13B
L13	Gannoruwa	7,2834	80,5984	WL	EZ2	Rock outcrop	13A
L14	Udawattakele	7,2992	80,6425	WL	EZ2	Central forest	14D
L14	Udawattakele	7,2981	80,6500	WL	EZ2	Central forest	14F
L14	Udawattakele	7,3965	80,6540	WL	EZ2	Disturbed forest	14E
L14	Udawattakele	7,2973	80,6419	WL	EZ2	Forest Edge	14A
L14	Udawattakele	7,2967	80,6424	WL	EZ2	Forest valley	14B
L14	Udawattakele	7,2959	80,6422	WL	EZ2	Grassland	14C
L2	Riverston	7,5498	80,7521	SM	EZ2	Central forest	2C
L2	Riverston	7,5364	80,7723	SM	EZ2	Forest Edge	2A
L2	Riverston	7,5383	80,7500	SM	EZ2	Forest Edge	2E
L2	Riverston	7,5383	80,7511	SM	EZ2	Forest Edge	2F
L2	Riverston	7,5491	80,7539	SM	EZ2	Grassland	2B
L2	Riverston	7,5522	80,7529	SM	EZ2	Hilltop	2D
L3	Dambulla	7,8577	80,6747	DL	EZ1	Central forest	3B
L3	Dambulla	7,8580	80,6755	DL	EZ1	Central forest	3C
L3	Dambulla	7,8591	80,6759	DL	EZ1	Central forest	3F
L3	Dambulla	7,8590	80,6753	DL	EZ1	Forest Edge	3D
L3	Dambulla	7,8582	80,6751	DL	EZ1	Grassland	3E
L3	Dambulla	7,8578	80,6739	DL	EZ1	Rock outcrop	3A
L4	Deenston	7,3310	80,8593	SM	EZ3	Abandon plantation	4A
L4	Deenston	7,3350	80,8597	SM	EZ3	Central forest	4D
L4	Deenston	7,3362	80,8591	SM	EZ3	Central forest	4E
L4	Deenston	7,3389	80,8510	SM	EZ3	Central forest	4F
L4	Deenston	7,3316	80,8611	SM	EZ3	Forest Edge	4B

L4	Deenston	7,3308	80,8620	SM	EZ3	Forest Edge	4C
L5	NuwaraEliya	6,9113	80,7948	MO	EZ4	Central forest	5B
L5	NuwaraEliya	6,9109	80,7943	MO	EZ4	Central forest	5C
L5	NuwaraEliya	6,9307	80,8134	MO	EZ4	Central forest	5E
L5	NuwaraEliya	6,9300	80,8136	MO	EZ4	Central forest	5F
L5	NuwaraEliya	6,9118	80,7949	MO	EZ4	Forest Edge	5A
L5	NuwaraEliya	6,9305	80,8136	MO	EZ4	Forest Edge	5D
L8	Hiyare	6,0564	80,3170	WL	EZ1	Central forest	8C
L8	Hiyare	6, 070	80,3161	WL	EZ1	Central forest	8E
L8	Hiyare	6, 092	80,3320	WL	EZ1	Central forest	8F
L8	Hiyare	6,0596	80,3150	WL	EZ1	Forest Edge	8A
L8	Hiyare	6, 057	80,3151	WL	EZ1	Forest Edge	8B
L8	Hiyare	6,0587	80,3154	WL	EZ1	Grassland	8D
L9	Kottawa	6,0971	80,3167	WL	EZ1	Central forest	9A
L9	Kottawa	6,0981	80,3161	WL	EZ1	Central forest	9C
L9	Kottawa	6,1000	80,3086	WL	EZ1	Central forest	9D
L9	Kottawa	6,1345	80,3000	WL	EZ1	Central forest	9E
L9	Kottawa	6,0980	80,3167	WL	EZ1	Forest Edge	9B
L9	Kottawa	6,1367	80,3456	WL	EZ1	Forest valley	9F

Table S8.2: Details of species, recorded localities and their presence

Morphospecies/ Location	L1	L8	L9	L12	L13	L14	L3	L2	L4	L5	L11	L6
Forest/Elevation zone	WL/EZ	WL/EZ	WL/EZ	WL/EZ	WL/EZ	WL/EZ	DL/EZ	SM/EZ	SM/EZ	MO/EZ	MO/EZ	MO/EZ
	1	1	1	2	2	2	1	2	3	4	5	5
<i>M. anderssoni</i>	0	0	0	0	0	0	0	0	1	0	0	0
<i>Sel. athukoralai</i>	0	0	0	0	0	0	0	1	0	0	0	0
<i>M. badullana</i>	0	0	0	0	0	0	0	0	0	1	1	0
<i>M. bandarawelana</i>	0	0	0	0	0	0	0	1	0	0	0	0
<i>M. breviatella</i>	0	0	0	0	0	1	1	0	0	0	0	0
<i>M. calcarata</i>	0	0	0	0	0	0	1	0	0	0	0	0
<i>M. cervicornis</i>	0	0	0	0	0	0	0	1	0	0	0	0
<i>M. cinnaberina</i>	1	0	0	0	0	0	0	0	0	0	0	0
<i>Sel. convexiuscula</i>	0	0	1	0	0	0	0	0	0	0	0	0
<i>M. coxalis</i>	1	0	0	0	0	0	1	0	0	0	0	0
<i>M. dambullana</i>	0	0	0	0	0	0	1	0	0	0	0	0
<i>N. dharmapriyai</i>	1	0	0	0	0	0	0	0	0	0	0	0
<i>M. dubia</i>	0	0	0	0	0	0	0	0	0	1	1	0
<i>Sel. fabriziae</i>	0	0	1	0	0	0	0	0	0	0	0	0
<i>M. fistulosa</i>	0	0	0	0	0	0	0	0	0	1	0	0
<i>Serica fusa</i>	0	0	0	0	0	0	0	0	0	1	1	0
<i>M. galdaththana</i>	1	0	0	0	1	0	0	1	0	0	0	0
<i>M. haniel</i>	0	0	0	0	0	0	0	0	1	0	0	0
<i>M. heveli</i>	0	0	0	0	0	0	1	0	0	0	0	0
<i>M. hortonensis</i>	0	0	0	0	0	0	0	0	0	0	1	0

<i>Sel. impexa</i>	0	1	0	0	0	0	0	0	0	0	0	0
<i>M. iuga</i>	0	0	0	0	0	0	0	0	1	0	0	0
<i>M. kandyensis</i>	0	0	0	0	1	1	0	0	0	0	0	0
<i>M. karunaratnae</i>	0	0	0	0	0	0	1	1	0	0	0	0
<i>M. kishi</i>	0	0	0	0	0	0	0	0	1	0	0	0
<i>M. laterita</i>	0	0	0	0	0	0	0	1	0	0	0	0
<i>M. lindulana</i>	0	0	0	0	0	0	0	0	1	0	0	0
<i>Serica lurida</i>	0	0	0	0	0	0	0	1	1	0	0	0
<i>Sel. maculicauda</i>	0	0	0	0	0	0	0	0	0	0	0	1
<i>M. mollis</i>	0	0	0	0	0	0	1	0	0	0	0	0
<i>Sel. nitida</i>	0	0	0	0	0	0	0	0	0	1	1	0
<i>Sel. nuwarana</i>	0	0	0	0	0	0	0	0	0	1	0	0
<i>M. padaviyaensis</i>	0	0	0	0	0	0	1	0	0	0	0	0
<i>N. pophami</i>	0	0	0	0	0	0	1	0	0	0	0	0
<i>Sel. praetexta</i>	0	0	0	0	1	1	0	1	0	0	0	0
<i>M. pubescens</i>	1	0	0	0	0	0	0	0	0	0	0	0
<i>Sel. pusilla</i>	0	0	0	0	0	0	1	1	0	0	0	0
<i>M. rotundata</i>	1	0	0	0	0	0	0	0	0	0	0	0
<i>M. rufocuprea</i>	1	1	0	0	0	0	1	1	1	0	0	0
<i>Sel. sororinitida</i>	0	0	0	0	0	0	0	0	1	0	0	0
<i>M. setosa</i>	0	0	0	0	0	0	1	0	0	0	0	0
<i>N. sexfoliata</i>	0	0	0	0	0	0	1	0	0	0	0	0
<i>M. tricuspidata</i>	0	0	0	0	0	0	1	0	0	0	0	0
<i>M. weligamana</i>	0	0	0	0	0	0	0	0	0	1	0	0
<i>M. windy</i>	0	0	0	0	0	0	0	0	1	0	0	0
<i>M. hiyarensis</i>	0	1	0	0	0	0	0	0	0	0	0	0
<i>M. deenstana</i>	0	0	0	0	0	0	0	0	1	0	0	0
<i>Apogonia sp1</i>	1	1	0	0	0	0	1	0	1	0	0	0
<i>A. glabrilinea</i>	1	1	1	0	0	0	0	1	1	0	0	0
<i>A. solida sp3</i>	1	0	0	0	0	0	0	0	0	0	0	0
<i>A. solida sp4</i>	0	0	0	0	0	0	1	0	0	0	0	0

<i>Apogonia sp5</i>	0	0	0	0	0	0	1	0	0	0	0	0
<i>A. comosa</i>	0	0	0	0	0	0	1	0	0	0	0	0
<i>Apogonia sp7</i>	0	0	0	0	0	0	1	0	0	0	0	0
<i>Apogonia sp8</i>	0	0	1	0	0	0	0	0	0	1	1	0
<i>A. coriacea</i>	0	0	0	0	0	0	0	0	1	1	1	0
<i>Apogonia sp10</i>	0	0	0	0	0	0	0	0	1	0	1	0
<i>A. ludificans</i>	0	0	0	0	0	0	0	1	1	0	0	0
<i>Apogonia sp12</i>	0	0	0	0	0	0	0	0	1	0	0	0
<i>Apogonia nietneri</i>	0	0	1	0	0	0	0	0	0	0	0	0
<i>Apogonia sp14</i>	0	0	0	0	0	0	1	0	0	0	0	0
<i>Apogonia sp15</i>	0	0	0	0	0	0	1	0	0	0	0	0
<i>Brahmina sp1</i>	0	0	0	0	0	0	0	0	0	1	0	0
<i>Holotrichia sp1</i>	1	0	0	0	0	0	0	0	0	0	0	0
<i>Holotrichia sp2</i>	1	0	0	0	0	0	0	0	0	0	0	0
<i>Holotrichia sp3</i>	0	0	0	0	0	0	1	0	0	0	0	0
<i>Holotrichia sp4</i>	0	0	0	0	0	1	0	0	0	0	0	0
<i>Holotrichia sp5</i>	0	1	1	0	0	0	0	0	1	0	0	0
<i>Holotrichia sp6</i>	0	0	0	0	0	0	0	0	1	0	0	0
<i>Holotrichia sp7</i>	1	0	0	0	0	0	0	0	0	0	0	0
<i>Leucopholis sp1</i>	1	0	0	0	0	0	0	0	0	0	0	0
<i>Leucopholis sp2</i>	1	1	1	0	0	0	0	0	0	0	0	0
<i>Sophraps sp1</i>	1	1	0	0	0	0	1	0	0	0	0	0
<i>Sophraps sp2</i>	0	1	1	0	0	0	1	1	1	0	0	0
<i>Sophraps sp3</i>	0	0	1	0	0	0	0	0	0	0	0	0
<i>Sophraps sp4</i>	0	0	0	0	0	0	1	1	0	0	0	0
<i>Sophraps sp5</i>	0	0	0	0	0	0	1	0	0	0	0	0
<i>Parastasia sp</i>	0	1	0	0	0	0	0	0	1	0	0	0
<i>Orphnus sp1</i>	1	0	0	0	0	0	0	0	0	0	0	0
<i>Eophileurus sp2</i>	0	0	0	0	0	0	1	0	0	0	0	0
<i>Orphnus sp1</i>	0	0	0	0	0	0	1	0	0	0	0	0
<i>Orphnus sp</i>	0	0	0	0	0	0	1	0	0	0	0	0

<i>Xylotrupes</i> sp5	1	1	1	1	0	0	0	0	0	0	0	0
<i>Eophileurus</i> sp6	0	0	0	0	0	0	0	0	1	0	0	0
<i>Oryctes</i> sp7	0	1	0	0	0	0	0	0	0	0	0	0
<i>Phyllognathus</i> sp8	1	0	0	0	0	0	0	0	0	0	0	0
<i>Adoretus</i> sp1	1	0	0	0	0	0	0	0	0	0	0	0
<i>Adoretus</i> sp2	0	0	0	0	0	0	1	1	0	0	0	0
<i>Adoretus</i> sp3	0	1	0	0	0	0	1	1	0	0	0	0
<i>Adoretus</i> sp4	0	0	0	0	0	0	0	0	0	1	1	0
<i>Adoretus</i> sp5	0	0	0	0	0	0	0	0	1	0	0	0
<i>Adoretus</i> sp6	0	0	0	0	0	1	0	0	0	0	0	0
<i>Adoretus</i> sp7	0	1	1	0	0	0	0	0	0	0	0	0
<i>Adoretus</i> sp8	0	0	0	1	0	0	0	0	0	0	0	0
<i>Adoretus</i> sp9	0	0	0	0	0	0	1	0	0	0	0	0
<i>Adoretus</i> sp10	0	0	0	0	0	0	1	0	0	0	0	0
<i>Adoretus</i> sp11	0	0	0	0	0	0	1	0	0	0	0	0
<i>Adoretus</i> sp12	0	0	0	0	0	0	1	0	0	0	0	0
<i>Anomala</i> sp1	1	1	0	0	1	0	1	0	0	0	0	0
<i>Anomala</i> sp2	1	0	0	1	0	0	0	0	0	0	0	0
<i>Anomala</i> sp3	0	0	0	0	0	0	1	0	0	0	0	0
<i>Anomala</i> sp4	0	0	0	0	0	0	1	0	0	0	0	0
<i>Mimela</i> sp1	0	1	0	0	0	0	0	0	0	0	0	0

Table S8.3: Individuals, observed species richness (Sobs) and percentages of inventory completeness and diversity indices of scarab beetles in all sampling locations.

Location	L1	L8	L9	L12	L13	L14	L3	L2	L4	L5	L11
Forest/Elevation zone	WL/EZ1	WL/EZ1	WL/EZ1	WL/EZ2	WL/EZ2	WL/EZ2	DL/EZ1	SM/EZ2	SM/EZ3	MO/EZ4	MO/EZ5
No. of species	19	16	12	3	4	5	38	16	19	12	9
No. of specimnes	231	55	42	9	28	8	1837	184	281	183	116
Choal	21,5	19	24	3	4,5	11	39,11	18	19,14	12	10
% completeness	88,37	84,21	50,00	100,00	88,89	45,45	97,16	88,89	99,27	100,00	90,00
Simpson_1-D	0,50	0,84	0,52	0,62	0,28	0,69	0,88	0,72	0,82	0,84	0,80
Shannon_H	1,41	2,28	1,37	1,03	0,61	1,39	2,54	1,73	2,06	2,06	1,81
Evenness_e^H/S	0,22	0,61	0,33	0,93	0,46	0,80	0,33	0,35	0,41	0,65	0,68

Table S8.4: Pearson correlation between the similarity of chafer assemblage sorted for body size and for separate lineages with geographic distance. Significant correlation coefficients ($p < 0.05$) are printed in bold.

Partition		R	p
Body size	small	-0.344	0.02
	medium	0.112	0.46
	large	-0.023	0.92
Lineage	Dynastinae	0.291	0.19
	Rutelinae	-0.110	0.42
	Sericini	0.239	0.07
	Melolonthinane	0.178	0.19

Table S8.5: Kruskal-Wallis test for species turnover in localities between four field campaigns.

	L1	L2	L3	L4	L5	L8	L9	L11	L12	L13	L14
p	<i>1,75E-03</i>	<i>0,005519</i>	<i>3,32E-06</i>	0,4761	0,4241	0,06445	0,004122	0,3914	0,7014	0,6516	1
Mean Beta diversity											
%	59,73	61,47	48,95	44,24	39,96	48,15	47,39	19,23	48,89	30,00	33,33

Table S8.6: Similarity (Jaccard measure) in species composition among campaigns for total assemblage and assemblage sorted for body size and lineages.

<i>Total assemblage</i>	2019I	2019II	2020I	2020II	<i>Sercini</i>	2019I	2019II	2020I	2020II
2019I	x				2019I	x			
2019II	0,31	x			2019II	0,34	x		
2020I	0,23	0,17	x		2020I	0,18	0,22	x	
2020II	0,49	0,44	0,25	x	2020II	0,55	0,44	0,32	x
<i>Large</i>	2019I	2019II	2020I	2020II	<i>Melolonthinae</i>	2019I	2019II	2020I	2020II
2019I	x				2019I	x			
2019II	0,25	x			2019II	0,34	x		
2020I	0,19	0,15	x		2020I	0,32	0,17	x	
2020II	0,29	0,40	0,18	x	2020II	0,45	0,52	0,20	x
<i>Medium</i>	2019I	2019II	2020I	2020II	<i>Dynastinae</i>	2019I	2019II	2020I	2020II
2019I	x				2019I	x			
2019II	0,29	x			2019II	0,17	x		
2020I	0,31	0,24	x		2020I	0,20	0,25	x	
2020II	0,49	0,39	0,33	x	2020II	0,20	0,25	0	x
<i>Small</i>	2019I	2019II	2020I	2020II	<i>Rutelinae</i>	2019I	2019II	2020I	2020II
2019I	x				2019I	x			
2019II	0,31	x			2019II	0,13	x		
2020I	0,08	0,04	x		2020I	0,29	0,06	x	
2020II	0,50	0,52	0,13	x	2020II	0,22	0,40	0,20	x

Table S8.7: Comparison of species occurrence in different months (only for Tribe Sericini).

Species	Jan	Feb	March	Apr	May	Jun	Jul	Aug	Sep	Oct	Nov	Dec
<i>M. anderssoni</i>			■							■		
<i>M. bandarwela</i>		■	■	■	■	■	■		■	■		
<i>M. bandullana</i>		■	■	■	■	■	■		■	■		
<i>M. batticaloana</i>						■					■	■
<i>M. bisornata</i>									■	■	■	■
<i>M. brincki</i>										■		
<i>M. cariniforms</i>		■	■	■		■						
<i>M. calcarata</i>	■	■	■	■	■	■		■	■	■	■	
<i>M. cinnaberina</i>	■	■	■				■	■	■	■		■
<i>M. coxalis</i>	■	■				■	■	■	■	■	■	
<i>M. diyalumana</i>			■			■	■	■	■	■		
<i>M. dubia</i>		■	■	■				■	■	■		■
<i>M. ekisi</i>								■	■			
<i>M. fistulosa</i>		■	■					■				■
<i>M. flinti</i>										■		
<i>M. hastata</i>		■	■								■	
<i>M. heveli</i>		■	■	■	■	■				■	■	■
<i>M. hortonensis</i>		■	■	■	■	■			■	■		■
<i>M. iuga</i>							■			■		
<i>M. kandyensis</i>		■	■				■					■
<i>M. krombeini</i>									■			
<i>M. kuruwitana</i>		■	■	■								
<i>M. lindulana</i>	■	■	■	■		■				■		■
<i>M. mavilluensis</i>	■	■	■	■	■	■	■	■	■	■	■	■
<i>M. mollis</i>	■	■	■	■	■	■	■	■	■	■	■	■
<i>M. nilaveliensis</i>											■	■



Sel. sinharajana
Sel. wilpattuensis
Serica fusa
Serica kitulgalana
Serica lurida
Serica maculicauda
Serica nana



Declaration

I declare, that this thesis has not been prepared for another examination or assignment, neither wholly nor partially. Contributions by co-authors to the original publication are at the beginning of each chapter listed.

Date:

Signature: